A Regional Approach for Estimating Design Storms in Canada

by

YOUNES ALILA

A Thesis Presented to the University of Ottawa
in Partial Fulfillment of the Requirements for the
Degree of Doctor of Philosophy
in Civil Engineering

DEPARTMENT OF CIVIL ENGINEERING
UNIVERSITY OF OTTAWA
Ottawa, Ontario, Canada

ISBN 0-612-15583-8

UNIVERSITÉ D'OTTAWA
UNIVERSITY OF OTTAWA

Abstract

The current design storm estimation method used in Canada is based on single site frequency analysis and single site intensity-duration-frequency relationships and involves large uncertainties, especially at short-term record stations and ungauged sites. To overcome the shortcomings of the current approach, a new improved method based on regional frequency analysis and regional depth-duration-frequency equations is proposed.

The L-moments are used in the three stages of regional frequency analysis, namely the delineation of homogenous regions, the identification of a regional parent distribution, and the estimation of distribution's parameters. Following a numerical analysis of short duration (5 minutes to 24 hours) rainfall extremes from 375 stations, it was found that Canada may be considered as one homogeneous region where L-skewness and L-kurtosis display no significant spatial variability. Also, based on mean annual precipitation (*map*), Canada may be subdivided into climatologically homogeneous sub-regions, wherein the L-coefficient of variation is virtually constant. The regional parent distribution was identified as the general extreme value (GEV), the parameters of which depend on the *map* and storm duration. These findings are different from the present method, where the extreme value type I (EV1) is used irrespective of storm duration.

A hierarchical regional approach is proposed for fitting the identified GEV distribution, where the L-skewness, L-coefficient of variation, and mean are estimated on a regional, sub-regional, and at-site basis, respectively. Monte Carlo simulation studies indicate that the hierarchical regional GEV frequency approach is substantially more accurate than the single site frequency method. In particular, it is shown that three times as much data are required for the single site method to provide the same accuracy as the hierarchical regional approach.

The depth-duration and depth-frequency ratios computed by the developed hierarchical regional GEV approach are used to assess the hypothesis that convective cells associated with short duration storms (i.e. less than 120 minutes) have common properties in different hydrologic regions. Depth-

duration ratios (defined as the ratios of the t-min to the 60-min rainfall depths of the same return period) are found to be independent of return period and geographical location for any storm less than 60 minutes. However, for storms of longer durations, depth-duration ratios depend on both the return period and the geographical location indexed by the at-site *map*. Depth-frequency ratios (defined as the ratios of the T-yr to the 10-yr rainfall depths of the same storm duration) are also found to depend on the return period and geographical location. Hence, the assumption of geographically independent depth-frequency ratios used in previous studies is incorrect.

Generalized expressions of depth-duration and depth-frequency ratios are combined to develop a set of regional depth-duration-frequency equations that are applicable in Canada. These equations are found to be more accurate than other regional equations developed in previous studies. Furthermore, a split sampling experiment has verified that the proposed equations reproduce the rainfall frequency data at long-term record stations in different hydrologic zones better than the existing single site AES equations.

Finally, the proposed hierarchical regional GEV approach and depth-duration-frequency equations are combined to develop a new design storm estimation method at ungauged sites. This method is shown to be a viable alternative to the current arbitrary interpolation procedure from isoline maps.

Acknowledgements

Grateful thanks to Dr. K. Adamowski of the University of Ottawa and Dr. P. J. Pilon of Environment Canada for their outstanding supervision, technical advice, constructive criticism, and encouragement throughout my PhD program.

I am also indebted to my colleague Brett Young of the Greater Vancouver Regional District for making many useful comments on the final manuscript of this thesis. Further grateful acknowledgement is extended to the Atmospheric Environment Services of Environment Canada for providing the necessary rainfall data required for the analysis.

Finally, I would like to express my sincere appreciation to the Tunisian Ministry of Higher Education and Scientific Research, the Canadian International Development Agency, and the National Science and Engineering Research Council of Canada for providing the financial support of my education at the University of Ottawa.

Contents

List of Appendices

List of Figures

List of Tables

Notations

λ_1	: Population mean in L-moment space
λ_2	: Population standard deviation in L-moment space
τ_2	: Population coefficient of variation in L-moment space
τ_3	: Population skewness in L-moment space
τ_4	: Population kurtosis in L-moment space
τ_r	: R-th population L-moment ratio
λ_r	: R-th population L-moment statistic
l_r	: R-th sample L-moment statistic
$t_r^{(i)}$	: R-th L-moment ratio at site i
t_2	: Sample coefficient of variation in L-moment space
t_3	: Sample skewness in L-moment space
t_4	: Sample kurtosis in L-moment space
C_s	: Sample skewness in moment space
$\bar{\lambda}_1$	: Weighted average mean in L-moment space
$\bar{\lambda}_2$	: Weighted average standard deviation in L-moment space
$\bar{t}_2$	: Weighted average coefficient of variation in L-moment space
$\bar{t}_3$	: Weighted average skewness in L-moment space
$\bar{t}_4$	: Weighted average kurtosis in L-moment space
$\bar{t}_r$	: R-th weighted average L-moment ratio
V_1, V_2, V_3	: Between-site variability measures of L-moment statistics
β	: Bias correction factor for L-kurtosis
N and K	: Number of sites in a homogeneous region
θ_0	: Statistical regional average parameter
K_e	: Equivalent number of independent sites in a region
σ^2	: Time sampling variance
ω^2	: Space sampling variance
a,b,c	: Site specific design storm parameters
a_1, b_1, c_1	: Site specific design storm parameters
I	: Rainfall intensity (mm/hr or in/hr)
C	: Regional location parameter used in IDF equations
$f(\cdot)$	: Probability density function

$\Gamma(\cdot)$	: Gamma function
n	: Number of observations in a sample
$F(x)$	: Cumulative distribution function of x
$x(F)$	: Quantile function of the distribution
$x_{i:n}$	: I-th observation of an ordered sample of size n
μ and α	: Location and scale parameters of the Gumbel Distribution
$\zeta, \alpha,$ *and* k	: Location, scale, and shape parameters of a distribution
μ_y and σ_y	: Location and scale parameters of the log-normal
$y = \ln(x)$	: Natural logarithm of the random variable x
μ_r	: R-th absolute moment
μ_r'	: R-th central moment about the origin
t	: Design storm duration
T	: Design storm return period
R_t^T	: T-yr t-min rainfall depth
R_t^{2yr}	: 2-yr t-min rainfall depth
R_t^{10yr}	: 10-yr t-min rainfall depth
R_t^{100yr}	: 100-yr t-min rainfall depth
R_{1hr}^T	: T-yr 24-hr rainfall depth
R_{60min}^T	: T-yr 60-min rainfall depth
R_{60min}^{2yr}	: 2-yr 60-min rainfall depth
R_{60min}^{10yr}	: 10-yr 60-min rainfall depth
R_{60min}^{100yr}	: 100-yr 60-min rainfall depth
R_{24hr}^T	: T-yr 24-hr rainfall depth
R_{24hr}^{2yr}	: 2-yr 24-hr rainfall depth
R_{24hr}^{10yr}	: 10-yr 24-hr rainfall depth

Abbreviations

AES	: Atmospheric Environment Services
CDF	: Cumulative distribution function
CFA	: Consolidated frequency analysis package
DDR	: Depth-duration ratio / relationship
DFR	: Depth-frequency ratio / relationship
DIST	: Frequency distribution
EV1	: Gumbel type I frequency distribution
GEV	: General extreme value frequency distribution
GLO	: General logistic frequency distribution
GLN	: Generalized log-normal frequency distribution
GPA	: General Pareto frequency distribution
H	: Homogeneity statistic by Hosking and Wallis (1993)
HRGEV	: Hierarchical regional general extreme value frequency model
IDF	: Intensity-duration-frequency
L-kurtosis	: Kurtosis coefficient in L-moment space
L-moments	: Linear moment statistics
L-skewness	: Skewness coefficient in L-moment space
map	: Mean annual precipitation
MSC	: Meteorological Survey of Canada
MSE	: Mean square error
NERC	: Natural Environment Research Council
N_{sim}	: Number of synthetic replications of homogeneous networks in Monte Carlo simulations
PIII	: Pearson type III or Gamma frequency distribution
PWM	: Probability weighted moments
RMSE	: Root mean square error
S	: Homogeneity statistics by Alila et al. (1992)
SEV1	: At-site Gumbel I frequency model
SGEV	: At-site general extreme value frequency model
RDDF	: Regional depth-duration-frequency equations
TCEV	: Two-component extreme value distribution
TP40	: US Weather Bureau technical paper No. 40
WMO	: World Meteorological Organization
Z	: Regional goodness-of-fit statistic

Chapter 1

Introduction

1.1 Motivation

The knowledge of design storms, defined as the rainfall intensity for various probability of occurrences or return periods, is of fundamental importance in hydrology. Design storms, in the form of intensity-duration-frequency (IDF) curves or empirical relationships, are needed in many hydrological models and procedures for computation of water quantity and quality characteristics.

In practice, design storms are computed based on a single site frequency analysis of annual maxima rainfall series of durations varying from 5 minutes to 1 day (WMO, 1983). The rainfall series are commonly assumed to have been drawn from a Gumbel or extreme value type I (EV1) distribution and

its parameters are estimated by the method of moments that relates sample statistics such as mean and standard deviation to the distribution parameters. Unfortunately, there are several sources of error and other drawbacks to this approach.

A first source of error in single site frequency analysis results from misidentification of the underlying probability distribution. The extent of such an error depends on how far off the assumed model is from the actual parent distribution. The choice of EV1 by many world wide meteorological organizations is mostly made for convenience and standardization purposes (Hershfield, 1961; Hogg and Carr, 1985). However, the World Meteorological Organization (WMO, 1983) does indicate that several other distributions could be chosen, whereby the best one is selected because it gives a 'better fit to the data'. Watt and Nozdryn-Plotnicki (1980) and Pilon et al. (1991a) demonstrated that the EV1 doesn't always give the 'best' fit to the annual rainfall extremes in Canada. Figure 1.1 shows an example of how the EV1 does not provide a good fit to the 2-hr rainfall extremes at the St. Thomas station in Ontario. It is evident from the lack of literature in this area that little effort is spent reviewing the appropriateness of the form of the distribution of short duration rainfall extremes.

A second source of error in single site frequency analysis is due to sampling deficiencies, where the sample length is not long enough for a reliable statistical analysis (especially for long return periods). This is particularly true in Canada as the average record length based on the available 500 rain

gauge network is less than 25 years, and only few stations have more than 40 years of record. These ranges of record lengths are sufficient to provide reasonable estimates of design storms with return periods of up to 10 years. However, for many engineering design purposes it is necessary to estimate values with return periods of at least 50 years. Bell (1969) showed that the 68 % lower and upper confidence limits for estimating the 50-yr design storm return period from 25 years of records using the single site EV1 frequency approach are 12 and 220 years, respectively. Using 100 years of records, he also demonstrated that these lower and upper limits could only be reduced to 25 and 100 years, respectively. This indicates how the extrapolation of design storms from short rainfall records is subject to a wide range of uncertainty.

Another inherent drawback to single site frequency analysis is that the approach is not directly applicable to ungauged locations. In the absence of local rainfall data, design storms are obtained through various transposition and interpolation schemes (WMO, 1983). According to Hershfield (1961), values interpolated from current United States Weather Bureau rainfall frequency maps have standard errors of at least 10 % for short return periods and 20 % or more for return periods of 50 or 100 years. Hogg and Carr (1985) also admitted that mapping IDF statistics might introduce large uncertainties and suggested safety factors ranging from 1.2 up to 2.0 to be applied in remote and mountainous areas.

To overcome the difficulty of using rainfall frequency maps when data transposition or interpolation is infeasible, several other studies (Hershfield

and Wilson 1958; Hershfield, 1961 and 1962; Bell, 1969; Ferreri and Ferro, 1990) have developed empirical IDF equations. These equations are based on the assumption that short duration convective storms have common characteristics irrespective of geographical location. These equations provide more reliable means of estimating design storms at both gauged and ungauged sites and extrapolating to higher return periods (Bell, 1969). However, there is little agreement in the literature (Chen, 1983; Ferreri and Ferro , 1990; Kothyari and Garde, 1992; Hogg, 1992; Ferreri and Ferro, 1992) as to the general form of such equations and they have never been validated for application in local Canadian conditions (Pugsley, 1981).

While current procedures for computing design storms are exclusively based on single site frequency analysis, it has long been recognized that regional analysis techniques have the ability to significantly reduce uncertainties in quantile estimates relative to that inherent in the single site approach (Lettenmaier et al., 1987; Hosking and Wallis, 1988; Pilon and Adamowski, 1992). Regionalization procedures can further be considered equivalent to an extension of the gauging network, and provide planners and designers with a better alternative for the estimation of design storms at ungauged sites than currently used rainfall frequency maps. The advantages of regional frequency models and the large uncertainties involved in the current single site approaches justify the need for a new regional methodology leading to more reliable design storm estimates at both short-term record and ungauged sites.

1.2 Scope

While previous rainfall studies were performed using the method of moments, the Linear moments or L-moments (Hosking, 1990), which are based on the linear combinations of order statistics, have recently gained considerable momentum in the regional analysis of hydrologic extreme variables (Chowdhury et al., 1991; Pilon et al., 1991a; Alila and Adamowski, 1992; Alila et al., 1992a and b; Angel and Huff, 1992; Pilon and Adamowski, 1992; Thomas and Olson, 1992; Vogel and Lin, 1992; Cong et al., 1993; Hosking and Wallis, 1993). The advantages of L-moments are that they can characterize a wider range of distributions than conventional moments, they are less sensitive to outliers in the data, they approximate their asymptotic normal distribution more closely, and they suffer less from the effect of sampling variability (Wallis, 1989; Hosking and Wallis, 1990). To the best of the author's knowledge, the use of L-moments has never been explored in the frequency analysis of rainfall extremes and the development of IDF relationships.

This study uses the L-moments to develop a regional rainfall frequency model for computing design storms at gauged stations. The numerical analysis is performed using annual maximum rainfall data from 375 stations across Canada for storm durations of 5, 10, 15, 30, 60 minutes and 2, 6, 12, 24 hours (Appendix C). The regional rainfall frequency model is developed in three stages, namely the delineation of homogeneous regions, the identification of the regional distribution, and the estimation of distribution's parameters.

A homogeneous region (zone of applicability of the regional model) is interpreted to mean that all sites within the same region could be characterized by the same fixed value of a particular L-moment statistic, such as L-kurtosis, L-skewness, or L-coefficient of variation. However, these L-moment statistics could be affected by various climatic factors such as rain forest environment and ocean and mountainous influences. To delineate homogeneous regions, it is proposed to assess the significance of the spatial variability of extreme rainfall characteristics using L-moment based statistical tests of homogeneity.

The identification of the regional distribution within each homogeneous region is performed using L-moment based goodness-of-fit tests (Hosking and Wallis, 1993). This procedure is more robust than the classical hypothesis testing methods since it uses regional, rather than single site data, to discriminate between alternative distributions (Cong et al., 1993). A first simulation study is conducted to assess the sensitivity of design storm estimates to misspecification of the identified regional distribution.

A hierarchical approach is developed for the estimation of parameters for the identified regional distribution in which higher order L-moments such as the L-kurtosis and L-skewness are estimated over larger areas than lower order L-moments such as the L-coefficient of variation and mean. The suggested hierarchical approach has been justified for use in the regionalization of flood data and has been reported to significantly improve the accuracy of estimating design floods, especially at sites with short record lengths (Fiorentino et al., 1987; Gabriele and Arnell, 1991; Ribeiro-Correa and Rouselle, 1993).

A second simulation study is conducted to assess the value of the hierarchical regional frequency model in improving the accuracy of design storms in comparison to the single site approach.

For illustration purposes, real data from long and short-term record stations (selected to represent various hydrologic conditions) is then used to compare the performance of the proposed hierarchical regional frequency model to the present single site EV1 frequency analysis method.

At each site, the 2, 5, 10, 20, 50, and 100 year design storms are computed for each duration using the proposed hierarchical regional frequency model. These results are in turn used to assess the assumption that the general properties of convective cells associated with short duration (i.e., less than 120 minutes) storms are similar in different hydrologic regions. In particular, the geographical variation of rainfall is evaluated in terms of (i) depth-duration ratios defined as the ratios of the t-min to the 1-hr rainfall depth of the same return period, and (ii) depth-frequency ratios defined as the ratios of the T-yr to the 10-yr rainfall depth of the same storm duration. These ratios are then used to develop a set of regional depth-duration-frequency equations for the estimation of design storms at ungauged locations. A split sampling experiment that uses real data at long-term record stations from different hydrologic regions will ascertain the validity of the form of the developed regional equations in comparison to the existing single site relationships.

In a sample application, the proposed regional depth-duration-frequency equations are used to estimate design storms at a set of ungauged sites selected to represent various hydrologic conditions. Results are then compared to the current interpolation procedure from the rainfall frequency maps of Hogg and Carr (1985).

In summary, this thesis presents an improved regional methodology to estimate design storms at both gauged and ungauged sites. While there has been vigorous research activity on the regionalization of flood data (Potter, 1987), very little effort has been devoted to the regionalization of short duration rainfall extremes. To the best of the author's knowledge, this thesis is one of the first large scale and comprehensive regional frequency analyses of short duration rainfall extremes.

1.3 Objectives

The primary objective of the thesis is to develop a new regional methodology for the estimation of design storms at both gauged and ungauged sites. The novel application of the L-moments to the regionalization of short duration rainfall extremes is investigated and a hierarchical regional frequency model, that leads to more reliable design storm estimates than the single site approach, is suggested. Design storms computed based on the proposed hierarchical model are in turn used to develop a set of regional depth-duration-frequency equations that provide a new frontier in the estimation of design

storms at ungauged sites in Canada and reduces uncertainties associated with current interpolation procedures from rainfall frequency maps.

Specific objectives of the thesis are as follows:

1. Delineate homogeneous climatic regions by assessing the spatial variability of key statistical characteristics of annual rainfall extremes using L-moment based statistical testing of homogeneity.

2. Identify the regional parent distribution within each delineated homogeneous region using regional and L-moment based goodness-of-fit testing.

3. Design and perform a first Monte Carlo simulation experiment to assess the sensitivity of design storm estimates to misspecification of the identified regional parent distribution.

4. Develop a hierarchical approach for fitting the identified regional distribution and perform a second Monte Carlo simulation experiment to evaluate the accuracy of such an approach relative to that of the single site frequency method.

5. Compute design storms by the proposed regional hierarchical frequency model at typical long and short-term record stations selected to cover a wide range of meteorological conditions in Canada. Compare with estimates obtained by the current single site EV1 frequency approach.

6. Develop regional depth-duration-frequency equations by evaluating the spatial variability of both depth-duration and depth-frequency ratios computed using the hierarchical regional frequency model.

7. Verify the validity of the proposed regional equations in comparison to existing single site relationships using a split sampling experiment.

8. Estimate design storms by the proposed regional equations at selected ungauged sites from different climatic zones and compare with values obtained by interpolation from existing rainfall frequency maps.

1.4 Thesis Overview

Chapter I presents the drawbacks of the current single site rainfall frequency analysis approach and highlights the need for a new regional methodology that improves on the accuracy of design storm estimates at both gauged and ungauged sites. A summary of the various stages proposed for the development of the new methodology and the evaluation of current practices is also given.

Chapter II reviews the literature related to single site and regional frequency analyses as well as the development of IDF equations. Unresolved problems and potential solutions by the proposed methodology are highlighted.

Chapter III presents the theory of L-moments with emphasis placed on their superiority to the conventional moments. The theoretical background is developed for a distribution's goodness-of-fit test and two statistical tests of homogeneity. A hierarchical approach for estimating distribution parameters is introduced and the Monte Carlo experiments are described.

Chapter IV describes the various climatic zones in Canada and the database used for the numerical analysis. Findings from various stages in the development of the regional hierarchical frequency model and the regional depth-duration-frequency equations are reported and new regional methodologies for estimating design storms at both gauged and ungauged locations are proposed. Finally, the evaluation results of the new regional methodologies using simulated and real data are presented and discussed.

Chapter V summarizes the major findings of the thesis and lists recommendations for further studies.

Chapter 2

Literature Review

2.1 Single Site Rainfall Frequency Analysis

Single site frequency analysis consists of two steps: (i) selecting a probability distribution, and (ii) fitting the distribution to the observed data. Design storms estimated by the fitted distribution are prone to errors. A possible source of error may be a misspecification of the parent distribution; i.e., model governing the population from which the observed sample of data is supposedly drawn (model error). Another source of error may be a deviation of the distribution's parameters from its 'true' values as a result of sampling deficiencies or inappropriate fitting techniques (sampling error).

2.1.1 Distribution selection

Many distributions have been investigated for the frequency analysis of extreme hydrologic variables (Alexander et al., 1969). However, there is no firm theoretical basis for the exclusive use of one distribution over others. Gumbel (1958) stated that the goodness-of-fit of any distribution cannot be foreseen from theory. In practice, more than one distribution is fitted to the same data and the one providing the 'best' fit based on the goodness-of-fit tests is chosen.

One such test is a graphical technique (Dalrymple, 1960; Farmer and Fletcher, 1972) in which plotting positions and appropriate probability papers are used to compare the observed data to the theoretical form of the distribution. However, this procedure can be quite subjective and limit the assessment of fit to the range of the observed data.

Other statistical goodness-of-fit tests include the Chi-Square, Kolmogorov Smirnov (Keeping, 1966), and Akaike Information Criterion (Akaike, 1974). Reservations against the use of such tests have been raised (Matalas and Wallis, 1973) because of the relative degree of subjectivity of the index of fit and the plotting position.

It is also possible to select a suitable distribution based on moment ratio diagrams utilizing the coefficients of skewness and kurtosis (Wu and Goodridge, 1974; Watt and Nozdryn-Plotnicki, 1980). This approach has

been the subject of much criticism because of the inherent sampling errors in estimating higher order moments associated with existing ranges of record lengths (Hazen, 1924; Wallis et al., 1974). Other, not fully developed techniques for discriminating between alternative distributions, include the Bayesian decision theory and nonparameteric statistics (Bodo and Unny, 1976).

Recent developments have made an attempt to avoid the parametric distribution selection by adopting the nonparametric methods (Adamowski, 1985; Wu and Woo, 1989). In the nonparametric approach to frequency analysis, there is no need for an a priori choice of distribution, and the parameter estimation problem is much less complex. However, it has been argued that the nonparametric estimators have virtually no tail and may lead to unreliable quantile estimates beyond the largest observed value (Schuster and Yakowitz, 1986; Bradsley, 1988).

Because of the lack of a theoretical basis for selecting an appropriate distribution in rainfall analysis, many national meteorological agencies have adopted some sort of procedural policies and standardization of IDF analysis (Gupta, 1970). The most frequently used probability distribution in a frequency analysis of rainfall data is the two-parameter EV1 distribution (WMO, 1981), with constant theoretical skewness and kurtosis of 1.14 and 5.4, respectively. Its density function is given by (Gumbel, 1958):

$$f(x) = \alpha \ \exp\left[-\alpha(x-\mu) - \exp\left(-\alpha\ (x-\mu)\right)\right] \qquad (2.1)$$

in which x is the rainfall quantile, and μ and α are the location and scale

parameters, respectively. Its cumulative distribution function is expressed as follows:

$$F(x) = \exp[-\exp(-\alpha(x-\mu))] \tag{2.2}$$

The second most frequently used distribution is the two-parameter log-normal (LN) (WMO, 1981), with constant theoretical skewness and kurtosis of 0.0 and 3.0, respectively. Its density function is defined as (Kite, 1975):

$$f(x) = \frac{1}{x\sigma_y\sqrt{2\pi}} \exp\left\{-\frac{(\ln(x)-\mu_y)^2}{2{\sigma_y}^2}\right\} \tag{2.3}$$

in which μ_y and σ_y are the mean and standard deviation of the natural logarithm of x ($y = \ln\ x$). In addition to goodness-of-fit tests, the arguments in favour of the use of these two models include: (i) the lower bound of the distribution is greater than zero, (ii) the upper bound is much greater than the maximum observed rainfall and, (iii) reduced bias in estimating distribution parameters caused by sampling deficiencies (two-parameter distributions do not require moments of higher order such as skewness).

Comparison between the 100-yr design storm estimates by these two distributions revealed small differences of up to 10 % (Hershfield and Wilson, 1958; Huff and Neill, 1959a; Hershfield and Kohler, 1962; Majumdar and Sawhney, 1965; Samuelson, 1972). On the other hand, comparison between estimates by EV1 and three-parameter distributions, with variable skewness and kurtosis values, revealed larger differences. Huff and Neill (1959a) and Reich (1970) showed that differences between 100-yr design storm estimate by EV1 and the extreme value type II (EV2) are as high as 80 %. Adamson and Zucchini (1983) found that in the range of return periods between 100

and 200 years, design storms estimated by EV1 averaged about 20 % smaller than those estimated by the log-Pearson type III (LP3) distribution.

In some studies, the suitability of a specific distribution has been attributed to climatic factors. Wurtele and Roe (1978) suggested the EV2 (with an effective lower bound but meteorologically no upper bound) in deserts, and the EV1 (with no effective lower bound) in regions with moderate-to-high rainfall intensity characteristics. In Russia, Kuznetsova (1964) had shown that in regions where the amount of rain is limited by low temperature and atmospheric condensation levels the binomial distribution gave a better fit than the LN. In climates favouring a wider range of rainfall with occasional extremely heavy storms leading to an asymmetric distribution, the LN did not always give the best fit to the daily maximum precipitation series.

In other studies, different distributions have been selected for different geographical regions. According to Uppala (1978), the EV2 distribution gave the best fit to rainfall data in western Finland, whereas, in eastern Finland the extreme value type III (EV3) was found to be more appropriate. Zeller et al. (1978) have shown that the annual rainfall maxima in north-eastern Switzerland were best fit by the EV1, while in other regions the EV2 distribution was more suitable. Krishnan and Kushwaha (1975) also found that rainfall data in India exhibits deviations from the EV1 distribution that are systematic with geographical pattern. In the United States, Hershfield (1962) did not detect any geographical pattern to the behaviour of rainfall distribution. However, this behaviour may be due to the greater consistency

and inflexibility associated with the two-parameter distributions considered in his analysis (EV1 and LN) as opposed to the more versatile and flexible three-parameter models.

Some other studies have adopted different distributions for different storm durations. Sneyers (1977 and 1978) fitted the EV1 distribution to the annual rainfall maxima in Belgium for storm duration of less than 30 minutes, the EV2 distribution for storm durations of 1 to 24 hours, and a mixture of both distributions for durations in between. Wu and Goodridge (1974) found that the annual rainfall maxima of storm duration less than 30 hours in California, USA, are best fitted by the Pearson type III (P3), while those of longer durations are best suited by the EV3 distribution. Rodda (1970) demonstrated that rainfall data of durations greater than five days tend to become normal or can at least be normalized. Pilon et al. (1991a) found that the rainfall data in Ontario, Canada, are best fitted by the general extreme value (GEV) distribution, the parameters of which depended on the storm duration. Also, in analyzing three long-term rain gauge stations in Canada (Victoria, St. Thomas, and Quebec) Watt and Nozdryn-Plotnicki (1980) observed that:

> *In general, the data, when plotted on EV1 probability paper, provide an equally good fit for shorter durations, but for durations above 30 minutes the fit deteriorates. As was the case for the LN the largest two or three events exceed the fitted value and this is reflected in the values of sample skewness which, on the average,*

exceed the EV1 population value of 1.14.

In summary, there seems to be no 'standard' distribution capable of describing rainfall extreme values irrespective of climate, geographical location, and storm duration. The choice of a distribution can affect to a great extent the magnitude of the estimated design storms, especially for relatively large return periods. In Canada, the EV1 distribution is recommended, not necessarily because of its statistical superiority, but mainly to promote a uniform and consistent rainfall frequency analysis (Hogg and Carr, 1985). Canada covers a wide range of climatic and physiographic conditions from the mountainous coastal rain-forest environment of British Columbia to the flat and relatively dry southern Prairies zone. To the best of the author's knowledge, there has been no comprehensive study of the effect of climate, other geographical factors, and storm duration on the selection of the probability distribution governing short duration rainfall extremes in Canada. Therefore, this study evaluates the current distribution assumption of EV1, identifies an appropriate parent distribution, and examines the effect of storm duration, climate, and geographical location on the characteristics of such a distribution. To overcome the drawbacks of classical goodness-of-fit tests, a recently developed test (Hosking and Wallis, 1993) that uses regional as opposed to relatively short-term single site records is applied.

2.1.2 Parameter estimation method

In single site frequency analysis, parameters of the selected distribution are estimated from the observed data sample. Due to sampling variability, this constitutes a second possible source of error in design storm estimates. The most common techniques for parameter estimation are the moments and maximum likelihood methods.

The method of moments is based on the relationships between the parameters of the distribution and its absolute or central moments. The r-th absolute moment is given by:

$$\mu_r = \int_{-\infty}^{+\infty} x^r f(x) dx \tag{2.4}$$

while the r-th central moment about the origin is expressed as:

$$\mu_r' = \int_{-\infty}^{+\infty} (x - \mu_1)^r f(x) dx \tag{2.5}$$

where r is the order of moment and μ_1 is the population mean. Most of the frequency models in hydrologic practices are adequately described by the first two or three moments. The location, scale, and shape parameters are a function of the first, second, and third order moments, respectively. The accuracy of estimating higher order moments from sample data deteriorates rapidly as its order r increases and the sample size decreases. Only the mean of the sample is an unbiased estimate of the population mean while the standard deviation and coefficient of skewness are quite biased (Hazen, 1924, Wallis et al., 1974). Therefore, quantile estimates by three parameter distributions are more prone to errors caused by sampling variability.

The maximum likelihood technique, first introduced by Fisher (1922), is based on the fact that the joint probability distribution of the n random observations in data sample of density function $f(x,\ a,\ b,\ c, ...)$, is proportional to the product:

$$L = \prod_{i=1}^{n} f(x_i,\ a,\ b,\ c, ...) \tag{2.6}$$

in which L is known as the likelihood function. The parameter values maximizing this product are called the maximum likelihood estimates.

Lowery and Nash (1970), Samuelson (1972), and Watt and Nozdryn-Plotnicki (1980) have shown that fitting the two-parameter EV1 distribution by both the moments and the maximum likelihood techniques produced nearly unbiased and almost equally efficient quantile estimates (bias is a measure of the deviation of an estimate from its true value while efficiency is a measure of the dispersion of estimates about their own mean). Hence, these authors have concluded that the method of moments is better to use because of its computational simplicity.

There is, however, no general agreement on the best technique for fitting a three-parameter distribution. The method of maximum likelihood is only more efficient for larger samples (Matalas and Wallis, 1973). Its efficiency deteriorates rapidly as the sample size decreases (Bobee and Robitaille, 1977), while Fisher (1941) and Thom (1958) have shown that both techniques produced poor parameter estimates for highly skewed data. Bias correction factors for the coefficient of skewness have been suggested in several studies but found to be dependent on both the distribution and sample size (Hazen,

1924; Matalas et al., 1975; Bobee and Robitaille 1975 and 1977; Bobee, 1975; Landwehr et al., 1979; Beard and Lall, 1982). The efficiency of the method of moments can also be affected by outliers - extremely high or low values in data samples that determine the tail behavior of the distribution (Jenkinson, 1969; Snyder, 1972; Klemes, 1987).

As a remedy, Greenwood et al. (1979) introduced probability weighted moments (PWM) - a method of interest for distributions that can be written in inverse form, such as the Wakeby and Weibull. The performance of the three methods: moments, maximum likelihood, and PWM have been studied by Landwehr et al. (1979). They showed that, unlike the two former techniques, the latter produces unbiased parameter estimates when sample data are drawn from a purely random process. Many studies (Hosking et al., 1985a and b; Lettenmaier and Potter, 1985; Wallis and Wood, 1985; Lettenmaier et al., 1987) used the PWM in regional frequency analysis and showed it to be a viable means of improving single site quantile estimates.

Hosking (1990) expanded the utility of PWM through the development of the linear moment statistics (L-moments). The L-moments, the theory of which is detailed in chapter 3, are virtually unbiased and less sensitive to outliers in data samples in comparison to the conventional moments (Royston, 1991). Fitting the GEV and generalized Pareto distributions (GPA), Hosking et al. (1985b) and Hosking and Wallis (1987) have shown that the method of L-moments is more efficient than the maximum likelihood technique for various sample sizes of up to 100.

In summary, population statistics of rainfall extremes such as the mean, standard deviation, and skewness are not known and can only be estimated from observed sample data. The existing short record lengths do not warrant unbiased sample statistics by either the method of moments or maximum likelihood (Hannan, 1987), especially when the behaviour of the observed data is better ascribed by a three-parameter distribution, as is demonstrated in this study. It is therefore suggested to use the method of L-moments for fitting short duration rainfall extremes in Canada.

2.2 Regional Rainfall Frequency Analysis

Regional analysis consists of transferring information between sites within a homogeneous region - zone of applicability of the regional model - in order to improve the accuracy of quantile estimates at short record stations and allows the estimation of information at ungauged locations.

Over the years, two methodologies have evolved in regional flood frequency analyses. These are the regression and the index techniques.

In the regression approach (Thomas and Benson, 1970), predictive models relating quantiles to physiographic and climatic variables governing the generation mechanisms of the extreme variable are derived using ordinary, weighted, and generalized-least squares (Stedinger and Tasker, 1985). While recent advances in the regression approach (Gingras et al., 1994) have demon-

strated its value in reducing the standard error of flood quantile estimates, its application to the regionalization of rainfall extremes remains limited due to the difficulties often encountered in parametrizing, using measurable quantities, physical factors that affect rainfall characteristics.

The index flood approach (Dalrymple, 1960) uses a regional probability distribution to describe how the quantiles vary with their probability of occurrence within the homogenous region. The parameters of such a distribution are in turn defined by functional relationships relating the statistical characteristics of the extreme event variable to hydrometeorological factors responsible for its generation mechanism. The procedure is further simplified by either proving or assuming that all but one (often the annual mean) of the extreme variable characteristics are constant within the homogeneous region and hence the number of functional relationships is reduced to one for a two parameter distribution such as the EV1.

Recent studies show that in nearly all practical situations the index regional estimators outperform single site estimators, particularly when the data indicate the need for a three-parameter distribution (Potter, 1987).

Wallis and Wood's (1985) simulation study has shown that the index flood regionalization technique, as applied to the GEV distribution fitted by the PWM, results in more accurate flood quantiles with nearly zero average bias and very tight average confidence limits than the single site approach. Lettenmaier et al. (1987) compared the performance of regional to single site flood frequency estimators when the parent distribution is an EV2. Using ex-

tensive simulation work, they showed that the index regional GEV approach yields more accurate flood quantiles than both the single site EV1 (results in the largest downward bias) and single site GEV (results in the largest root mean square error).

Potter and Lettenmaier (1990) have also demonstrated using bootstrapping, a resampling technique that does not require the assumption of a parent distribution, that the index flood approach applied to the GEV produces more accurate 100-yr flood quantiles than its single site counterpart.

Pilon and Adamowski (1992) evaluated the use of L-moments in regional flood frequency analysis by Monte Carlo simulations and demonstrated that the regional GEV model is more accurate than either the single site EV1 or single site GEV. In particular, they found that at least twice the amount of data is required by the single site techniques to be as accurate as the regional GEV model.

In summary, many researchers have shown that regional flood frequency analysis improves the accuracy of quantile estimates in comparison to its single site counterpart. However, current IDF curves and relationships are exclusively derived using single site rainfall frequency analysis, and the author is unaware of any study that addresses the value of regional information in estimating design storms. Thus, a regional rainfall frequency model is proposed as part of this study and its performance is evaluated in comparison to the current single site approach.

2.2.1 Identification of homogeneous regions

The accuracy of regional frequency models have been shown to depend on the proper delineation of homogeneous regions (Kuczera, 1983; Hosking and Wallis, 1988). A homogeneous region is formed by a group of sites that have similar meteorological and physiographic characteristics governing the generation processes of the hydrologic extreme variable.

In the direct regression approach, homogeneous regions are obtained through the visual assessment of the mapped regression residuals (Stedinger and Tasker, 1985). This approach has limited application in the domain of regional rainfall frequency analysis because of the difficulties in quantifying physiographic and climatic factors affecting the rainfall generation mechanisms, and the complexity of the physical laws governing the process of rainfall.

When Dalrymple (1960) applied the index method to flood data, his perception of homogeneity was limited to geographically defined regions. He suggested the 'funnel' test that compares the variability of the 10-yr quantile estimates from each site in the stipulated region with that expected if sampling noise alone was responsible for the difference between sites. Cole (1966), Chong and Moore (1983), and others applied the test successfully. However, Benson (1962) and Wiltshire (1986a and b) pointed out the deficiencies of Dalrymple's 'funnel' test. They suggested that either the test was not particularly powerful or was not sensitive to a wide variety of extreme

value characteristics. When the region has become too large to 'supposedly' assume homogeneity, common practice has been to delineate geographical sub-regions with little or no statistical testing (Matalas et al., 1975; NERC, 1975). Difficulties associated with this approach are the subjective definition of sub-regions and the discontinuities in quantile estimates that can arise across sub-regional boundaries.

The geographical approach to homogeneity is not always valid since the factors that control the generation mechanism of the extreme event (flood or rainfall) may not be conducive to spatial mapping. In addition, neighboring basins within a region can be physically and hydrologically very different (Acreman and Sinclair, 1986). As a remedy, other alternative criteria have been formulated and, irrespective of geographical location, groups of gauged basins have been categorized as homogeneous using different classification philosophies such as cluster (Mosley, 1981), discriminant (Waylen and Woo, 1984; Burn, 1990), variance (Wiltshire, 1985 and 1986b), factor (White, 1975), and canonical correlation (Cavadias, 1989) analyses. These new techniques involve a great deal of subjectivity in determining the dimensions of the problem, the type of variables used for classification purposes, and the number of sub-groups (Wiltshire, 1986b).

The identification of homogeneous regions for use in regional frequency analysis of extreme hydrologic event variables remains an active field of research. The wide range of approaches using different classification philosophies, yet employing more or less the same algorithms, is a testimony to the

complexity of the problem. While the more recent non-geographical techniques represent a substitute for the arbitrary delineation of geographical regions, they remain subjective as they are not based on any statistical test of homogeneity.

Among the sparse studies of regional rainfall frequency analysis are Aron et al. (1987) and Schaefer (1990). In the first study, Pennsylvania State, USA, was divided into five geographically defined sub-regions, and regional IDF curves were developed for each sub-region using the LP3 distribution. However, no attempt was made to statistically test the homogeneity within each sub-region. In the second study, Schaefer fitted the GEV distribution by the ordinary method of moments to the precipitation data in Washington State, USA, following an index regional approach. He showed that the coefficient of variation and the skewness vary systematically with the at-site mean annual precipitation (*map*). The study area was found to be climatically heterogeneous, and independent homogeneous regions were delineated within the heterogeneous area based on *map* values. However, recent studies for both flood and rainfall data (Versace et al., 1987; Fiorentino et al., 1987; Alila et al., 1992b; Ribeiro-Correa and Rouselle, 1993) indicate that different statistics can be assumed to be approximately constant over different spatial scales. In particular, the skewness and kurtosis were found to be constant over a larger area than the coefficient of variation, which in turn varies less in space than the mean value. When these characteristics of sample statistics are hypothesized, such an analysis is known as the *hierarchical regionalization*. The rationale of this approach lies in the fact that sampling

uncertainty associated with short record lengths increases with higher order statistics. Hence, more samples of a given size are required to estimate the skewness to a specific level of accuracy than the regional coefficient of variation.

Fiorentino et al. (1987) adopted a hierarchical approach for the regionalization of flood data in Italy using the two component extreme value (TCEV) distribution fitted by the maximum likelihood (ML) method. Through Monte Carlo simulation, they showed that the regional hierarchical approach yields significantly more accurate flood quantiles than the classical regional index and the single site methods.

Gabriele and Arnell (1991) also assessed the benefits of the hierarchical approach to the regionalization of flood data based on the TCEV and GEV distributions fitted by both the PWM and ML methods. They determined that the hierarchical TCEV and GEV models result in more accurate flood estimates for all ranges of sample sizes and return periods. Particularly, they found that dividing a heterogeneous area into independent rather than hierarchical regions increased the root mean square error of quantile estimates. Furthermore, they showed that the TCEV distribution is less robust to the underlying form of the parent distribution than the GEV-PWM procedure.

More recently, Ribeiro-Correa and Rousselle (1993) adopted a regional hierarchical approach in fitting the LP3 distribution by an empirical Bayes technique. Their simulation work has shown that the hierarchical approach performs appreciably better than the single site LP3 when fitted by the

method of moments. In applying the new method to flood data in Ontario, they showed that the hierarchical approach reduces the variability of flood quantile estimates at short record stations.

Based on the above, it is clear that a hierarchical approach is preferable to the classical index method and, for the first time, is adopted in this study to the regionalization of short duration rainfall data. To justify the need for this approach, two recently developed L-moment based statistical tests of homogeneity (Alila et al., 1992b; Hosking and Wallis, 1993) are examined. This is discussed in detail in chapter 3.

2.2.2 Identification of the regional distribution

While regional frequency estimators are usually associated with less sampling variance than single site estimators, they both still suffer from the same complicating factor; namely the form of the underlying distribution is not known, nor can it necessarily be assumed on theoretical grounds (Potter and Lettenmaier, 1990).

As is the case for single site frequency analysis, the selection of the probability distribution is based either on standardization of practices (NERC, 1975; USWRC, 1982) or on empirical goodness-of-fit tests. However, it has been demonstrated in several studies that some regional estimators are not robust with respect to assumed parent distribution; i.e., a misspecification of the regional parent may induce large biases in regional estimation (Letten-

maier et al., 1987).

The GEV distribution is the most frequently studied parent distribution in regional flood frequency analysis (Greis and Wood, 1981; Wallis, 1982a and b; Stedinger et al., 1983; Hosking et al., 1985a and b; Wallis and Wood, 1985; Lettenmaier and Potter, 1985; Acreman and Sinclair, 1986; Hosking and Wallis, 1986; Lettenmaier et al., 1987; Landwehr et al., 1987; Hosking and Wallis, 1988; Wallis, 1988; Jin and Stedinger, 1989; Boes et al., 1989; Potter and Lettenmaier, 1990; Schaefer, 1990; Chowdhury et al., 1991; Pearson and Woods, 1991; Pilon and Adamowski, 1992; Pilon et al., 1991a and b; Alila et al., 1992a and b). In most of these regional studies, the GEV distribution was proven to have many desirable properties. In a review paper on flood frequency analysis, Potter (1987) stated:

> *Among those regional methods which have been carefully studied, the index flood methods based on probability-weighted moments using the GEV distribution or one of the three extreme value distributions perform very well in a variety of situations. In fact, for any reasonably homogeneous region the main source of variability in probability-weighted moments index flood methods appears to be the uncertainty in estimating the at-site means used to standardize the individual flood series. Any improvement in estimating the at-site mean would significantly enhance these methods.*

Lettenmaier et al. (1987) investigated the robustness of a class of regional PWM estimators to misspecification of the assumed distribution form and to regional heterogeneity in moments of order higher than one. In their conclusions they stated:

> *Whereas two-parameter distributions - belonging to the extreme value family - perform quite well when the form of the underlying distribution is close to that of the fitted distribution, large biases can result when the distribution is misspecified. The three parameter GEV distribution, when fitted using the regional PWM method, has been shown to be relatively insensitive to violations of the distribution assumption, and to have low variability and bias.... It is shown that regional estimation methods using the three-parameter GEV distribution are relatively insensitive to modest regional heterogeneity in the coefficient of variation and quite insensitive to regional variation in the skew coefficient.*

In a regional context, this thesis shows that the GEV distribution provides a better fit to short duration rainfall extremes in Canada. Hence, the assumption of EV1 distribution with a constant theoretical skewness value of 1.14 in current single site rainfall frequency analyses is not generally valid. The identification of this regional parent distribution is performed by the recently developed and L-moment based regional goodness-of-fit test (Hosking and Wallis, 1993), the detail of which is presented later.

2.3 Intensity-Duration-Frequency Relationships

Single site rainfall frequency analysis is not directly applicable when local rainfall data are not available. In practice, the estimation of design storms at an ungauged location is often based on interpolation from rainfall frequency (isopluvial) maps.

To facilitate mapping of design storms for various return periods and to reduce the number of required maps, Hershfield (1961) hypothesized that for short duration storms the ratios of the t-min to the 60-min rainfall depth, referred to as depth-duration ratios (DDRs), may be considered independent of geographical location and return period. He derived empirical DDRs of the 5, 10, 15, 30 minutes to the 60-min rainfall depths, which were 0.292, 0.450, 0.569, and 0.790, respectively for the USA. Their estimated average errors varied from 5 % to 8 %, and these were deemed to be in the same order of magnitude as the errors due to sampling deficiencies.

Hershfield (1961) discovered, however, that this geographical independence of DDRs does not hold for durations longer than 60 minutes. While appearing independent of return period, the ratio of the 24-hr to 1-hr rainfall depths (R^T_{24hr}/R^T_{1hr}) varied spatially from 10 to 1.7 with an average value of 2.5. He then suggested linearly interpolating the values of ratios of other durations between 1 and 24 hours from the depth-duration diagram shown

in Figure 2.1. Despite the averaging process and the assumption of linearity of DDRs, Hershfield (1961) used this diagram together with four isopluvial maps (2-yr 1-hr, 2-yr 24-hr, 100-yr 1-hr, and 100-yr 24-hr) to construct 45 out of the 49 isopluvial maps of the United States Weather Bureau Technical Paper Number 40 (TP40). Hershfield indicated that design storms interpolated from TP40 have standard errors of at least 10 % for short return periods and more than 20 % for return periods of 50 or 100 years. In discussing Hershfield's procedure, Frederick et al. (1977) stated that:

> *... while these average ratios are valid in many specific sections in the USA, they have an observed describable geographic pattern, it has also been found that the ratios vary with the return period.*

Using measured rainfall data, Peterson (1987) also found that actual DDRs in Billings, Montana, are 13 % to 69 % higher than those derived by interpolation from TP40.

Bell (1969) expressed the DDRs as a function of storm duration:

$$\frac{R_t^T}{R_{60min}^T} = 0.54\ t^{0.25} - 0.50 \tag{2.7}$$

in which R_t^T and R_{60min}^T are the t-min and 60-min rainfall depths of the same return period T, respectively. Equation (2.7) applies for short storm durations (5 min $\leq$ t $\leq$ 60 min) and for return periods ranging from 2 to 100 years.

Bell suggested further that depth-frequency ratios (DFRs), defined as the ratios of rainfall depth of specific return periods to the rainfall depth of a base frequency (such as 1, 2, or 10 year return periods) for the same duration, are independent of geographical location and storm duration. He developed the following empirical DFR formulas for any return period between 2 and 100 years and for any storm duration between 5 and 120 minutes:

$$\frac{R_t^T}{R_t^{10yr}} = 0.21 \ \ln (T) + 0.52 \tag{2.8}$$

$$\frac{R_t^T}{R_t^{2yr}} = 0.35 \ \ln (T) + 0.76 \tag{2.9}$$

in which R_t^{2yr} and R_t^{10yr} are the 2-yr t-min and 10-yr t-min rainfall depths in inches. However, he cautioned that some systematic variations in the DDRs and DFRs may exist but such variations were deemed small in comparison with sampling errors and other sources of uncertainties.

To further reduce errors of interpolating from isopluvial maps, Bell combined equations (2.7) to (2.9) and proposed the following IDF relationships:

$$R_t^T = (0.21 \ln T + 0.52)(0.54 \ t^{0.25} - 0.5) R_{60min}^{10yr} \tag{2.10}$$

$$R_t^T = (0.35 \ln T + 0.76)(0.54 \ t^{0.25} - 0.5) R_{60min}^{2yr} \tag{2.11}$$

in which all the terms are as previously defined. Both formulations were developed for storm durations ranging from 5 to 120 minutes and return periods from 2 to 100 years. Knowing either the 10-yr 60-min or the 2-yr 60-min rainfall depth at any site in the USA, any design storms can be determined either using equation (2.10) or (2.11). The standard error of

design storm estimates ranges from 5 % to 7 % for equation (2.10) and 20 % to 32 % for equation (2.11). Although the variability of rainfall estimates from equation (2.11) seems considerably large, it has been suggested that this is partly compensated for by smaller sampling errors in the derivation of the 2-yr design storms. While equations (2.10) and (2.11) were derived from USA rainfall data, Bell further suggested that both equations can still be applicable to other areas of the world such as Australia, South Africa, Hawaii, Alaska, and Puerto Rico.

For a more generalized form of IDF equation, Chen (1983) provided the following relationship:

$$R_t^T = \frac{a_1 R_{60min}^{10yr} \log\left(10^{(2-x)} T^{(x-1)}\right) t}{60\,(t+b_1)^{c_1}} \tag{2.12}$$

in which $x = \frac{R_t^{100yr}}{R_t^{10yr}}$; R_t^{100yr} is the 100-yr t-min rainfall depth in inches; a_1, b_1, and c_1 are storm parameters dependent on geographical location. Equation (2.12) is developed for any storm duration ranging from 5 minutes to 24 hours and any return period greater than or equal to 1 year. Chen devised a functional relationship between parameters a_1, b_1, and c_1, and the ratio of the 1-hr to the corresponding 24-hr rainfall depths as shown in Figure 2.2. Thus, if the site specific 10-yr 1-hr (R_{60min}^{10yr}), 10-yr 24-hr (R_{24hr}^{10yr}), and 100-yr 1-hr (R_{60min}^{100yr}) rainfall depths are known, any design storm can be computed for any return period T and storm duration t.

Chen verified the performance of equation (2.12) for the Chicago rainfall data and found errors within 8 %. However, it is important to mention that the Chicago rainfall frequency data, as well as the original data used for developing equation (2.12), are interpolated from isopluvial maps of TP40, which has been subject to criticism as noted earlier. Thus, the curve fitting exercise used by Chen to develop his IDF relationship (equation 2.12) is not based on the actual at-site frequency data, which may explain the tight range of error (8 %) found in verifying the performance for Chicago data.

Using the EV1 frequency distribution as a reference, Kothyari and Garde (1992) applied equation (2.12) for rainfall data at 20 long-term stations in India and found results to be within a ±50 % error, for 90 % of the time. This was considered unsatisfactory and a new rainfall depth-duration-frequency relationship was proposed for Indian conditions:

$$R_t^T = C\frac{T^{0.2}}{t^{0.71}}(R_{24hr}^{2yr})^{0.33}(\frac{60}{t}) \tag{2.13}$$

where C is a regional location parameter and R_{24hr}^{2yr} is the 2-yr 24-hr rainfall depth at the site of interest. The application of equation (2.13) to five climatic regions in India, with distinct values of C, resulted in errors of ±18 %. Kothyari and Garde considered this accuracy to be satisfactory, particularly because of the given estimation method, measurement, and cartographic errors in the analysis. Equation (2.13) was also applied to limited data in Sri Lanka and several stations in the USA and results were found to be within a maximum error of ±30 % and ±25 %, respectively, for 90 % of the time.

Pagliara and Viti (1993) compared rainfall intensities given by equation (2.13) to those estimated by single site EV1 frequency analysis at 247 stations in Tuscany, Italy, and found results to be within ±20 %. It was further suggested that a better agreement between the data may be achieved through the use of the following relationship:

$$R_t^T = 2.29\ t^{0.3} T^{0.18} \left(R_{24hr}^{2yr}\right)^{0.59} \tag{2.14}$$

They discovered, however, that any rainfall intensity estimated by equation (2.14), used together with the R_{24hr}^{2yr} isopluvial map, still have a ±20 % error.

Ferreri and Ferro (1990) verified the applicability of Bell's DDR equation (2.7) in both Sicily and Sardinia, Italy, giving the following empirical ratio expressions:

$$In\ \ Sicily \qquad \frac{R_t^T}{R_{60min}^T} = 0.208\ t^{0.386} \tag{2.15}$$

$$In\ \ Sardinia \qquad \frac{R_t^T}{R_{60min}^T} = 0.246\ t^{0.345} \tag{2.16}$$

As shown in Figure 2.3, these relations give values quite comparable to those computed by Bell's equation (2.7). More recently, however, Ferro (1993) compared the performance of equations (2.15) and (2.16) to Kothyari and Garde's equation (2.13) and provided yet another empirical DDR formula:

$$\frac{R_t^T}{R_{60min}^T} = \left(\frac{t}{60}\right)^s \tag{2.17}$$

where 's' is a coefficient having a different value for each geographical region (0.386 in Sicily, 0.345 in Sardinia, 0.227 in Molise-Abruzzo, 0.451 in the USA, and 0.290 in India).

Hogg (1992) admitted that IDF equations could prove quite useful in the regionalization and mapping of IDF statistics. However, no attempt was made to develop regional IDF relationships applicable for Canadian conditions (Pugsley, 1981). Instead, existing single site IDF equations have the following two forms (Hogg et al., 1989):

$$I = \frac{a}{(t+c)^b} \tag{2.18}$$

$$I = a\, t^b \tag{2.19}$$

where I is the rainfall intensity in mm/hr (or in/hr), a, b, and c are site-specific parameters, and t is the storm duration in minutes ranging from 5 minutes to 24 hours. These equations were developed for the purpose of interpolating from one storm duration to another for the same return period and the same location, instead of using IDF curves. However, these equations were established by regression analysis of single site frequency data only. Therefore, they cannot be considered as regional equations, and they cannot be used for estimation at ungauged sites.

Hogg compared the performance of Ferreri and Ferro's equations (2.15) and (2.16) to equation (2.19) at a sample of Canadian stations and found that DDRs may not be independent of geography or return period. However, such comparison may yield to questionable results as the performance of supposedly regional relationships are assessed against single site equations. In addition, 3 of the 9 durations used for fitting equations (2.18 and 2.19) are longer than 2 hours exceeding, hence, the range of storm durations for which equations (2.15) and (2.16) are applicable. Several authors (Hershfield,

1961 and 1962; Bell, 1969; Penta et al., 1972; Ferreri and Ferro, 1990 and 1992) recognized that short duration rainfall events ($t \leq 2$ hr) and long duration rainfall events ($t > 2$ hr) follow different IDF equations because of the different meteorological factors responsible for each range of storms. The IDF curves at Kingston, Ontario, pumping station displayed in Figure 2.4 is an example that shows how a better fit for each return period could be obtained if storms with durations smaller than 2 hours are considered separately.

Since both single site equations (2.18) and (2.19) cannot be used when rainfall data are not available, the estimation of design storms at an ungauged location in Canada involves the interpolation from existing isoline maps for both the mean and standard deviation of annual rainfall extremes for each duration. The Rainfall Frequency Atlas of Canada (Hogg and Carr, 1985) contains 18 such maps, two for each storm duration (5, 10, 15, 30, 60 minutes and 3, 6, 12, 24 hours). As is the case for gauged sites, the EV1 distribution is assumed to apply and appropriate frequency factors are used to compute design storms for different return periods.

In this procedure, the mapping of standard deviations and frequency factors can, however, introduce large uncertainties in the estimation of design storms at ungauged sites. Both the frequency factors and standard deviation are dependent on the record length of the station, while the frequency factor is also a function of the return period. This dependency causes spatial discontinuity as a result of different record lengths. In addition, there is may

be little or no physical reason to support any geographical trend of the standard deviation. Diaconis and Efron (1983) noted that, if the geographical attribute to be mapped is subject to random variability, its isolines must be interpreted cautiously. In particular, they showed that corridors of low values of the attribute on an original isoline map can become islands on subsequent maps generated using the same data by nonparametric bootstrapping. Hogg and Carr (1985) stated that mapping IDF statistics may introduce large uncertainties and, consequently, suggested safety factors ranging from 1.2 up to 2.0 to be applied to design storms in mountainous areas that are computed by interpolation from maps.

In summary, there are large uncertainties involved in the estimation of design storms at ungauged locations using isoline or isopluvial maps. Regional IDF relationships represent a viable alternative to current interpolation procedures. While several studies have been carried out in several countries, and formulas have been proposed, there seems to be little agreement on the form of these formulas. Hence, no 'universal' equation can describe rainfall characteristics irrespective of geographical location. In addition, the IDF relationships reviewed were exclusively derived using single site rainfall frequency data assuming an EV1 distribution, which may explain the large range of errors encountered in their application.

In this thesis, generalized IDF relationships are developed using regional rather than single site rainfall frequency data. The development of these relationships is based on a regression analysis in space and applies the same

concept as the index flood regionalization approach of Dalrymple (1960). Consequently, the proposed IDF equations provide a more reliable means of extrapolating for longer return periods at short-term record stations and a viable alternative for transferring information from gauged to ungauged sites. It is also demonstrated that the developed IDF relationships minimize uncertainties induced in current interpolation procedures by significantly reducing the number of required isoline maps.

Chapter 3

Theoretical Background and Development

3.1 Theory of L-Moments

The linear moments are the expectations of certain linear combinations of order statistics. Hosking (1990) defined the r-th L-moment of a random variable x to be:

$$\lambda_r = \int_0^1 x(F) P^*_{r-1}(F) dF \tag{3.1}$$

where

$$P^*_r = \sum_{k=0}^{r} (-1)^{r-k} \binom{r}{k} \binom{r+k}{k} F^k, \tag{3.2}$$

$F(x)$ is the cumulative distribution function of x, and $x(F)$ is the quantile function of the distribution. The first L-moment, λ_1, is the arithmetic mean, while the second L-moment, λ_2, is a measure of dispersion analogous to the standard deviation. Hosking found it convenient to standardize the higher L-moments such that the r-th L-moment ratio is given by:

$$\tau_r = \frac{\lambda_r}{\lambda_2} \tag{3.3}$$

where τ_3 is a measure of the symmetry of the sample and is referred to as L-skewness; τ_4 is considered a measure of peakedness and is referred to as L-kurtosis; and the L-coefficient of variation is denoted by $\tau_2 = \lambda_2/\lambda_1$.

For a random sample $x_1, x_2, ..., x_n$, let $x_{1:n} \leq x_{2:n} \leq .... \leq x_{n:n}$ be the ordered sample. The r-th sample L-moment, l_r, can be estimated by:

$$l_r = \binom{n}{r}^{-1} \sum_{1 \leq i_1} \sum_{\leq i_2} .... \sum_{i_r \leq n} r^{-1} \sum_{k=0}^{r-1} (-1)^k \binom{r-1}{k} x_{i_{r-k}:n} \tag{3.4}$$

In particular:

$$l_1 = n^{-1} \sum_i x_i \tag{3.5}$$

$$l_2 = \frac{1}{2}\binom{n}{2}^{-1} \sum_i \sum_{>j} (x_{i:n} - x_{j:n}) \tag{3.6}$$

$$l_3 = \frac{1}{3}\binom{n}{3}^{-1} \sum_i \sum_{>j} \sum_{>k} (x_{i:n} - 2x_{j:n} + x_{k:n}) \tag{3.7}$$

$$l_4 = \frac{1}{4}\binom{n}{4}^{-1} \sum_i \sum_{>j} \sum_{>k} \sum_{>l} (x_{i:n} - 3x_{j:n} + 3x_{k:n} - x_{l:n}) \tag{3.8}$$

or alternatively

$$\bar{\lambda}_r = \sum_{i=1}^{n} P^*_{r-1}(p_{i:n})\, x_{i:n} \tag{3.9}$$

where the probability $p_{i:n}$ is estimated using an empirical plotting position formula. Hosking (1990) indicated that $\bar{\lambda}_r$ is asymptotically equivalent to l_r, but that $\bar{\lambda}_r$ is not an unbiased estimator of λ_r. Rather, the bias is of stochastic order n^{-1}.

Since, in practical experience, plotting position estimators sometimes yield better estimate of parameters and quantiles when a distribution is fitted to the data, equation (3.9) has been suggested to estimate L-moments. In this thesis, equation (3.9) is applied in conjunction with the plotting position formula given by:

$$p_{i:n} = \frac{(i - 0.35)}{n} \tag{3.10}$$

This plotting position has been shown to give satisfactory results when using the GPA distribution (Hosking and Wallis, 1987), and the GEV distribution (Hosking et al., 1985b).

For a finite sample, the L-moment ratio is estimated by $t_r = (\bar{\lambda}_r/\bar{\lambda}_2)$; where t_r is the r-th sample L-moment ratio. The sample coefficient of variation in L-moments space is estimated by the ratio $t_2 = (\bar{\lambda}_2/\bar{\lambda}_1)$.

3.2 Theoretical Properties of L-Moments

(i) Robustness

A sample statistic is said to be robust when its performance is unaffected by small changes in the tails of the distribution. This means that the difference in performance between estimates of the same statistic from one data sample to another, containing moderate outliers but from the same population, is kept to a minimum.

Non-robustness in the method of moments is induced by the process of quadruplicating (x^4), cubing (x^3), and squaring (x^2) of data, which give heavier weighting to the larger observations in the sample, especially when estimating the skewness and kurtosis. Royston (1991) demonstrated that L-moments are generally less sensitive to extreme outliers, especially in asymmetric distributions. Through a nonparametric sampling experiment, he showed that sub-samples with no outliers produced different values of skewness and kurtosis from those obtained from sub-samples containing an outlier. However, the L-skewness and L-kurtosis of the same sub-samples were shown to be fairly consistent and stable around their population values.

(ii) Bias

An estimator of sample statistics is said to be unbiased when the expected value equals the quantity being estimated. In general, estimates of sample statistics deviate from their population values as the sample size decreases. However, Royston (1991) illustrated that L-moments can be much less biased than the conventional moments. Using nonparametric resampling, it was found that while both skewness and kurtosis have a tendency of decreasing as the sample size decreases, their L-moment counterparts displayed no perceivable trends.

Wallis (1989) used parametric bootstrapping to demonstrate how L-moments are less biased than ordinary moments. Using the EV1 distribution, he generated 100 samples with n=10, 25, 40, and 100 and, for each sample size, the skewness and kurtosis were estimated by both methods and plotted as shown in Figure 3.1. These plots show how the L-moment estimates of skewness and kurtosis are much less biased, have a smaller variance, and are normally distributed about their respective population values when compared to the ordinary moment estimates.

Figure 3.1 also shows how, even for a sample size of 40, the points in the moments space appear to cluster around a value away from the theoretical skewness of 1.14 and kurtosis of 5.4. This implies that if one is sure that the 100 samples were originally from the same but unknown distribution, average skewness and kurtosis would certainly misidentify the original par-

ent. This is particularly important in the process of identifying and testing homogeneous regions in regional analysis, since a error in the selection of the parent distribution may cause a homogeneous region to be perceived as heterogeneous.

(iii) Efficiency and unboundedness

Among several unbiased estimators, the most efficient is the one that produces estimates with the smallest sampling variance. In this regard, the method of maximum likelihood has been shown to be asymptotically more efficient than the method of moments, especially when the data indicate the need for three-parameter distributions. Unfortunately, the asymptotic theory does not always lead to the smallest sampling variance when the range of sample sizes are as typically found in the frequency analysis of hydrologic variables (Hannan, 1987). Fitting the GEV and GPA distributions Hosking et al. (1985b) and Hosking and Wallis (1987) have shown that the method of L-moments is more efficient than the maximum likelihood technique for various sample sizes of up to 100.

The mathematical boundedness of ordinary skewness and kurtosis is another serious drawback of the method of moments (Kirby, 1974). Shape indices computed from existing observed samples are bounded, and cannot reach or cover the full range of the population values. The mathematical bound of skewness, while independent of the parent distribution, is a func-

tion of sample size and is given by (Kirby, 1974):

$$| C_s | \leq \frac{(n-2)}{\sqrt{n-1}} \tag{3.11}$$

Hosking (1986) demonstrated, however, that both L-skewness and L-kurtosis computed from samples with sizes larger than four can take values covering the full range of the population values (τ_3 and τ_4).

In summary, L-moments are generally more robust, less biased, and more efficient estimators than conventional moments. These characteristics present significant advantages in the regionalization of short duration rainfall extremes. In this study, the L-moments are used in the development of the hierarchical regional rainfall frequency model and the regional IDF relationships.

3.3 Testing of Homogeneous Regions

The time and space variability of L-moments are hypothesized to reflect the time and space variability of environmental factors, such as physiographic characteristics and meteorological conditions, governing the rainfall generation mechanisms. Thus, the variability of a particular L-moment reflects the likeness of sites (or homogeneity) to respond to their environmental factors. If the site responses are a function of factors that vary significantly, then the variability of the resulting L-moments may be larger than the variance caused by random sampling errors.

In this study, the statistical testing of homogeneity for a network of sites is based on the assessment of the time and space sampling characteristics of a pre-specified parent regional distribution. In this testing, data at each site in the homogeneous network are assumed to be drawn from the same distribution. Two alternative statistical tests of homogeneity are suggested for the analysis of Canadian rainfall data, namely the H and S statistics.

(i) H statistic:

In the H test, a group of gauged basins having similar statistical characteristics is first hypothesized to be homogeneous. Therefore, weighted average L-moment statistics would be the best representative parameters of the whole network. If the network has N sites, each with n_i length of record, its L-moment ratios are computed as follows (Hosking and Wallis, 1993):

$$\bar{t}_r = \frac{\sum_{i=1}^{N} n_i t_r^{(i)}}{\sum_{i=1}^{N} n_i} \tag{3.12}$$

where $t_r^{(i)}$ is the value of t_r at site i. The hypothesized homogeneous region is then tested using a Monte Carlo simulation procedure, which is detailed in section 3.6. To avoid any early commitment to a particular two or three-parameter distribution, the four-parameter Kappa distribution (Hosking, 1988) is used for the Monte Carlo simulations. The Kappa distribution is then fitted using the weighted average L-moments l_1, $\bar{t}_2$, $\bar{t}_3$, and $\bar{t}_4$. Samples drawn from this parent are arranged to replicate the number of sites and the number of observations at each. The generated data for each site

are independent and identically distributed from the presumed parent. A large number ($N_{sim} = 500$) of synthetically generated networks are then replicated, and the following three measures of the between-site variability of sample L-moments are computed for each time:

1. based on the L-coefficient of variation (t_2) only, the weighted standard deviation of t_2 is calculated as V_1,

$$V_1 = \frac{\sum_{i=1}^{N} n_i (t_2^{(i)} - \bar{t}_2)^2}{\sum_{i=1}^{N} n_i} \tag{3.13}$$

2. based on t_2 and t_3, the weighted average distance from the site to the network's mean on the t_2 versus t_3 space is then calculated as V_2,

$$V_2 = \frac{\sum_{i=1}^{N} n_i \sqrt{(t_2^{(i)} - \bar{t}_2)^2 + (t_3{}^{(i)} - \bar{t}_3)^2}}{\sum_{i=1}^{N} n_i} \tag{3.14}$$

3. based on t_3 and t_4, the weighted average distance from the site to the network weighted mean on the t_3 versus t_4 space is calculated as V_3,

$$V_3 = \frac{\sum_{i=1}^{N} n_i \sqrt{(t_3{}^{(i)} - \bar{t}_3)^2 + (t_4{}^{(i)} - \bar{t}_4)^2}}{\sum_{i=1}^{N} n_i} \tag{3.15}$$

If V denotes any of the three quantities V_1, V_2, or V_3, the measure of homogeneity is given by (Hosking and Wallis, 1993):

$$H = \frac{(V_{obs} - \mu_v)}{\sigma_v} \tag{3.16}$$

where V_{obs} is the real network value of either V_1, V_2, or V_3, and μ_v and σ_v are the mean and standard deviation of the N_{sim} values of their synthetic counterparts.

While sample L-moments are considered virtually unbiased even for short sample lengths ($n \leq 20$), this statement is more accurate for the L-skewness than for the L-kurtosis. A bias correction factor is, hence, adopted for the L-kurtosis and is given by (Hosking and Wallis, 1993):

$$\beta = \frac{1}{N_{sim}} \sum_{m=1}^{N_{sim}} (\bar{t}_4^{(m)} - \bar{t}_4) \tag{3.17}$$

in which $\bar{t}_4$ is the parent value of L-kurtosis used for the synthetic generation and $\bar{t}_4^{(m)}$ is the weighted average counterpart for the m-th generated network.

Through Monte Carlo experiments, Hosking and Wallis (1993) suggested that the region under testing should be regarded as operationally 'acceptably homogeneous' if $H < 1$, 'possibly heterogeneous' if $1 \leq H < 2$ and 'definitely heterogeneous' if $H \geq 2$. These values of H account for the difference between statistical and operational homogeneity. Operational homogeneity, in this context, is defined as the acceptable degree of heterogeneity in a region for which the regional analysis is still considered more accurate than the single site approach.

(ii) S statistic:

The second statistical homogeneity test proposed in this study is based on parametric bootstrapping and hypothesis testing. In this test, the between-site variability of sample L-moments in a network of N sites, each with n_i record length, is measured by:

1. weighted variance of L-coefficient of variation (t_2),

$$\sigma^2{}_1 = \frac{\sum_{i=1}^{N} n_i (t_2^{(i)} - \bar{t}_2)^2}{\sum_{i=1}^{N} n_i} \tag{3.18}$$

2. weighted variance of the L-skewness (t_3),

$$\sigma^2{}_2 = \frac{\sum_{i=1}^{N} n_i (t_3{}^{(i)} - \bar{t}_3)^2}{\sum_{i=1}^{N} n_i} \tag{3.19}$$

3. weighted variance of the L-kurtosis (t_4),

$$\sigma^2{}_3 = \frac{\sum_{i=1}^{N} n_i (t_4{}^{(i)} - \bar{t}_4)^2}{\sum_{i=1}^{N} n_i} \tag{3.20}$$

If σ^2 denotes any of the three quantities $\sigma^2{}_1$, $\sigma^2{}_2$, or $\sigma^2{}_3$, then the homogeneity measure is defined by (Pilon et al., 1991b; Alila and Adamowski, 1992; Alila et al., 1992b):

$$S(\%) = \frac{(\sigma^2{}_{obs} - \mu_{\sigma^2})}{\sigma^2{}_{obs}} 100 \tag{3.21}$$

where $\sigma^2{}_{obs}$ is the variance of the L-statistic under scrutiny for the network ($\sigma^2{}_1$, $\sigma^2{}_2$, or $\sigma^2{}_3$), and μ_{σ^2} is its synthetic counterpart based on N_{sim} replications of the same network generated by the four-parameter Kappa distribution. The μ_{σ^2} quantifies the amount of variation (sampling error or 'noise') of L-statistics that would be expected had the network been homogeneous and of the assumed parent distribution. In comparison, σ^2_{obs} represents a combination of sampling error and process 'signal'. Therefore, S represents the percentage of signal that is evident in the network and the percentage of noise in the network is thus equal to $100 - S$. Differences between the observed and synthetic variances of each L-statistic can be tested for significance using Fisher's F-test.

The three S statistics allow the testing of homogeneity or the similarity of synthetic to natural variability for each of the L-moments independently, while two of the three H statistics measure the homogeneity of L-moments pair-wise. While both tests are used in this study, the S statistic is more suited for the proposed hierarchical regionalization approach, in which different L-moments are assumed constant over different spatial scales and, hence, the number of sites within each delineated homogenous region is not necessarily equal for all L-moments.

3.4 Identification of Regional Distribution

Once a region is determined to be homogeneous by following the procedure described in section 3.3, data at all sites within this region are assumed to be drawn from the same regional parent distribution. The L-skewness and L-kurtosis of such a parent are represented by the regional average values based on data from all sites within the homogeneous region. The L-moment ratio diagrams of Figure 3.2 are used in the preliminary selection of the regional parent distribution. The locations of the observed regional L-skewness and L-kurtosis on this diagram identify a possible distribution that may be assumed to represent the rainfall data in that region.

The identified distribution is further verified by a goodness-of-fit test. This test is different from classical goodness-of-fit tests in two ways: (i) it uses regional data and, (ii) it combines both the selection of the distribution and

the method of parameter estimation. This approach was recently reported by Cong et al. (1993) as being:

> *... reasonably efficient when the form of the underlying distribution is close to that of the fitted, and not grossly inaccurate when the distribution is misspecified.*

The test discriminates between the most frequently used five distributions in the analysis of extreme hydrologic variables, namely the:

1. Generalized extreme value (GEV), with its cumulative distribution function (CDF)

$$F(x) = \exp\{-[1 - k(\frac{x-\zeta}{\alpha})]^{1/k}\} \quad for \quad k \neq 0 \qquad (3.22)$$

$$F(x) = \exp\{-\exp[-(\frac{x-\zeta}{\alpha})]\} \quad for \quad k = 0 \qquad (3.23)$$

2. Pearson type III (P3), with its CDF

$$F(x) = \frac{1}{\alpha\Gamma(k)} \int_{\zeta}^{x} (\frac{x-\zeta}{\alpha})^{k-1} exp\{\frac{-(x-\zeta)}{\alpha}\} dx \qquad (3.24)$$

3. Generalized log-normal (GLN), with its CDF

$$F(x) = \Phi\left\{\frac{[\log(x-\zeta) - \alpha]}{k}\right\} \qquad (3.25)$$

4. Generalized logistic (GLO), with its inverse CDF

$$x = \zeta + \frac{\alpha}{k}\left\{1 - \left[\frac{1-F(x)}{F(x)}\right]^{k}\right\} \qquad (3.26)$$

5. Generalized Pareto (GPA), with its inverse CDF

$$x = \zeta + \frac{\alpha}{k}\left\{1 - [1 - F(x)]^k\right\} \tag{3.27}$$

where ζ, α, and k are the respective distribution parameters.

The suitability of fit of a specific distribution (DIST) is judged by the difference between the theoretical L-kurtosis of the distribution and the regional L-kurtosis. The significance of this difference is assessed through the statistic (Hosking and Wallis, 1993):

$$Z^{DIST} = \frac{\left\{(\bar{t}_4) - ({\tau_4}^{DIST})\right\}}{\sigma_{\bar{t}_4}} \tag{3.28}$$

where $\bar{t}_4$ is the regional weighted average L-kurtosis of the observed network and $({\tau_4}^{DIST})$ is the theoretical τ_4 for the same regional L-skewness of the observed network of sites $(\bar{t}_3)$. The $\sigma_{\bar{t}_4}$ is the standard deviation of $\bar{t}_4$ obtained by repeated simulations of a homogeneous region with the DIST frequency distribution as a parent. Since the test is applied to discriminate between different alternative three-parameter distributions with the same skewness and to avoid extensive simulations, $\sigma_{\bar{t}_4}$ is assumed to be the same for all distributions. As proposed by Hosking and Wallis (1993), the four-parameter Kappa distribution is used for the determination of $\sigma_{\bar{t}_4}$. In computing the regional L-kurtosis values of the synthetically generated homogeneous networks, the same bias correction factor of equation (3.17) is used. The statistic Z is based on asymptotic normality and the fit is declared satisfactory at the 90 % confidence level if $\mid Z \mid \leq 1.64$.

The first assumption underlying the use of such a significance test is that the region must be exactly homogeneous. Exact homogeneity, as defined by constant shape parameters (equivalently L-skewness and L-kurtosis) across the region, allows the scale and location parameters to vary from one location to another. Such an assumption is more compelling than that implied in other recently developed goodness-of-fit tests (Chowdhury et al., 1991) where only the scale parameter is allowed to vary within a homogeneous region. The second assumption is that the data from different sites within the same homogeneous region be independent. While this hypothesis is made to simplify the analysis, it may be supported by: (i) the adopted non-geographical definition of homogeneous regions and, (ii) the fact that convective storms have limited areal coverage.

3.5 Proposed Hierarchical Approach for Fitting the Regional GEV Distribution

Section 4.2.3 shows that short duration rainfall extremes in Canada are best described by the GEV distribution. The GEV is a generalization of the extreme value distributions types I, II, and III (Fisher and Tippett, 1928). Following the parametrization done by Jenkinson (1955), the cumulative distribution function of the GEV (equations 3.22 and 3.23) is given by:

$$F(x) = \exp\{-[1-k(\frac{x-\zeta}{\alpha})]^{1/k}\} \quad for \quad k \neq 0 \qquad (3.29)$$

$$F(x) = \exp\{-\exp[-(\frac{x-\zeta}{\alpha})]\} \quad for \quad k = 0 \tag{3.30}$$

where ζ, α, and k are the location, scale, and shape parameters, respectively. These CDF equations translate to the following quantile functions:

$$x(F) = \zeta + \frac{\alpha}{k}\{1 - [-\log\ F(x)]^k\} \quad for \quad k \neq 0 \tag{3.31}$$

$$x(F) = \zeta - \alpha\{\log[-\log\ F(x)]\} \quad for \quad k = 0 \tag{3.32}$$

where

$$\begin{aligned} &for\ Type\ I && k = 0 && -\infty < x < \infty \\ &for\ Type\ II && k < 0 && \zeta + \frac{\alpha}{k} \leq x < \infty \\ &for\ Type\ III && k > 0 && -\infty < x \leq \zeta + \frac{\alpha}{k} \end{aligned}$$

The parameters ζ, α, and k are related to the theoretical L-moment statistics of the GEV distribution by the following relationships (Hosking, 1990):

$$\lambda_1 = \zeta + \frac{\alpha}{k}[1 - \Gamma(1+k)] \tag{3.33}$$

$$\lambda_2 = \frac{\alpha}{k}(1 - 2^{-k})\Gamma(1+k) \tag{3.34}$$

$$\tau_3 = \frac{2(1-3^{-k})}{(1-2^{-k})} - 3 \tag{3.35}$$

The location, scale, and shape parameters are estimated using the L-skewness, L-standard deviation, and the mean of the observed data. A framework for the estimation of these parameters has been articulated by Matalas and Gilroy (1968) (and later adopted by Fiorentino et al., 1987; Versace et al., 1987; Gabriele and Arnell, 1991, Adamowski et al., 1992; and Ribeiro-Correa and Rousselle, 1993) based on the relative importance of their temporal and

spatial variability. Matalas and Gilroy (1968) showed that estimating a regional parameter θ_0 from a region containing K sites using:

$$\hat{\theta}_0 = \sum_{j=1}^{K} \frac{\hat{\theta}_j}{K} \tag{3.36}$$

will lead to an overall accuracy measured in terms of the mean square error (MSE) as:

$$MSE(\hat{\theta}_0) = E[(\hat{\theta}_0 - \theta_0)^2] = \frac{\sigma^2}{K_e} + \omega^2(1 - \frac{1}{K}) \tag{3.37}$$

where E is the expected value, and σ^2 and ω^2 are the time and space sampling variances, respectively. The parameter K_e is the equivalent number of independent stations given by:

$$K_e = \frac{K}{1 + (K-1)\bar{\rho}_\theta} \tag{3.38}$$

in which $\bar{\rho}_\theta$ is the mean inter-site correlation within the defined region.

Equations (3.37) and (3.38) suggest that the accuracy of regional estimators is affected by the: (i) time sampling variance, (ii) space sampling variance, and (iii) inter-station correlation. They also imply that the time sampling variance can be reduced by considering larger regions. This may induce a space sampling variance and violates the assumption of homogeneity. However, Kuczera (1983), Stedinger (1983), and Hosking and Wallis (1988) showed that even when the basic assumptions of regional frequency analysis are moderately violated; i.e., when both heterogeneity and inter-site dependence are present and the form of the distribution is misspecified, regional estimators improve the accuracy of quantiles in comparison to their single site counterparts.

Theoretically, a regional model should be a time-space trade-off that maximizes the benefits of pooling data while minimizing the consequences of defining larger regions. This justifies the need for a hierarchical procedure for fitting the regional GEV distribution to short duration rainfall extremes in Canada. In the hierarchical procedure, different regional parameters are estimated from different, but nested, subsets of data. In other words, the L-skewness, L-standard deviation, and mean are estimated on regional, sub-regional, and at-site basis (i.e., more sites are used to estimate higher order L-moments).

In section 4.2.1, it is shown that Canada can be considered one homogeneous region in L-skewness as the observed variance among the different sites appears to be due to time sampling error. As such, the best regional estimate of L-skewness is given by:

$$\bar{t}_3 = \frac{\sum_{i=1}^{N} n_i t_3^{(i)}}{\sum_{i=1}^{N} n_i} \tag{3.39}$$

where N is the total number of network sites and n_i is the record length at site i. Also, the weighted average is used as opposed to simple average (equation 3.36) because the variance of estimated parameters of statistical models is inversely proportional to the sample length (Wallis, 1982b; Hosking and Wallis, 1991).

In contrast, the L-coefficient of variation of rainfall extremes across Canada is shown in section 4.2.2 to have two components: (i) a time-sampling portion, and (ii) a significant space-disturbance portion. This has lead to the further delineation of Canada into sub-regions, in which the L-coefficient of

variation is assumed to be approximately constant. The sub-regional estimates of the L-coefficient of variation are given by:

$$\bar{t}_2 = \frac{\sum_{i=1}^{N} n_i t_2^{(i)}}{\sum_{i=1}^{N} n_i} \tag{3.40}$$

Consequently, the L-standard deviation is selected to match the at-site mean using the sub-regional L-coefficient of variation computed by equation (3.40).

The hierarchical approach in regional parameter estimation is composed of three different levels. At the first level, the L-skewness is estimated based on the entire network of rain gauges in Canada. At the second level, the L-coefficient of variation and, hence, the L-standard deviation is computed for each homogeneous sub-region within the same region. At the third level, the mean is allowed to vary from one site to another across Canada. The computed regional L-skewness, sub-regional L-standard deviation, and at-site mean are then used to fit the GEV distribution using the L-moments technique (equations 3.33 to 3.35).

The above methodologies for the delineation of homogeneous regions and the identification and fitting of the regional distribution within each region are used in the development of the proposed hierarchical regional GEV frequency model and applied to short duration rainfall extremes in Canada. A Monte Carlo simulation experiment (detailed in section 4.4) will demonstrate how the proposed regional model results in more accurate design storm estimates than the single site approach, and thus should be adopted in preference to the current single site EV1 method.

3.6 Simulation Experiment

A Monte Carlo simulation experiment uses a known distribution to generate synthetic data that replicate real-world conditions. Monte Carlo experiments are used extensively in statistical hydrology to better understand the probabilistic behavior of extreme hydrologic variables such as floods and low flows (Potter and Lettenmaier, 1990).

Three Monte Carlo experiments are designed in this study. The first is performed to assess the homogeneity of a pre-specified network of sites and identify an appropriate regional parent distribution for the same network; the second experiment (section 4.4.2) is designed to assess the sensitivity of design storm estimates to misidentification of the regional parent distribution, while the third (section 4.4.1) is used to evaluate the performance of the hierarchical regional frequency model in comparison to the single site approach. Only the first experiment is presented in this section, the second and third are detailed in section 4.4.

The simulation procedures involved in the assessment of homogeneity and the identification of a regional probability distribution consist of the following steps:

1. Compute for the observed network of sites the following:

   (a) the mean (l_1), L-standard deviation (l_2), L-coefficient of variation (t_2), L-skewness (t_3), and L-kurtosis (t_4) at each site,

(b) the between-site L-moment variability measures V_1, V_2, and V_3 (equations 3.13 to 3.15),

(c) the between-site L-moment variability measures ${\sigma_1}^2$, ${\sigma_2}^2$, and ${\sigma_3}^2$ (equations 3.18 to 3.20),

(d) the average regional weighted L-moment parameters $\bar{l_1}$, $\bar{l_2}$, $\bar{l_3}$, and $\bar{l_4}$ using equation (3.12).

2. Use the observed network values of $\bar{l_1}$, $\bar{l_2}$, $\bar{l_3}$, and $\bar{l_4}$ to fit the four-parameter Kappa distribution defined (Hosking, 1988) by its CDF function:

$$F(x) = \left[1 - h\left\{1 - \frac{k}{\alpha}(x - \zeta)\right\}^{1/k}\right]^{1/h} \tag{3.41}$$

where ζ is its location parameter, α is its scale parameter, and k and h are its shape parameters.

3. Generate a synthetic network with the same number of sites and the same record length at each site using the quantile function of the four-parameter Kappa distribution defined by:

$$x(F) = \zeta + \frac{\alpha}{k}\left[1 - \left\{\frac{1 - (F(x))^h}{h}\right\}^k\right] \tag{3.42}$$

where all parameters are as defined previously.

4. Compute for the synthetic network of sites the following:

(a) the L-coefficient of variation (t_2), L-skewness (t_3), and L-kurtosis (t_4) at each site,

(b) the between-site L-moment variability measures V_1, V_2, and V_3 (equations 3.13 to 3.15),

(c) the between-site L-moment variability measures ${\sigma_1}^2$, ${\sigma_2}^2$, and ${\sigma_3}^2$ (equations 3.18 to 3.20).

5. Compute based on 500 replications of steps 3 and 4 above the following:

   (a) the mean (μ_v) and standard deviation (σ_v) of each of the quantities V_1, V_2, and V_3,

   (b) the mean (μ_{σ^2}) of each of the quantities ${\sigma_1}^2$, ${\sigma_2}^2$, and ${\sigma_3}^2$,

   (c) the standard deviation (σ_{t_4}) of the regional weighted average L-kurtosis of the synthetic networks.

6. Compute the homogeneity statistics H (equation 3.16) and S (equation 3.21) and the regional goodness-of-fit statistic Z (equation 3.28).

A Fortran computer program was developed to perform the simulation experiment. The program calls standard routines published by IBM Research Center (Hosking, 1991) to compute sample L-moments and to fit the four-parameter Kappa distribution by the method of L-moments.

In this experiment, the homogeneity of a network of sites is examined by quantifying the time and space sampling variability of various L-moments for both the observed and synthetic data. The statistical significance of differences in the L-moments sampling variability of the two worlds is then

assessed by using the H and S tests described in section 3.4. Once a network of sites is accepted as being homogeneous, the most appropriate parent distribution is selected by using the Z test (equation 3.28) to evaluate the statistical significance of the difference between the observed weighted average L-kurtosis of the network and its theoretical counterpart for various candidate distributions.

3.7 Development of Regional Depth-Duration-Frequency Equations

Section 4.8 shows that the proposed hierarchical regional frequency model allows design storms at ungauged sites to be estimated by using isoline maps of mean annual rainfall extremes for each duration and a single regional map of mean annual precipitation. This in itself constitutes an improvement over current interpolation procedures (Hogg and Carr, 1985), since there is no need for isoline maps of the standard deviation for each storm duration. In addition, an isoline map of the mean annual precipitation has a better resolution and is more reliable than an isoline map of standard deviation. In Canada for instance, the mean annual precipitation is measured at a network of 2500 stations, whereas the standard deviation of storms with durations less than 24 hours can only be computed at approximately 500 sites.

To further reduce interpolation uncertainties from isoline maps and to

make the estimation of design storms at ungauged locations more independent of the availability of pluviometric data, regional depth-duration-frequency equations are developed. This study focuses only on extreme rainfall values having durations of 2 hours or less, which are the most significant in urban hydrologic applications. Furthermore, most of these storms are convective in nature and can be shown to have similar properties irrespective of geographical location. This allows a high degree of generalization in estimating design storms.

The development of the proposed equations is performed in five main steps:

1. Use the regional L-skewness, sub-regional L-coefficient of variation, and the at-site mean to fit the regional GEV distribution by the method of L-moments at each site and for each storm duration (5, 10, 15, 30, 60, and 120 minutes).

2. Compute, using the hierarchical regional GEV frequency model, the arbitrarily selected 2, 5, 10, 20, 50, and 100 year design storms for each site and duration.

3. Formulate, using a least squares regression, regional linear depth-duration relationships defined as:

$$R_t^T = a\, R_{60min}^T + b \tag{3.43}$$

where R_t^T and R_{60min}^T are the T-yr t-min and T-yr 60-min rainfall depths, respectively; and 'a' and 'b' are site specific parameters.

4. Formulate, using a least squares regression, regional logarithmic depth-frequency relationships defined as:

$$\frac{R_t^T}{R_t^{10yr}} = c \ln(map) + d \tag{3.44}$$

where R_t^T and R_t^{10yr} are the T-yr t-min and 10-yr t-min rainfall depths, respectively, and 'c' and 'd' are site specific parameters.

5. Combine the depth-duration and depth-frequency relationships of steps 3 and 4 to formulate the final regional depth-duration-frequency (RDDF) equations that relate the T-yr t-min design storm to the corresponding 10-yr 60-min value at the same site.

Through the assessment of standard error of estimates and coefficients of determination of equation (3.43), section 4.6 shows that parameters 'a' and 'b' are independent of geographical location and return period for storms with durations less than 60 minutes. To simplify the analysis for longer duration storms, Canada is delineated into various homogeneous climatic zones where depth-duration ratios can be considered approximately constant. It is also shown in section 4.6 that, while parameters 'c' and 'd' of equation (3.44) are independent of storm duration, they vary systematically with the return period.

The regression analyses in steps 3 and 4 above are performed in space; i.e., one data point from each site. Hence, both depth-duration and depth-frequency relationships (equations 3.43 and 3.44) may be considered as generalized regional forms of frequency distributions that are based on the same

concept as the index regionalization approach of Dalrymple (1960). As such, both equations result in more accurate design storm estimates than single site rainfall frequency analysis based on short-term record data.

Bell (1969) followed a similar approach for the regionalization of short duration rainfall extremes in USA, but failed to detect that depth-duration and depth-frequency ratios (equations 2.7 to 2.9) may depend on both the return period and geographical location. Furthermore, Bell used the single site EV1 frequency data for the development of his depth-duration and depth-frequency relationships, which could explain the discrepancies in his findings. However, section 4.4 demonstrates that regional frequency estimators yield more accurate design storms than the single site models. Thus, parameter estimates in the depth-duration and depth-frequency relationships are more reliable when the regional frequency data are used in the regression analyses as proposed in this study.

The performance of the final RDDF equations is measured by their ability to reproduce design storms estimated by the hierarchical regional GEV frequency model at a site. Data from long-term record stations representative of various climatic zones in Canada are used to validate the proposed RDDF equations by a split sampling experiment.

Chapter 4

Numerical Analysis

4.1 Introduction

4.1.1 Data selection

The numerical analysis in this study is conducted on annual maxima rainfall series for storm durations of 5, 10, 15, 30, and 60 minutes (which are typical times of concentration for small urban catchments) and 2, 6, 12, and 24 hours (which are typical times of concentration for larger rural watersheds). The rainfall records for a total of 375 rain gauges are obtained from Environment Canada's Atmospheric Environment Services (AES). The name, number, and location of these stations are listed in Appendix (C).

The majority of stations are concentrated in the southern areas of high population density, where most of urban development activity usually takes place. In the northern part of Canada, most of the precipitation is in the form of snow and flooding problems are mainly caused by snowmelt. Thus, rainfall information is more vital to urban developments in southern Canada.

Tables 4.1a and 4.1b summarize the stations' record length information for the various durations on a national and provincial basis, respectively. In Canada, the network of rain gauges is fairly new, with only 150 stations having more than 20 years of data and only 10 stations with over 40 years of record. Table 4.1b further shows that Ontario, Quebec, and British Columbia contain the largest concentration of rain gauges. However, British Columbia has the lowest average record length, where 72 % of the stations have less than 18 years of record.

The network of rain gauges consists of 320 stations equipped with Meteorological Survey of Canada (MSC) tipping buckets (Meteorological Branch, 1952) recording hourly and daily maximum rainfall intensities between 5 minutes and 24 hours. However, the remaining 55 stations are equipped with Fisher and Porter long-duration automatic digital recording gauges. Measurements from these rain gauges have limited time resolution and, hence, the number of stations available for analysis is reduced from 375 to 320 for storm durations less than 30 minutes. Furthermore, to correct for inconsistencies between the two devices, Atmospheric Environment Services (AES) of Environment Canada applies standard adjustment factors to rainfall val-

ues measured by the tipping buckets to match those of the Fisher Porter gauge (Pugsley, 1981).

As published by AES, the quality of data is considered to be satisfactory. Standard AES practices are geared to reduce both random and systematic measurement errors. Random errors include misreading recorded data and gauge mal-functioning. However, systematic errors that are inherent to the specific gauge design include: (i) water loss as a result of adhesion on the gauge surface, (ii) evaporation between the end of precipitation and the time of measurement, and (iii) splashing out from the gauge and water gained as a result of splashing into the gauge.

Stations with only a minimum record length of 10 years are used in the analysis to reduce uncertainties involved in estimating long return period values from small samples. In section 4.7, eight long-term record stations are used in a split sampling experiment to verify the proposed generalized depth-duration-frequency equations.

The annual maxima rainfall time series are assumed to be independently and identically distributed. This assumption is verified using the nonparametric tests for independence, trend, randomness, and homogeneity as outlined in the Consolidated Frequency Analysis (CFA) package (Pilon and Harvey, 1993). Furthermore, rainfall records from different sites are assumed to be statistically independent. This assumption is especially valid for shorter storms, because of the limited aerial coverage of convective storm activity.

4.1.2 Precipitation regimes in Canada

In mesoscale climatology, the climate in Canada is categorized into seven main regions. These regions are shown in Figure 4.1 and are the Pacific, Cordillera, Prairies, Boreal, Arctic, Great Lakes - St. Laurence, and the Atlantic (Hare and Thomas, 1979). The regional boundaries shown in Figure 4.1 are drawn rather arbitrarily.

Figure 4.2 shows the *map* isolines for Canada. The basic structure of the Canadian precipitation pattern can be approximated by these contour lines. As shown, two wet areas, separated by a saddle of medium rainfall in the northern Prairie Provinces, are distinguishable. The western Cordillera is the first wet area with total precipitation decreasing rapidly east of the Rocky Mountains. While areas west of the Rockies encounter variable rainfall, most upland sites and west facing slopes are excessively wet. The *map* on the west coast of Vancouver is as large as 5000 mm at some sites and decreases rapidly in the Coast Mountains. Disturbances from moist Pacific air swept by westerly winds are the basic generating precipitation mechanism in the western wet area.

The third of Canada southwest of a line from Winnipeg to southern Baffin Island constitutes the second wet area. While this area has less precipitation than the western wet area, the pattern is more uniformly distributed in space. Annual precipitation of over 1250 mm is experienced in the Laurentians and the hilly parts of the Atlantic Provinces. The main driving source of precip-

itation in this region is moisture from Atlantic and the Gulf of Mexico via the USA-Midwest.

The larger part of Canada consisting mainly of the Arctic and western Boreal regions is considered a relatively dry area, with *map* typically below 500 mm and may fall as low as 125 mm in the far northern Islands. The other dry area consists of the southern Prairies and the deep valley systems of southern British Columbia. The dryness of this region is caused partly by the rain-shadow effect of the Western Cordilleran ranges.

From a microscale climatology perspective, convective and frontal types of storms are both typically encountered in Canada. Tropical storms are also known to occur, although relatively seldom. Hence, the study area for this thesis covers a wide spectrum of climatic conditions that may affect the rainfall generation mechanisms and, consequently, the governing probability distribution of rainfall extremes in Canada.

4.2 Development of a Hierarchical Regional Frequency Model

4.2.1 Delineation of homogeneous region in L-skewness and L-kurtosis

In this thesis, the initial hypothesis is made that Canada is one homogeneous region in L-skewness (t_3) and L-kurtosis (t_4) for each of the nine storm durations. The hypothesis is then verified using both the H and S statistics (equations 3.16 and 3.21, respectively) and results are listed in Table 4.2. Values of S indicate that the synthetic space variance in sample t_3 and t_4 are practically similar to the observed variances. In other words, the signal portion of the variability is relatively small in comparison with the noise for all storm durations. At the 90 % confidence limits, the difference in variability of t_3 and t_4 between the observed and synthetic networks is not significant. Since the synthetic replication at each site uses the observed record length structure of the network, it may also be stated that the between site variability of t_3 and t_4 is almost completely explained by the time sampling variability.

The hypothesis that Canada is one homogeneous region in t_3 and t_4 is further supported by the H statistics with values in the 'acceptably homogeneous' range ($H < 1$). The calculated H statistics are relatively higher for shorter duration storms. This could be explained by the fact that more

variability in both time and space are expected for shorter duration storms. The averaging process of rainfall depths over longer durations reduces data variability within each site and from one site to another within the same network. Moreover, the three H measures of homogeneity are not independent. For instance, an extreme heterogeneity in L-coefficient of variation will affect the H value for t_3.

Plots of t_3 and t_4 are made against the *map* in order to visually ascertain if these L-statistics vary with *map*. Scatter plots of t_3 and t_4 for all storm durations showed no discernible pattern. Hence, it is assumed that both are independent of *map*.

Both L-moment based statistical tests of homogeneity indicate that the spatial variability of the L-skewness and L-kurtosis of annual rainfall extremes for all storm durations is attributed to random sampling. This implies that the spatial variability of the environmental factors governing the rainfall generation mechanisms have an insignificant effect on the L-skewness and L-kurtosis values. Hence, Canada may be considered as a single homogeneous region in both L-skewness and L-kurtosis.

4.2.2 Delineation of homogeneous sub-regions in L-coefficient of variation

The hypothesis that Canada is one homogeneous region in L-coefficient of variation (t_2) is tested using the H and S statistics and results are given in Table 4.2. For a region to be 'acceptably homogeneous', the H values should be less than unity. However, as shown in Table 4.2 the H values for t_2 for all storm durations range from 6.3 to 8.5. The S statistic values further indicate that around 50 % of the spatial variability of t_2 is attributed to noise caused by random sampling. The remaining 50 % of the observed variance in t_2 is attributed to signal and is assumed to be the result of spatial variability in the environmental factors governing the rainfall generation mechanisms. Thus, results of both tests indicate that Canada cannot be considered homogenous in t_2 and further delineation into sub-regions is required. For the purpose of this study, a sub-region is defined as a group of sites that are not necessarily contiguous in space.

The validity of any statistic in delineating and testing homogeneous regions should also be supported by some physical evidence. For example, a group of sites that are homogeneous and portray similar statistical characteristics may reflect similar climatic conditions. For this purpose, the *map* values can numerically describe arid and wet climates and, as such, can be used to explain some of the behavior in the variation of L-moments in space. Thus, groups of 12 to 15 stations within a small range of *map* were formed for each storm duration. Each group of sites is assumed to constitute a homo-

geneous sub-region in t_2 terms. The assumption that t_2 should be constant for each sub-region is further verified using both the S and H statistics for which 28 out of 30 sub-regions passed the test of homogeneity. Hence, the *map* is used to define climatologically homogeneous sub-regions in which the variability in t_2 is not in excess of that normally caused by random sampling.

The sub-regional values of t_2 are plotted against the mid-point of the range of *map* for each storm duration. The scatter plots of the L-coefficient of variation versus *map* reveal a definable and systematic trend across Canada for all storm durations. As shown in Figures 4.3a and 4.3b, smaller values of t_2 are associated with rain-forests and coastal areas (where the *map* is usually high), whereas larger values of t_2 are associated with arid areas such as the Prairies zone. A least squares regression of the sub-regional value of t_2 versus *map* is performed for each storm duration and the resulting power or logarithmic relationships are given in Table 4.3. The general goodness-of-fit of these relationships can be seen in Figures 4.3a and 4.3b and is further verified by the relatively small magnitudes of the standard error of estimates and high coefficients of determination in Table 4.3. These relationships allow the sub-regional values of t_2 to be expressed as continuous variables instead of conventional fixed values, and eliminate the boundary problems normally associated with the geographic region definition. Similar relationships using the method of moments have been suggested by Schaefer (1990) but only for 2, 6, and 24 hour rainfall data of Washington State, USA. Section 4.8 further shows that these relationships are useful in the proposed new procedure for estimating design storms at ungauged locations.

4.2.3 Identification of regional probability distribution

As the variance of the L-skewness and L-kurtosis are mostly due to noise, their weighted averages (with respect to sample length) are considered representative of regional parameters (Hosking and Wallis, 1993). These regional t_3 and t_4 values are computed for each storm duration and are given in Table 4.4. Each duration's pair of t_3 and t_4 are superimposed on a theoretical L-moment ratio diagram and is shown in Figure 4.4. Their values correspond closely with the line described by the GEV distribution. The Z statistic (equation 3.28) is further used to assess the fit of the GEV to the data for each storm duration. Among the five distributions tested including the GLO, GLN, GEV, P3, and GPA, Table 4.4a shows that the GEV gives the best fit at the 90 % confidence level.

As noted earlier, the GEV is the most common distribution used in the regional analysis of extreme hydrologic variables (Potter, 1987). The GEV distribution fitted by the probability weighted moments (which form the basis of L-moments) has also been shown to be relatively insensitive to violations of the distributional assumptions and to yield more accurate and less biased design floods (Lettenmaier et al., 1987).

The EV1 distribution, which is used in Canada irrespective of storm duration, is a particular case of the GEV and has a constant theoretical L-skewness of 0.1699. However, Figure 4.5 shows that the regional L-skewness

varies with the storm duration and has values greater than the lower bound of the EV2 distribution. The EV2 distribution has also been recommended for the analysis of rainfall extremes in Illinois, USA, by Huff and Neill (1959b), in Belgium by Sneyers (1978), in Finland by Uppala (1978), in Switzerland by Zeller et al. (1978), and in Ontario by Pilon et al. (1991a).

In summary, the above regional goodness-of-fit testing and L-moments analysis have shown that the current EV1 assumption in the estimation of IDF curves and equations for all storm durations in Canada is not valid. The GEV, and in particular the EV2, seems to provide a better fit to short duration rainfall extremes. The effect of misspecifying the parent distribution on the accuracy of design storm estimates is addressed by simulation experiments in section 4.4.

4.3 Proposed New Design Storm Estimation Method at Gauged Stations

The analysis presented in the previous section shows that Canada can be considered as a homogeneous region in both the L-skewness and L-kurtosis of short duration rainfall extremes as they are independent of geographical location. Furthermore, Canada has been delineated into homogeneous non-geographically based sub-regions in which the L-coefficient of variation may be considered approximately constant or can be estimated by a mathematical

model relating t_2 to *map*. These findings justify the need for a hierarchical regional rainfall frequency approach in which different statistical parameters of short duration rainfall extremes are estimated using different, but nested, subsets of data. Thus, in this study the author proposes a new hierarchical regional frequency approach for estimating design storms at any gauged site in Canada. For each storm duration, the approach consists of the following steps:

1. Select the regional value of L-skewness from Table 4.4. This is termed Level I of the hierarchy in which the third order L-moment ratio is estimated from regional information.

2. Compute the sub-regional value of the L-coefficient of variation using the measured at-site *map* and the relationships of Table 4.3. This is termed Level II of the hierarchy in which the second order L-moment ratio is estimated from sub-regional information.

3. Compute the mean of annual rainfall maxima using at site observed records. This is termed level III of the hierarchy in which the mean is estimated from at-site information.

4. Compute the sub-regional L-standard deviation that matches the L-coefficient of variation of Level II and the at-site mean of Level III.

5. Fit the GEV distribution to the estimated regional L-skewness, sub-regional L-standard deviation, and at-site mean by L-moments (equations 3.33 to 3.35).

6. Compute the design storms at required return periods using the quantile function of the GEV distribution (equation 3.31).

The above hierarchical regional GEV approach, henceforth termed the HRGEV frequency model, is summarized by the flowchart in Figure 4.6. The HRGEV model reduces uncertainties usually associated with estimating distribution parameters from short-term at-site record, especially when the data are ascribed by a three-parameter distribution as demonstrated in this study. Using Monte Carlo simulations, the following section shows that the proposed HRGEV model yields more accurate design storm estimates than the single site frequency method.

4.4 Simulation Study

4.4.1 Comparison of regional and single site models

To assess the accuracy of the proposed HRGEV rainfall frequency model in comparison to single site GEV (SGEV) analysis, a Monte Carlo experiment is conducted. In this experiment identically distributed, stationary, stochastic random variables are generated from a GEV distribution. The parent GEV has a mean of 23.4 mm, a L-coefficient of variation of 0.202, and a L-skewness of 0.227. These values are assumed arbitrarily, but are typical of average Canadian conditions for a 2-hr storm (see Figure 4.5 or Table 4.4). The

GEV is then fitted by L-moments (equations 3.33 to 3.35). The resulting population values of scale (α), location (ζ), and shape (k) parameters are 6.247, 19.177, and -0.087, respectively.

The Monte Carlo experiment consists of synthetically generating a large number of samples (10000) of size n=10, 20, 30, 50, 75, and 100 using the prescribed GEV parent distribution. Each sample is fitted to the GEV distribution by L-moments. In the SGEV model, the GEV is fitted using the actual statistics computed from each sample. However, in the HRGEV model the GEV is fitted using L-skewness and L-coefficient of variation equal to the regional population estimates of 0.227 and 0.202, respectively. The population values of the design storms are 21.5, 29.2, 34.7, 38.4, 48.2, 54.5, 61.2, and 70.7 mm for the 2, 5, 10, 20, 50, 100, 200, and 500 year return periods, respectively.

To evaluate the relative performance of both the HRGEV and SGEV models, two statistical measures are used in the simulation experiment, namely bias and root mean square error (RMSE). Bias refers to the difference between the estimated and population value of a statistic caused by random sampling. An approach is said to be biased if it yields estimates that are on average significantly larger or smaller than the population values. The precision is measured by the variance and refers to the dispersion of estimates about their mean. However, the RMSE (used in this study and referred to us a measure of accuracy) reflects the dispersion of estimates about the

population's mean and comprises both the bias and precision as defined by:

$$RMSE = \left[(Bias)^2 + (Variance)\right]^{1/2} \quad (4.1)$$

The simulation results for different return periods and sample sizes are summarized in Tables 4.5 and 4.6. The results listed in Table 4.5 confirm that the method of L-moments provide virtually unbiased estimators of the quantiles regardless of sample size. This is true for both the SGEV and HRGEV models and confirms the findings of Hosking et al. (1985b) and Pilon and Adamowski (1992).

The RMSE values in Table 4.6 reveal that while both models are in reasonably good agreement for return periods less than 10 years, the HRGEV model substantially outperforms the SGEV model for larger return periods. Figure 4.7 displays the variation of the RMSE (mm) with the return period for both frequency models when the sample size is 20 (typical of average Canadian conditions). As shown, the 100-yr design storm estimate by the HRGEV is about 1.7 times more accurate than the SGEV estimate. Figure 4.8 displays the variation of the RMSE with sample size for the 100-yr design storm. In this plot, the RMSE is presented as a percent of the design storm itself. It is seen that about three times as much data are required for the SGEV model to be as accurate as the HRGEV model.

4.4.2 Sensitivity of design storm estimates to misspecifications in the GEV shape parameter

The EV1 distribution is only a special case of the GEV distribution with a shape parameter k (equation 3.32) equal to zero and a L-skewness value of 0.1699. However, it is shown in this study (Table 4.4) that regional L-skewness values of rainfall data in Canada are larger than 0.1699 and vary with the storm duration (Figure 4.5). Therefore, a second Monte Carlo experiment was conducted to quantify the errors in estimating the T-yr design storm caused by a misspecification of the population L-skewness value and, consequently, the shape parameter 'k'.

As with the first experiment, identically distributed, stationary, stochastic random variables are generated from the same GEV population. The Monte Carlo experiment consists of synthetically generating a large number of samples (10000) with the same sample size using the prescribed GEV distribution of section 4.4.1. Each of these samples is fitted by L-moments to the EV1 frequency distribution. In each case, the scale and location parameters are computed from actual L-statistics of the sample while the shape parameter is assumed to be zero.

The results of the experiment are shown in Figure 4.9, where the RMSE is presented as a percent of design storm itself for various return periods and sample sizes. It is clear that the accuracy of design storms estimated by a single site EV1 model deteriorates rapidly as the sample size decreases.

In summary, both Monte Carlo experiments have demonstrated that while the choice between EV1 and EV2 distributions becomes more critical as the sample size decreases, the hierarchical regional GEV approach is substantially more accurate than its single site counterpart. Therefore, based on the results of this study, the author recommends that the GEV distribution, fitted by L-moments using the regional hierarchical approach developed in section 4.3, be used to estimate design storms in Canada. These findings are of particular significance in urban hydrology as the storm duration usually selected for small basins is in the order of the durations analyzed in this study.

4.5 Comparison of Regional and Single Site Frequency Models at Gauged Stations

The simulation results in section 4.4 show that the hierarchical regional frequency model yields more accurate design storm estimates than the single site approach. Also, it is demonstrated that about three times as much data are required for the single site model to provide as accurate design storm estimates as the hierarchical regional model. Thus, using an appropriate parent distribution and parameter estimation technique, the sample size is the predominant factor in determining the accuracy of a frequency model. Theoretically, the performance of both regional and single site models should converge as the at-site sample size increases when using the same parent distribution and parameters estimation technique. As regional models are based

on longer effective record lengths than single site models, their merits should be more apparent when applied at short-term record stations.

To illustrate the merits of the proposed hierarchical regional frequency approach, the performance of the HRGEV model is compared to the current single site EV1 distribution fitted by the method of moments, henceforth denoted as the SEV1 model, for samples of long and short-term record stations in Canada.

It is recognized that both the HRGEV and SEV1 models use different parent distributions and parameter estimation techniques. However, this study demonstrates, as shown in section 4.2.3, that short duration rainfall extremes are better described by the GEV distribution. Also, as noted in chapter 3, the method of L-moments is more efficient, less biased, and less sensitive to outliers in the data than the conventional method of moments.

4.5.1 Comparison at long-term record stations

A comparison of the performance of the regional HRGEV and single site SEV1 frequency models in estimating design storms is made for the seven long-term record stations listed in Table 4.7. These stations were selected to represent various climatic and hydrologic conditions across Canada. The sample length ranges from 39 to 57 years (average of 48 years) and the *map* from 345.0 to 1130.1 mm.

Comparison between the two models is made at both the 10-yr and 100-yr design storms. The 10-yr and 100-yr return periods are chosen arbitrarily, but are representative of the lower and upper range of return periods used in practical applications.

Design storms are first computed by the HRGEV model using the algorithm in Figure 4.6. For further illustration, the detailed application of the HRGEV model at the long-term record station 5023222 - Winnipeg international airport - is presented. Columns 2, 4, and 5 of Table 4.8 give the at-site mean, sub-regional L-standard deviation, and regional L-skewness for the station. For each storm duration, the regional L-skewness is selected from Table 4.4, while the sub-regional L-standard deviation is selected to match the at-site mean and the sub-regional L-coefficient of variation. The L-coefficient of variation is in turn computed using the at-site measured *map* and the regional relationships of Table 4.3. For each storm duration, the at-site mean, sub-regional L-standard deviation, and regional L-skewness are then used to fit the GEV distribution by L-moments (equations 3.33 to 3.35).

For comparison purposes, design storms at station 5023222 are also computed using the SEV1 model, in which the at-site mean and at-site standard deviation (columns 2 and 3 of Table 4.8) are used to fit the EV1 distribution by the method of moments.

The 10-yr and 100-yr return period design storms for the nine durations at station 5023222 computed by the two models are given in Table 4.9. Design storms at the remaining six long-term stations are computed by both models

in the same manner and results are displayed in Figures 4.10 to 4.16.

Table 4.9 shows that at station 5023222, with 39 years of data and a *map* of 525.5 mm, the 5-min 100-yr design storm estimated by the SEV1 is 21 % lower than that computed by the HRGEV. However, for the 10, 15, 30, and 60 minute durations design storms computed by the SEV1 are about 6 % and 13 % lower than those estimated by the HRGEV for the 10-yr and 100-yr return periods, respectively. For longer storm durations, both models are in agreement for the 10-yr return period but differ by about 6 % for the 100-yr return period.

Figures 4.10 to 4.16 show similar findings with the SEV1 consistently underestimating rainfall intensities for all storm durations at five out of the seven long-term stations analyzed. To further quantify this underestimation, Table 4.10 gives the absolute deviation between the design storms computed by the two models for the 5 and 60 minute durations as:

$$\textit{Absolute Deviation}\ (\%) \;=\; 100\,\frac{\mid R_{HRGEV} - R_{SEV1} \mid}{R_{HRGEV}} \qquad (4.2)$$

where R_{HRGEV} and R_{SEV1} are the design storms in mm/hr computed by the HRGEV and SEV1 models, respectively.

Table 4.10 shows that the deviation increases with the return period. This may be explained by the fact that statistical inference in regional models are based on longer effective record lengths than single site models. On average, differences between the two models (computed for seven sites) are 7 % and 10 % for the 10-yr and 100-yr design storms, respectively. As shown in Table

4.10, these differences reach a maximum of 21 % and 23 % for the 100-yr return period at stations 5023222 in Winnipeg and 1018610 in Victoria, respectively.

4.5.2 Comparison at short-term record stations

The proposed HRGEV model is also applied at the seven short-term record stations listed in Table 4.11 and results are compared to the SEV1 model. The sample length ranges from 10 to 16 years and the at-site *map* from 453.7 to 3322.0 mm. Design storms at each station for the 10-yr and 100-yr return periods are computed by the two models following the same procedures described in section 4.5.1 and results are presented in Figures 4.17 to 4.23.

These figures indicate that the SEV1 model underestimates rainfall intensities at all storm durations for five out of the seven stations and differences between the two models increase with the return period. The absolute deviations between design storms estimated by the two models for the 5 and 60 minute durations are listed in Table 4.12. On average, these deviations are 9 % and 16 % for the 10-yr and 100-yr design storms, respectively. However, Table 4.12 indicates that these deviations may be as high as 27 % as is the case for station 7057574 in Quebec.

Deviations between the two models at short-term record stations are relatively higher than those at long-term stations. Hence, the merits of applying the proposed HRGEV model are more apparent at short-term record sta-

tions where sampling variability can have an adverse effect on the single site frequency approach.

To summarize, a regional frequency model is developed in this study for the analysis of short duration rainfall extremes in Canada. The proposed model uses the GEV distribution fitted by L-moments using a hierarchical approach, where the L-skewness, L-standard deviation, and mean are estimated on a regional, sub-regional, and at-site basis, respectively. The simulation experiments described in section 4.4 showed that the proposed hierarchical regional GEV frequency model is more accurate than the single site frequency approach. Using real data at typical long and short-term record stations, it is demonstrated that the current single site approach using the EV1 distribution fitted by moments underestimates design storms on an average of 9 % and 16 % for the 10-yr and 100-yr return periods. It has also been shown that this underestimation may reach 27 % at some stations.

Based on the above findings, the author suggests that the developed hierarchical regional GEV frequency model be used in preference to the single site EV1 approach for IDF analyses in Canada.

4.6 Development of Regional Depth-Duration-Frequency Equations

Regional depth-duration-frequency (RDDF) equations are developed to make the estimation of design storms at ungauged locations less dependent on the availability of pluviometric data and to reduce uncertainties associated with current interpolation procedures from isoline maps (Hogg and Carr, 1985) These equations relate the t-min to the 60-min design storms at a site.

The development of the RDDF equations is achieved through the use of curve fitting procedures. At each site and for each of the 5, 10, 15, 30, 60, and 120 minute storm durations, the regional L-skewness, sub-regional L-coefficient of variation, and at-site mean are used to fit the regional GEV distribution by the L-moments following the proposed hierarchical approach of section 4.3. The 2, 5, 10, 20, 50, and 100 year return period rainfall depths at each site are then computed using the quantile function of the fitted GEV distribution (equation 3.31). A least squares regression analysis is performed on these rainfall depths for all gauged stations in the network to formulate depth-duration and depth-frequency relationships. These are in turn combined to formulate the final RDDF equations. Finally, a set of eight long-term record stations that were not originally used in the regression analyses are employed to verify the developed equations through a split sampling experiment.

4.6.1 Regional depth-duration relationships

At first, rainfall frequency data are generalized through the use of linear depth-duration formulations that relate the rainfall depths of a particular storm duration to the corresponding 60 minute base value for the same return period as follows:

$$R_t^T = a\, R_{60min}^T + b \tag{4.3}$$

where R_t^T and R_{60min}^T are the t-min T-yr and 60-min T-yr rainfall depths, respectively. These linear depth-duration relationships are found to have a definite consistency with respect to geographical location. To illustrate this, sample plots of the 30-min versus 60-min rainfall depths computed by the HRGEV frequency model at all gauge stations are provided in Figures 4.24 and 4.25 for the 10-yr and 100-yr return periods, respectively. These figures indicate that parameters 'a' and 'b', which represent the slope and intercept of the straight line passing through the plotted points, may be considered independent of geographical location.

A least squares regression of equation (4.3), using the rain gauge network HRGEV frequency data, is performed for the arbitrarily assumed return periods of 2, 5, 10, 20, 50, and 100 years and for storm durations of 5, 10, 15, and 30 minutes. Detailed results of this analysis are presented in Tables 4.13a to 4.13d. As shown in these tables, the overall goodness-of-fit of equation (4.3) to the data is verified by the high coefficients of determination and low standard error of estimates. This further indicates that more than 90 % of the spatial variability of the T-yr t-min rainfall depth (R_t^T) may be explained

by that of the T-yr 60-min (R^T_{60min}).

Tables 4.13a to 4.13d also indicate that the slope 'a' is independent of return period and has values of 0.347, 0.500, 0.625, and 0.851 for the 5, 10, 15, and 30 minute storm durations, respectively. The variation of slope with the storm duration is displayed in Figure 4.26 and may be expressed by:

$$a = 0.183\, t^{0.433} \tag{4.4}$$

in which 't' is the storm duration in minutes. The goodness-of-fit of equation (4.4) to the data is justified by a high coefficient of determination of 0.98 and a standard error of estimate of 0.07.

The intercept 'b', while varying systematically with storm duration and return period as shown in Figure 4.27, is insignificantly small and, hence, is assumed constant and equal to zero for the 5, 10, 15, and 30 minute storm durations.

The substitution of slope 'a' from equation (4.4) into equation (4.3) yields the following regional depth-duration relationship:

$$R^T_t = 0.183\, t^{0.433}\, R^T_{60min} \tag{4.5}$$

Equation (4.5) applies to any storm duration of less than 60 minutes and any return period between 2 and 100 years. Equation (4.5) supports the same hypothesis advocated in several other studies (Bell, 1969; Cao et al., 1969; Maksimov, 1964; Ferreri and Ferro, 1990) that suggests that depth-duration ratios (R^T_t / R^T_{60min}) for storms of less than 60 minutes are independent of

geographical location. Table 4.14a shows that the computed depth-duration ratios from Canadian rainfall data are in close agreement to those of the USA, Australia, Italy, and India. For comparison purposes, a least squares regression of DDRs is also performed using:

$$\frac{R_t^T}{R_{60min}^T} = \left(\frac{t}{60}\right)^s \tag{4.6}$$

which yielded a 's' value of 0.393. Table 4.14b gives the 's' values reported for other countries and Figure 4.28 shows the corresponding plots of depth-duration ratios as a function of storm duration. The difference in 's' values between countries, although small, may reflect real climatic differences and/or spatial and temporal sampling variability. The statistical significance of these differences can be tested, but this requires the knowledge of mean and standard deviation of 's' values from other studies, which are not available. Nevertheless, Figure 4.28 indicates that, at the 5 % confidence level, the difference in depth-duration ratios between Canada, USA, and Italy is not highly significant.

To further verify that the depth-duration ratios are independent of geographical location within Canada, the ratio of the 30-min to 60-min rainfall depths for the 100-yr return period is plotted against the *map* at each site. Figure 4.29 indicates that the 30-min depth-duration ratio may be considered approximately constant for all sites with a *map* less than 1200 mm. This constitutes about 90 % of the Canadian rain gauge network and is henceforth denoted as subnetwork I. The 30-min depth-duration ratios at sites with *map* larger than 1200 mm (subnetwork II) are relatively smaller but vary in

a fairly stable manner around a constant average value. Similar findings are also observed for the remaining storm durations and return periods.

To verify whether the difference between the average depth-duration ratios of the two subnetworks of rain gauges is statistically significant, their respective regression results (equation 4.3) are compared. Figure 4.30 shows the 90 % confidence limits of the computed slopes (a) at each subnetwork for various storm durations. From this figure, it may be concluded that for any storm duration less than 60 minutes the detected difference in slope of both subnetworks is not significant enough to declare the depth-duration ratios to be dependent on geographical location. However, Figure 4.30 indicates that the difference in slope between the two subnetworks becomes significant for storm durations greater than 60 minutes. For this reason, a different regional depth-duration relationship for each subnetwork is proposed for the 2-hr storm duration. Detailed regression results for the 2-hr rainfall frequency data are given in Tables 4.15a and 4.15b.

The above tables show that the slope is also independent of return period and has an average value of 1.08 for subnetwork I and 1.18 for subnetwork II. However, the intercept, while independent of the *map*, varies systematically with the return period as shown in Figure 4.27 and may be expressed by:

$$b = 1.23\ ln(T) + 1.6 \qquad (4.7)$$

Bell (1969) hypothesized that the slope 'a' and intercept 'b' are independent of the return period and geographical location and assumed a constant value (R^T_{120min}/R^T_{60min}) of 1.25 across all of the USA. Thus, based on the above

findings Bell's assumption is clearly invalid for Canada.

The substitution of both 'a' and 'b' into equation (4.3) yields the following regional depth-duration relationships for the 2-hr storm duration:

(a) For sites with map $\leq$ 1200 mm:

$$R^T_{120min} = 1.08 R^T_{60min} + [1.23\ ln(T)\ +\ 1.6] \tag{4.8}$$

(b) For sites with map > 1200 mm:

$$R^T_{120min} = 1.18 R^T_{60min} + [1.23\ ln(T)\ +\ 1.6] \tag{4.9}$$

The same depth-duration relationships do not hold for storms with durations greater than 120 minutes. The linear regression of the t-min rainfall against the 60-min rainfall for the same return period results in deteriorating coefficients of determination for durations of 6, 12, and 24 hours. This suggests that the T-yr 60-min rainfall depth (R^T_{60min}) is unable to explain the spatial variability of any T-yr t-min rainfall depths (R^T_t) for durations greater than 2 hours.

In summary, ratios of the t-min to the 60-min rainfall depths for any storm duration less than 60 minutes across Canada are found to be independent of both return period and geographical location. However, the ratio of the 120-min to 60-min rainfall depths is found to depend on both the return period and geographical location as indexed by the *map*. This high degree of consistency in short duration rainfall frequency data implies that local convective

rainfall cells have similar physical properties irrespective of geographical location. While this hypothesis has never been verified for Canadian conditions, it has been advocated in other studies (Hershfield, 1961, 1962; Bell, 1969; Ferreri and Ferro 1990). The proposed regional depth-duration relationships are key to the development of the final depth-duration-frequency equations detailed in section 4.6.3.

4.6.2 Regional depth-frequency relationships

Rainfall frequency data are also generalized through the use of depth-frequency ratios (DFRs). DFRs are defined as the ratios of any particular T-yr rainfall depth to the corresponding value of an arbitrarily chosen 10-yr return period for the same storm duration.

In Canada, DFRs depend on the geographical location as indexed by the at-site *map* value. Figure 4.31 shows how the ratio of the 100-yr to 10-yr rainfall depths for the 30 minute storm duration varies with the *map* across Canada. Sites in the coastal Maritimes region and the mountainous rain-forest environment of British Columbia have lower values of DFRs while those in the low lying coastal areas of British Columbia and the Prairies zone have higher values of DFRs. Similar findings have also been observed for DFRs of 5, 10, 15, 60, and 120 minute storm durations and other return periods.

At first glance, it may appear that the hierarchical regional GEV ap-

proach adopted for the computation of the at-site rainfall frequency data could be responsible for the correlation between DFR and *map* values. In the HRGEV model, the sub-regional L-coefficients of variation used to fit the GEV distribution to the at-site rainfall data are computed using the regional relationships of Table 4.3, where the at-site *map* is the independent variable. However, Figure 4.32 shows that this correlation is apparent even when the DFRs are computed by the single site EV1 distribution fitted by the method of moments. Furthermore, it is interesting to note by comparing Figures 4.31 and 4.32 that the sampling variability in the single site EV1 approach results in DFRs with higher random noise than in the hierarchical regional GEV approach. This reflects the advantage of using regional rainfall frequency data in the development of IDF relationships. In previous studies, IDF relationships were developed using single site rainfall frequency data exclusively.

The correlation between DFRs and *map* values is better described by the following logarithmic relationship:

$$\frac{R_t^T}{R_t^{10yr}} = c\, ln(map) + d \qquad (4.10)$$

where R_t^T and R_t^{10yr} are the T-yr t-min and 10-yr t-min rainfall depths, respectively. A least squares regression of equation (4.10), using the HRGEV frequency data at all network stations, is performed for arbitrarily assumed return periods of 2, 5, 20, 50, and 100 years and for storm durations of 5, 10, 15, 30, 60, and 120 minutes. Detailed results of this analysis are presented in Tables 4.16a to 4.16f. As shown in these tables, the goodness-of-fit of

equation (4.10) to the data is verified by the high coefficients of determination and low standard error of estimates. This implies that the spatial variability of the rainfall depth for any return period between the 2 and 100 years may be explained by the spatial variability of the 10-yr rainfall depth of the same storm duration and the *map* value.

Tables 4.16a to 4.16f show also that the slope 'c' may be considered independent of storm duration and has average values of 0.061, 0.026, -0.026, -0.062, and -0.090 for the 2, 5, 20, 50, and 100 year return periods, respectively. Tables 4.16a to 4.16f further indicate that the intercept 'd' may also be considered independent of storm duration, having average values of 0.185, 0.666, 1.310, 1.785, and 2.139 for the 2, 5, 20, 50, and 100 year return periods, respectively. The variability of the slope and intercept with the return period is displayed in Figures 4.33 and 4.34 and may be expressed by:

$$c = -0.038\ ln(T) + 0.088 \tag{4.11}$$

$$d = 0.495\ ln(T) - 0.152 \tag{4.12}$$

Estimates of 'c' and 'd' using these equations have average standard errors of 2 % and 1 %, respectively. The substitution of 'c' and 'd' from equations (4.11) and (4.12) into equation (4.10) yields the following regional depth-frequency relationship:

$$R_t^T = [(-0.038ln(T) + 0.088)ln(map) + (0.495ln(T) - 0.152)]R_t^{10yr} \tag{4.13}$$

Equation (4.13) is applicable for any return period from 2 to 100 years and any storm duration from 5 to 120 minutes. Hershfield (1961) and Bell

(1969) hypothesized that depth-frequency relationships are independent of geographical location and suggested that their equations (2.8 and 2.9) were applicable in many parts of the world such as the USA, Australia, South Africa, Hawaii, Alaska, and Puerto Rico. However, the results of this study demonstrate that their hypothesis can not be accepted and that depth-frequency relationships are indeed dependent on geographical location as indexed by the at-site *map* value. The proposed regional depth-frequency relationship in equation (4.13) is a key factor in the development of the final depth-duration-frequency equations detailed in the following section.

4.6.3 Regional depth-duration-frequency equations

The depth-duration and depth-frequency relationships derived in section 4.6.1 and 4.6.2 are combined to form a generalized set of regional depth-duration-frequency (RDDF) equations.

First, the depth-frequency equation (4.13) is applied to the 60 minute reference storm duration which leads to:

$$R^{T}_{60min} = [(-0.038ln(T) + 0.088)ln(map) + (0.495ln(T) - 0.152)]R^{10yr}_{60min} \tag{4.14}$$

Then, the substitution of R^{T}_{60min} from equation (4.14) into the depth-duration relationship given by equations (4.5), (4.8), and (4.9) gives the generalized RDDF equations:

(1) For storms of durations less than 60 minutes:

$$R_t^T = [(-0.038ln(T)+0.088)ln(map)+(0.495ln(T)-0.152)][0.183t^{0.433}]R_{60min}^{10yr} \tag{4.15}$$

(2) For the 120 minute storm:

(a) For sites with map $\leq$ 1200 mm:

$$\begin{aligned} R_{120min}^T &= 1.08[(-0.038ln(T)+0.088)ln(map)+(0.495ln(T)-0.152)]R_{60min}^{10yr} \\ &\quad + [1.23ln(T)+1.60] \end{aligned} \tag{4.16}$$

(b) For sites with map > 1200 mm:

$$\begin{aligned} R_{120min}^T &= 1.18[(-0.038ln(T)+0.088)ln(map)+(0.495ln(T)-0.152)]R_{60min}^{10yr} \\ &\quad + [1.23ln(T)+1.60] \end{aligned} \tag{4.17}$$

Knowing the 10-yr 60-min rainfall depth at any location in Canada, any rainfall depth with a storm duration in the range of 5 to 120 minutes and a return period of 2 to 100 years can be computed using equations (4.15) to (4.17). It is important to point out that because of their highly empirical nature, these equations should not be used beyond the ranges of values from which they are developed.

In summary, a set of RDDF equations for use in Canada are developed in this study. The validity of these equations is verified in the next section by a

split sampling experiment using representative long-term record stations from different climatic zones. It is also shown that the proposed RDDF equations yield more accurate design storms than the current single site AES equations.

4.7 Verification of Proposed Regional Equations

The validity of the developed RDDF equations is verified by their ability to reproduce the HRGEV frequency data. In Figures 4.35 and 4.36 the R_i^T computed at each site using equation (4.15) is compared with its corresponding 'observed' value estimated by the HRGEV frequency model for the 30-min 10-yr and 100-yr rainfall depths, respectively. These figures show that the developed RDDF equations are systematically biased yet give results within a maximum error range of ±15 %, for 90 % of the time. Similar findings were also observed for the remaining storm durations and return periods. The ±15 % error range is considered satisfactory (Bell, 1969) in comparison to the errors caused by sampling variability in single site frequency analysis or to the uncertainties associated with interpolation procedures from isoline maps. In other studies, published depth-duration-frequency equations gave results with higher ranges of error in the order of ±20 % for Italy (Pagliara and Viti, 1993) and ±18 %, ±25 %, and ±30 % for India, USA, and Sri Lanka, respectively (Kothyari and Garde, 1992).

To further assess the relative performance of the developed equations for different climatic zones in Canada, the error (E) at any site is computed by:

$$E(\%) = 100\left[\frac{(R_t^T)_{observed} - (R_t^T)_{computed}}{(R_t^T)_{observed}}\right] \tag{4.18}$$

where 'observed' refers to rainfall estimates by the HRGEV frequency model and 'computed' denotes those estimated by RDDF equations. Figures 4.37a and 4.37b show that the error (E) of the RDDF equations varies with the at-site *map* for the 10-yr and 100-yr 30-min rainfall depths, respectively. At 90 % of the sites where the *map* is less than 1200 mm, there seems to be no apparent correlation between the error and *map* and the error varies stably and tightly around an average value of 5 %.

However, at the remaining 10 % of the sites where the *map* is greater than 1200 mm, the RDDF equations result in relatively higher rainfall estimates than the HRGEV frequency model with the error tending to increase with the *map* value. Figures 4.37a and 4.37b further indicate that these sites are exclusively located in the coastal mountainous regions of British Columbia and the Maritimes. This may be explained by the fact that rainfall measurements in mountainous areas are often underestimated as a result of wind effects upon rain gauges (Warnick, 1956; Neff, 1977; Jones, 1990). This results in rainfall estimates based on at-site records that are lower than the actual values. To compensate for this underestimation in current interpolation procedure from isoline maps, Hogg and Carr (1985) suggested safety factors ranging from 1.5 to 2.0 be applied to rainfall intensities in mountainous areas. The use of the proposed RDDF equations can compensate for this

underestimation by providing greater estimates closer to the actual values since 90 % of the sites used for developing these equations are located in relatively flat areas where rain gauges are often sheltered and subject to less wind effect.

The increase of error with the *map* value may also be explained by the fact that sites in mountainous areas often have relatively shorter record lengths and a large component of error can be attributed to sampling variability. Figures 4.38a and 4.38b show how the error varies with the sample size for the 10-yr and 100-yr 30-min rainfall depths, respectively. Both figures indicate that, in general, the error decreases as the at-site record length increases and sites in the coastal regions of Canada present no exception. It is interesting to note by comparing Figures 4.37 and 4.38 that sites with the largest *map* (i.e., located at higher altitudes) and the largest error values in British Columbia and the Maritimes correspond to those sites with the lowest record lengths. This consistent decrease of error with the increase in sample size, which has also been observed for the other storm durations and return periods, supports the correctness of the proposed RDDF equations.

To further validate the developed RDDF equations, a split sampling experiment in space is used. For this purpose, the data at eight long-term record stations not originally used for establishing the equations are employed. These eight stations, listed in Table 4.7, represent typical meteorological localities of the Pacific West (British Columbia), Rocky Mountains (Alberta), Prairies (Saskatchewan and Manitoba), Centraleast (Ontario), Northeast (Quebec), and Atlantic (Maritimes) areas in Canada. The record length ranges from 34 to 57 years (average of 46 years) and the at-site *map* from 345.0 to 1130.1 mm.

Figures 4.39 to 4.46 show the 10-yr and 100-yr IDF curves computed by the HRGEV frequency model and the proposed RDDF equations for one long-term record station in each of Quebec, Ontario, Alberta, Manitoba, Saskatchewan, and the Maritimes and two long-term stations in British Columbia. From these figures, it can be seen that the RDDF equations developed in this study satisfactorily reproduce the HRGEV frequency model. The RDDF equations result in slightly higher rainfall estimates at station 1018610 in British Columbia and 8401700 in the Maritimes.

For comparative purposes, the 10-yr and 100-yr IDF curves computed by the current single site SEV1 frequency model and AES equation (2.19) are plotted at each of the eight long-term sites in Figures 4.47 to 4.54. A cross-comparison between Figures 4.39 to 4.46 and Figures 4.47 to 4.54 shows that, contrary to the almost perfect fit between the HRGEV frequency model and the RDDF equations in at least six of the eight long-term stations, the AES

equation (2.19) is not able to reproduce the SEV1 frequency data used in its own development.

The 10-yr and 100-yr design storms estimated by the HRGEV and SEV1 frequency models and the RDDF and AES equations at each of the long-term record stations are also given in Tables 4.17 to 4.24. At the long-term stations located in Ontario, Quebec, Manitoba, and Saskatchewan, Tables 4.17 to 4.20 show that the absolute average deviation between the AES equation and SEV1 model (based on the 6 storm durations) is twice as high as that between the RDDF equations and the HRGEV model. This may be explained by the fact that the AES equations are developed for storm durations of up to 24 hours while the RDDF equations are developed for only storm durations less than 2 hours. Thus, a better fit to the observed data is obtained in this study by separating short duration ($t \leq 2$ hr) from long duration ($t > 2$ hr) rainfall events since short duration convective storms are physically based on different meteorological factors from longer duration frontal storms. As indicated earlier, several other studies (Hershfield, 1961, 1962; Bell, 1969; Penta et al., 1972; Ferreri and Ferro, 1990 and 1992; Ferro, 1993) have also recognized that the two types of storms follow different IDF relationships.

Tables 4.21 and 4.22 indicate that the fit of the AES equation to the SEV1 frequency model is as good as that of the RDDF equations to the HRGEV model at station 3012208 in Alberta and 1108447 in British Columbia. Furthermore, Tables 4.23 and 4.24 show that while the AES equation provides a better fit to the SEV1 model 8401700 at station 1018610 in British Columbia

and 8401700 in the Maritimes, it underestimates design storms by as much as 39 % and 24 %, respectively.

To summarize, the RDDF equations developed in this thesis are shown to be more accurate than other regional equations developed in Italy, India, USA, and Sri Lanka. Errors of the developed RDDF equations have a significant sampling variability component that decreases rapidly as the sample size increases. The split sampling verification technique using real data at long-term record stations from different hydrologic zones in Canada, demonstrates that the developed RDDF equations more satisfactorily reproduce the at-site rainfall frequency data than the current single site AES equations. Furthermore, it is found that the proposed RDDF equations yield rainfall intensities greater than those estimated from at-site records in mountainous areas. This may be considered as compensation for the expected underestimation of rainfall measurements due to wind effect upon rain gauges at higher altitudes.

The developed RDDF equations are also superior to the single site AES equations since they allow the transfer of rainfall frequency information from gauged to ungauged sites. In the next two sections, it is shown how the proposed RDDF equations make the estimation of design storms at ungauged locations less dependent on the availability of rainfall data and how they reduce uncertainties associated with current procedure involving interpolation from isoline maps.

4.8 Proposed New Design Storm Estimation Method at Ungauged Locations

The developed HRGEV frequency model and RDDF equations are regional in concept and, hence, they allow the transfer of rainfall information from gauged to ungauged sites. In this study, a new and improved method for estimating design storms at ungauged sites in Canada is proposed by combining the HRGEV model and RDDF equations.

The procedure for estimating the 1, 6, 12, and 24 hour design storms at ungauged sites is based on the developed HRGEV frequency model and consists of the following steps:

1. Select the regional value of L-skewness for the appropriate storm duration from Table 4.4.
2. Interpolate the values of at-site *map* and the at-site mean of annual rainfall maxima from existing maps.
3. Compute the sub-regional value of the L-coefficient of variation using the *map* value of step 2 and the relationships given in Table 4.3.
4. Compute the sub-regional L-standard deviation that matches the L-coefficient of variation of step 3 and the mean value from step 2.
5. Fit the GEV distribution to the estimated regional L-skewness, sub-

regional L-standard deviation, and at-site mean by L-moments (equations 3.33 to 3.35).

6. Compute the design storms at the required return periods using the quantile function of the GEV distribution (equation 3.31).

On the other hand, the procedure for estimating the 5, 10, 15, 30, and 120 minute design storms is based on the developed RDDF equations and consists of the following steps:

1. Compute the 10-yr 60-min design storm following the procedure described above.
2. Interpolate the at-site *map* from existing maps.
3. Compute the design storms at the required return periods using the 10-yr 60-min design storm of step 1, the at-site *map* from step 2, and the developed RDDF equations (4.15 to 4.17).

In the method proposed above, the relationships in Table 4.3 that relate the sub-regional L-coefficient of variation to the at-site *map* eliminate the need for isoline maps of the standard deviation of annual rainfall maxima for the 1, 6, 12, and 24 hour storms. In addition, the use of the RDDF equations eliminates the need for isoline maps of both the mean and standard deviation of the 5, 10, 15, 30, and 120 minute storms. As such, the proposed design storm estimation method for ungauged locations significantly reduces uncertainties usually associated with the current interpolation procedure.

4.9 Comparison of the Proposed Estimation Method with the Current Interpolation Procedure

A comparison between the proposed method described in section 4.8 and the interpolation procedure from rainfall frequency atlas maps of Hogg and Carr (1985) is made at the seven ungauged sites listed in Table 4.25.

The 10 and 100 year IDF curves computed by the two procedures for each of the seven ungauged sites are given in Figures 4.55 to 4.61. These figures indicate that the interpolation procedure from existing rainfall frequency maps underestimates the design storms at three locations and overestimates the design storms at the other four sites. There is no consistency in the overall performance since the interpolation from rainfall frequency maps involves a great deal of subjectivity, especially at remote locations.

The 10-yr and 100-yr design storm values computed by the two procedures are also given in Tables 4.26 to 4.32. Absolute deviations between the two procedures are also reported in these tables. As shown, the deviations tend to increase with return period. While on average, the absolute deviation amounts to 9 % and 12 % for the 10-yr and 100-yr design storms, differences between the two procedures are relatively higher for short duration storms. As shown in Tables 4.28 through 4.32, the interpolation procedure underestimates design storms by as much as 20 %, 25 %, and 37 % at the ungauged

sites in Alberta, Ontario, and British Columbia, while overestimating design storms by as much as 35 %, 20 %, 19 %, and 24 % at the ungauged sites in Quebec, Manitoba, Saskatchewan, and the Maritimes, respectively. These differences may have a significant impact on estimated water quantity and quality characteristics in urban drainage design and consequently on the economical and environmental outcome of water management.

It is the author's opinion that there are severe limitations to using the current interpolation procedure which is based on single site frequency approach. However, the method in section 4.8 is based on the developed regional HRGEV frequency model and RDDF equations which are both shown to provide more accurate design storm estimates than the single site EV1 and AES equations. As such, the proposed method represents a viable alternative for the estimation of design storms at ungauged locations that is recommended in preference to the current interpolation procedure.

Chapter 5

Conclusions and Recommendations

5.1 Summary of the Study

The Canadian practice of calculating design storms using the single site frequency approach and intensity-duration-frequency (IDF) relationships is evaluated in this thesis. As demonstrated, there are several weaknesses in the current practice especially for short term record stations and ungauged locations. Therefore, a new and improved regional approach is proposed.

The L-moments which are less biased, more efficient, and less sensitive to outliers in the data than the conventional moments are used in the regional

frequency analysis of short duration rainfall extremes in Canada. The three stages of the analysis are the delineation of homogeneous regions, the identification of regional parent distribution, and the estimation of distribution's parameters.

The simulations and statistical testing of homogeneity conducted show that the spatial variability of the L-skewness and L-kurtosis for storm durations of 5, 10, 15, 30, 60 minutes and 2, 6, 12, and 24 hours may be attributed to random sampling. This implies that the spatial variability of the environmental factors governing the rainfall generation mechanisms have an insignificant effect on the L-skewness and L-kurtosis. Therefore, Canada may be considered as a single homogeneous region in both L-skewness and L-kurtosis. However, the spatial variability of the L-coefficient of variation of annual rainfall extremes for the nine storm durations analyzed is found to be in excess of that normally caused by random sampling. Environmental factors are responsible for approximately 50 % of the spatial variability of the L-coefficient of variation and the remaining 50 % is attributed to noise caused by random sampling.

Climatologically homogeneous sub-regions within Canada are defined in terms of the *map*, rather than geographic location. This eliminates the boundary problems usually associated with the classical geographic definition of homogeneous sub-regions. The sub-regional values of L-coefficient of variation across Canada are found to vary systematically with the *map*. Logarithmic and power functions relating the L-coefficient of variation to the

map are developed for each storm duration. These functions allow the sub-regional L-coefficients of variation to be expressed as continuous variables rather than the conventional fixed values. Also, these functions are useful in the proposed estimation procedures of IDF data at ungauged locations as they eliminate the need for interpolating for the standard deviation from existing rainfall frequency maps.

Theoretical L-moment ratio diagrams and regional goodness-of-fit testing revealed that annual rainfall extremes are better described by the GEV family of distributions. The observed regional L-skewness of rainfall extremes is found to vary systematically with the storm duration, having values that correspond to the EV2 distribution. Hence, the current assumption of the EV1 distribution with a constant theoretical L-skewness of 0.1699 irrespective of storm duration is generally not valid.

A new hierarchical approach is developed for fitting the identified regional GEV distribution by L-moments in which the L-skewness, L-coefficient of variation, and mean are estimated based on a regional, sub-regional, and at-site basis, respectively. Simulation experiments have shown that, while the choice between EV1 and EV2 is not critical for the range of observed regional L-skewness values, the hierarchical regional GEV (HRGEV) frequency model is substantially more accurate than its single site counterpart. The application of the developed HRGEV model at sample rain gauge stations covering a wide range of climatic conditions in Canada for the 10-yr and 100-yr return periods produced design storm estimates on average 9 % and

16 % higher than those computed by current single site EV1 distribution fitted by moments. However, it was noted that these differences may be as high as 27 % at some stations. Therefore, based on these findings the author recommends that the GEV distribution fitted by L-moments following the hierarchical regional approach be used to estimate design storms at gauged stations in Canada in preference to the current single site EV1 frequency method.

The design storms estimated by the developed HRGEV frequency model are used to assess the spatial variability of depth-duration and depth-frequency ratios across Canada. The depth-duration ratios for storm durations less than 60 minutes are found to be independent of return period and geographical location. However, the ratio of the 120-min to the 60-min rainfall depths is found to depend on both the return period and geographical location as indexed by the at-site *map* value. This is consistent with other rainfall studies in the USA, Italy, Australia, India, and Russia. These findings, while never verified for Canadian conditions, support the hypothesis advocated by several authors that suggests convective rainfall mechanisms responsible for high-intensity short-duration rainfalls have common properties in many parts of the world.

The depth-frequency ratios are found to vary systematically with the return period and geographical location. Sites in the coastal Maritimes region and mountainous rain-forest environment of British Columbia are found to have lower values of depth-frequency ratios, while those in the low-lying

coastal areas of British Columbia and the Prairies zone have higher values. The hypothesis of geographically independent depth-frequency ratios adopted in previous studies is clearly incorrect. However, the reason for this hypothesis may be explained by the uncertainties introduced by using the single site EV1 frequency approach to compute these ratios.

For the first time in Canada, the generalized expressions of depth-duration and depth-frequency ratios are combined to formulate a set of regional depth-duration-frequency (RDDF) equations that relate the frequency data of the 5, 10, 15, 30, and 120 minute storms to the 60 minute storm frequency data. As shown, the proposed RDDF equations are found to be more accurate than other regional equations developed in Italy, India, USA, and Sri Lanka. Errors of the proposed RDDF equations are shown to have a significant sampling variability component that decreases rapidly as the record length increases. This is particularly true in mountainous areas, where rain gauges installed at high elevations generally have relatively shorter record lengths. A split sampling verification technique has demonstrated that the proposed RDDF equations better reproduce rainfall frequency data at long-term record stations than the single site AES equations. The main advantage of the developed RDDF equations is that they allow the transfer of rainfall information from gauged to ungauged sites. In practice, the adoption of these regional equations will reduce the work involved in dissecting records, extrapolating to long return periods, and efficiently presenting the data to potential users.

Finally, a new design storm estimation method that uses the HRGEV frequency model and the RDDF equations is proposed for ungauged locations. This method is found to significantly reduce the uncertainties associated with current interpolation procedures by eliminating the need for isoline maps. The application of the proposed method at sample ungauged locations from different climatic zones in Canada has produced design storms that differ from those estimated by the interpolation procedure by as much as 37 %. Since these differences may have a significant impact on the economical and environmental outcome of urban water management, the proposed method represents a viable and attractive alternative to using the current Canadian rainfall frequency atlas.

5.2 Major Conclusions

Several conclusions having a significant implication on the current Canadian practice of computing design storms are obtained from this study.

1. Short duration rainfall extremes are best described by the generalized extreme value family of distributions. The observed regional values of L-skewness for the analyzed durations lie above the lower bound of the extreme value type II and are dependent on the duration of the storm. Therefore, the extreme value type I distribution typically used in the frequency analysis of rainfall data is not generally valid.

2. The proposed hierarchical approach for fitting the identified regional extreme value distribution by the L-moments technique produces more accurate design storm estimates than the single site frequency method, especially at short-term record stations. Three times as much data are required for the single site frequency method to produce the same accuracy as the hierarchical regional frequency approach.

3. The regional depth-duration-frequency equations developed in this study are more accurate than other previously proposed regional relationships for Italy, USA, India, and Sri Lanka. These equations reproduce the long-term at-site rainfall frequency data better than the current single site AES equations. Also, they are superior to the single site AES equations since they allow the transfer of rainfall frequency information from gauged to ungauged sites.

4. The proposed regional method makes the estimation of design storms at ungauged locations less dependent on the availability of pluviometric data and reduces the uncertainties associated with current interpolation procedures from isoline maps.

5.3 Recommendations

1. In light of the findings of this study, the author recommends that the Rainfall Frequency Atlas of Canada be updated. The new version of the atlas should be composed of: (i) contour maps of the mean annual

rainfall of the 60 minute and 6, 12, and 24 hour storms only, (ii) a contour map of the *map* covering all of Canada, and (iii) the proposed regional depth-duration-frequency equations.

2. The errors involved in using these contour maps should also be quantified. This will allow a standard error of estimate to be allocated to IDF data computed at ungauged locations. Nonparametric resampling or bootstrapping, as suggested by Diaconis and Efron (1983), may be used for this purpose.

3. Regional analysis is conceptually based on the incorporation of spatial randomness to complement the limited time sampling record. Therefore, regional statistical inference is based on an effectively independent record length greater than the record length at any individual station. This effective independent record length should be determined to set-up an upper limit on the extrapolation to higher return period when using the proposed regional model. A possible approach for this purpose has been articulated by Schaefer (1990) for his proposed regional rainfall frequency model in the State of Washington, USA.

4. In this study, the spatial variability of the L-coefficient of variation was shown to have a much greater effect on design storm estimates than that of both shape indices - L-skewness and L-kurtosis. This leads to questions about the optimum number of gauges and lengths of record required to provide regionalized estimates that meet minimum accuracy criteria and budgetary constraints. The space-time trade-off in rain-

gauge network design in Canada has not been adequately studied and should be examined in detail so as to improve regional data collection approaches for maximizing the information content of regional models.

5. Attempts should be made to devise regional equations that estimate the 6, 12, and 24 hour rainfall intensities at ungauged locations using other available data, such as the mean annual precipitation, the mean annual number of days with rain, the mean annual number of thunderstorm days, etc. A summary of these equations derived for other countries is provided in WMO (1983). The justified adoption of such equations for application in Canada would further reduce interpolation errors from contour maps.

6. The findings of this thesis support the hypothesis advocated in other studies that suggests short duration convective rainfall cells have common properties irrespective of geographical location. To verify the universality of the proposed regional depth-duration-frequency equations data measured at long-term record stations from other parts of the world should be used.

Chapter 6

Bibliography

[1] Acreman, M. C. (1987), *Regional Flood Frequency Analysis in the United Kingdom, Recent Research, New Ideas*, Institute of Hydrology, Wallingford, United Kingdom.

[2] Acreman, M. C. and G. D. Sinclair (1986), *Regional Flood Frequency Analysis from Basin Characteristics in Scotland,* Journal of Hydrology, 84, 365-380.

[3] Adamowski, K. (1985), *Nonparametric Kernel Estimation of Flood Frequencies,* Water Resources Research, 21(11), 1585-1590.

[4] Adamowski, K., Y. Alila, and P. J. Pilon (1992), *Hierarchical Approach in Homogeneous Region Delineation of Extreme Rainfall Events in Canada*, EOS Transaction, American Geophysical Union, 73(14), Spring Meeting Supplement, 107 (Abstract).

[5] Adamson, P. T. and W. Zucchini (1983), *On the Application of a Censored Log-Normal Distribution to Partial Duration Series of Storms*,

Technical Report, Branch of Scientific Services, Department of Environment Affairs, Pretoria, South Africa.

[6] Akaike, H. (1974), *A New Look at the Statistical Model Identification*, IEEE Transactions on Automatic Control, AC-19(6), 716-721.

[7] Alexander, G. N., A. Karoly, and A. B. Sust (1969), *Equivalent Distributions with Application to Rainfall as an Upper Bound to Flood Distributions*, Journal of Hydrology, 9(3), 322-344 and 9(4), 345-373.

[8] Alila, Y. and K. Adamowski (1992), *Comprehensive Analysis and Interpretation of Extreme Flood Data and Regionalization of Hydrologic Parameters in the Nelson - Saskatchewan River Basin*, A Report Prepared for Environment Canada, Conservation and Protection, Inland Waters Directorate, Water Resources Branch, Manitoba and Northwestern District, Winnipeg, Manitoba.

[9] Alila, Y., K. Adamowski, and P. J. Pilon (1992a), *Regional Homogeneity Testing of Low-Flows Using L-Moments*, Proceedings of the 12th Conference on Probability and Statistics in the Atmospheric Sciences, American Meteorological Society, June 22-26, Toronto, Ontario, Canada, 242-246.

[10] Alila, Y., P. J. Pilon, and K. Adamowski (1992b), *An Evaluation of Rainfall Frequency Data for Canada Using L-Moments*, Proceedings of the 12th Conference on Probability and Statistics in the Atmospheric Sciences, American Meteorological Society, June 22-26, Toronto, Ontario, Canada, 237-241.

[11] Angel, J. R. and F. A. Huff (1992), *Comparing Three Methods for Fitting Extreme Rainfall Distributions: L-Moments, Maximum Likelihood, and Graphical Fit*, Proceedings of the 12th Conference on Probability and Statistics in the Atmospheric Sciences, American Meteorological Society, June 22-26, Toronto, Ontario, Canada, 255-260.

[12] Aron, G., D. J. Wall, E. L. White, and C. N. Dunn (1987), *Regional Rainfall Intensity - Duration - Frequency Curves for Pennsylvania*, Water Resources Research, 23(3), 479-970.

[13] Beard, L. R. and U. Lall (1982), *Estimation of Pearson Type III Moments*, Water Resources Research, 12(2), 1563-1569.

[14] Bell, F. C. (1969), *Generalized Rainfall - Duration - Frequency Relationships*, Journal of the Hydraulics Division, American Society of Civil Engineers, 95(1), 331-327.

[15] Benson, M. A. (1962), *Evolution of Methods for Evaluating the Occurrence of Floods*, U.S. Geological Survey Water Supply Paper 1550-A.

[16] Bobee, B. (1975), *The Log-Pearson Type III Distribution and its Application in Hydrology*, Water Resources Research, 11(5), 681-689.

[17] Bobee, B. and R. Robitaille (1975), *Correction of Bias in the Estimation of the Coefficient of Skewness*, Water Resources Research, 11(6), 851-854.

[18] Bobee, B. and R. Robitaille (1977), *The Use of the Pearson Type III and the Log-Pearson Type III Distributions Revisited,* Water Resources Research, 13(2), 427-443.

[19] Bodo, B. and T. E. Unny (1976), *Model Uncertainty in Flood Frequency Analysis and Frequency - Based Design*, Water Resources Research, 12(6), 1109-1117.

[20] Boes, D. C., J. H. Heo, and J. D. Salas (1989), *Regional Flood Quantile Estimation for Weibull Model,* Water Resources Research, 25(5), 979-990.

[21] Bradsley, W. E. (1988), *Comment on 'Nonparametric Kernel Estimation of Flood Frequencies' by Adamowski K.*, Water Resources Research, 24(6), 890.

[22] Burn, D. B. (1990), *An Appraisal of the 'Region of Influence' Approach to Flood Frequency Analysis,* Hydrologic Sciences, 35(2), 149-165.

[23] Cao, C., G. Pazzaglia, and P. V. Puddu (1969), *Determinazione Statistica delle Curve di Possibilita Pluviometrica, Applicazione alle Piogge di Durata Inferiori alle 24 Ore in Sardegna*, Proceedings National Congress on l'Idrologia e la Sistemazione dei Piccoli Bacini, Associatone Idrotecnica Italina, Roma, Italy, 293-315 (in Italian).

[24] Cavadias, G. S. (1989), *Regional Flood Estimation by Canonical Correlation,* Proceeding of the Annual Conference of the Canadian Society for Civil Engineers, June 8-10, St. John's, Newfoundland, Canada, 212-231.

[25] Chen, C. L. (1983), *Rainfall Intensity - Duration - Frequency Formulas*, Journal of the Hydraulics Division, American Society of Civil Engineers, 109(12), 1603-1621.

[26] Chong, S. and S. M. Moore (1983), *Flood Frequency Analysis for Small Watersheds in Southern Illinois*, Water Resources Bulletin, 19(2), 227-282.

[27] Chowdhury, J. U., J. R. Stedinger, and L. Lu (1991), *Goodness-of-fit Tests for Regional Generalized Extreme Value Flood Distributions*, Water Resources Research, 27(7), 1765-1776.

[28] Cole, G. (1966), *An Application of the Regional Analysis of Flood Flows*, Symposium on River Flood Hydrology - Session B 39-57, Institutions of Civil Engineers, London.

[29] Cong S., Y. Li, J.L. Vogel, and J.C. Schaake (1993), *Identification of the Underlying Distribution Form of Precipitation by Using Regional Data*, Water Resources Research, 29(4), 1103-1111.

[30] Dalrymple, T. (1960), *Flood Frequency Analysis*, U.S. Geological Survey Water Supply, Paper 1543-A.

[31] Diaconis, P. and B. Efron (1983), *Computer-Intensive Methods in Statistics*, Scientific American, 248(5), 116-130.

[32] Farmer, E. E. and J. E. Fletcher (1972), *Rainfall Intensity - Duration - Frequency Relations for the Kasatch Mountains of Northern Utah*, Water Resources Research, 8(1), 266-271.

[33] Ferreri, G. B. and V. Ferro (1990), *Short Duration Rainfalls in Sicily*, Journal of the Hydraulics Division, American Society of Civil Engineers, 116(3), 430-435.

[34] Ferreri, G. B. and V. Ferro (1992), *Closure to 'Short Duration Rainfalls in Sicily'*, Journal of the Hydraulics Division, American Society of Civil Engineers, 118(1), 109-111.

[35] Ferro, V. (1993), *Comment on 'Rainfall Intensity-Duration-Frequency Formula for India' by Kothyari, U. C. and R. J. Garde*, Journal of the Hydraulics Division, American Society of Civil Engineers, 119(8), 960-962.

[36] Fisher, R. A. (1922), *On the Mathematical Foundations of Theoretical Statistics,* Philosophical Transactions of the Royal Society of London, Series A, 222, 309-368.

[37] Fisher, R. A. (1941), *Statistical Methods for Research Workers*, 8th Edition, Oliver and Boyd, London.

[38] Fisher, R. A. and L. H. C. Tippett (1928), *Limiting Forms of the Frequency Distribution of the Largest or Smallest Member of a Sample,* Proceedings Cambridge Philosophy Society, 24, 180-190.

[39] Fiorentino, M., S. Gabriele, F. Rossi, and P. Versace (1987), *Hierarchical Approach for Regional Flood Frequency Analysis,* in Regional Flood Frequency Analysis, Edited by V. P. Singh, D. Reidel, Norwell, Mass., 35-49.

[40] Frederick, R. H., V. A. Meyers, and E. P. Auciello (1977), *Five- to 60-Minute Precipitation Frequency for Eastern and Central United States*, NOAA Tech. Memo, NWS Hydro-35, National Oceanic and Atmospheric Administration, National Weather Service, Office of Hydrology, Silver Spring, Madison.

[41] Gabriele, S. and N. Arnell (1991), *A Hierarchical Approach to Regional Flood Frequency Analysis,* Water Resources Research, 27(6), 1281-1289.

[42] Gingras, D., K. Adamowski, and M. Alvo (1994), *Regional Flood Relationships by Nonparametric Regression*, Submitted to Nordic Hydrology.

[43] Greenwood, J. A., T. A. Landwehr, N. C. Matalas, and J. R. Wallis (1979), *Probability Weighted Moments*, Water Resources Research, 15(5), 1409-1054.

[44] Greis, N. P. and E. F. Wood (1981), *Regional Flood Frequency Estimation and Network Design,* Water Resources Research, 17(4), 1167-1174, Correction Water Resources Research, 19(2), 589-590, 1983.

[45] Gumbel, E. J. (1958), *Statistics of Extremes*, Columbia University Press, New York.

[46] Gupta, V. (1970), *Selection of Frequency Distribution Models*, Water Resources Research, 6(4), 1193-1198.

[47] Hannan, E. J. (1987), *The Cochrane and Orcutt Papers,* in Specification Analysis in the Linear Model, International Library of Economics, London, Routledge and Kegan Paul, 9-18.

[48] Hare, F. K. and M. K. Thomas (1979), *Climate Canada,* 2nd Edition, John Wiley and Sons Canada Limited.

[49] Hazen, A. (1924), *Discussion on Theoretical Frequency Curves and their Application to Engineering Problems*, Transactions of the American Society of Civil Engineers, 87, 143-173.

[50] Hershfield, D. M. (1961), *Rainfall Frequency Atlas of the United States*, United States Weather Bureau, Technical Paper No. 40.

[51] Hershfield, D. M. (1962), *Extreme Rainfall Relationships*, Journal of the Hydraulic Division, American Society of Civil Engineers, 88(6), 73-92.

[52] Hershfield, D. M. and M. A. Kohler (1962), *An Empirical Comparison of the Predictive Value of Three Extreme - Value Procedures*, Journal of Geophysical Research, 67(4), 1535-1542.

[53] Hershfield, D. M. and W. T. Wilson (1958), *Generalizing of Rainfall - Intensity - Frequency Data*, IUGG/IASH Publication, 43, 499-506.

[54] Hogg, W. D. and D. A. Carr (1985), *Rainfall Frequency Atlas for Canada*, Environment Canada, Atmospheric Environment Service.

[55] Hogg, W. D. (1992), *Comment on 'Short Duration Rainfalls in Sicily' by Ferreri, G. B. and V. Ferro*, Journal of the Hydraulics Division, American Society of Civil Engineers, 118(1), 107-109.

[56] Hogg, W. D., D. A. Carr, and B. Routeledge (1989), *Rainfall Intensity - Duration - Frequency Values for Canadian Locations*, CLI-1-89, Atmospheric Environment Service, Downsview, Ontario, Canada.

[57] Hosking, J. R. M. (1986), *The Theory of Probability Weighted Moments,* IBM Research Report 12210, IBM, Yorktown Heights, N. Y.

[58] Hosking, J. R. M. (1988), *The 4-Parameter Kappa Distribution,* Research Report, RC13412, IBM Research, Yorktown Heights, N. Y.

[59] Hosking, J. R. M. (1990), *L-moments: Analysis and Estimation of Distribution Using Linear Combination of Order Statistics,* Journal of the Royal Statistical Society, Series B, 52(1), 105-124.

[60] Hosking, J. R. M. (1991), *Fortran Routines for Use with the Method of L-Moments, Version 2,* IBM Research Report 75864, IBM, Yorktown Heights, N.Y.

[61] Hosking, J. R. M. and J. R. Wallis (1986), *Regional Flood Frequency Analysis Using Log - Normal Distribution,* Transactions EOS, American Geophysical Union, 67, 953 (Abstract).

[62] Hosking, J. R. M. and J. R. Wallis (1987), *Parameter and Quantile Estimation for the Generalized Pareto Distribution,* Technometrics, 29, 339-349.

[63] Hosking, J. R. M. and J. R. Wallis (1988), *The Effect of Inter-site Dependence on Regional Flood Frequency Analysis,* Water Resources Research, 24(4), 588-600.

[64] Hosking, J. R. M. and J. R. Wallis (1990), *Regional Flood Frequency Analysis Using L-Moments,* Research Report, RC 15658, IBM Research, Yorktown Heights, New York.

[65] Hosking, J. R. M. and J. R. Wallis (1991), *Some Statistics Useful in Regional Frequency Analysis*, Research Report, RC 17096, IBM Research, Yorktown Heights, New York.

[66] Hosking, J. R. M. and J. R. Wallis (1993), *Some Statistics Useful in Regional Frequency Analysis*, Water Resources Research, 29(2), 271-281.

[67] Hosking, J. R. M., J. R. Wallis, and E. F. Wood (1985a), *Appraisal of the Regional Flood Frequency Procedure in the United Kingdom Flood Studies Report,* Journal of Hydrological Sciences, 30(1), 85-109.

[68] Hosking, J. R. M., J. R. Wallis, and E. F. Wood (1985b), *Estimation of the Generalized Extreme Value Distribution by the Method of Probability Weighted Moments,* Technometrics, 27(30), 251-202.

[69] Huff, F. A. and J. C. Neill (1959a), *Comparison of Several Methods for Rainfall Frequency Analysis,* Journal of the Geophysical Research, 64(5), 541-547.

[70] Huff, F. A. and J. C. Neill (1959b), *Frequency Relations for Storm Rainfall in Illinois,* III-rd State Water Survey Bulletin, 46.

[71] Jenkinson, A. F. (1955), *The Frequency Distribution of the Annual Maximum (or Minimum) Values of Meteorological Events*, Quarterly Journal of Royal Meteorological Society, 81, 158-171.

[72] Jenkinson, A. F. (1969), *Statistics of Extremes,* in Estimation of Maximum Floods, WMO Technical Note 98, 183-228.

[73] Jin, M. and J. R. Stedinger (1989), *Flood Frequency Analysis with Regional and Historical Information*, Water Resources Research, 25(5), 925-936.

[74] Jones, D. E. (1990), *Need for the New Manual of Practice for the Design and Construction of Urban Stormwater Management Systems*, Proceedings on the Workshop on the Manual of Practice for the Design and Construction of Urban Stormwater Management Systems, Water Pollution Control Federation, Alexandria, VA.

[75] Keeping, E. S. (1966), *Distribution-Free Methods in Statistics*, Statistical Methods in Hydrology, Proceedings of Hydrology Symposium No.5, McGill University, Montreal, Canada.

[76] Kite, G. W. (1975), *Confidence Limits for Design Events*, Water Resources Research, 11(1), 48-53.

[77] Kirby, W. (1974), *Algebraic Boundedness of Sample Statistics*, Water Resources Research, 10(2), 220-222.

[78] Klemes, V. (1987), *Hydrologic and Engineering Relevance of Flood Frequency Analysis*, in Hydrologic Frequency Modeling, Edited by V.P. Singh, 1-18.

[79] Kothyari, U. C. and R. J. Garde (1992), *Rainfall Intensity - Duration - Frequency Formula for India*, Journal of the Hydraulics Division, 118(2), 323-336.

[80] Krishnan, A. and R. S. Kushwaha (1975), *Comparison of Gumbel and Jenkinson's Methods of Estimating Probable Maximum Rainfall Intensities Over India for Different Return Periods,* Central Board Irrigation Power Journal, 30(2), 233-234.

[81] Kuczera, G. (1983), *Effect of Sampling Uncertainty and Spacial Correlation on an Empirical Bayes Procedure for Combining Site and Regional Information*, Journal of Hydrology, 83, 373-398.

[82] Kuznetsova, L. P. (1964), *The Use of Cumulative Probability Curves in Processing Daily Maximum Precipitation*, Transaction Voyeykov Main Geophysical Observations, 162, 7-21 (translation from Russian).

[83] Landwehr, J. M., N. C. Matalas, and J. R. Wallis (1979), *Probability Weighted Moments Compared with some Traditional Techniques in Estimating Gumbel Parameters and Quantiles*, Water Resources Research, 15(5), 1055-1064.

[84] Landwehr, J. M., G. D. Tasker, and R. D. Jarrett (1987), Discussion on: *Relative Accuracy of Log-Pearson Type III Procedures*, by J. R. Wallis and E. F. Wood, Journal of the Hydraulics Division, American Society of Civil Engineers, 111(7), 1206-1210.

[85] Lettenmaier, D. P. and K. W. Potter (1985), *Testing Flood Frequency Estimation Methods Using a Regional Flood Generation Model,* Water Resources Research, 21(12), 1903-1914.

[86] Lettenmaier, D. P., J. R. Wallis, and E. F. Wood (1987), *Effect of Regional Heterogeneity on Flood Frequency Estimation*, Water Resources Research, 23(2), 313-324.

[87] Lowery, M. D. and J. E. Nash (1970), *A Comparison of Methods of Fitting the Double Exponential Distribution*, Journal of Hydrology, 10, 259-275.

[88] Majumdar, K. C. and R. P. Sawhney (1965), *Estimates of Extreme Values by Different Distribution Functions*, Water Resources Research, 1(3), 429-434.

[89] Maksimov, V. A. (1964), *An Outstanding Rainstorm in the Donbas*, Soviet Hydrology: Selected Papers, No. 1, English Translation, Published by the American Geophysical Union.

[90] Matalas, N. C. and E. J. Gilroy (1968), *Some Comments on Regionalization in Hydrologic Studies*, Water Resources Research, 4, 1361-1369.

[91] Matalas, N. C., J. R. Slack, and J. R. Wallis (1975), *Regional Skew in Search of a Parent*, Water Resources Research, 11(6), 815-841.

[92] Matalas, N. C. and J. R. Wallis (1973), *Eureka! It Fits a Pearson Type 3 Distribution*, Water Resources Research, 9(2), 281-289.

[93] Meteorological Branch (1952), *The Tipping-Bucket Rain Gauge*, Instrument Manual 41, Atmospheric Environment Service, Downsview, Ontario, Canada.

[94] Mosley, M. P. (1981), *Delimitation of New Zealand Hydrological Regions,* Journal of Hydrology, 49, 173-192.

[95] Neff, E. L. (1977), *How Much Rain Does a Rain Gage Gage?*, Journal of Hydrology, 35, 230-220.

[96] NERC - Natural Environment Research Council (1975), *Flood Studies Report Volume I - Hydrologic Studies,* Water Resources Publications, Fort Collins, Colorado.

[97] Pagliara, S. and C. Viti (1993), *Comment on Rainfall Intensity - Duration - Frequency Formula for India' by Kothyari, U. C. and R. J. Garde,* Journal of the Hydraulics Division, American Society of Civil Engineers, 119(8), 962-966.

[98] Pearson, C. P. and R. A. Woods (1991), *Regional Frequency Analysis of Western Australian Data Using L-Moments*, Internal Paper, Hydrology Center, Christchurch, New Zealand.

[99] Penta, A., G. Rasulo, and F. Rossi (1972), *Curve di Probabilita Pluviometrica*, Proceedings of Giornata di Studio Della I Sezone CIGR, 3, 317-339 (in Italian).

[100] Peterson, M. M. (1987), *Short - Duration Precipitation for Billings, Montana,* Journal of the Hydraulics Division, American Society of Civil Engineers, 112(11), 1089-1093.

[101] Pilon, P. J. and K. Adamowski (1992), *The Value of Regional Information to Flood Frequency Analysis Using the Method of L-Moments,* Canadian Journal of Civil Engineering, 19, 137-147.

[102] Pilon, P. J., K. Adamowski, and Y. Alila (1991a), *Regional Analysis of Annual Maxima Precipitation Using L-moments,* Atmospheric Research Journal, 27, 81-92.

[103] Pilon, P. J., Y. Alila, and K. Adamowski (1991b), *Assessment of Risk of Flooding Based on Regional Information,* Presented at the NATO Advanced Study Institute on Risk and Reliability in Water Resources and Environmental Engineering, 18-28 May, Porto Carras, Greece.

[104] Pilon, P. J. and K. D. Harvey (1993), *Consolidated Frequency Analysis (CFA) Package - Version 3.1,* Systems and Information Branch, Environment Canada, Ottawa.

[105] Potter, K. W. (1987), *Research on Flood Frequency Analysis: 1983 - 1986,* Reviews of Geophysics, 25(2), 113-118.

[106] Potter, K. W. and D. P. Lettenmaier (1990), *A Comparison of Regional Flood Frequency Estimation Methods Using a Resampling Method,* Water Resources Research, 26(3), 424-451.

[107] Pugsley, W. I. (1981), *Flood Hydrology Guide for Canada: Hydrometeorological Design Techniques,* CLI-3-81, Atmospheric Environment Service, Downsview, Toronto, Ontario, Canada.

[108] Reich, B. M. (1970), *Flood Series Compared to Rainfall Extremes*, Water Resources Research, 6(6), 1655-1667.

[109] Ribeiro-Correa, J. and J. Rousselle (1993), *A Hierarchical and Empirical Bayes Approach for the Regional Pearson Type III Distribution*, Water Resources Research, 29(2), 435-444.

[110] Rodda, J. C. (1970), *Rainfall Excesses in the United Kingdom,* Trans. Inst. British Geograph., 49, 49-60.

[111] Royston, P. (1991), *Which Measures of Skewness and Kurtosis are Best,* Statistics in Medicine, 10, 1-11.

[112] Samuelson, B. (1972), *Statistical Interpretation of Hydrometeorological Extreme Values*, Journal of Northern Hydrology, 3(4), 199-213.

[113] Schaefer, M. G. (1990), *Regional Analysis of Precipitation Annual Maxima in Washington State,* Water Resources Research, 26(1), 119-131.

[114] Schuster, E. and S. Yakowitz (1986), *Parametric / Nonparametric Mixture Density Estimation with Application to Flood - Frequency Analysis*, Water Resources Bulletin, American Water Resources Association, 21(5), 797-804.

[115] Sneyers, R. (1977), *L' Intensite Maximale des Precipitation en Belgique*, Publication Serie B, 86, Bruxelles (in French).

[116] Sneyers, R. (1978), *L'Influene du Relief sur les Valeurs Extremes de l'Intensite et la Duree des Precipitations en Belgique*, 15.Int. Tag f.alp. Meterologie, Grindelwald, 19-23 September, 281-283 (in French).

[117] Snyder, W. M. (1972), *Fitting of Distribution Functions by Nonlinear Least Squares*, Water Resources Research, 8(6), 1423-1432.

[118] Stedinger, J. R. (1983), *Estimating a Regional Flood Frequency Distribution*, Water Resources Research, 19(2), 503-510.

[119] Stedinger, J. R. and G. D. Tasker (1985), *Regional Hydrologic Analysis 1- Ordinary, Weighted, and Generalized Least Squares Compared,* Water Resources Research, 21(9), 1421-1432.

[120] Stedinger, J. R., K. Potter, D. F. Kibler, and G. Tasker (1983), *Comment on: Regional Flood Frequency Estimation and Network Design,* by Greis N. P. and E. F. Wood, Water Resources Research, 19, 1343-1345.

[121] Thom, H. C. S. (1958), *A Note on the Gamma Distribution,* Monthly Weather Review, 86(4), 117-121.

[122] Thomas, D. M. and M. A. Benson (1970), *Generalization of Streamflow Characteristics*, U. S. Geological Survey, Water Supply Paper 1975.

[123] Thomas, W. D. and S. A. Olson (1992), *Regional Analysis of Minimum Streamflow*, Proceedings of the 12th Conference on Probability and Statistics in the Atmospheric Sciences, American Meteorological Society, June 22-26, Toronto, Ontario, Canada, 261-266.

[124] Uppala, S. (1978), *Extreme Distribution Functions for Daily and Monthly Precipitation in Finland,* Geophysica, 15(1).

[125] USWRC - U.S. Water Resources Council (1982), *Guidelines for Determining Flood Flow Frequency*, Bulletin 17B, Hydrology Committee, Washington, D.C.

[126] Versace, P., E. Ferrari, M. Fiorentino, S. Gabriele, and F. Rossi, (1987), *Valutazione Delle Piene in Calabria,* Geodata 30, Ist. Di Ric. per la Prot. Idrogeol., Cosenza, Italy (in Italian).

[127] Vogel, J.L. and B. Lin (1992), *Precipitation Return Frequencies and L-Moment Statistics*, Proceedings of the 12th Conference on Probability and Statistics in the Atmospheric Sciences, American Meteorological Society, June 22-26, Toronto, Ontario, Canada, 251-254.

[128] Wallis, J. R. (1982a), *Probable and Improbable Rainfall in California,* Research Report RC 9350, IBM, Yorktown Heights, New York.

[129] Wallis, J. R. (1982b), *Hydrologic Problems Associated with Oilshale Development,* Environmental Systems and Management, Edited by S. Rinaldi, 85-102., North-Holland, New York.

[130] Wallis, J. R. (1988), *Catastrophes, Computing and Containment: Living in our Restless Habitat,* Speculations in Science and Technology, 11(4), 295-315.

[131] Wallis, J. R. (1989), *Regional Frequency Studies Using L-Moments*, IBM Research Report, R.C. 14597.

[132] Wallis, J. R., N. C. Matalas, and J. R. Slack (1974), *Just a Moment!*, Water Resources Research 10(2), 211-219.

[133] Wallis, J. R. and E. F. Wood (1985), *Relative Accuracy of Log - Pearson III Procedures,* Journal of the Hydraulics Division, American Society of Civil Engineers, 11(7), 1043-1056.

[134] Warnick, C. C. (1956), *Influence of Wind on Precipitation Measurements at High Altitudes*, University of Idaho, Engineering Experimental Station, Bulletin No. 10.

[135] Watt, W. E. et al. (1989), *Hydrology of Floods in Canada: A Guide to Planning and Design*, National Research Council Canada, Associate Committee on Hydrology.

[136] Watt, W. E. and M. J. Nozdryn-Plotnicki (1980), *Rainfall Frequency Analysis for Urban Design*, Proceedings Canadian Hydrology Symposium, National Research Center, Ottawa, Ontario, Canada, 34-52.

[137] Waylen, P. R. and M. Woo (1984), *Regionalization and Prediction of Floods in the Fraser River Catchment,* B.C. Water Resources Bulletin, 20(6), 941-949.

[138] White, E. L. (1975), *Factor Analysis of Drainage Basin Properties: Classification of Flood Behavior in Terms of Basin Geomorphology*, Water Resources Bulletin 11(4), 676-686.

[139] Wiltshire, S. E. (1985), *Grouping Basins for Regional Frequency Analysis,* Hydrological Sciences Journal, 30(1), 151-159.

[140] Wiltshire, S. E. (1986a), *Regional Flood Frequency Analysis, I: Homogeneity Statistics,* Hydrological Sciences Journal, 31(3), 321-33.

[141] Wiltshire, S. E. (1986b), *Regional Flood Frequency Analysis, II: Multivariate Classification of Drainage Basins in Britain,* Hydrological Sciences Journal, 31(3), 334-346.

[142] WMO (1981), *Selection of Distribution Types for Extremes of Precipitation*, Operational Hydrology Report No. 15, WMO-No. 560, Geneva, Switzerland.

[143] WMO (1983), *Guide to Hydrologic Practices, Vol. II, Analysis, Forecasting and Other Applications*, WMO-No. 168, Geneva, Switzerland.

[144] Wu, B. and J. D. Goodridge (1974), *On the Selection of Probability Distributions for Hydrologic Frequency Analysis*, Paper Presented at American Geophysical Union Fall Annual Meeting.

[145] Wu, K. and M. K. Woo (1989), *Estimating Annual Flood Probability Using Fourier Series Method*, Water Resources Bulletin, 24(4), 743-750.

[146] Wurtele, M. G. and J. M. Roe (1978), *Fisher - Tippett Representations of Extreme Rainfall and Temperature Data,* Transaction EOS, American Geophysical Union, 59(12), 1603 (Abstract).

[147] Zeller, J., H. Geiger, and G. Roethlisberger (1978), *Starkniederschlage des Schweizerischen Alpen - Und Alpenrandgebietes,* Teil 1-3, Eidg. Anstalt fur das Forstliche, Versuchswesen, Birmensdorf, Schweiz (in German).

Appendix A

Figures

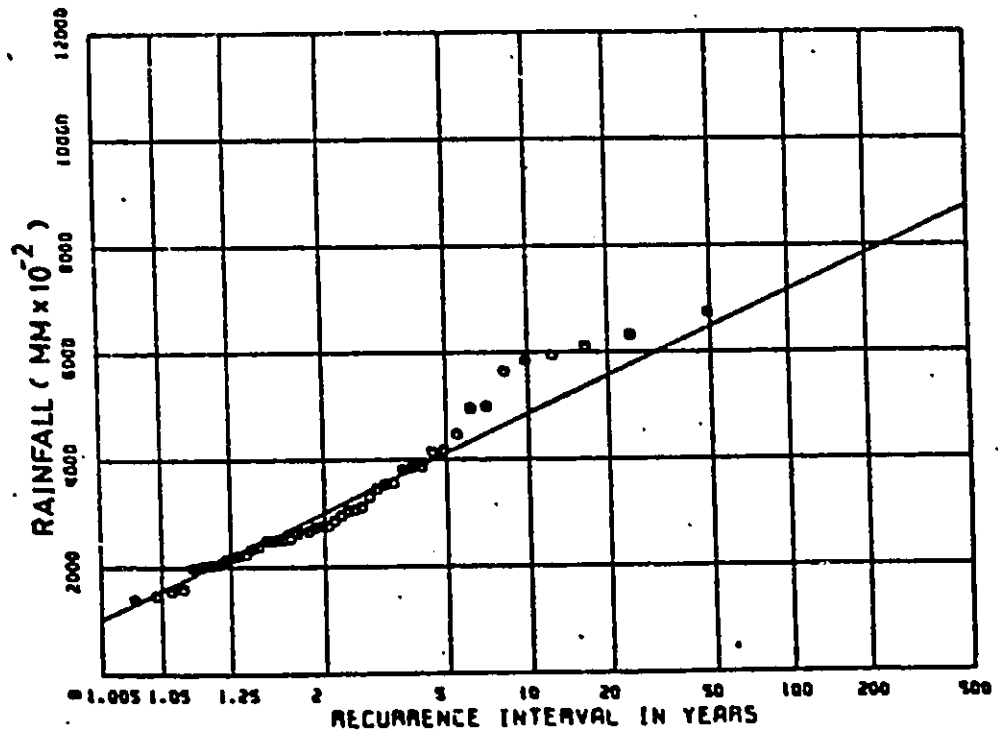

Figure 1.1: Graphical Fit of EV1 Distribution to 2-hr Rainfall Extremes at the Long-Term Record Station 6137362 - St. Thomas WPCP, Ontario (Watt and Nozdryn-Plotnicki, 1980)

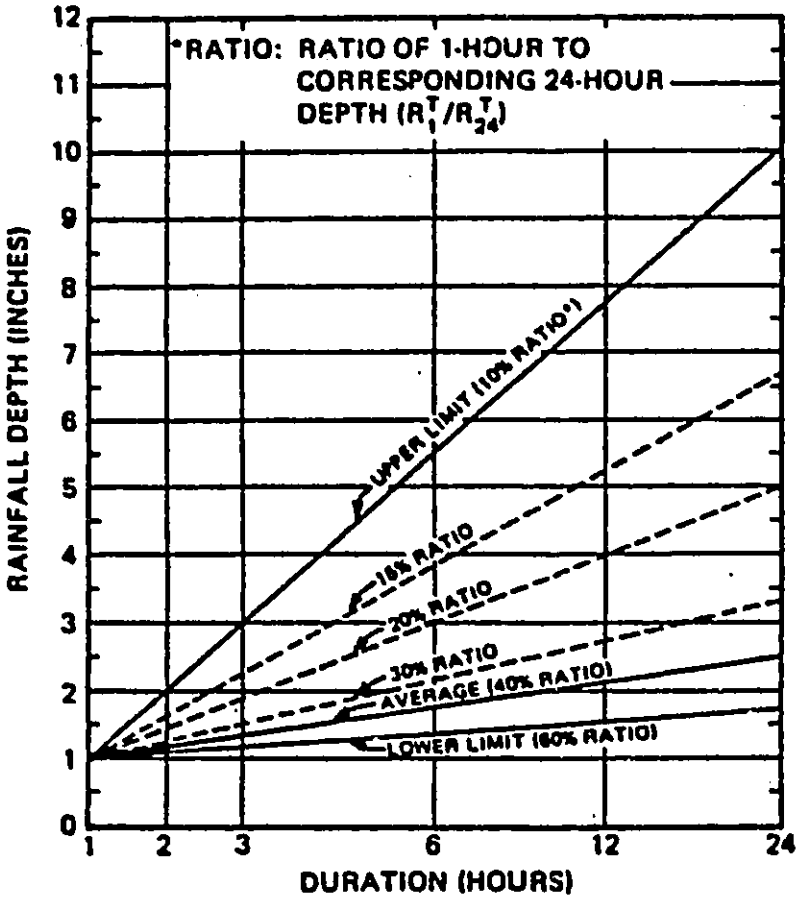

Figure 2.1: Rainfall Depth-Duration Diagram After United States Weather Bureau Technical Paper No. 40 (Hershfield, 1961)

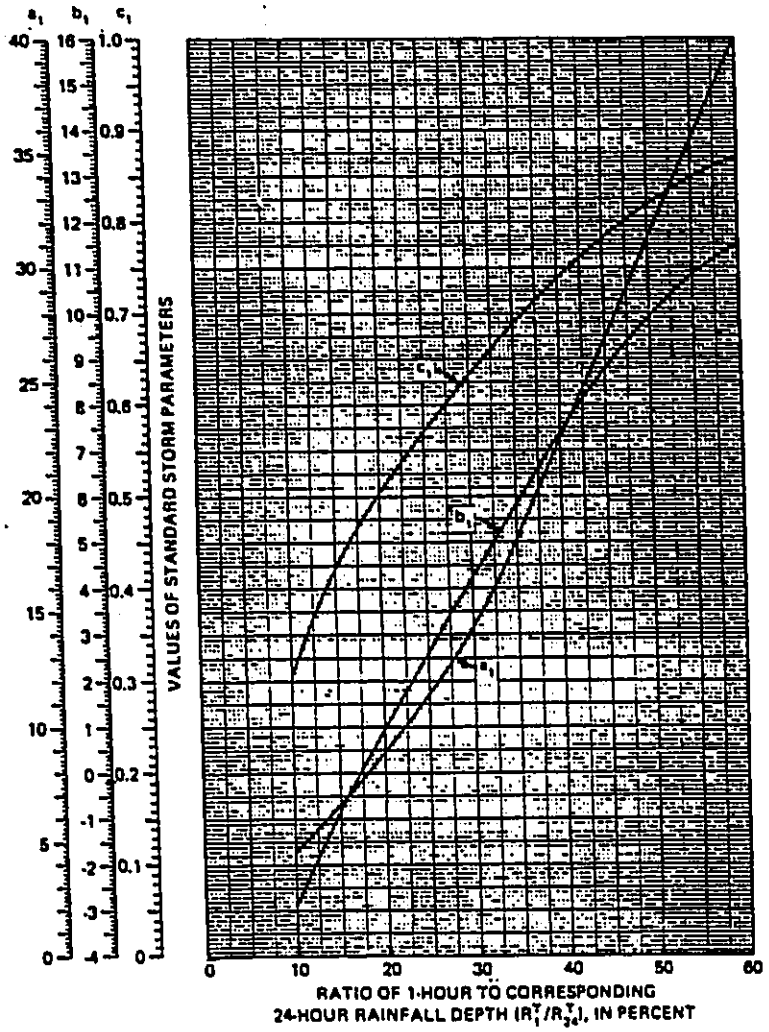

Figure 2.2 : Relations Between Standard Storm Parameters and Ratio of the 1-hr to the Corresponding 24-hr Rainfall Depth (Chen, 1983)

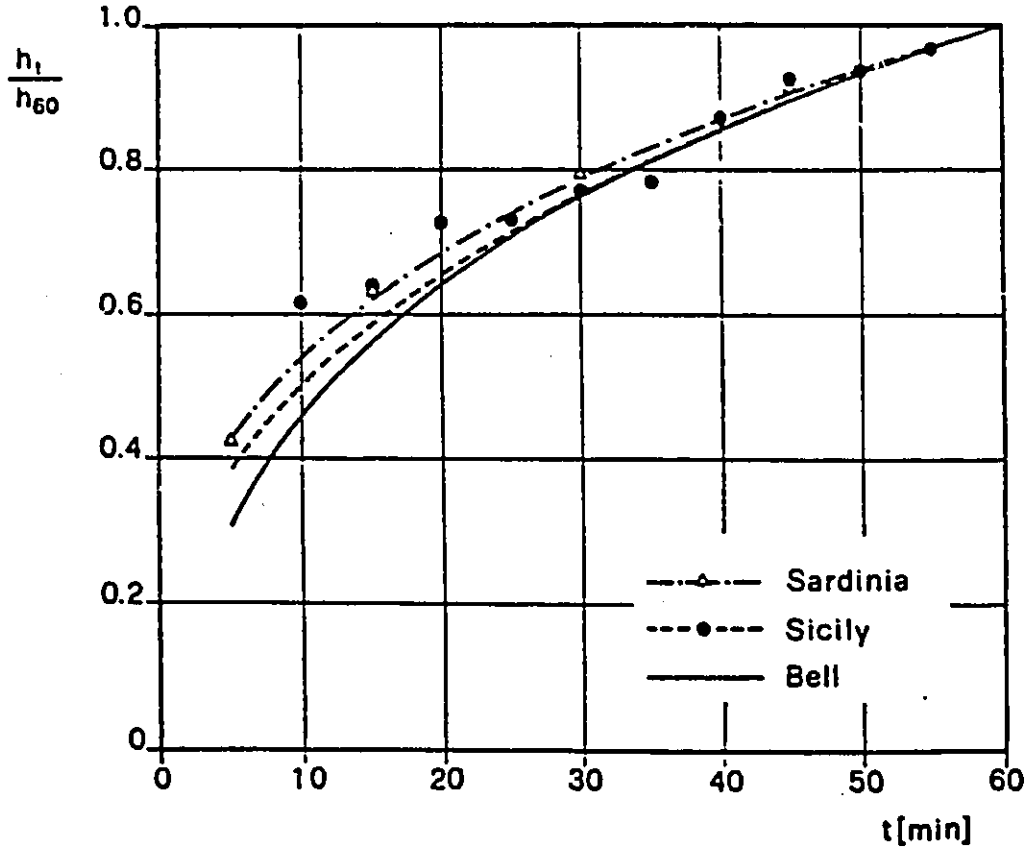

Figure 2.3: Comparison of Depth-Duration Ratios for United States and Italy (Ferreri and Ferro, 1990)

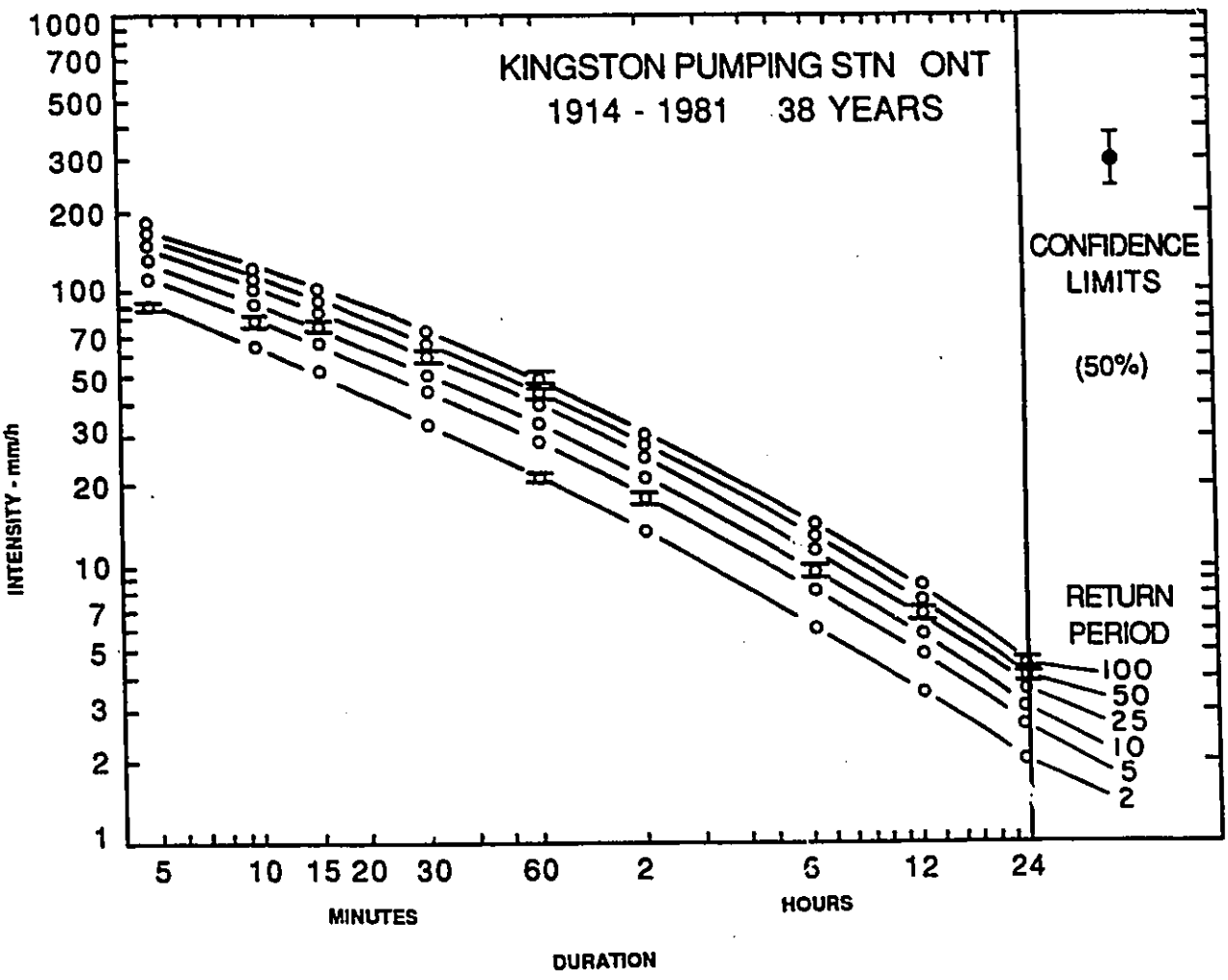

Figure 2.4: Rainfall Intensity-Duration-Frequency Curves at Station 6104175 - Kingston Pumping Station, Ontario (Watt et al., 1989)

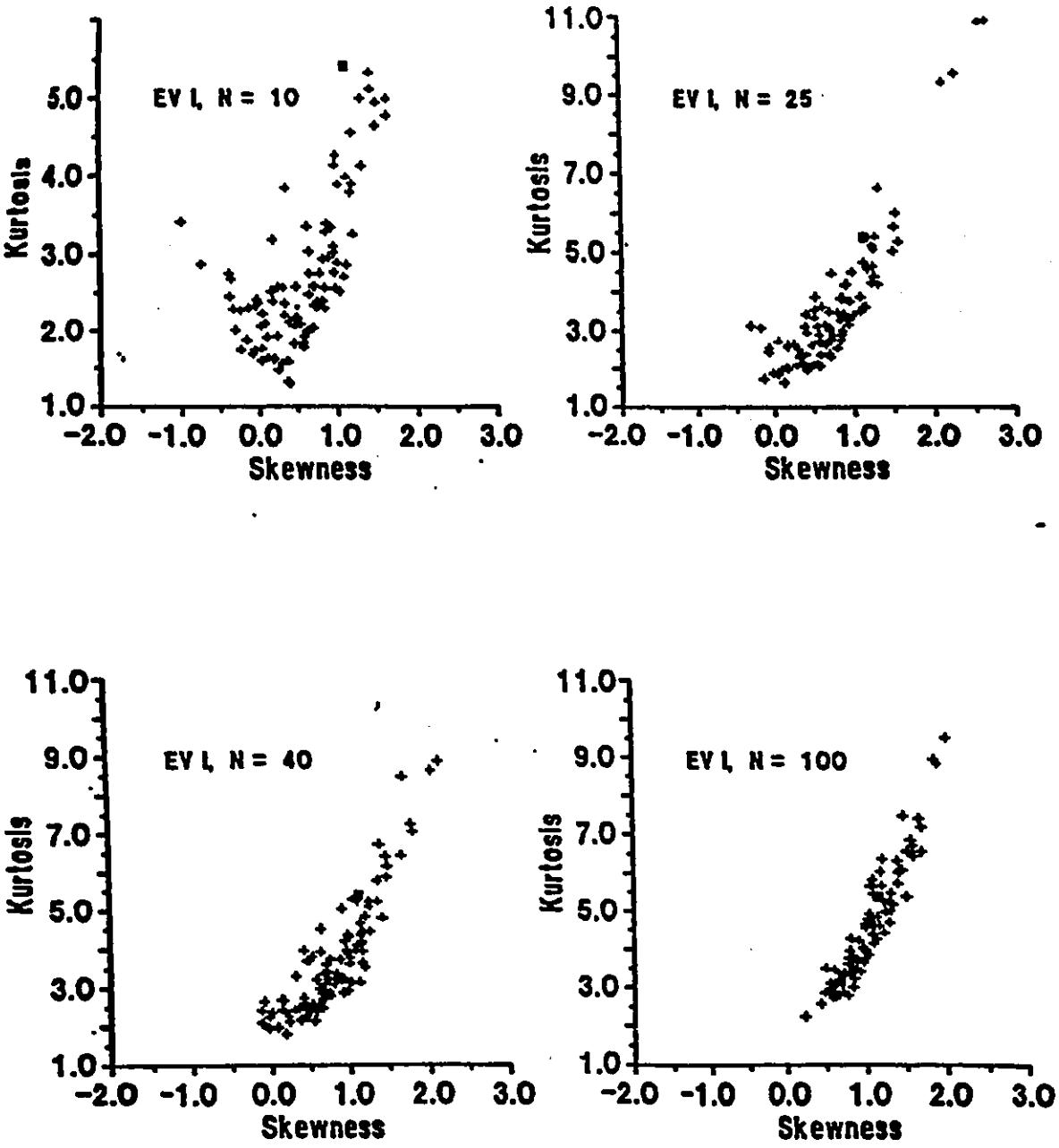

Figure 3.1a: Plot of Skewness vs. Kurtosis for EV1 Distribution (1.14 vs. 5.4) and Estimates for 100 Samples with n=10, 25, 40, and 100 (Wallis, 1989)

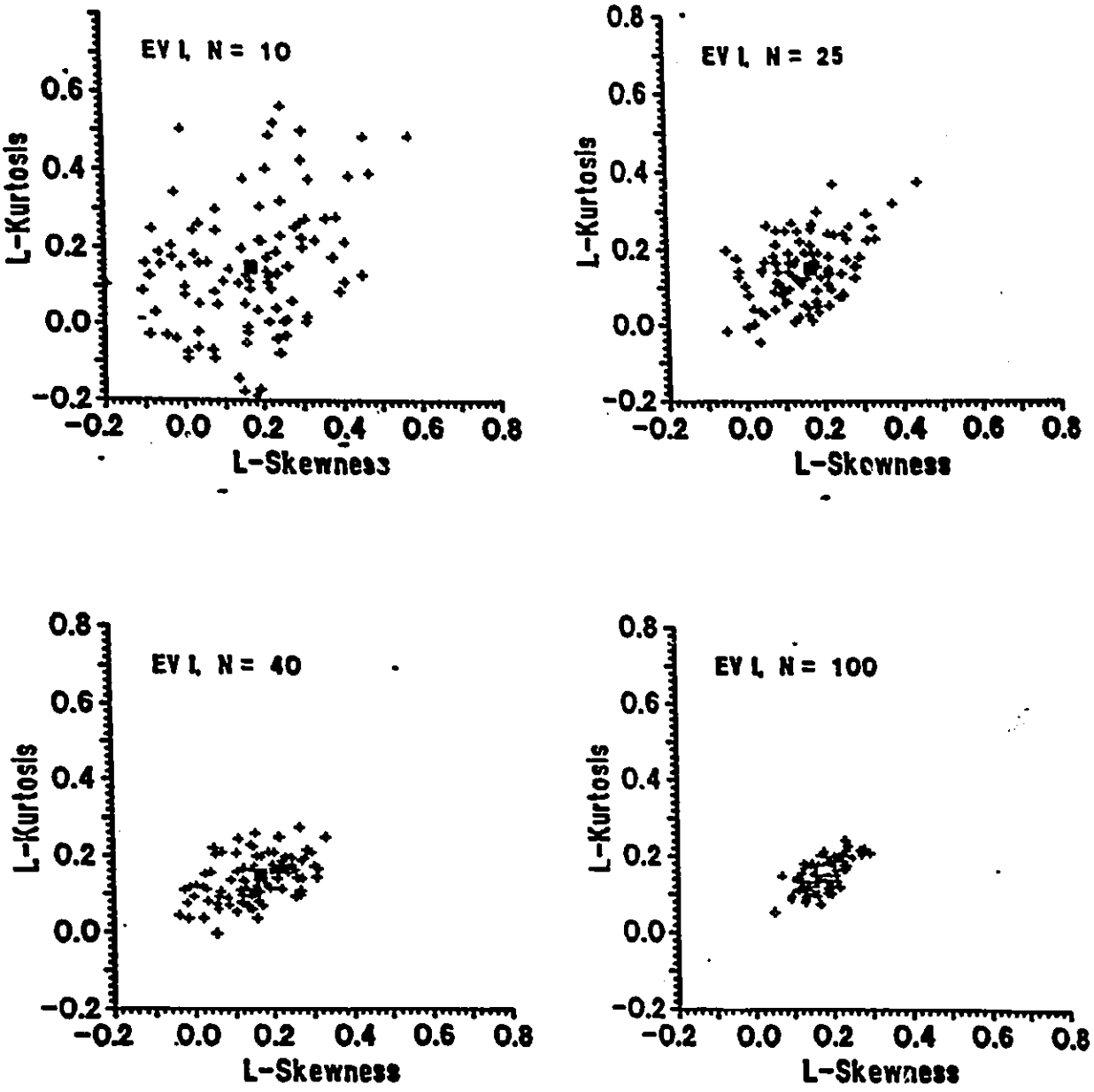

Figure 3.1b: Plot of L-Skewness vs. L-Kurtosis for EV1 Distribution (1.14 vs. 5.4) and Estimates for 100 Samples with n=10, 25, 40, and 100 (Wallis, 1989)

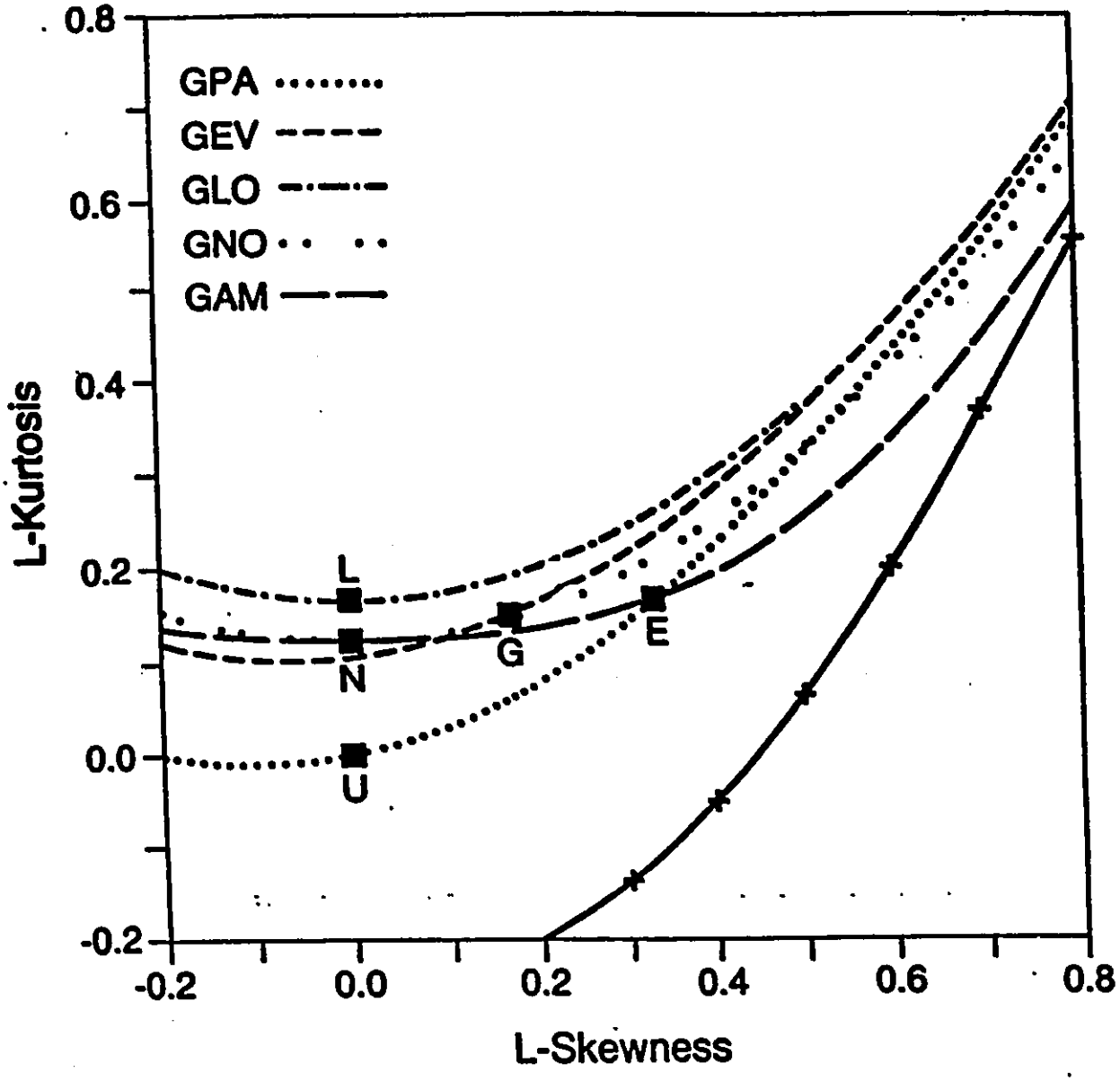

L-moment ratios of some common distributions for the values of usual interest E = exponential, G = Gumbel, L = logistic, U = uniform, GPA = generalized Pareto, GEV = generalized extreme value, GLO = generalized logistic, GNO = generalized normal, GAM = gamma, while vertical crosses are the lower bound for all other distributions.

Figure 3.2 : L-Moment Ratios of Some Common Distributions (After Hosking, 1989, 1990)

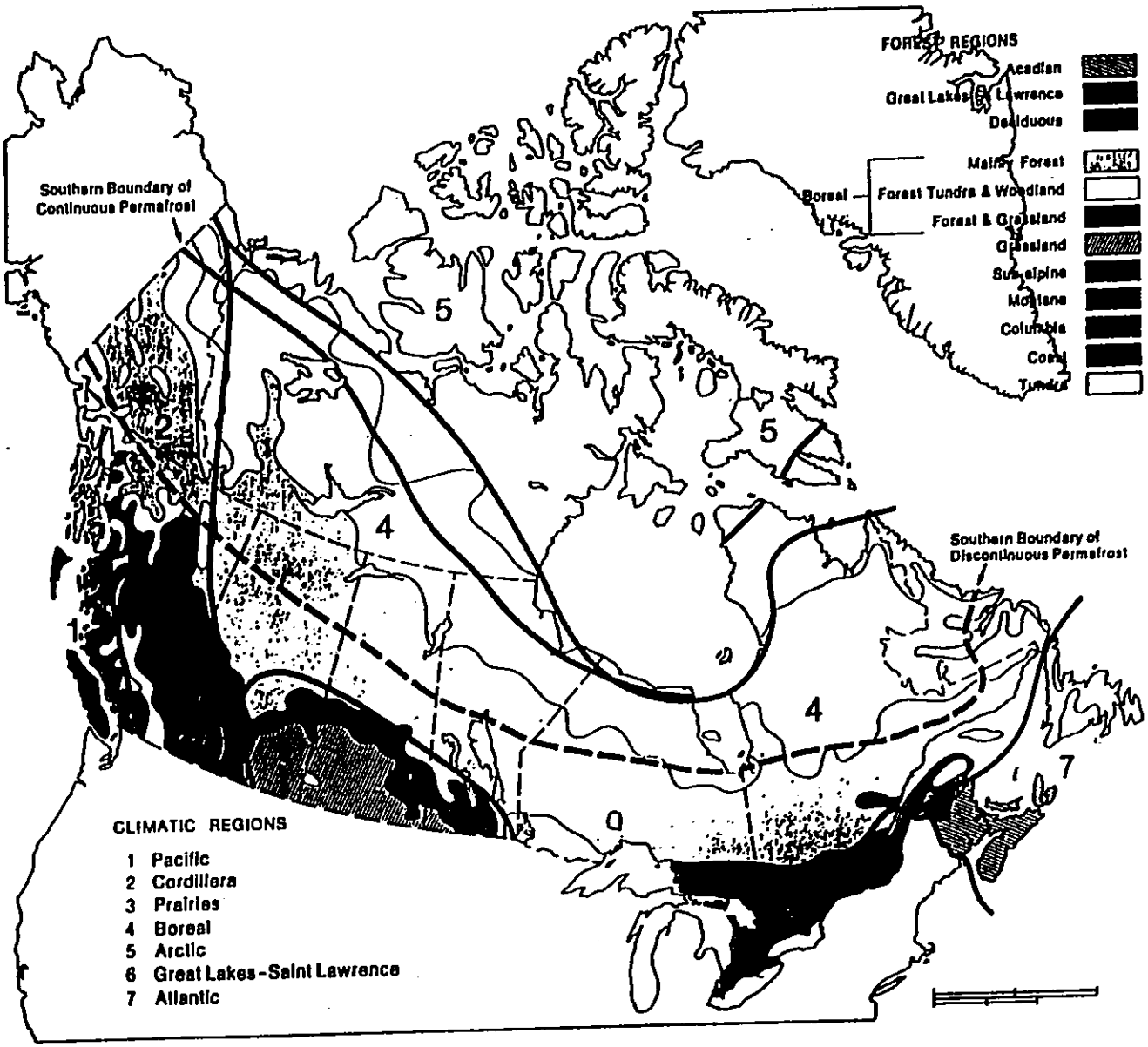

Figure 4.1 : Canada's Macrogeography; Coastlines, Vegetation and Climatic Regions, with Zones of Continuous and Discontinous Permafrost (Hare and Thomas, 1979)

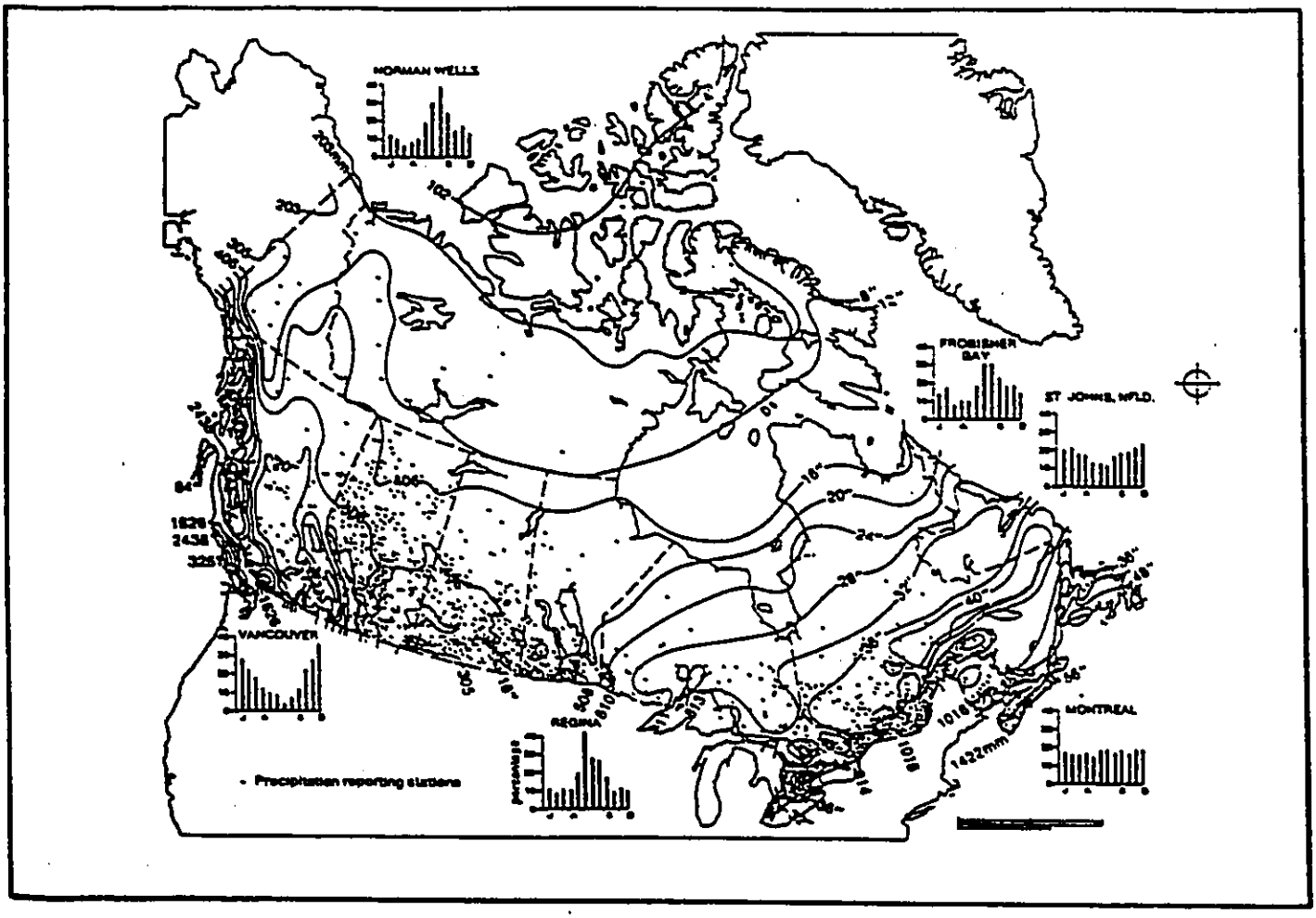

Figure 4.2 : Mean Annual Amount of Precipitation (inches and millimiters) with Reporting Stations (Hare and Thomas, 1979).

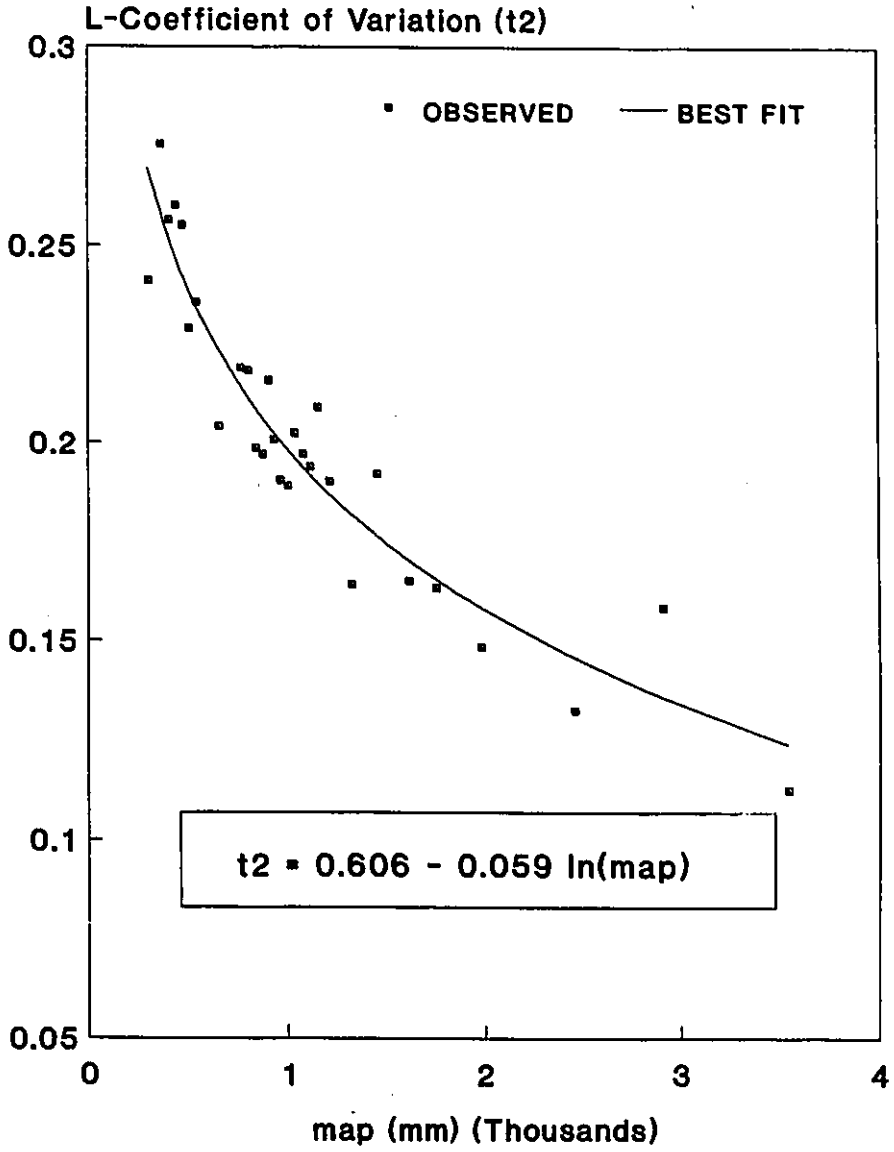

Figure 4.3a: Sub-Regional Solution for the L-Coefficient of Variation as a Function of map for the 60-min Storm

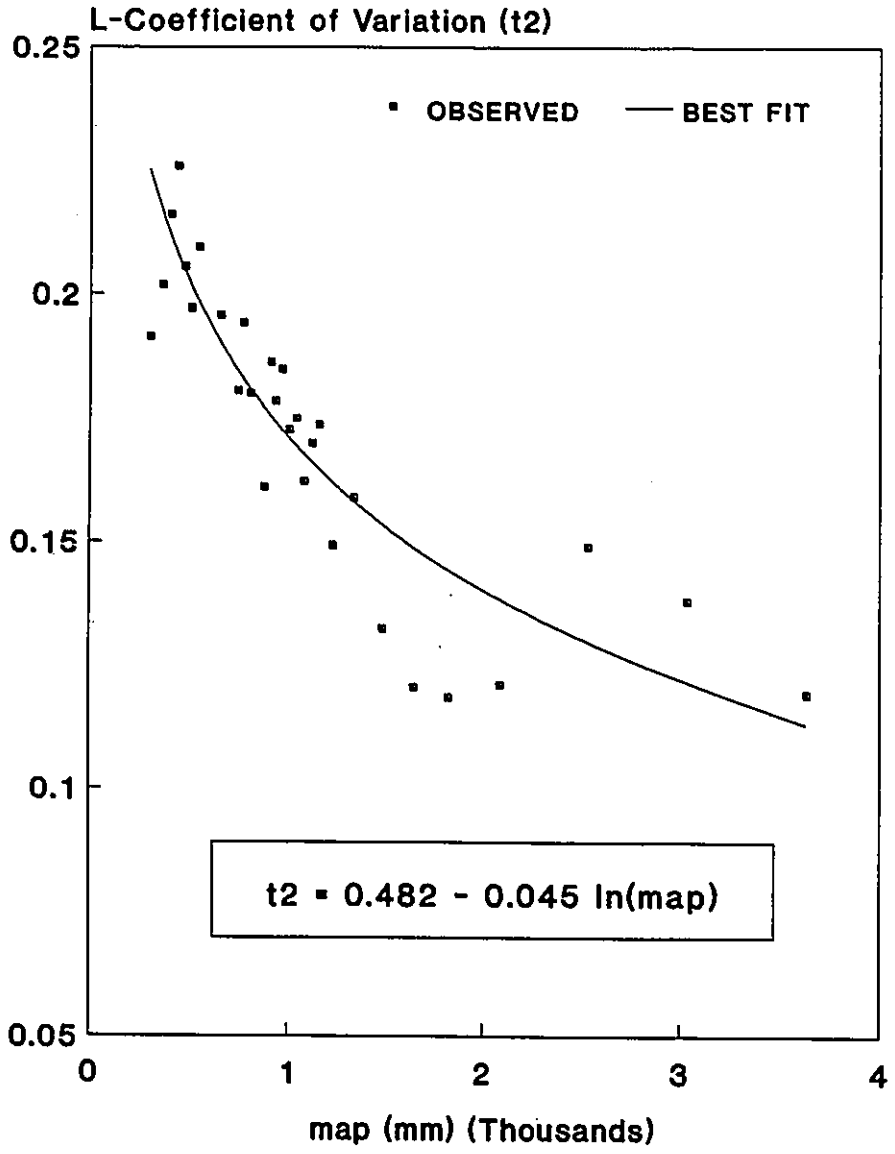

Figure 4.3b: Sub-Regional Solution for the L-Coefficient of Variation as a Funtion of map for the 12-hr Storm

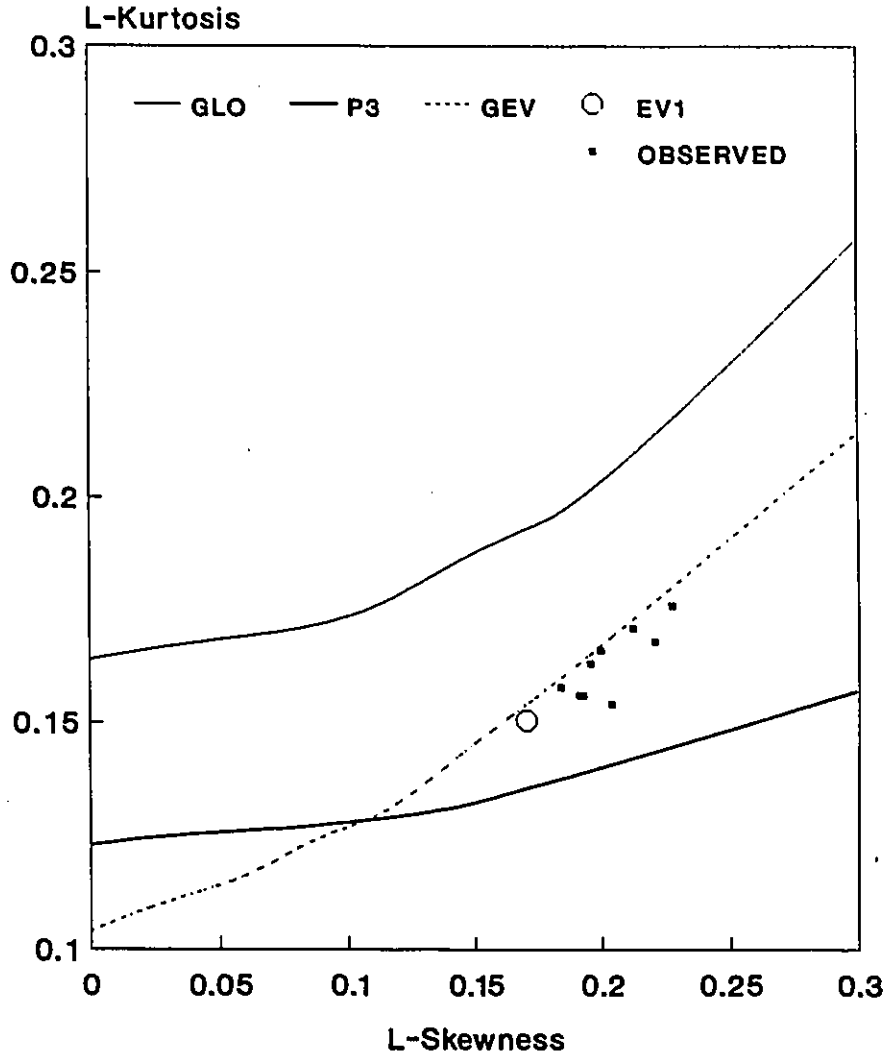

Figure 4.4: Average Relationships for Regional L-Kurtosis and L-Skewness of the 5, 10, 15, 30, 60 minutes and 2, 6, 12, and 24 hours Annual Rainfall Extremes in Canada

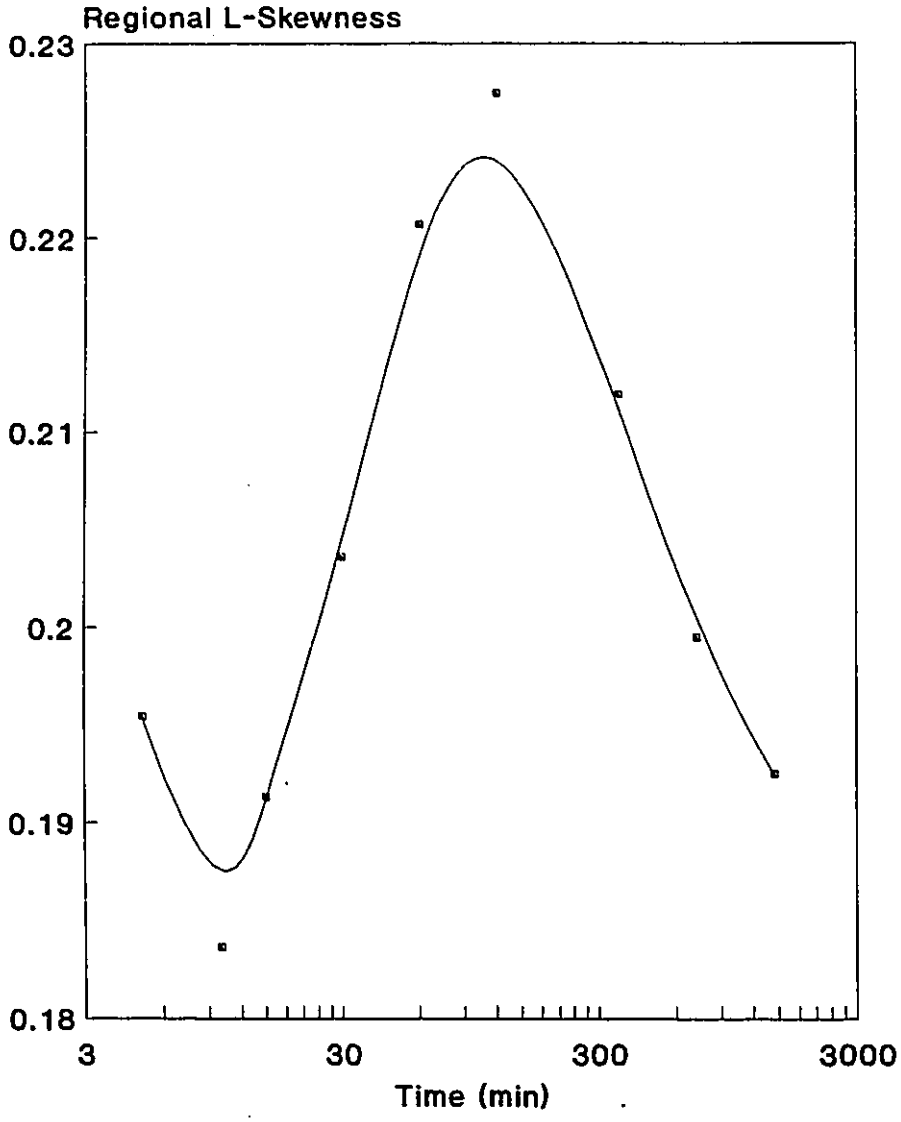

Figure 4.5: Regional Average L-Skewness as a Function of Storm Duration for Canadian Rainfall Extremes

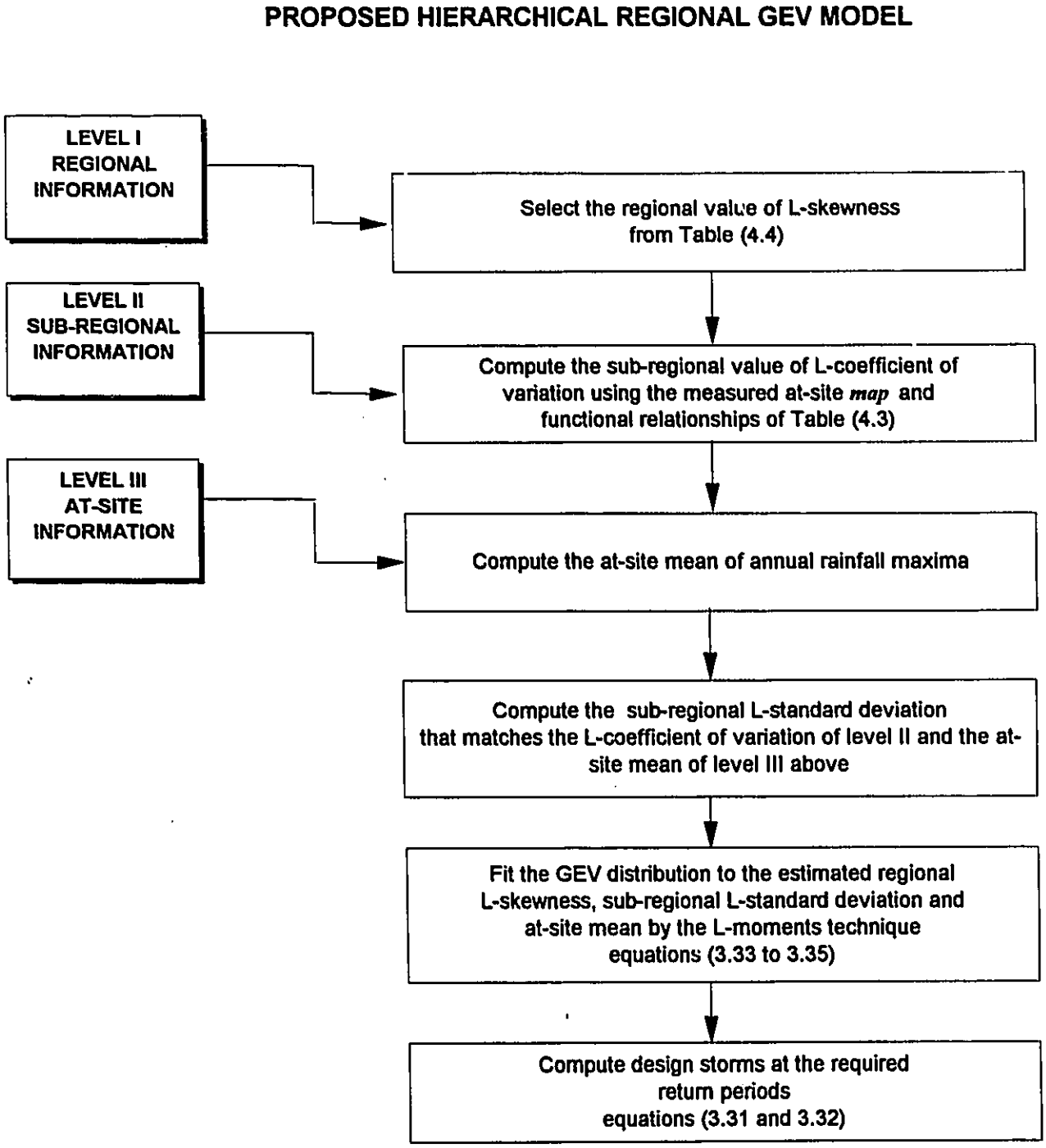

Figure 4.6: Proposed Procedure for Design Storm Estimation at Gauged Stations (valid for 5, 10, 15, 30, 60 min and 2, 6, 12, 24 hr)

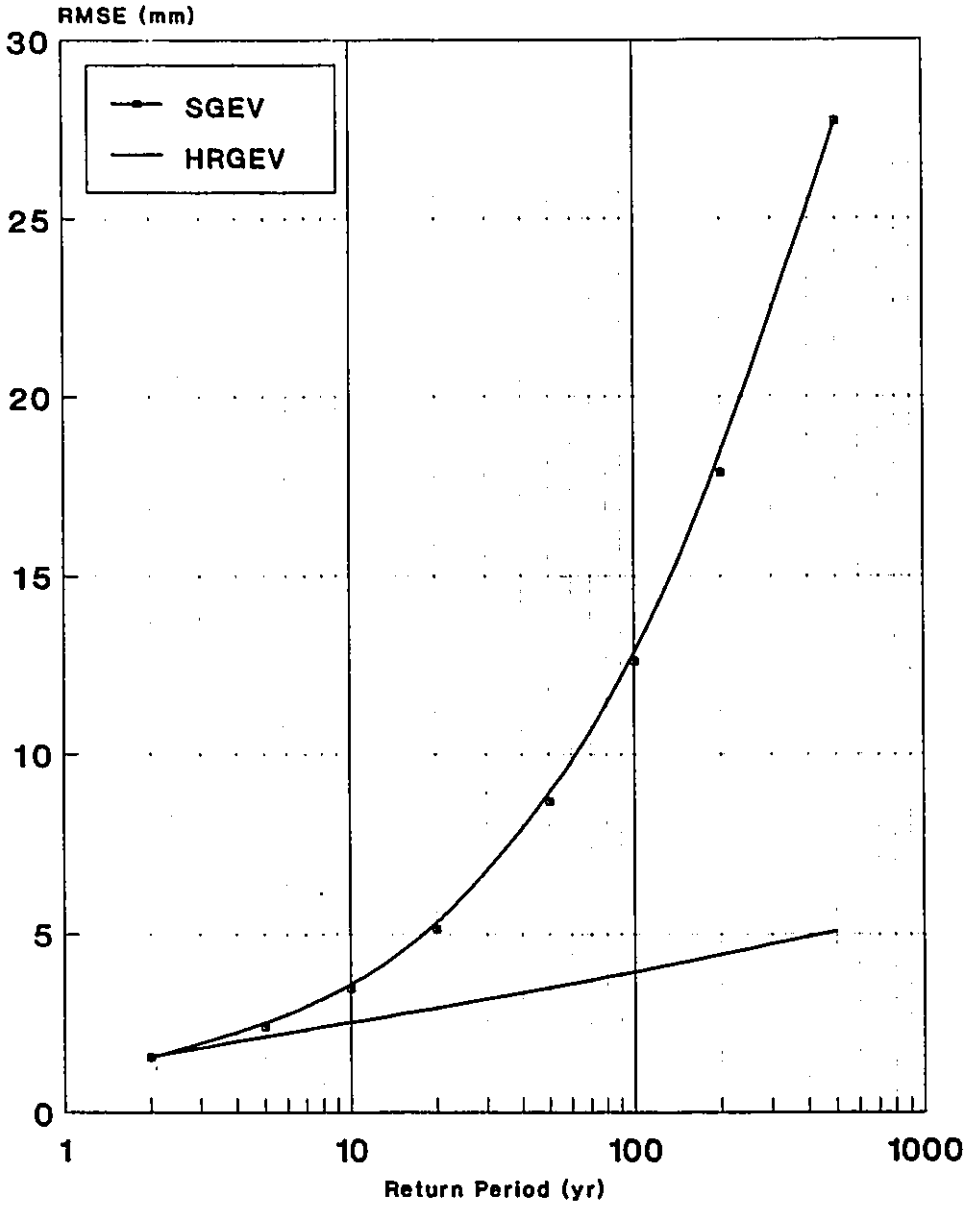

Figure 4.7: Accuracy of Estimating Design Storms for Various Return Periods when the Sample Size is 20.

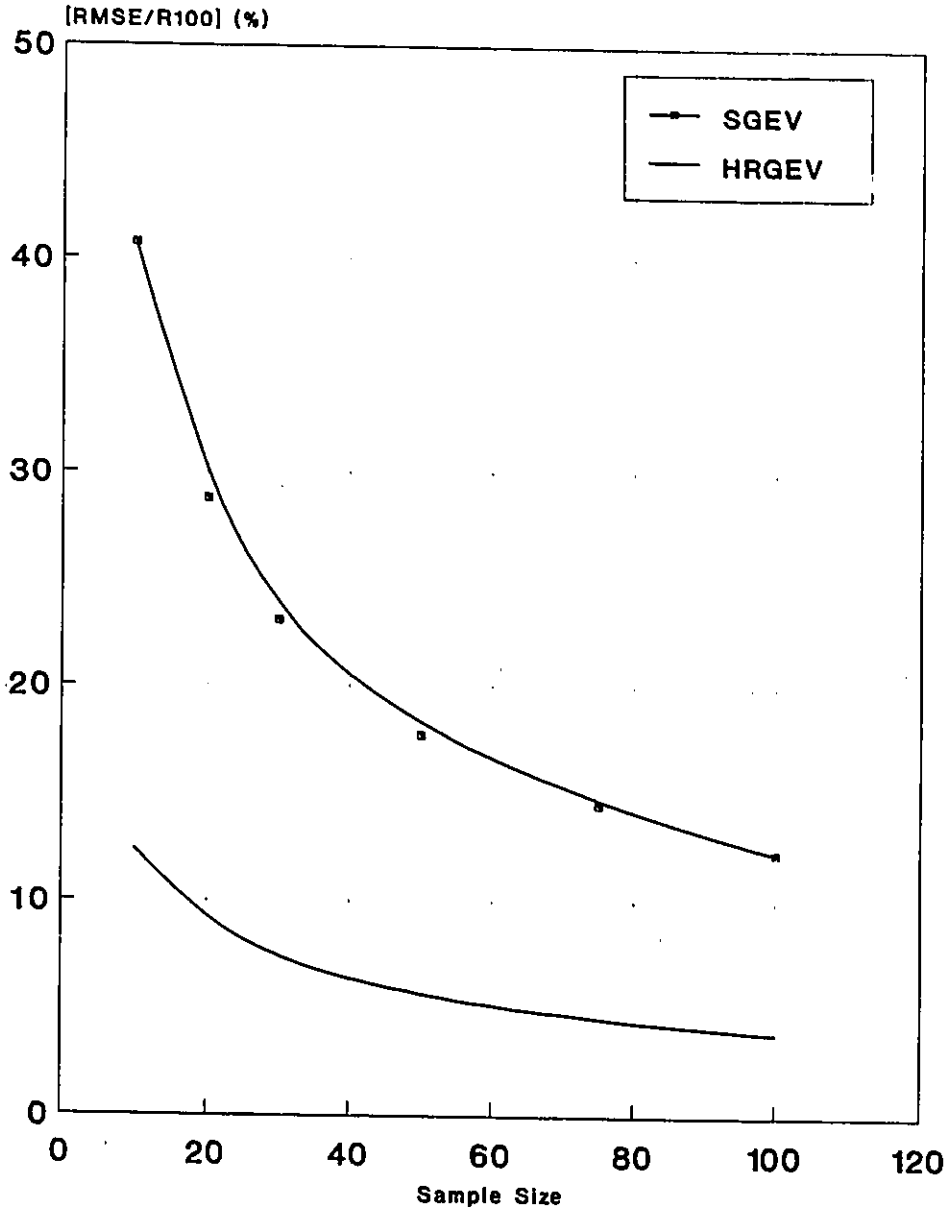

Figure 4.8: Influence of Sample Size on the Accuracy of 100-yr Design Storm

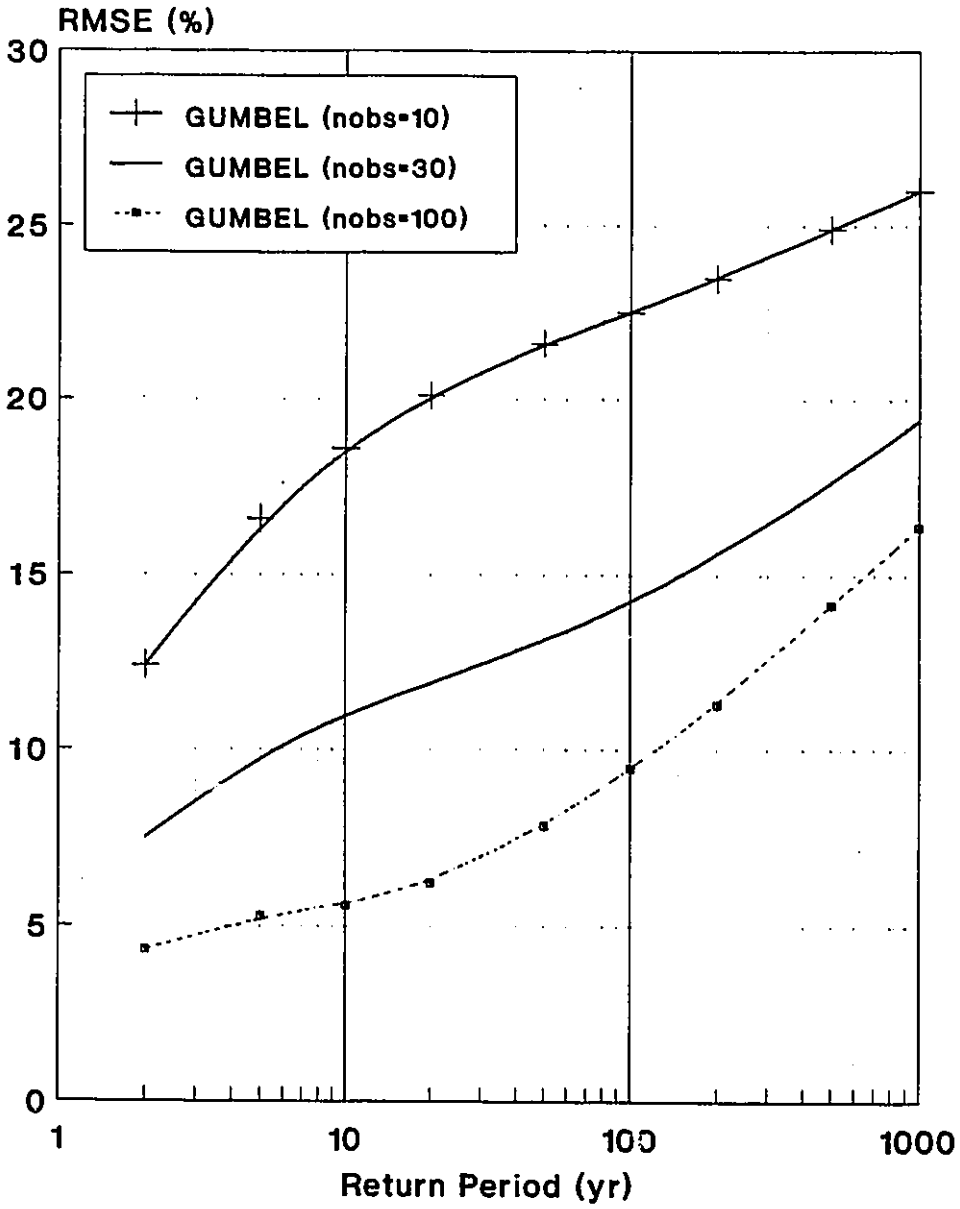

Figure 4.9: Sensitivity of the T-yr Design Storm Estimate to Gumbel Distribution Assumption for Various Sample Sizes

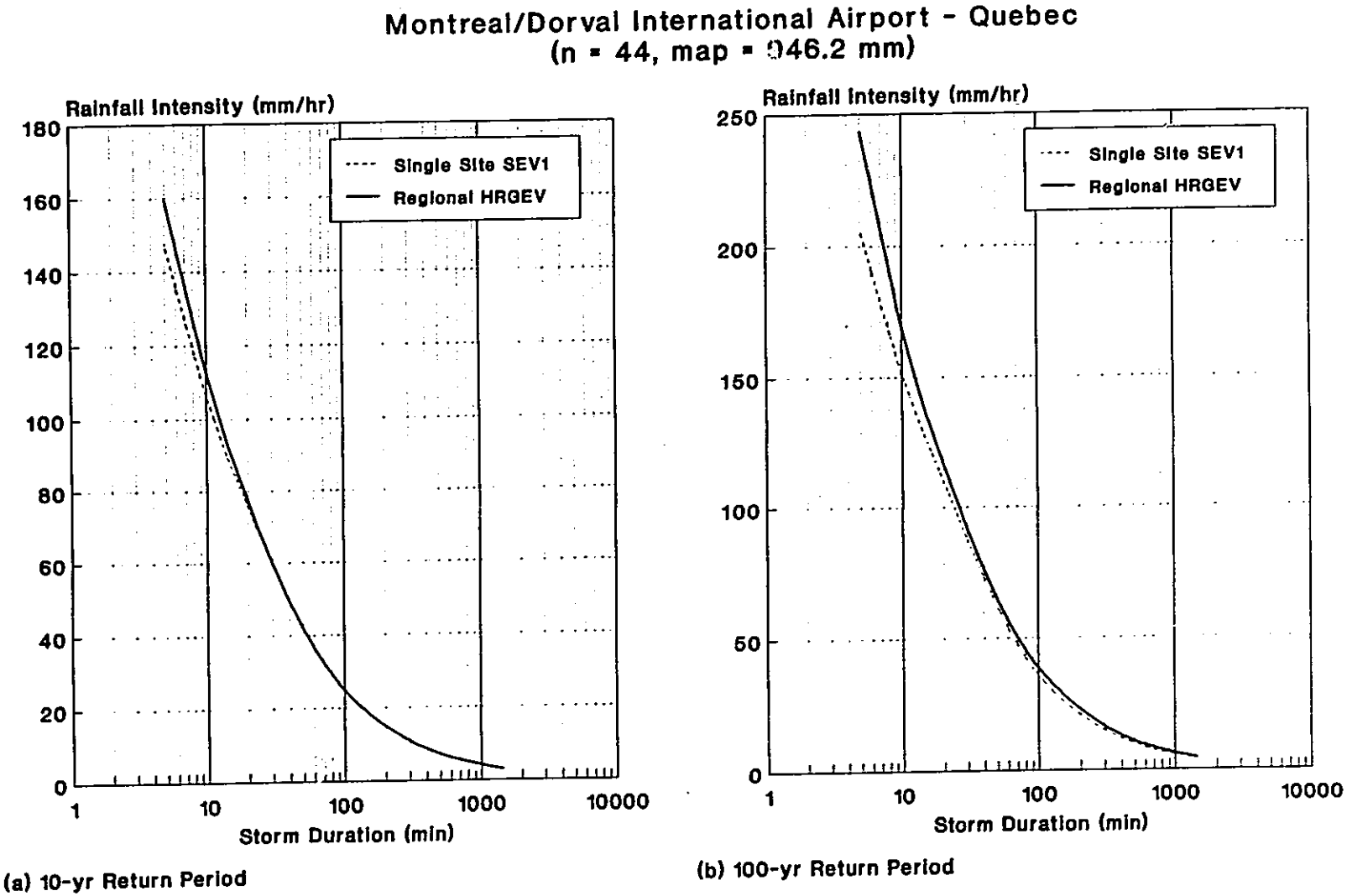

Figure 4.10: Comparison of IDF Curves Estimated by the HRGEV and SEV1 Models at Long-Term Record Station - 7025250

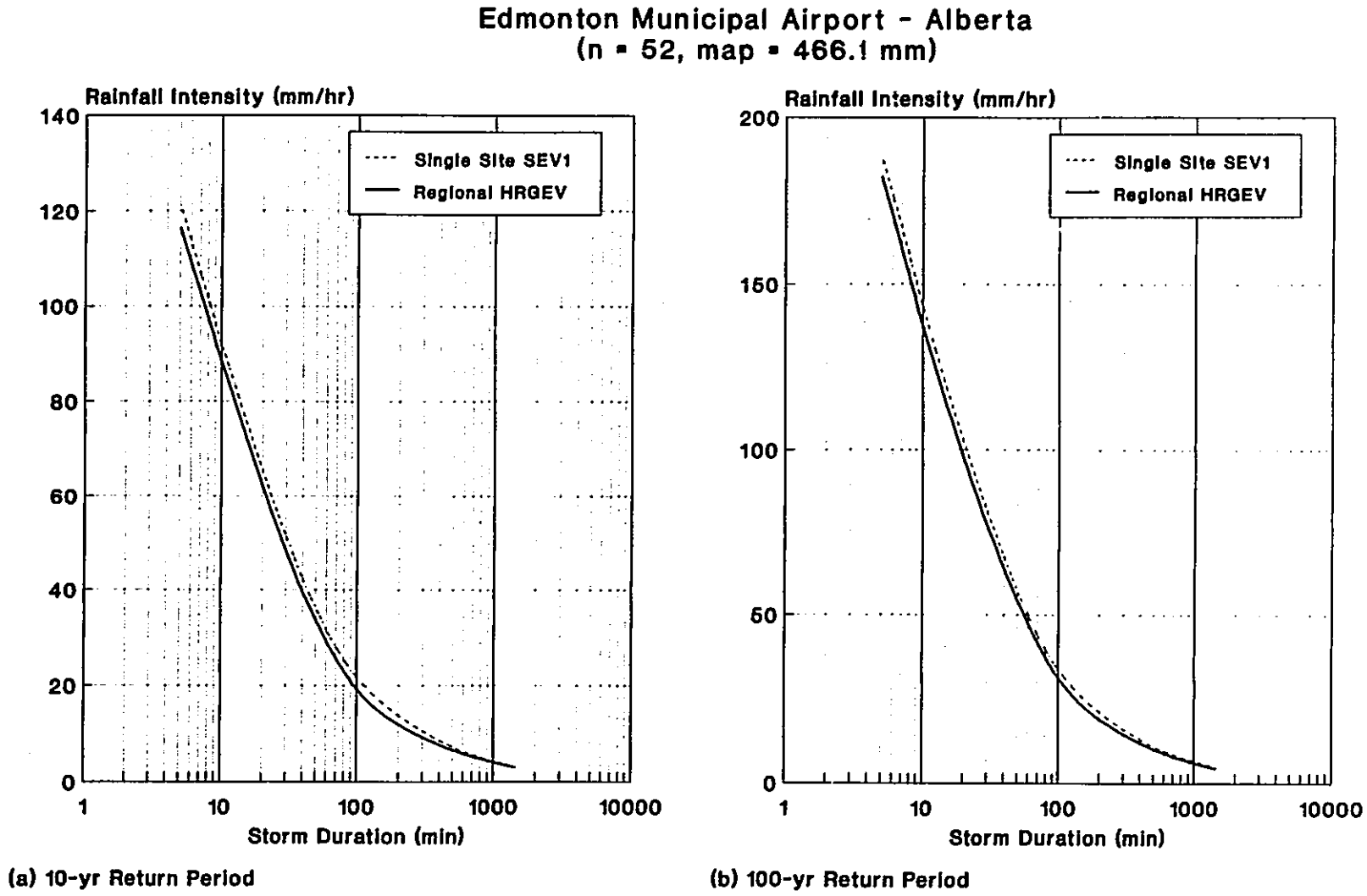

Figure 4.11: Comparison of IDF Curves Estimated by the HRGEV and SEV1 Models at the Long-Term Record Station - 3012208

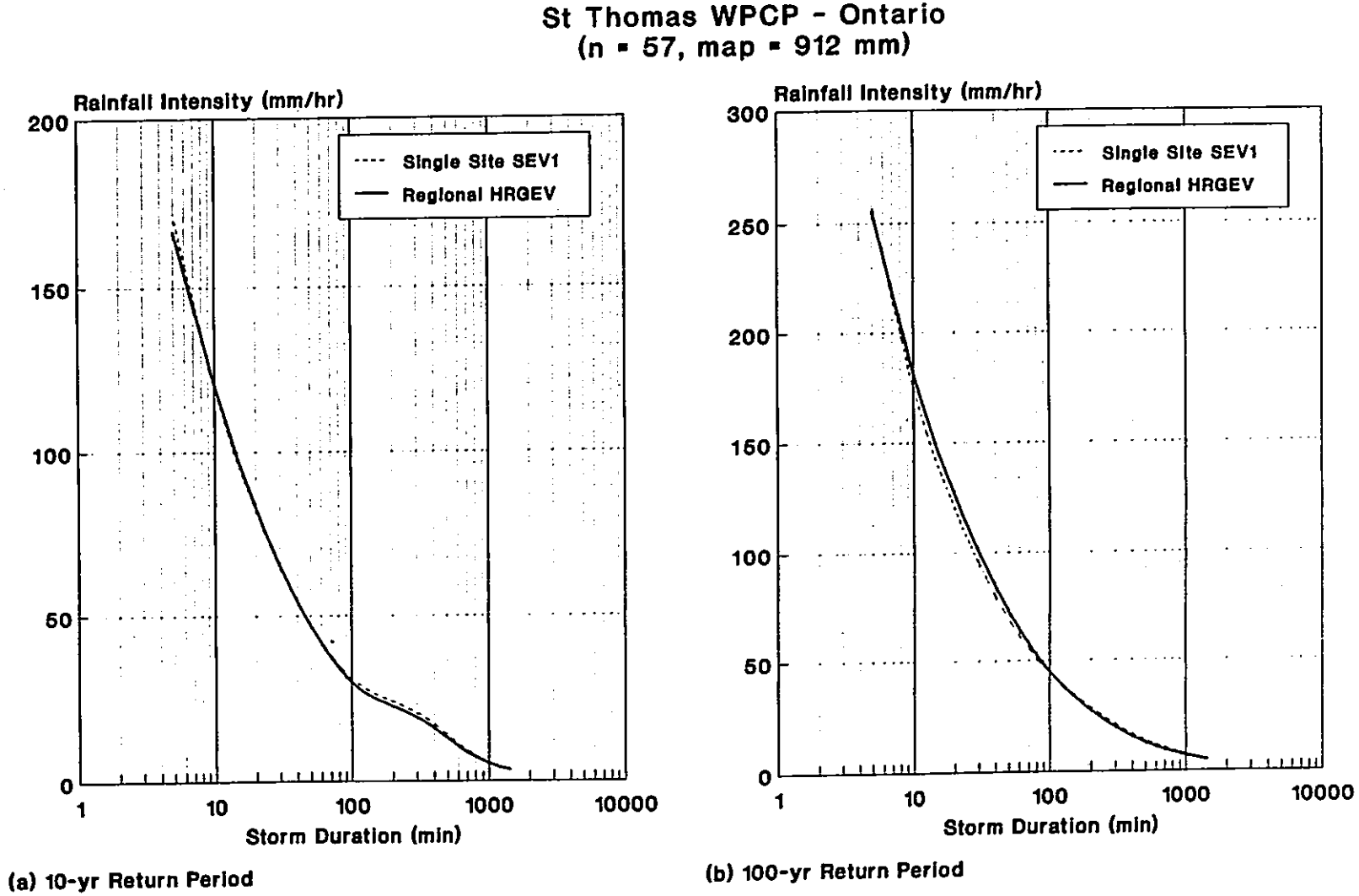

Figure 4.12: Comparison of IDF Curves Estimated by the HRGEV SEV1 Models at the Long-Term Record Station - 6137362

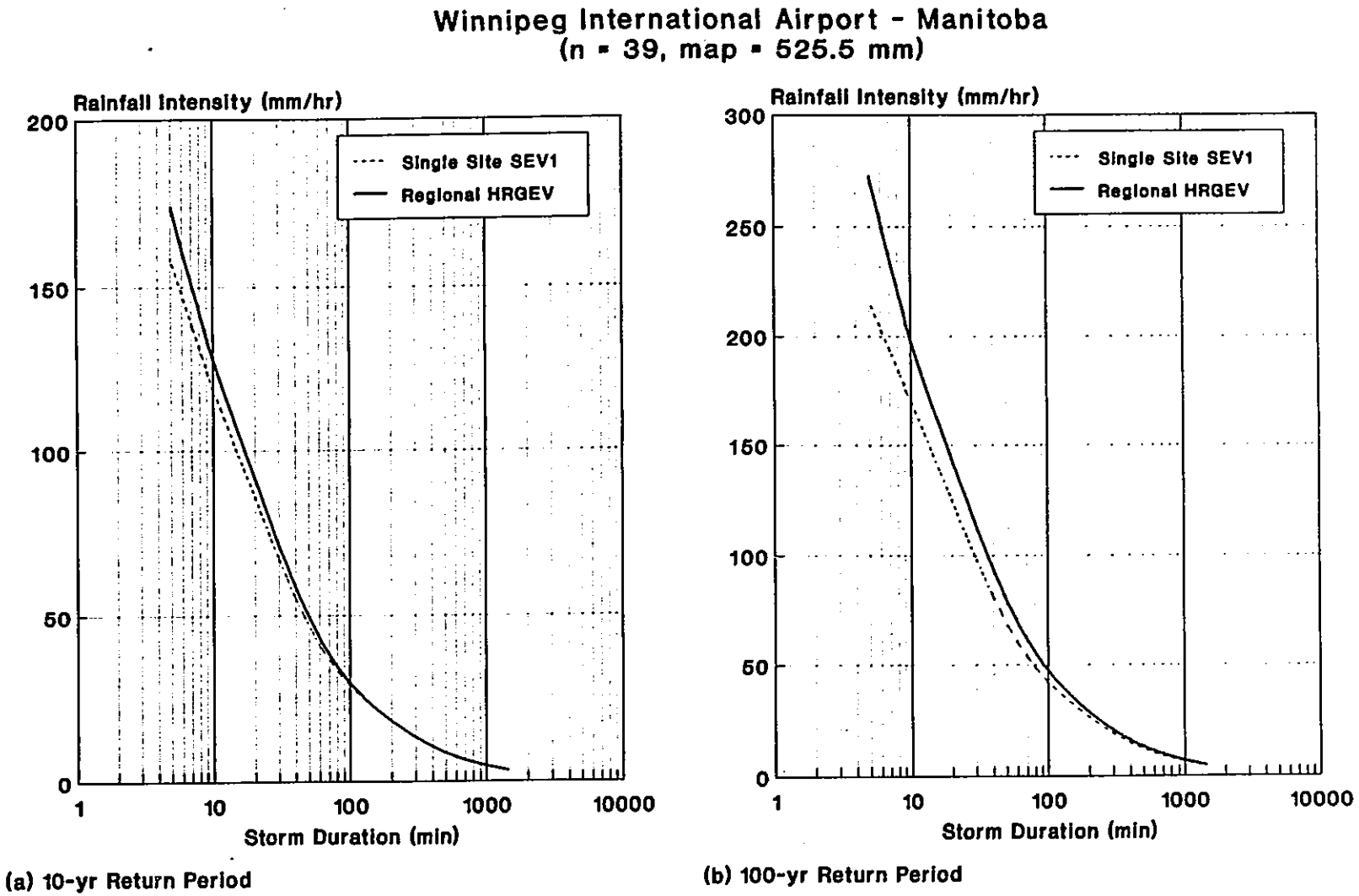

Figure 4.13: Comparison of IDF Curves Estimated by the HRGEV and SEV1 Models at the Long-Term Record Station - 5023222

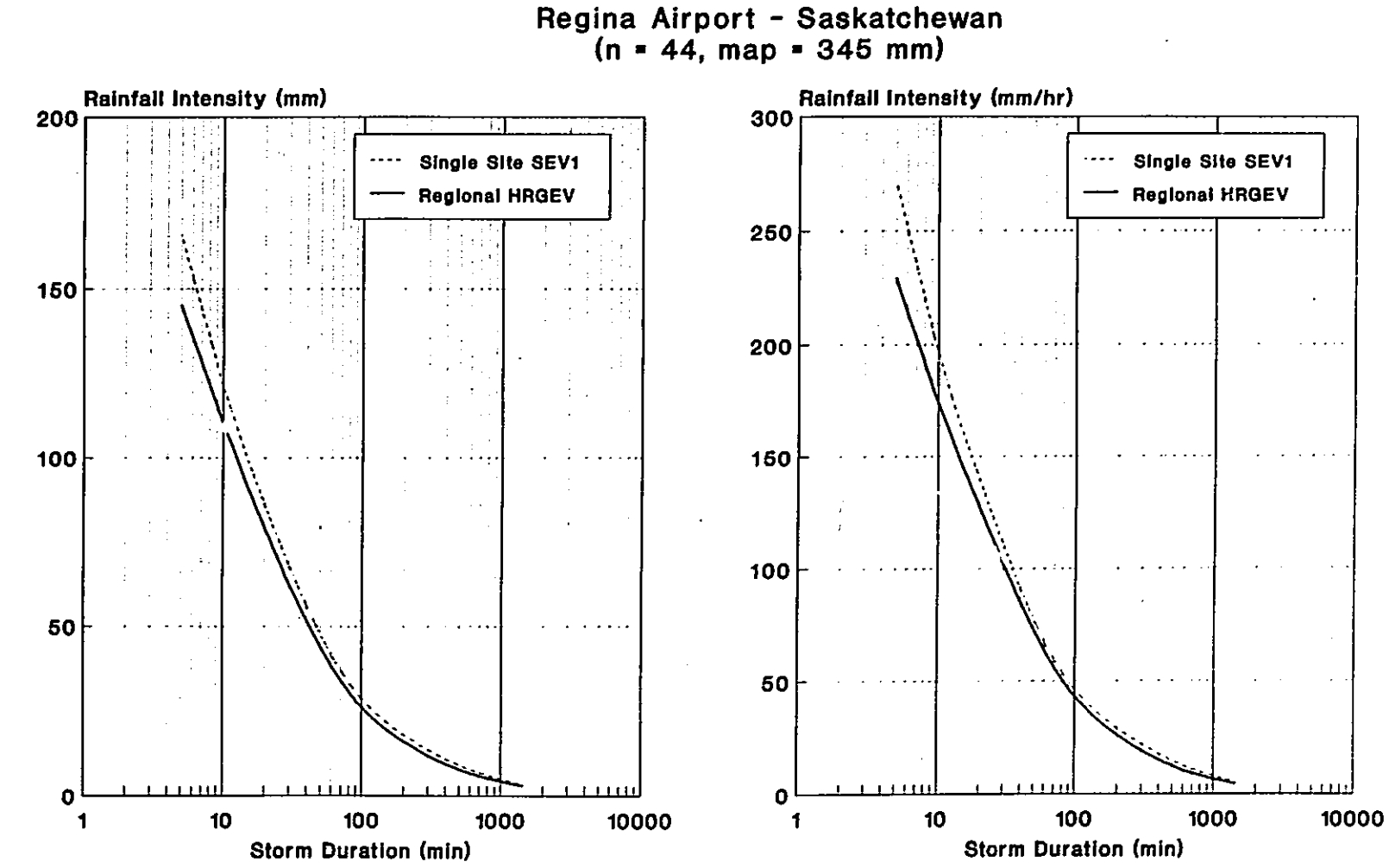

Figure 4.14: Comparison of IDF Curves Estimated by the HRGEV SEV1 Models at the Long-Term Record Station - 4016560

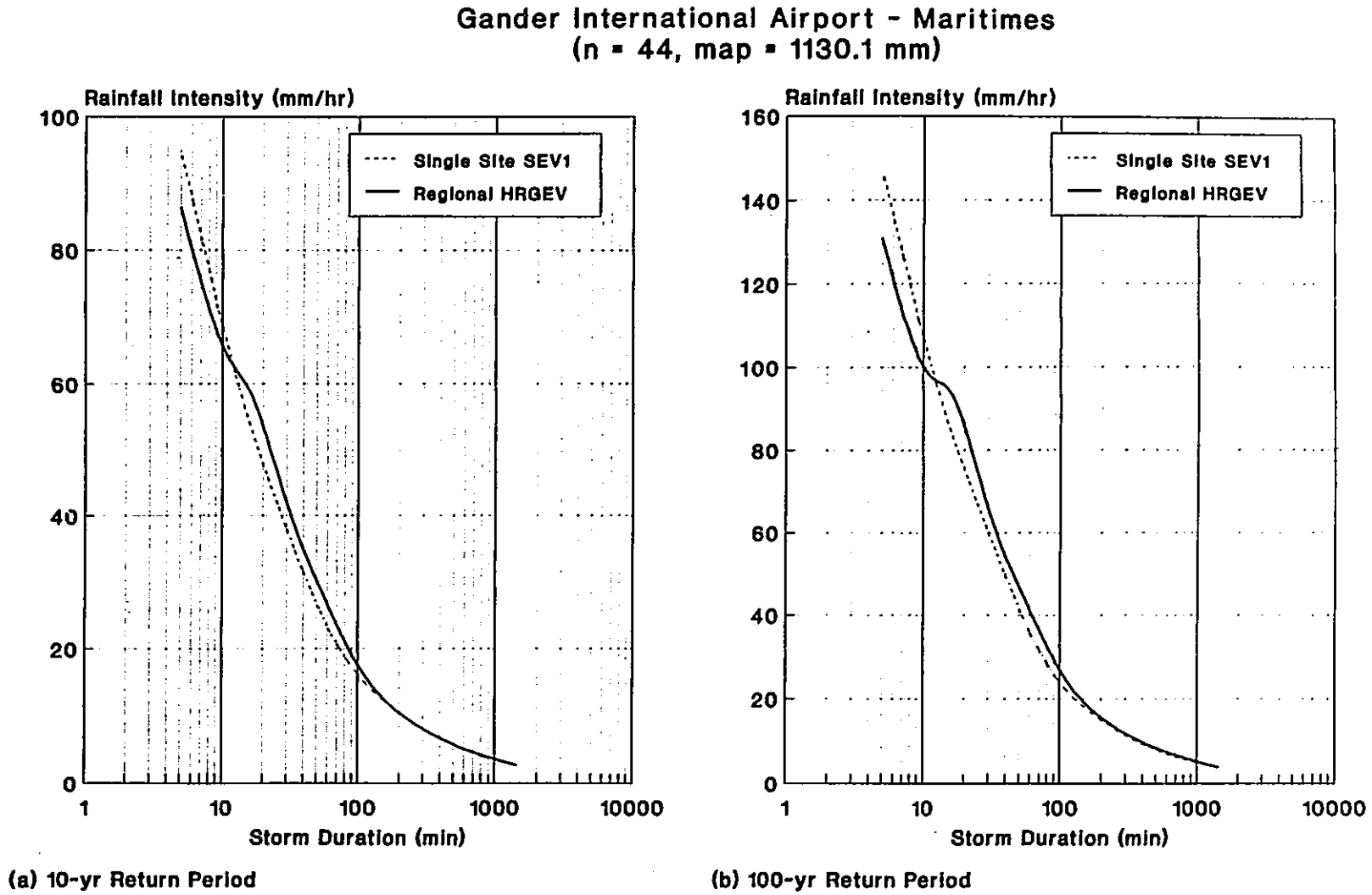

Figure 4.15: Comparison of IDF Curves Estimated by the HRGEV and SEV1 Models at the Long-Term Record Station - 8401700

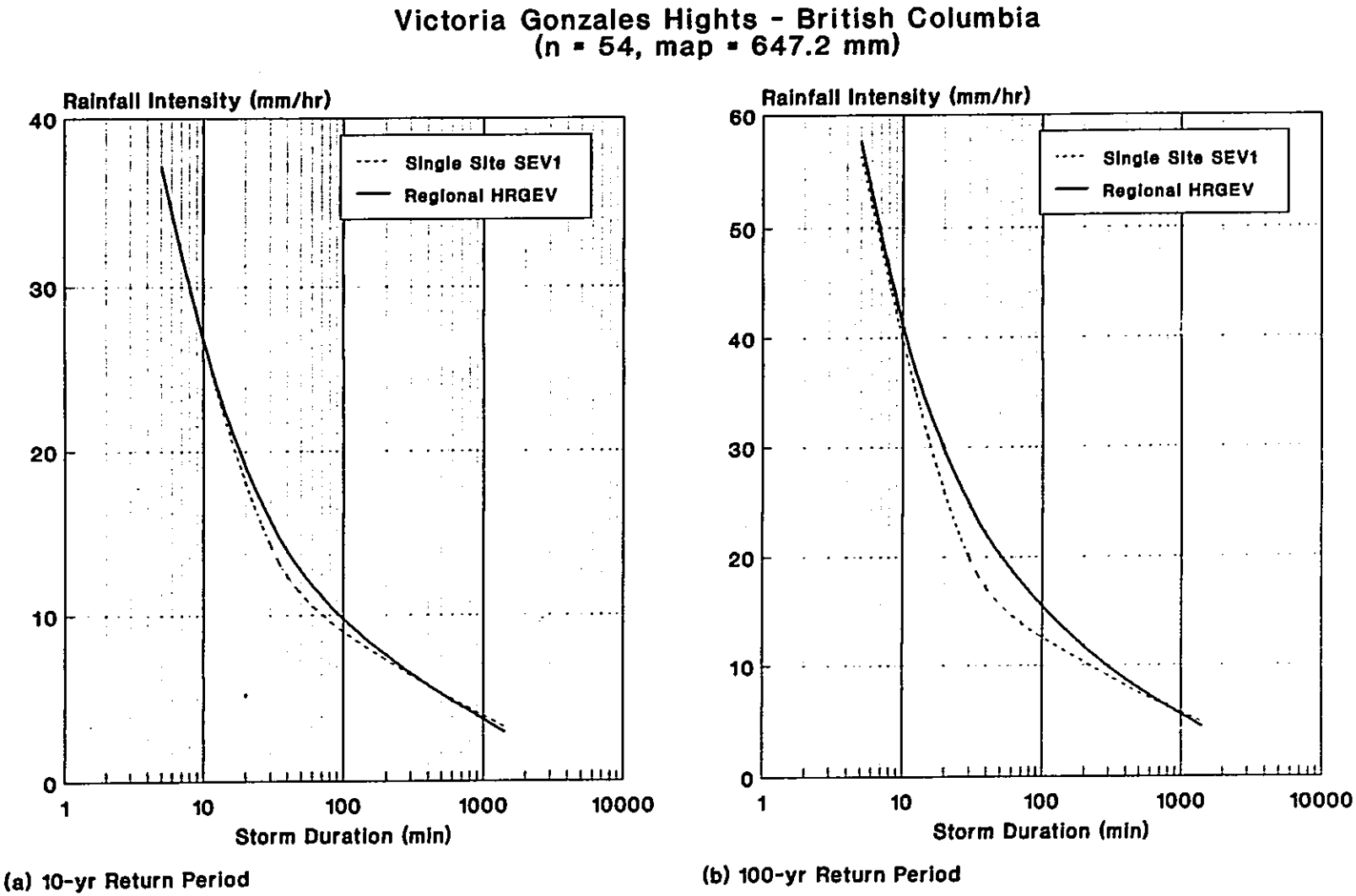

Figure 4.16: Comparison of IDF Curves Estimated by the HRGEV and SEV1 Models at the Long-Term Record Station - 1018610

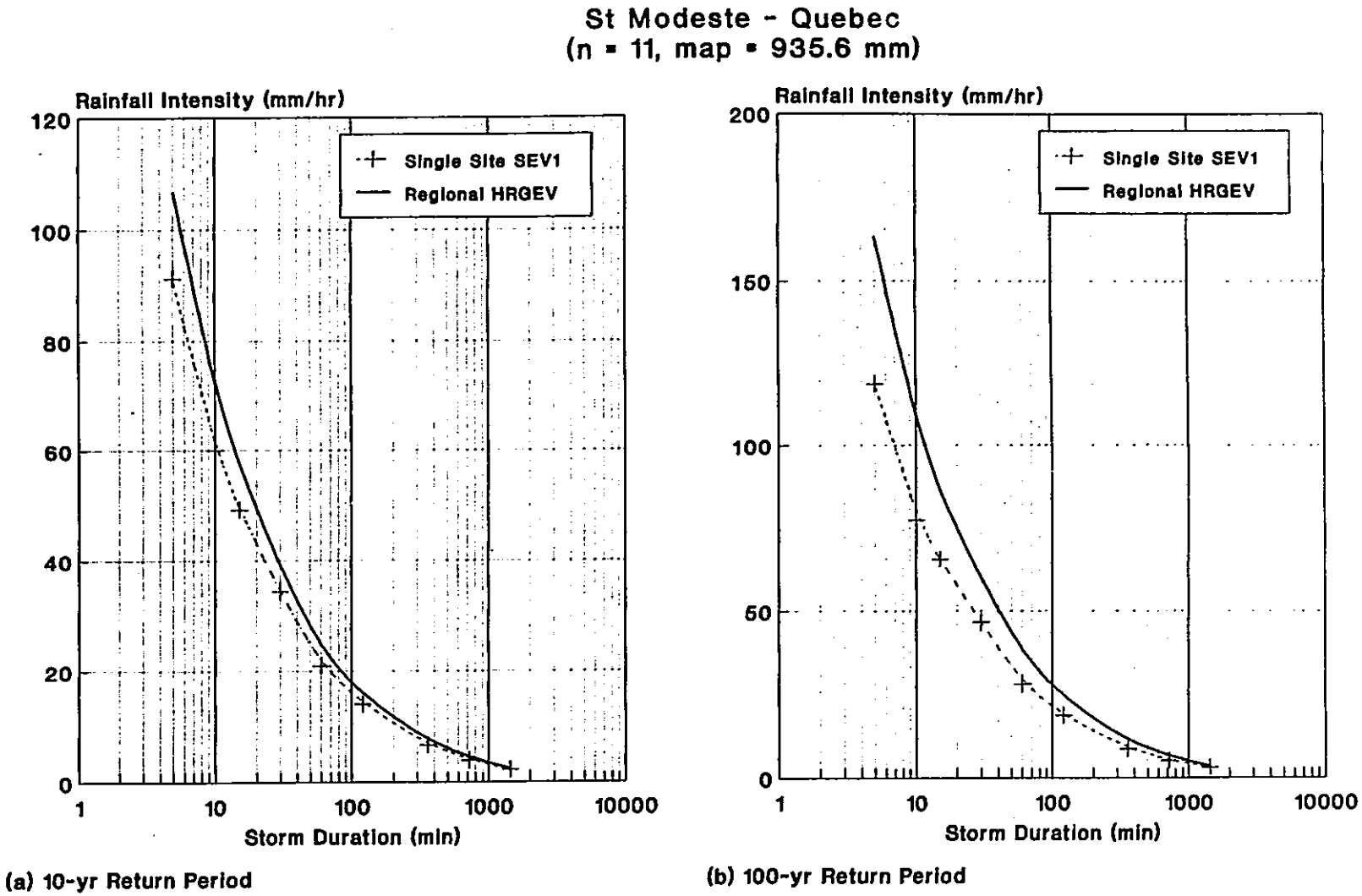

Figure 4.17: Comparison of IDF Curves Estimated by the HRGEV and SEV1 Models at the Short-Term Record Station - 7057574

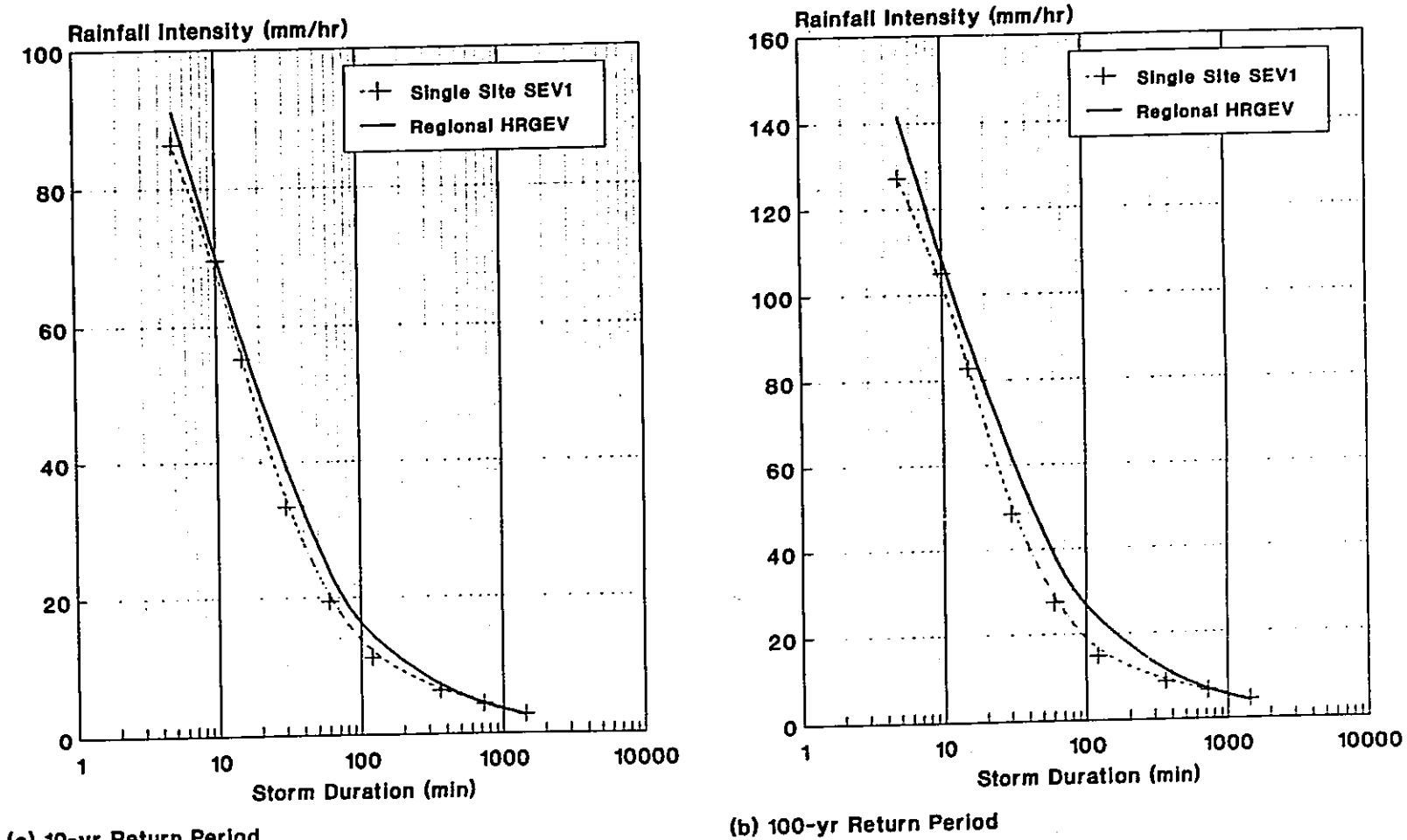

Figure 4.18: Comparison of IDF Curves Estimated by the HRGEV and SEV1 Models at the Short-Term Record Station - 3066001

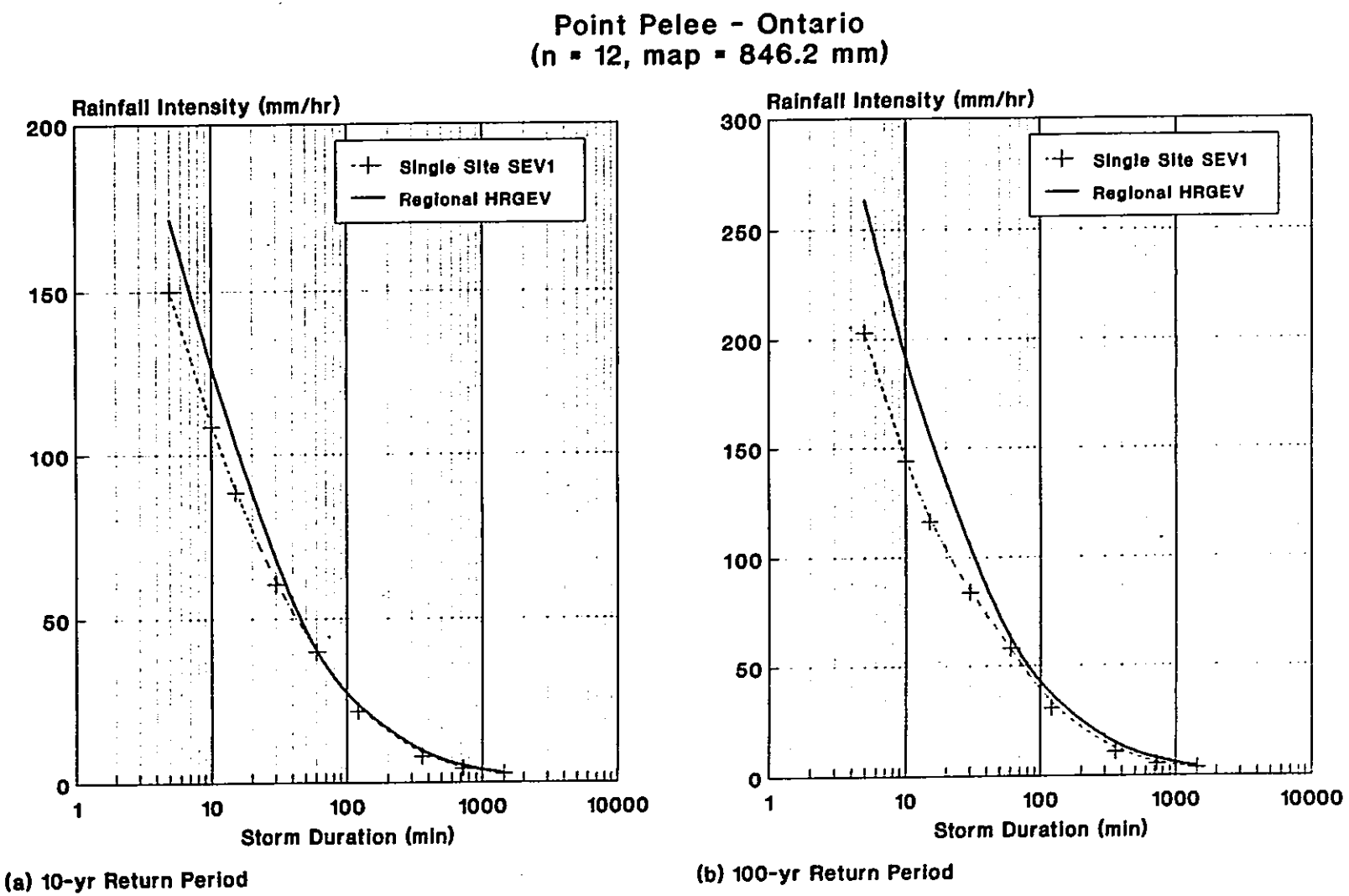

Figure 4.19: Comparison of IDF Curves Estimated by the HRGEV and SEV1 Models at the Short-Term Record Station - 613FN58

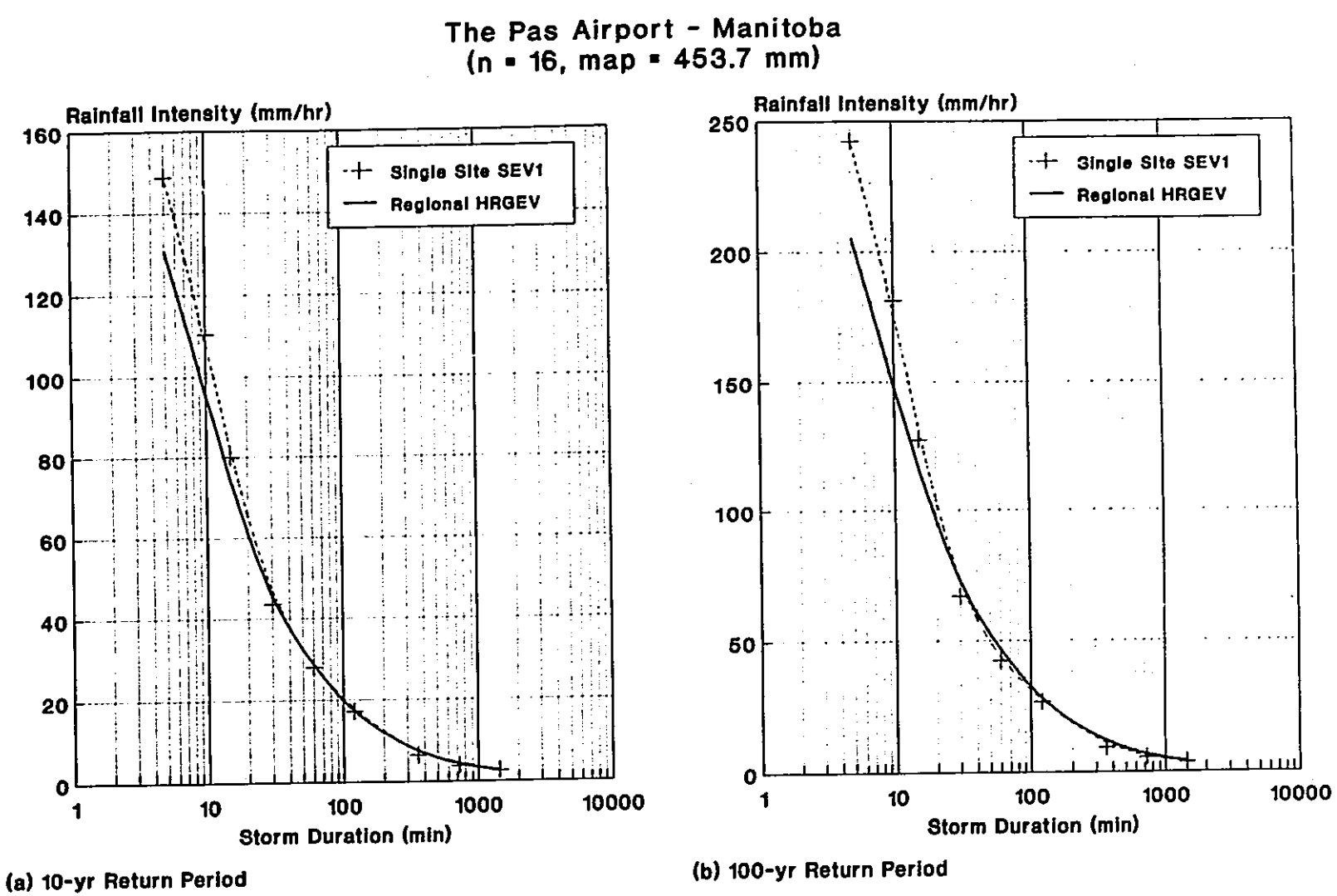

Figure 4.20: Comparison of IDF Curves Estimated by the HRGEV and SEV1 Models at the Short-Term Record Station - 5052880

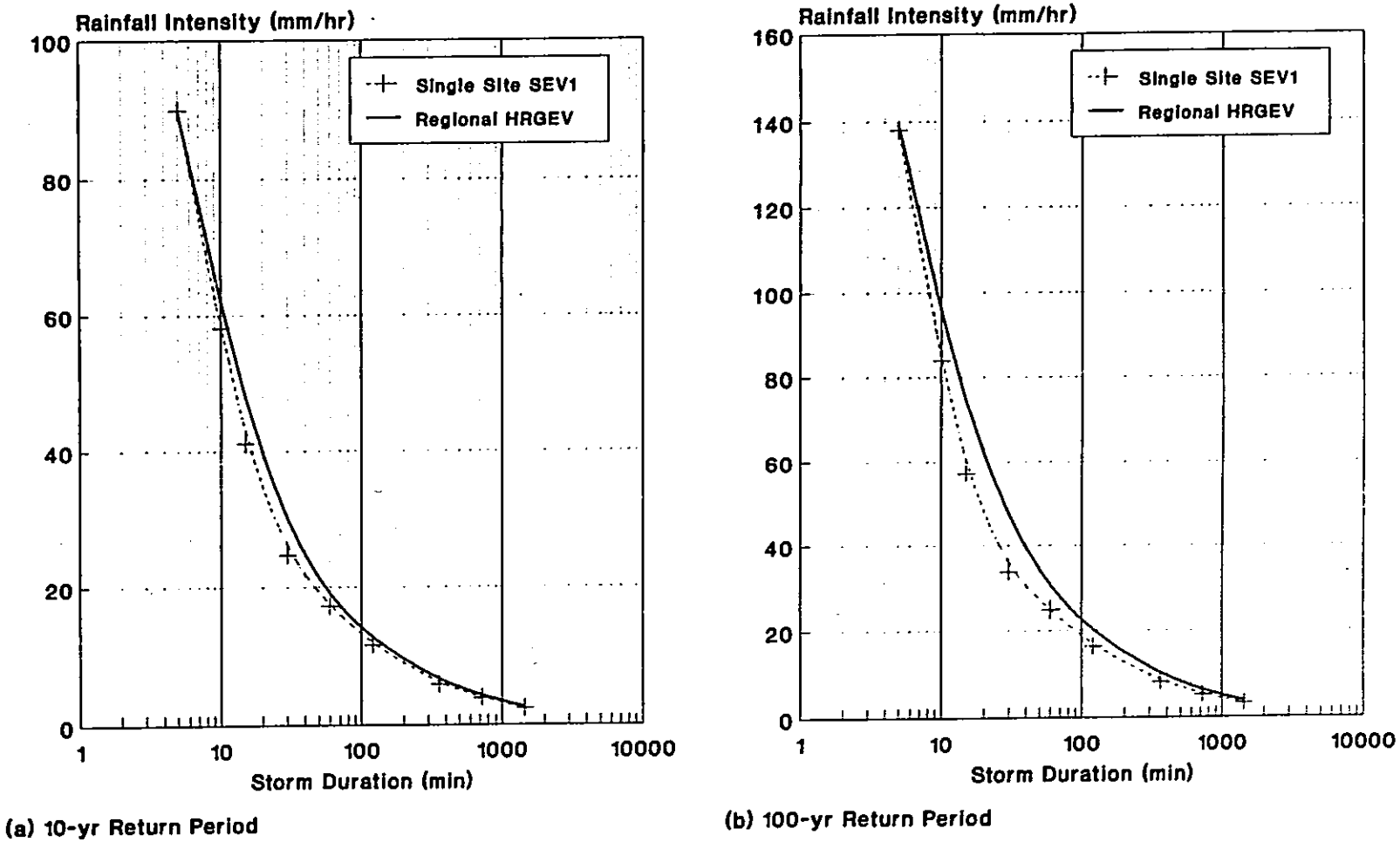

Figure 4.21: Comparison of IDF Curves Estimated by the HRGEV and SEV1 Models at the Short-Term Record Station - 4061630

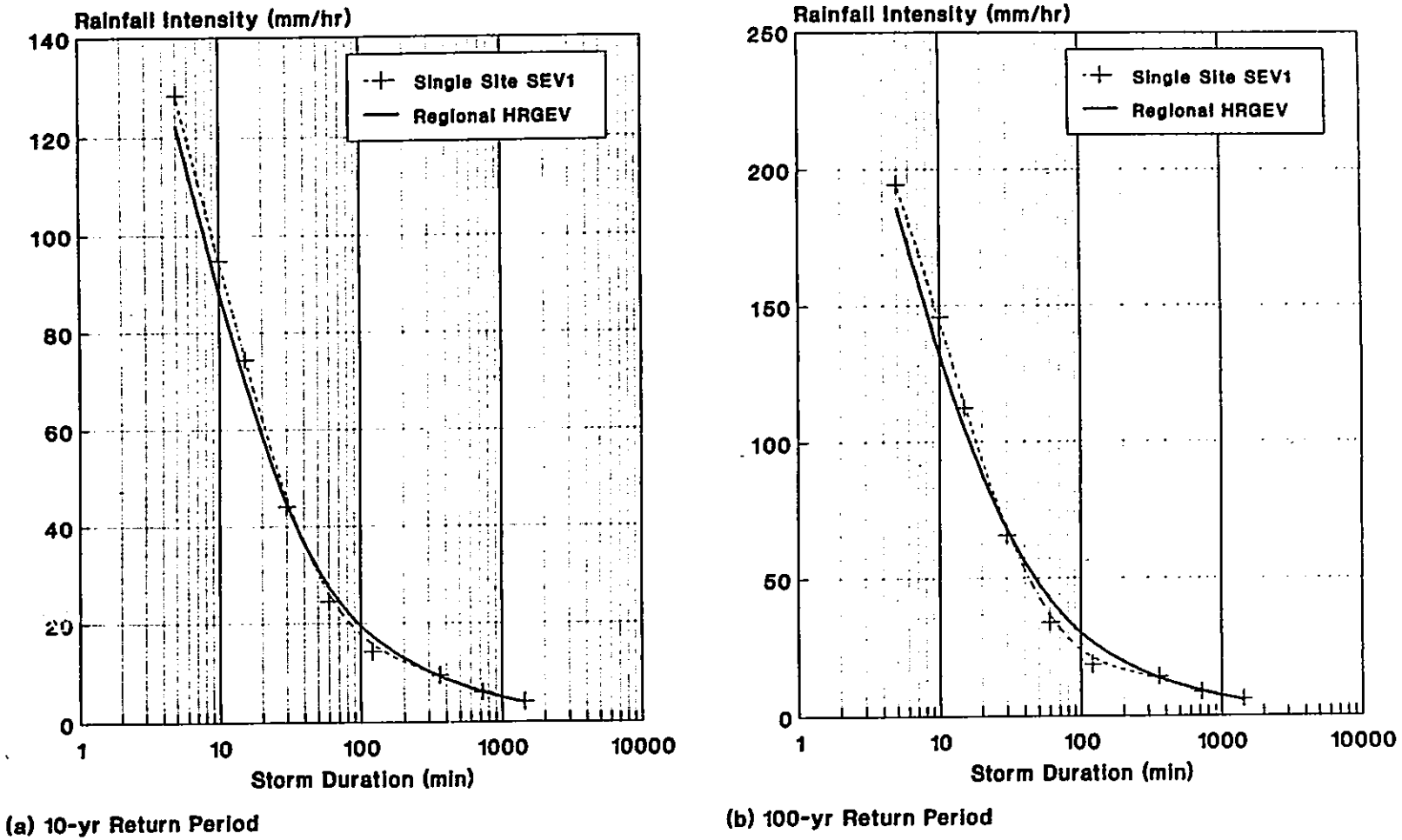

Figure 4.22: Comparison of IDF Curves Estimated by the HRGEV and SEV1 models at the Short-Term Record Station - 8100512

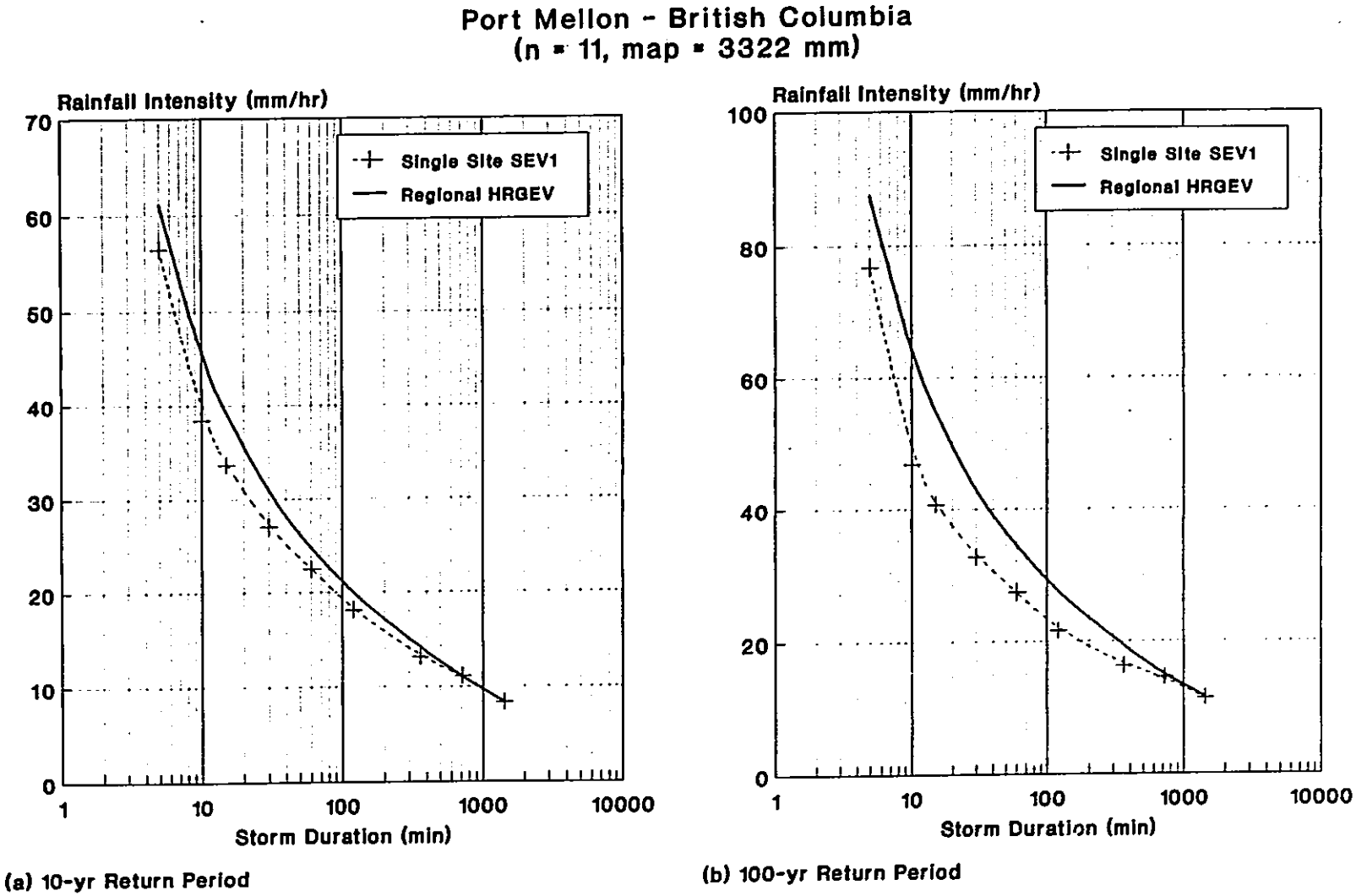

Figure 4.23: Comparison of IDF Curves Estimated by the HRGEV and SEV1 Models at the Short-Term Record Station 1046330

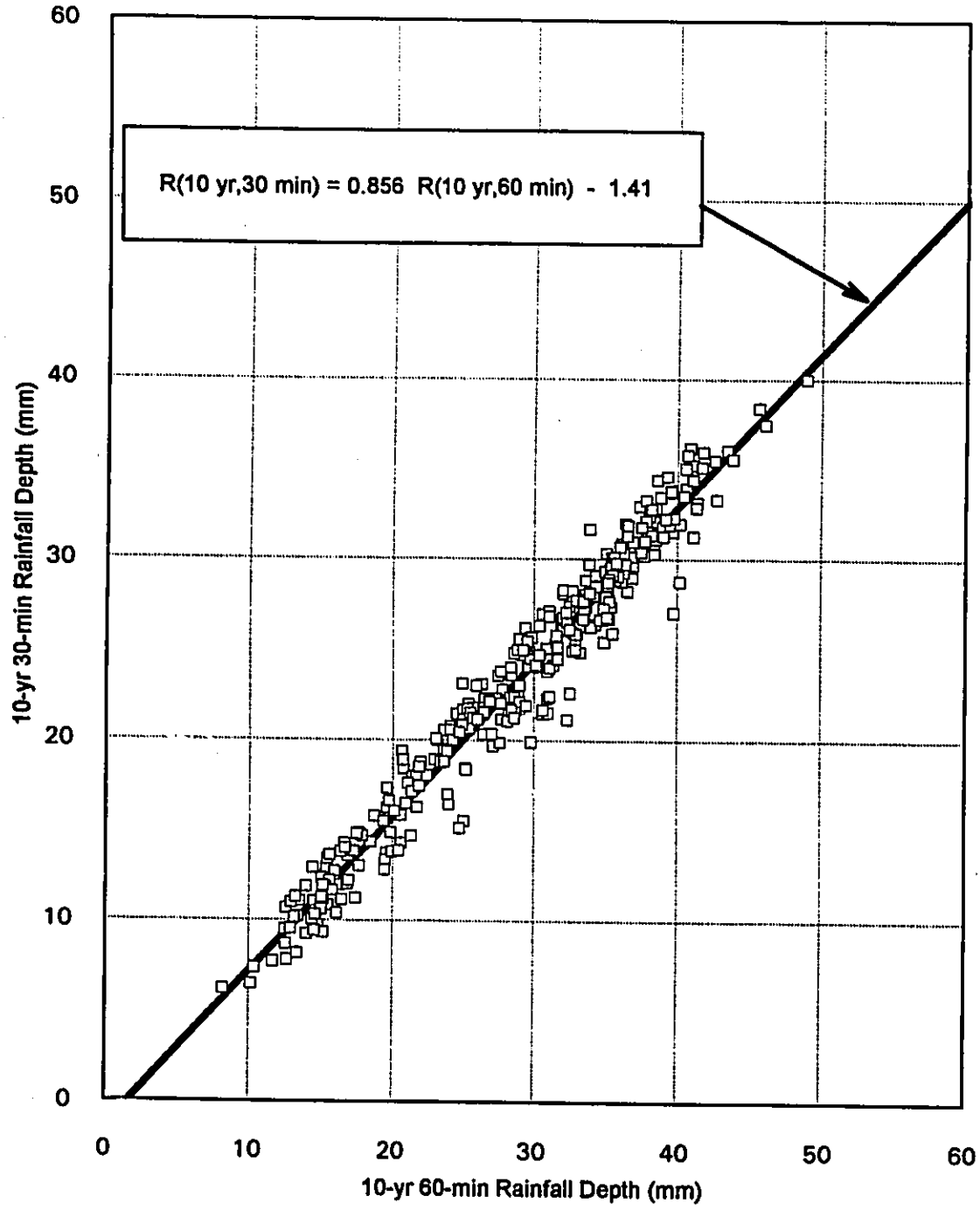

Figure 4.24: Depth-Duration Linear Relationship for the 10-yr 30-min Storm, with 60 minutes as the Base Duration

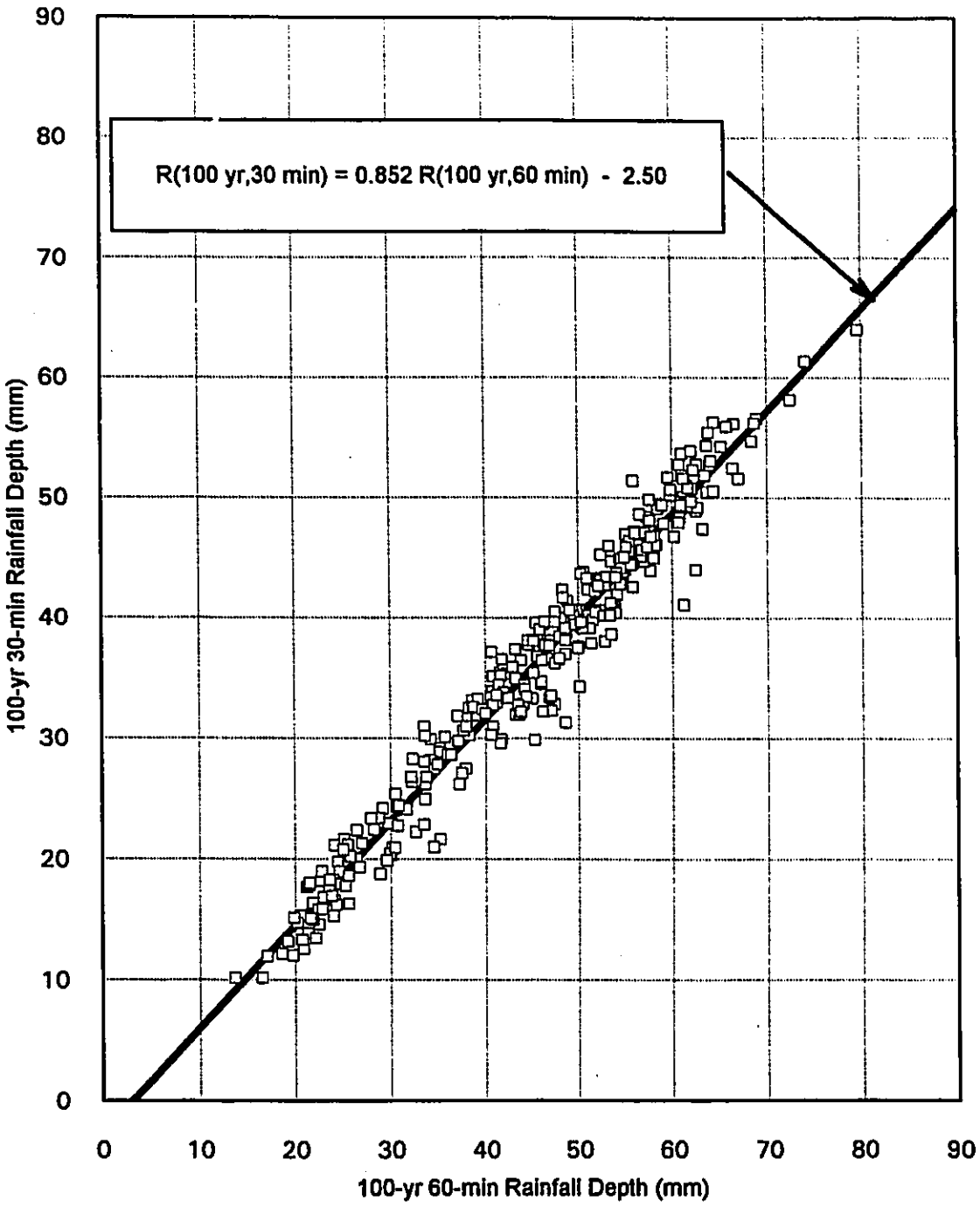

Figure 4.25: Depth-Duration Linear Relationship for the 100-yr 30-min Storm, with 60 minutes as the Base Duration

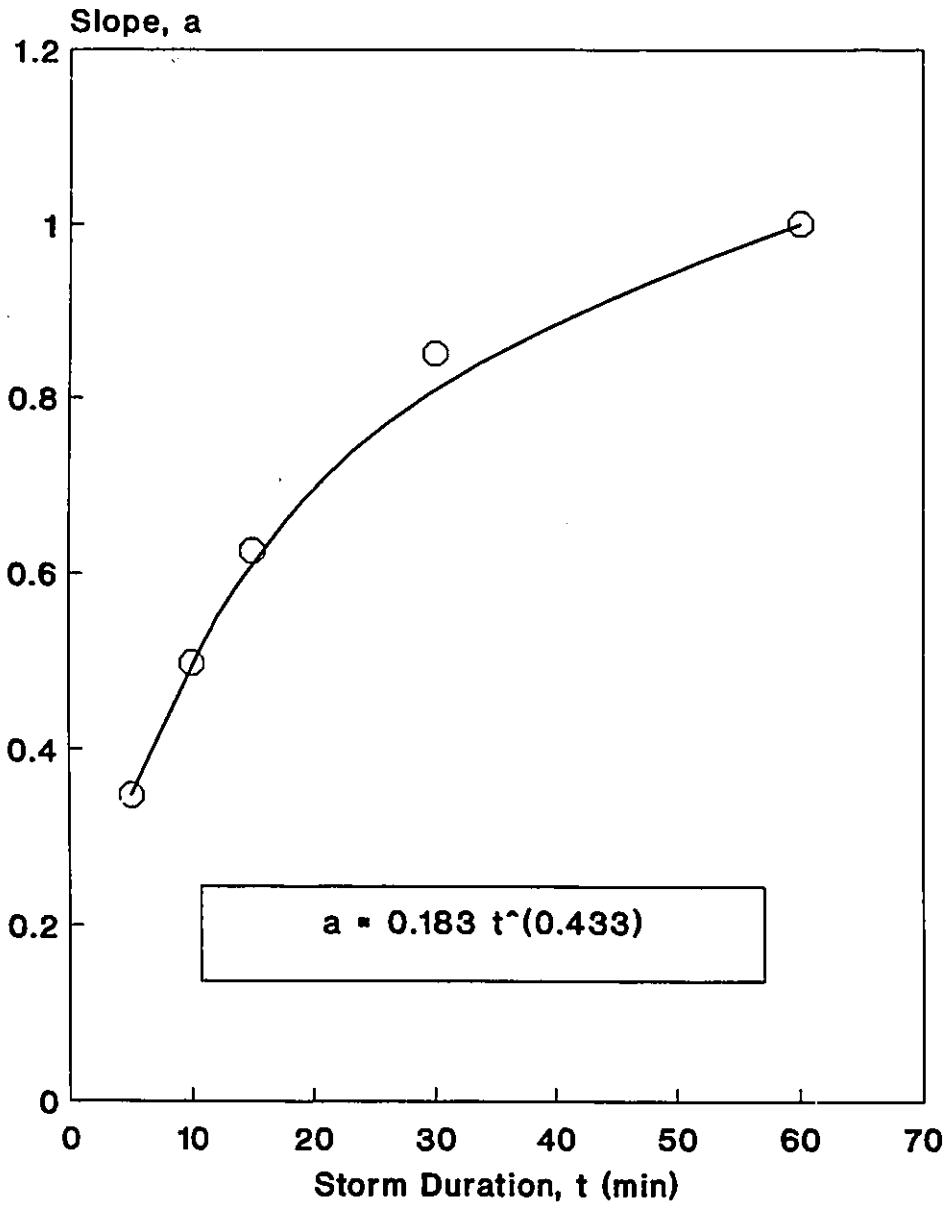

Figure 4.26: Slope 'a' in the Linear Depth-Duration Relation (equation 4.3) as a Function of Storm Duration

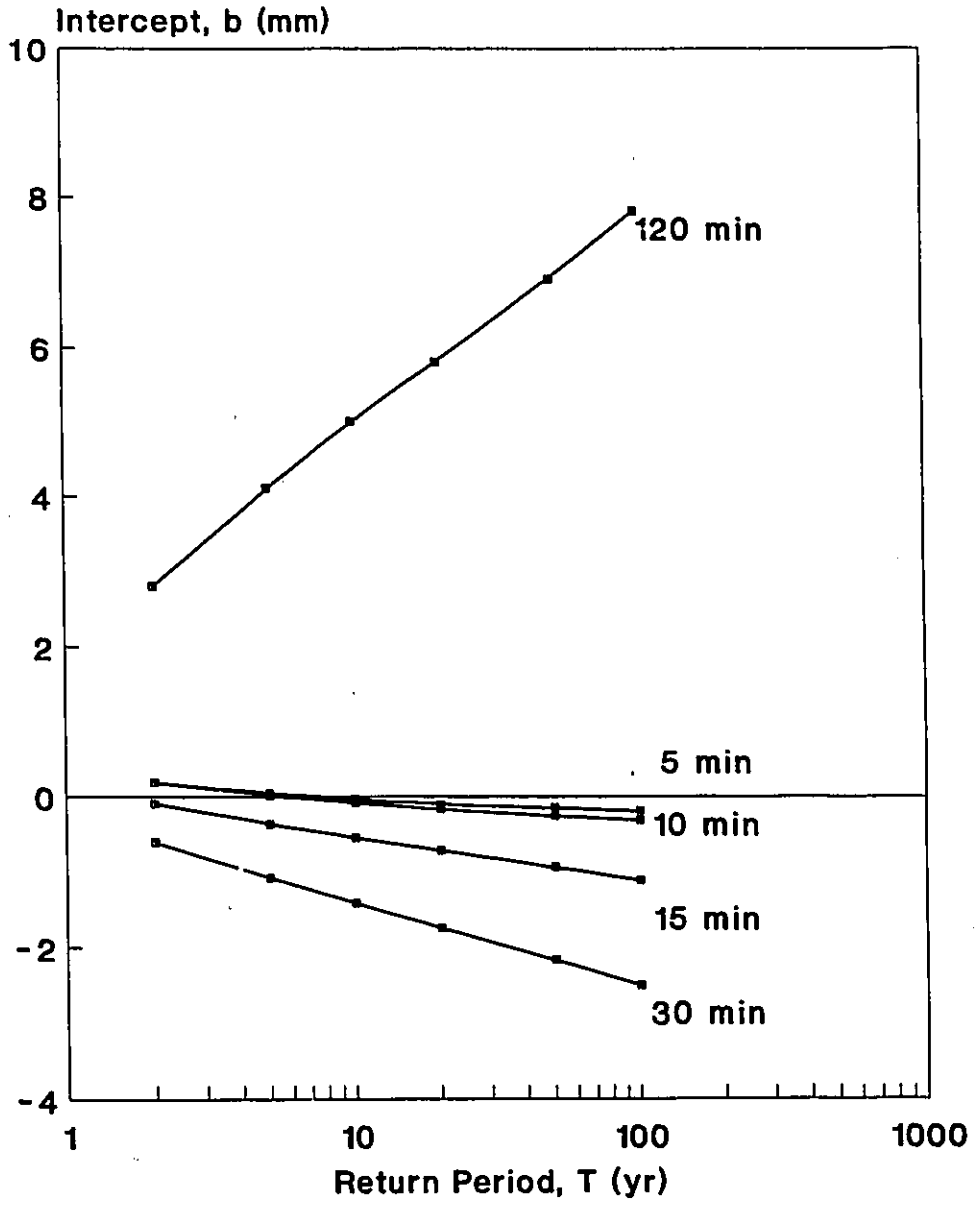

Figure 4.27: Intercept 'b' in Linear Depth-Duration Relation (equation 4.4) as a Function of Return Period for Various Storm Durations.

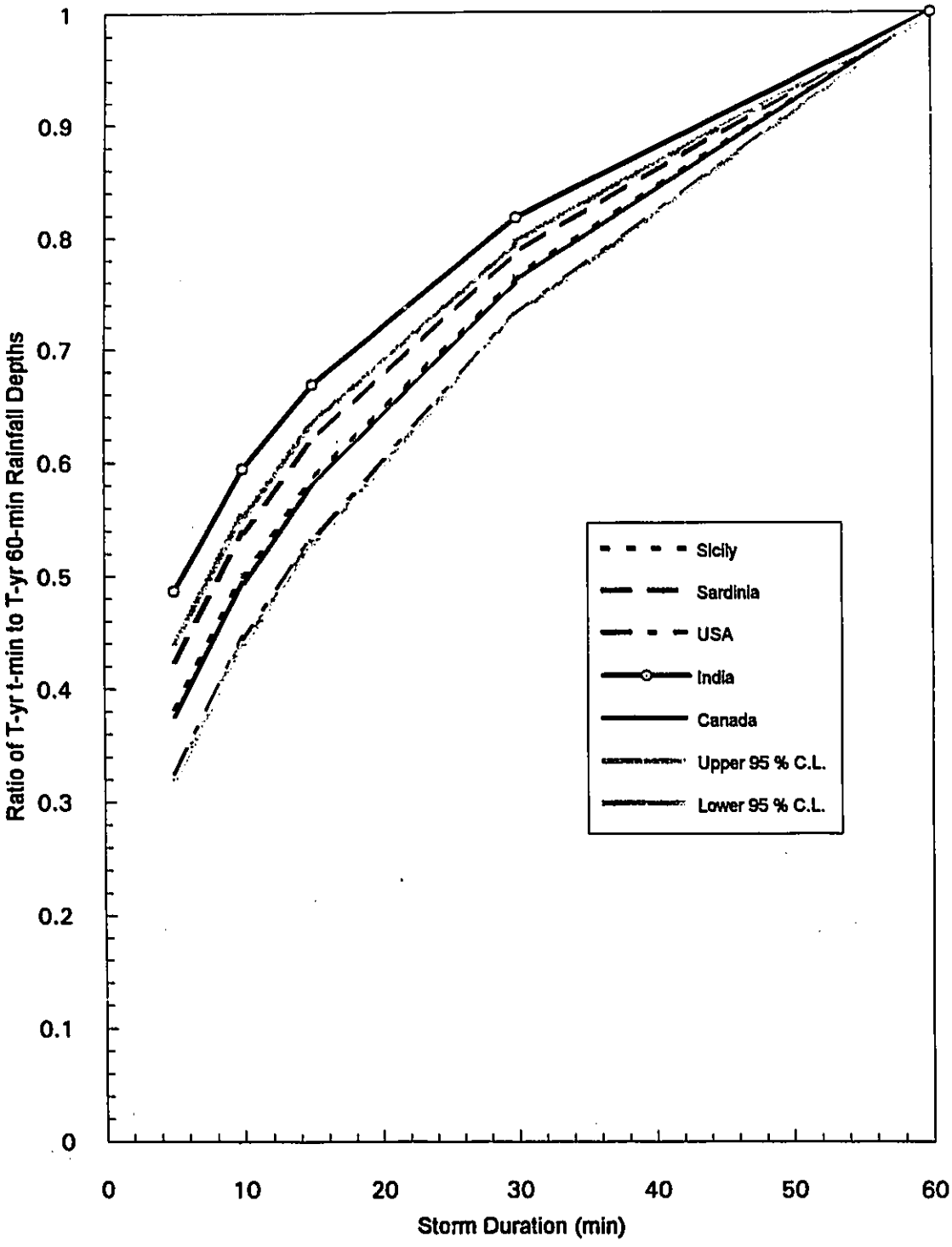

Figure 4.28: Comparison of Depth-Duration Ratios for Canada and for other Countries

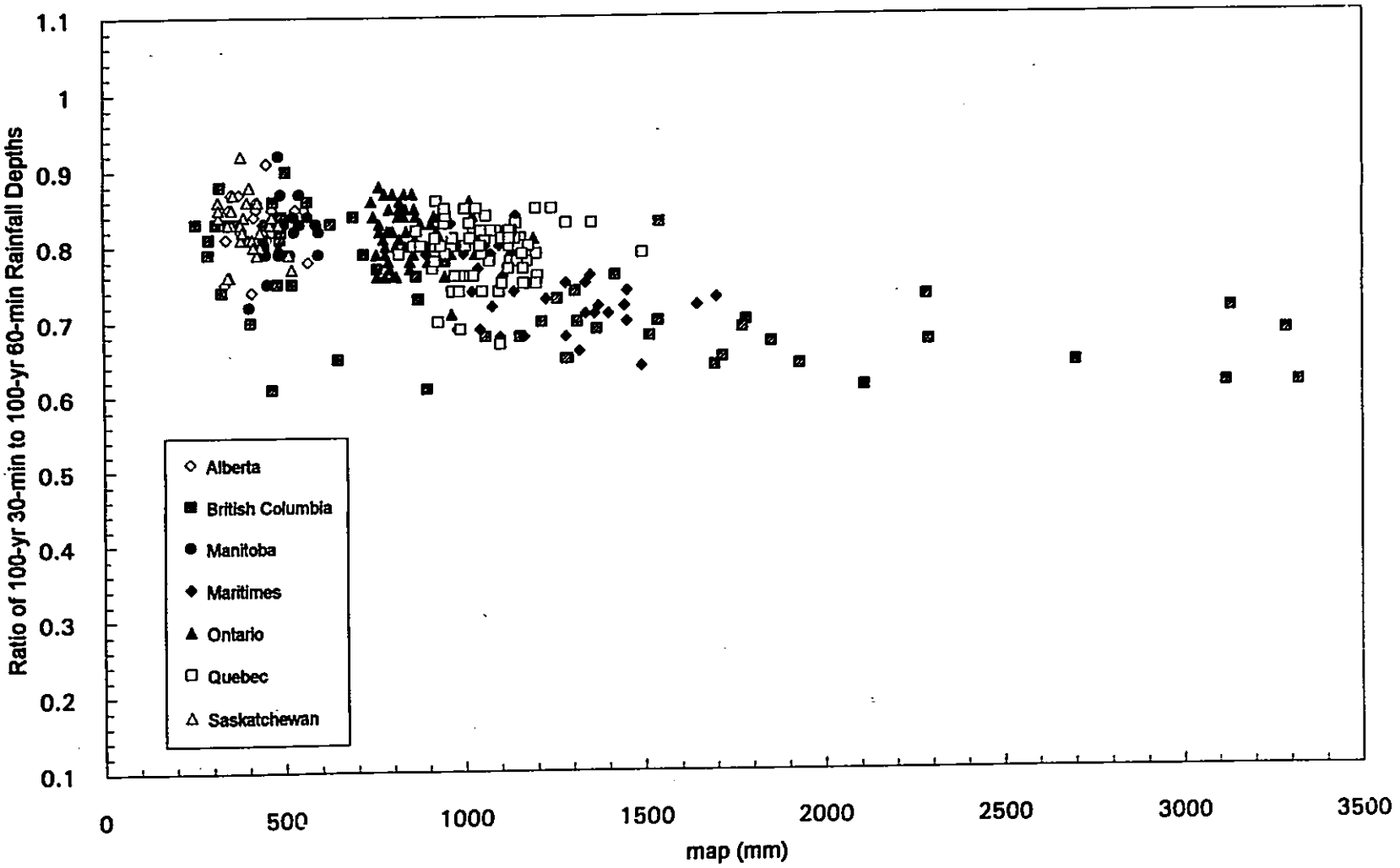

Figure 4.29: Ratio of 30-min to 60-min Rainfall Depths for the 100-yr Return Period as a Function of map

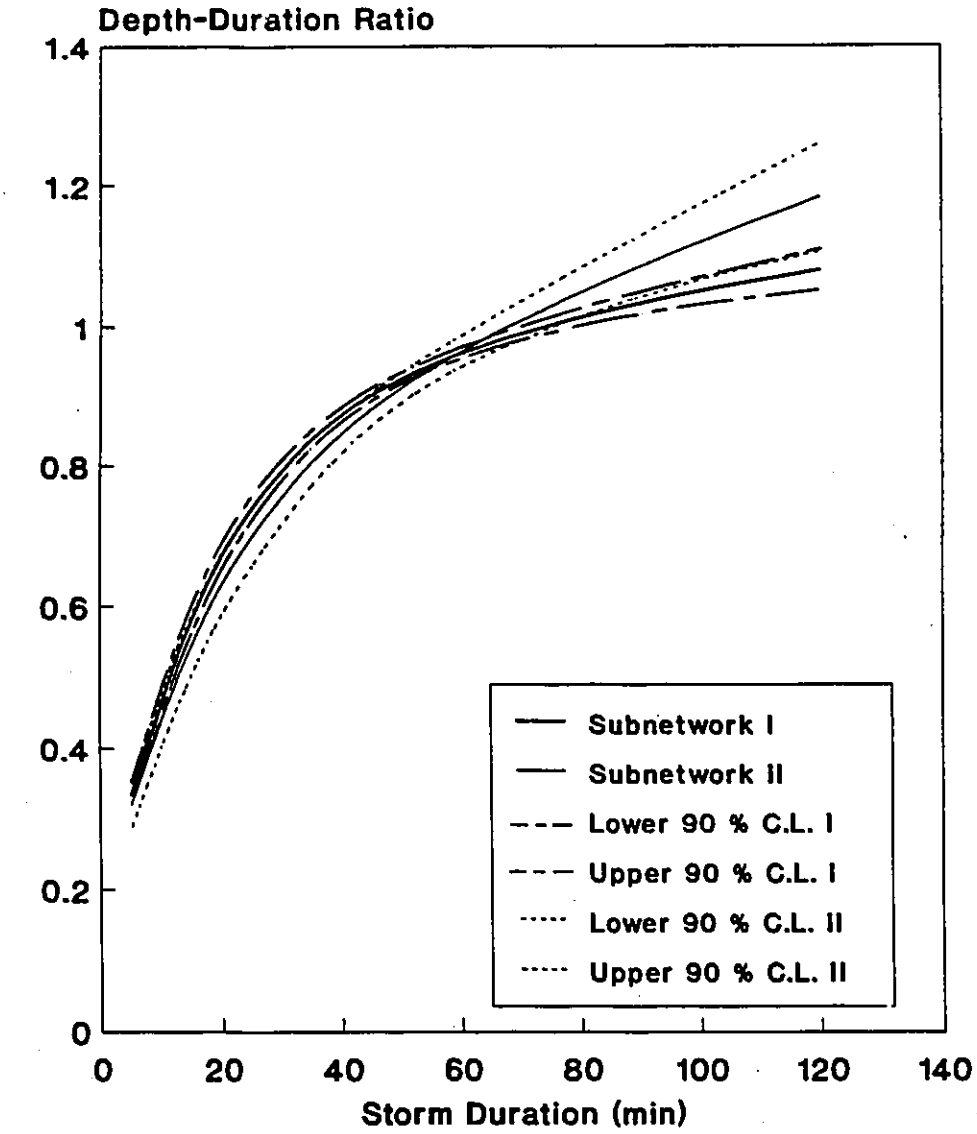

Figure 4.30: The 90 % Confidence Limits on Computed Regional Depth-Duration Ratios for Two Network of Sites Delineated Based on map Values

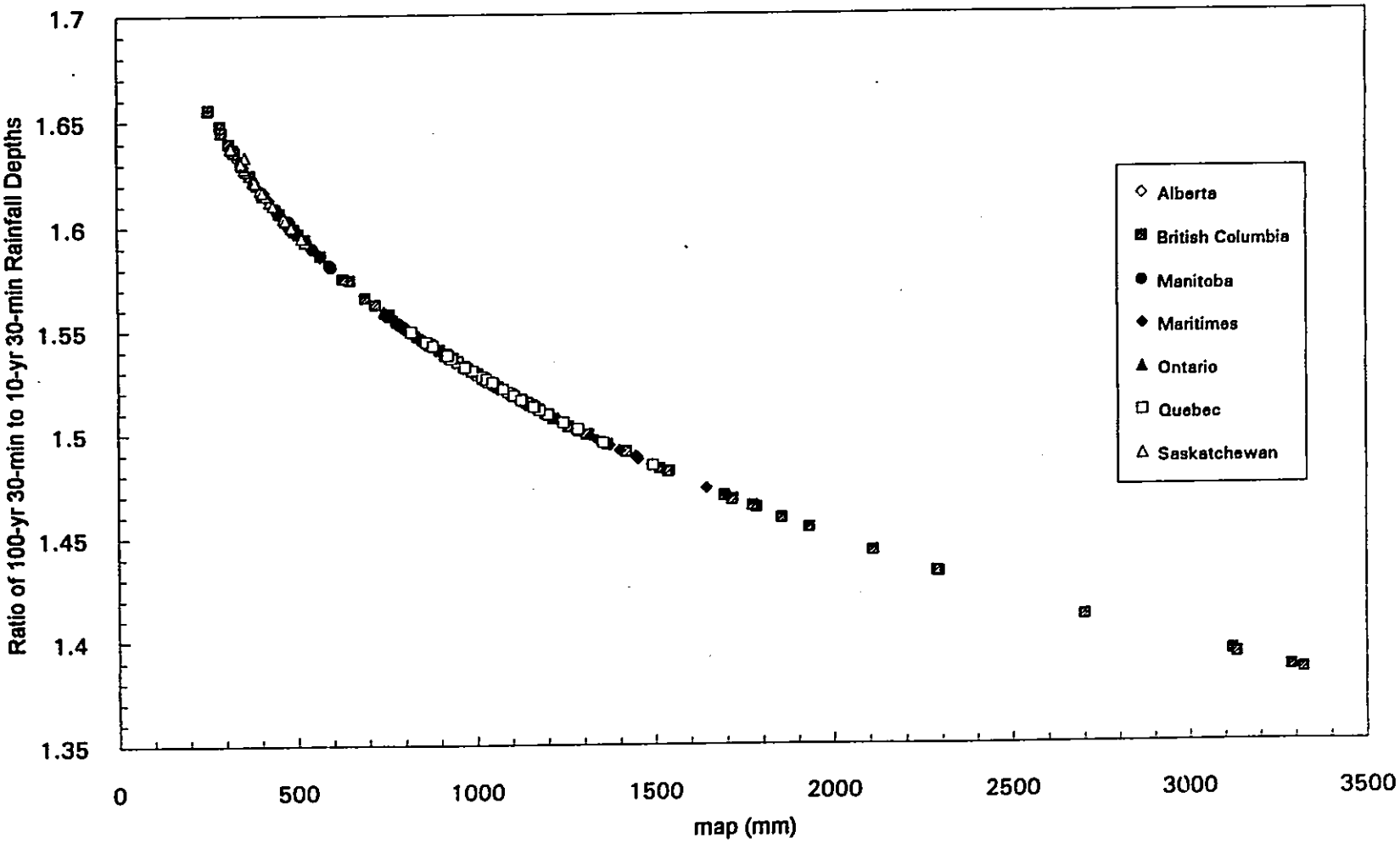

Figure 4.31: Ratio of 100-yr to 10-yr Rainfall Depths for the 30-min Storm as a Function of map

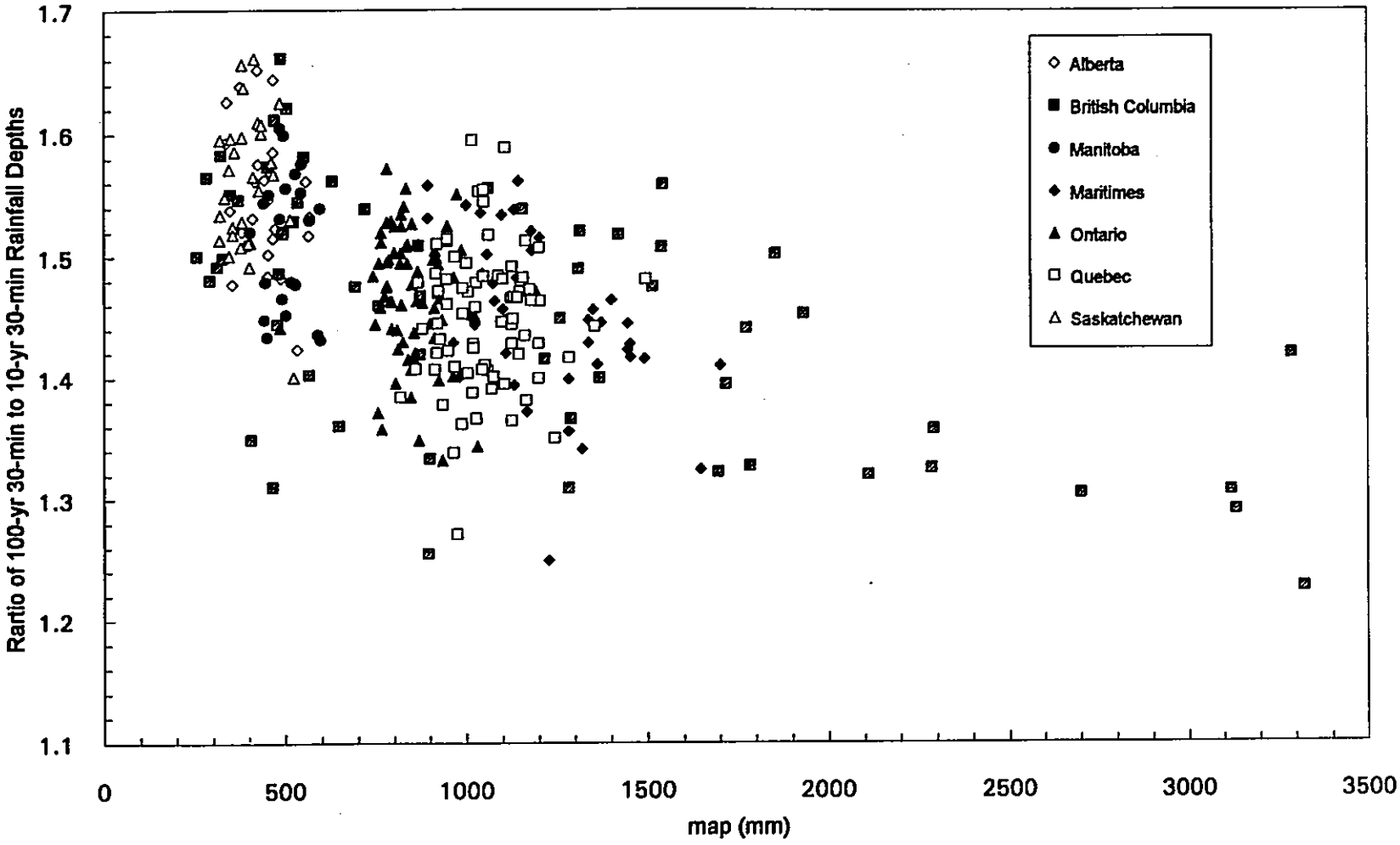

Figure 4.32: SEV1 Based Ratio of 100-yr to 10-yr Rainfall Depths for the 30-min Storm as a Function of map

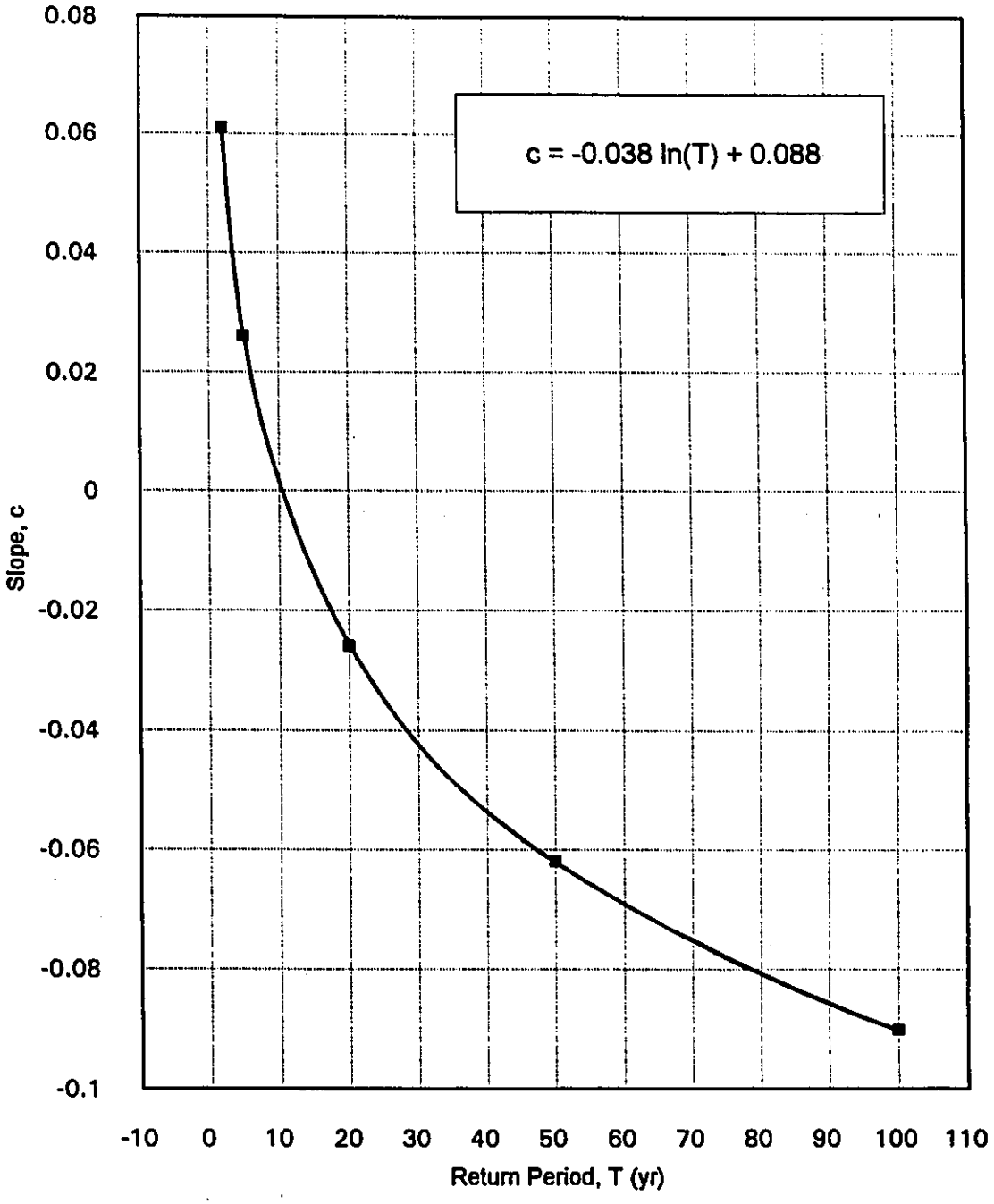

Figure 4.33: Slope 'c' in Depth-Frequency Logarithmic Relationship (Equation 4.10) as a Function of Return Period for Storm Durations of 5 to 120 minutes

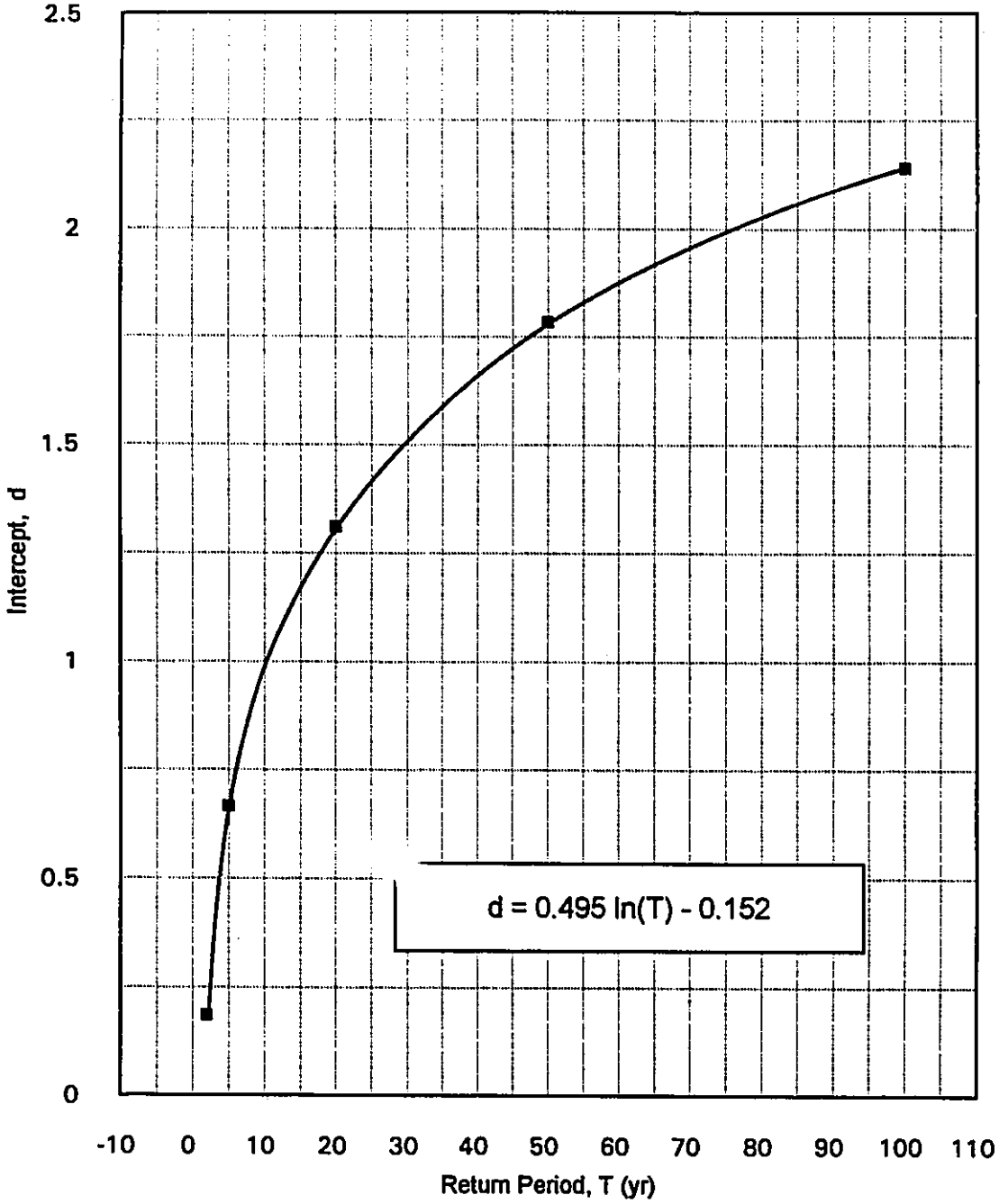

Figure 4.34: Intercept 'd' in Depth-Frequency Logarithmic Relationship (Equation 4.10) as a Function of Return Period for Storm Durations of 5 to 120 minutes

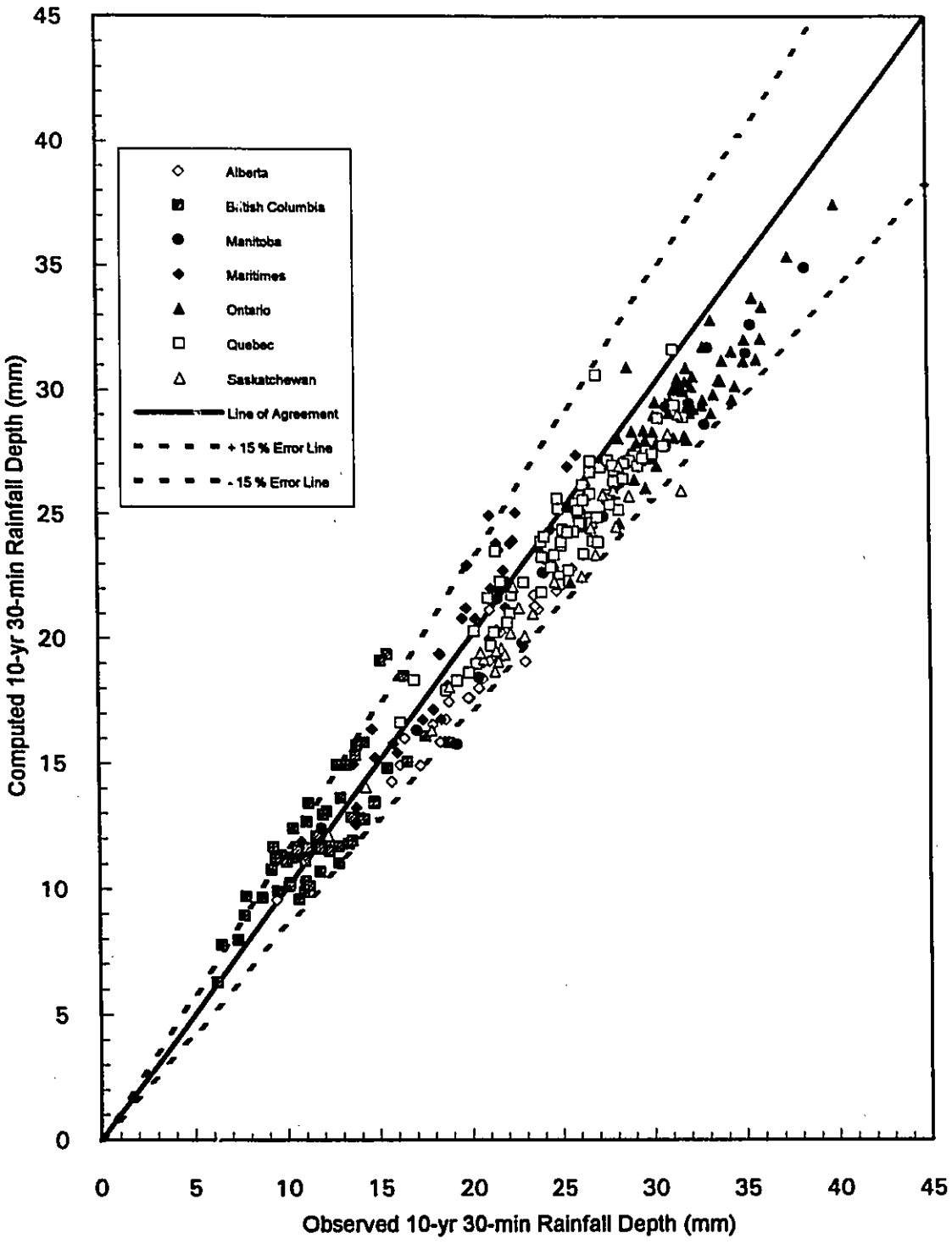

Figure 4.35: Performance of Proposed RDDF Equation (4.15) for the 10-yr 30-min Design Storm

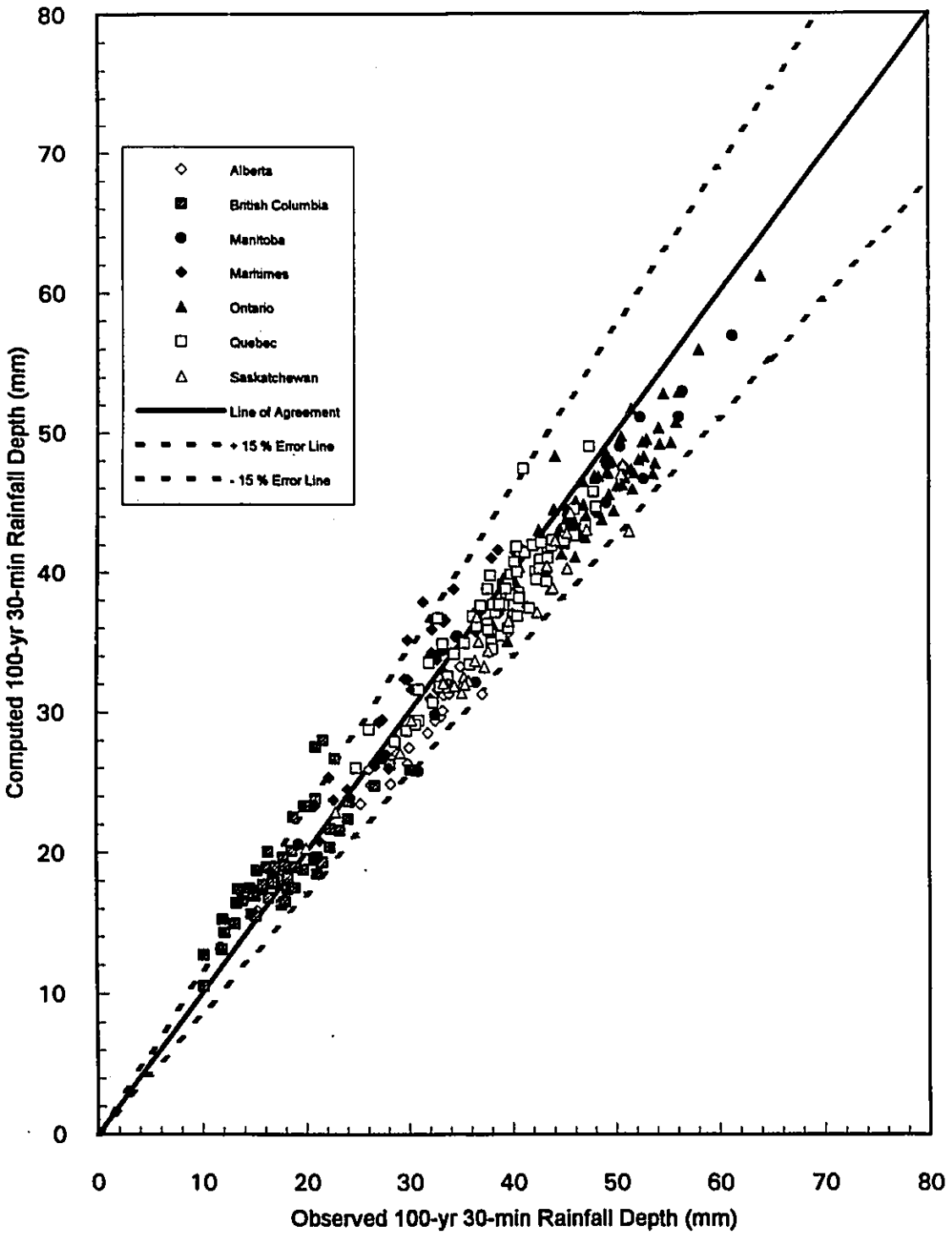

Figure 4.36: Performance of Proposed RDDF Equation (4.15) for the 100-yr 30-min Design Storm

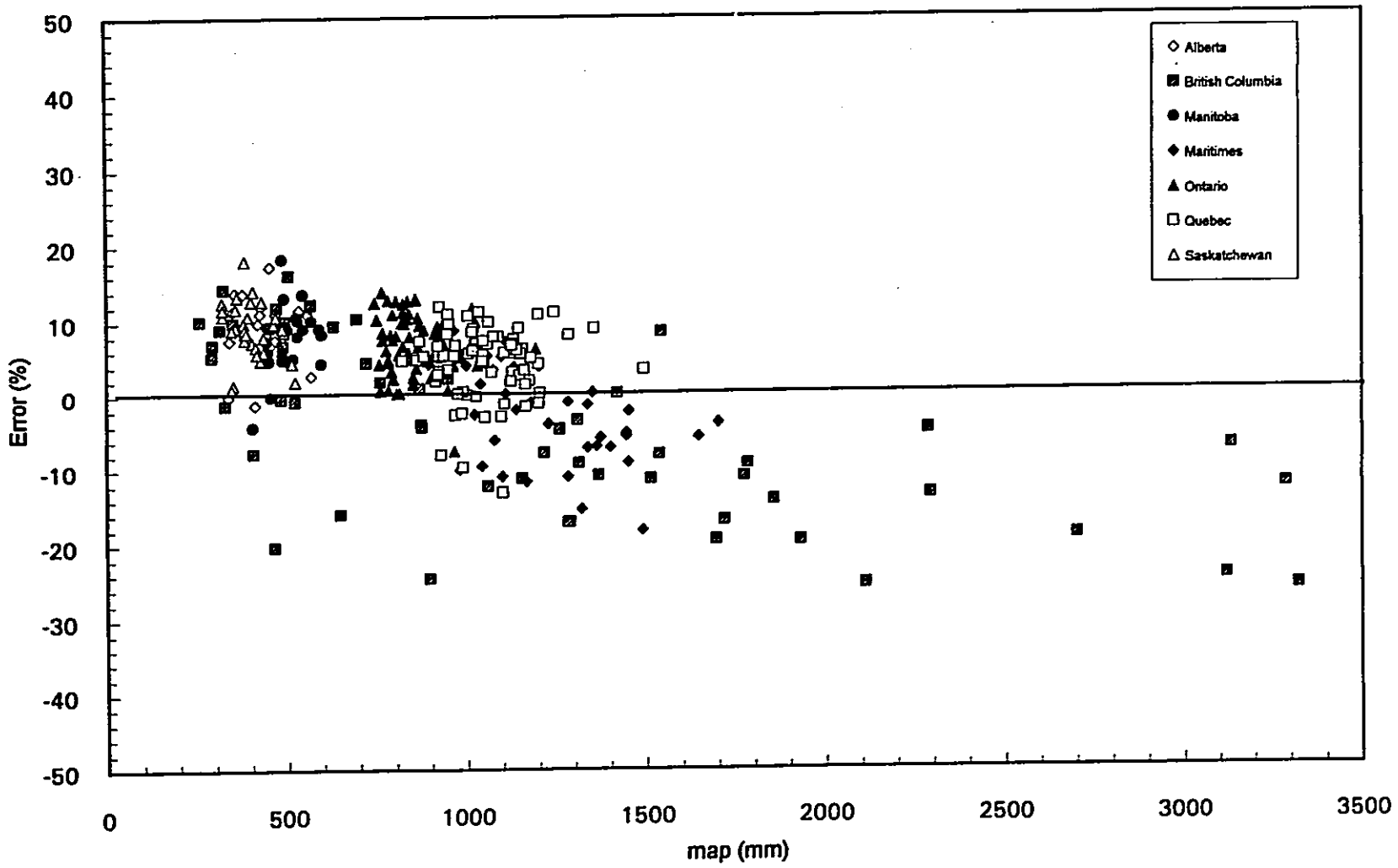

Figure 4.37a: Error of Proposed RDDF Equation (4.15) in Estimating the 10-yr 30-min Design Storm as a Function of map

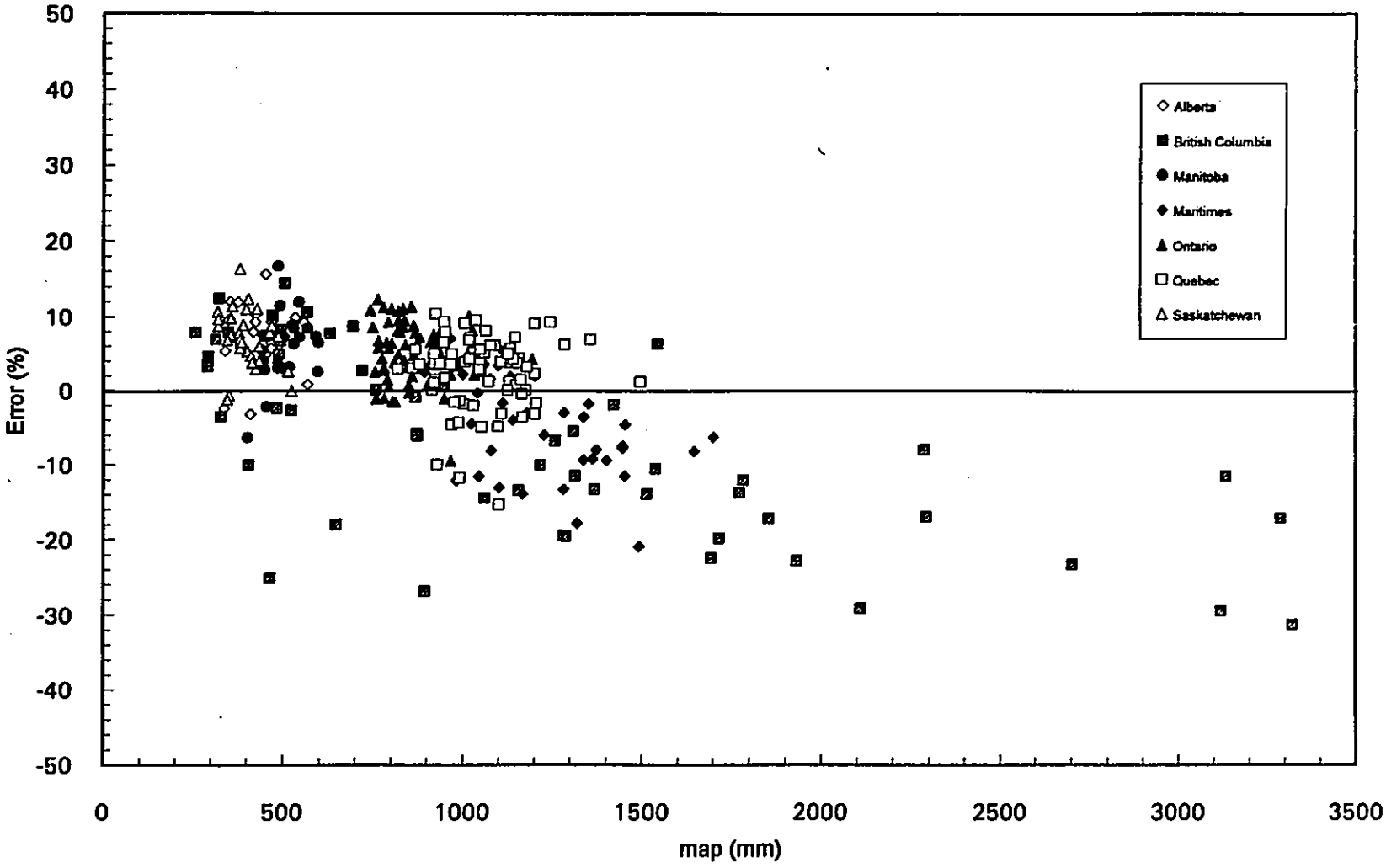

Figure 4.37b: Error of Proposed RDDF Equation (4.15) in Estimating the 100-yr 30-min Design Storm as a Function of map

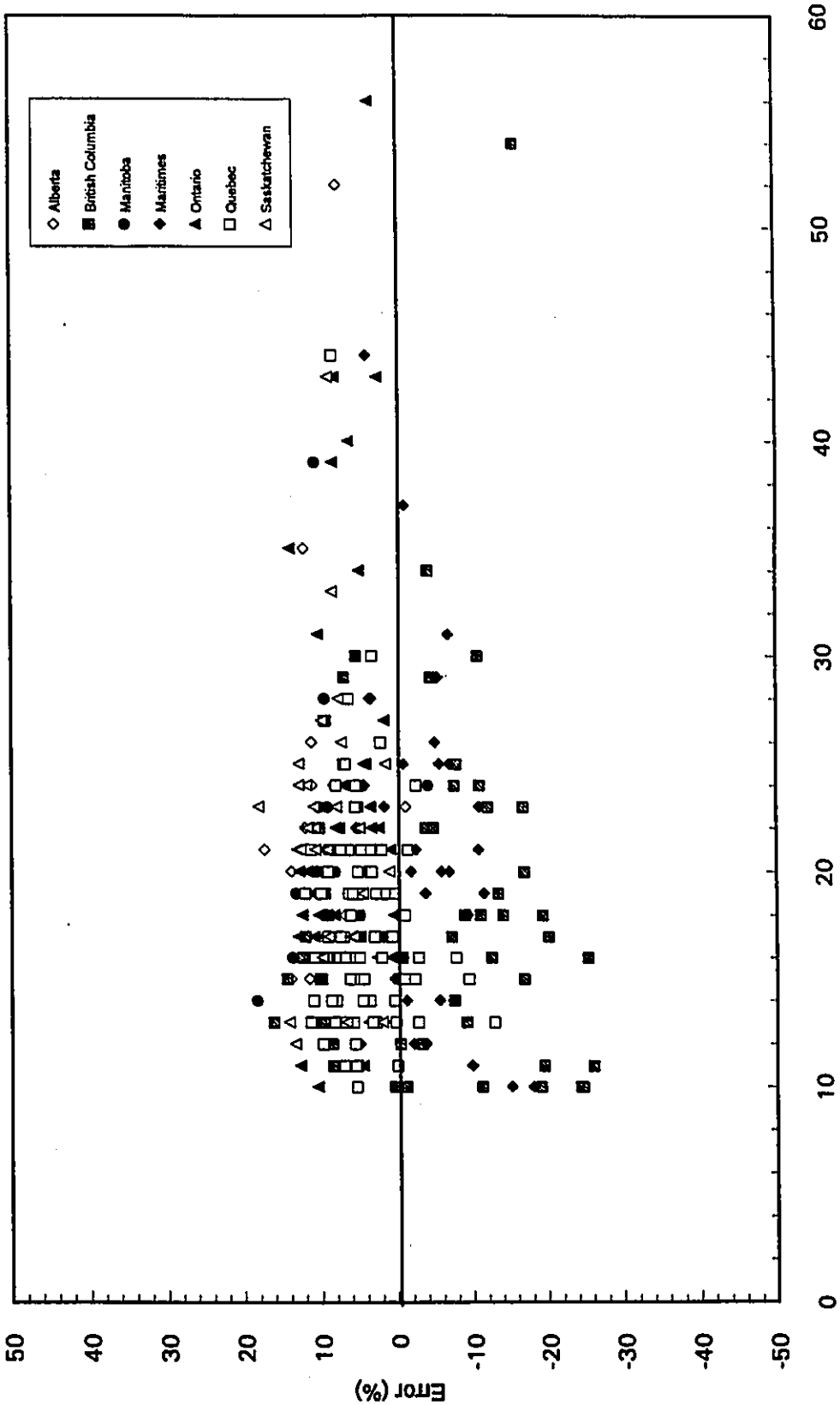

Figure 4.38a: Error of Proposed RDDF Equation (4.15) in Estimating the 10-yr 30-min Design Storm as a Function of Record Length

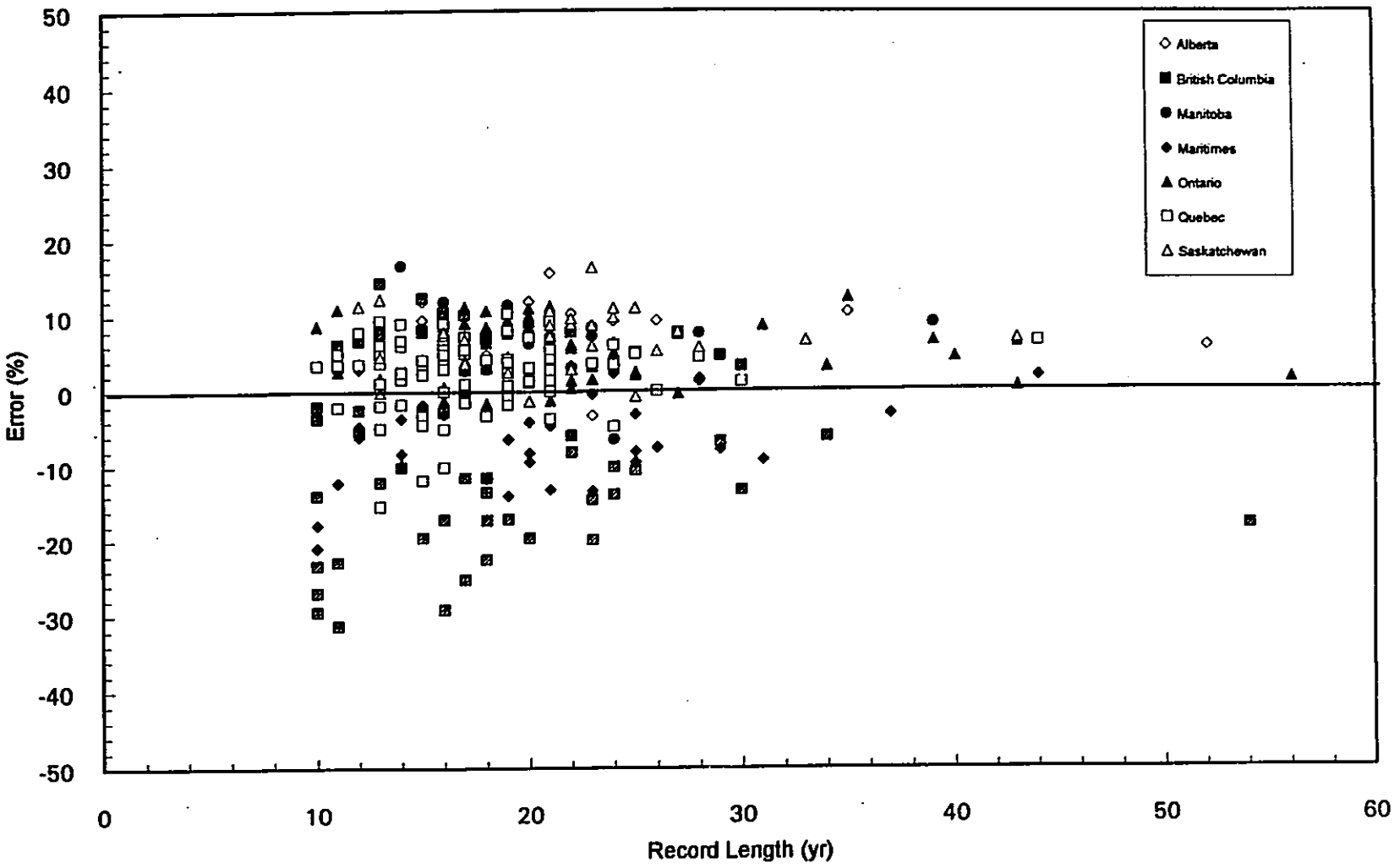

Figure 4.38b: Error of Proposed RDDF Equation (4.15) in Estimating the 100-yr 30-min Design Storm as a Function of Record Length

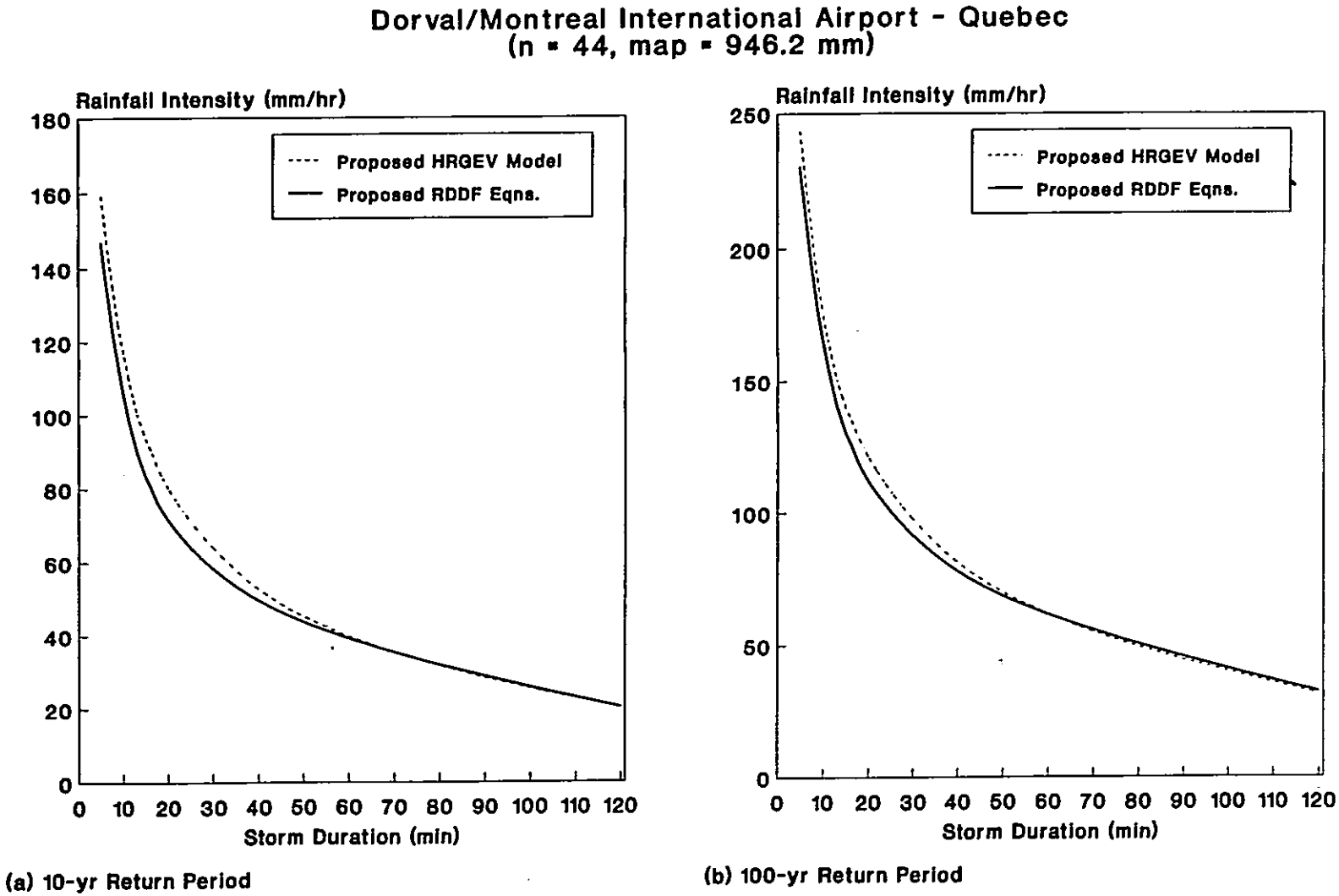

Figure 4.39: Verification of RDDF Equations (4.15) to (4.17) at the Long-Term Record Station 7025250

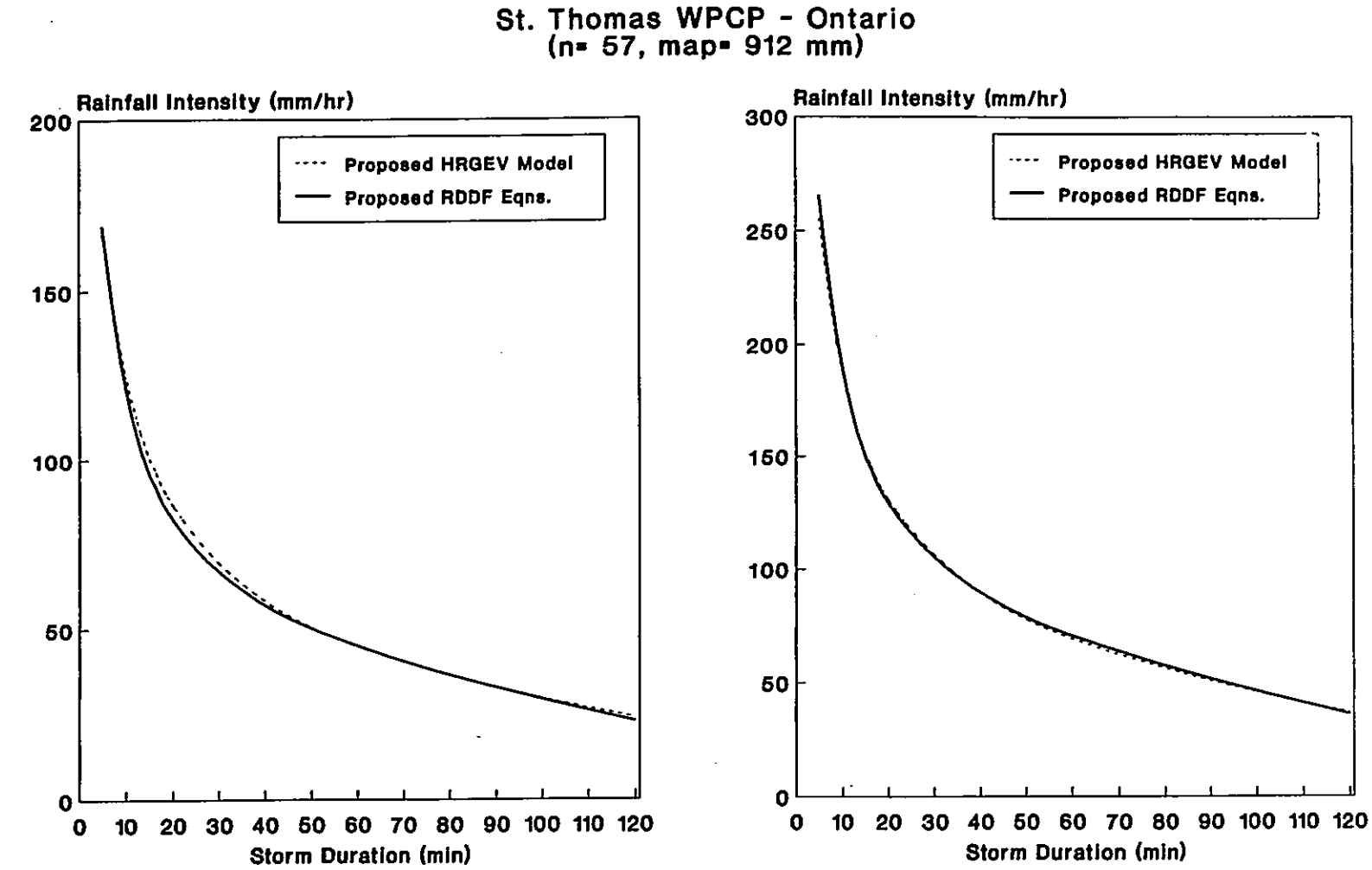

Figure 4.40: Verification of RDDF Equations (4.15) to (4.17) at the Long-Term Record Station 6137362

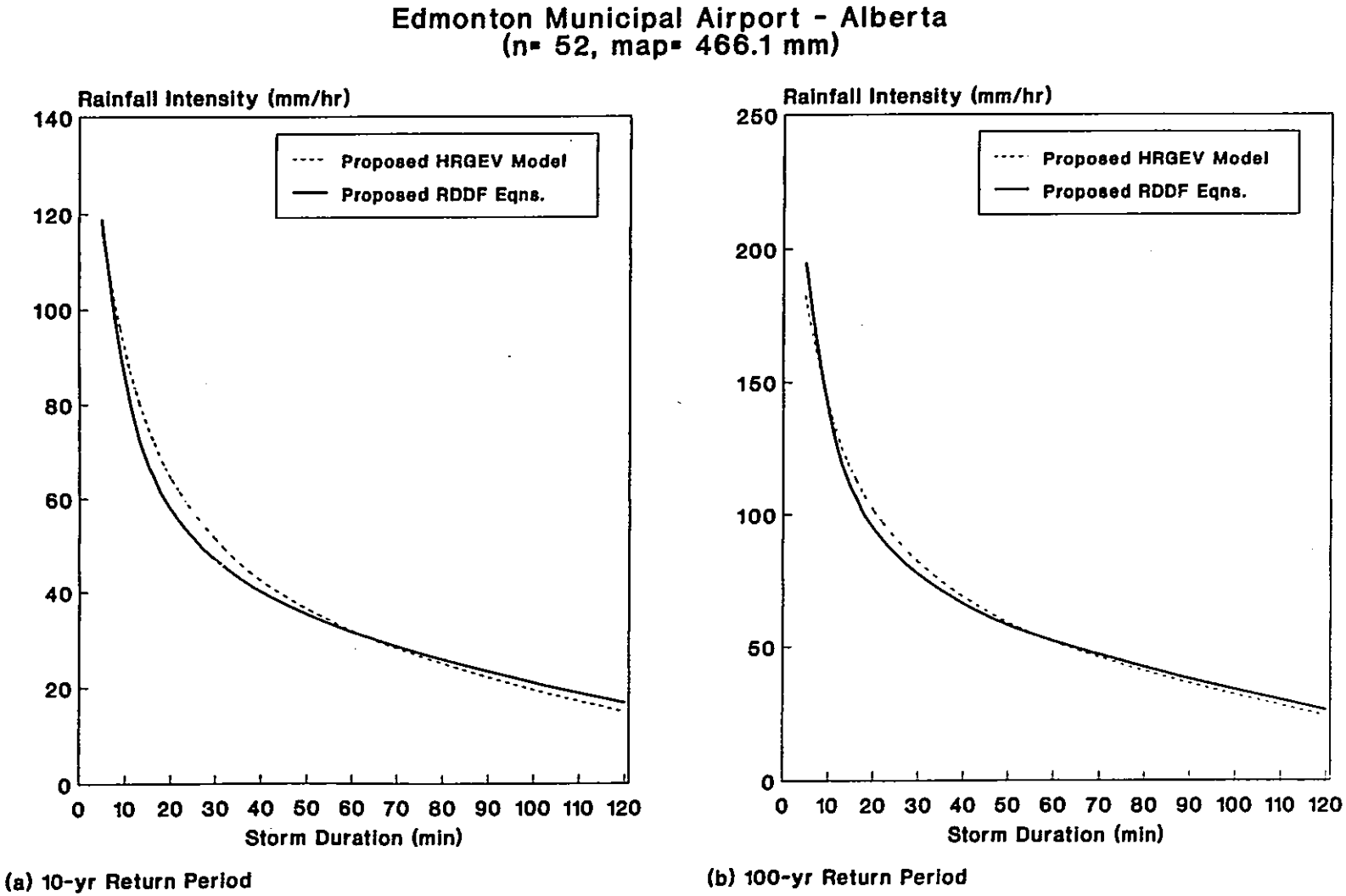

Figure 4.41: Verification of RDDF Equations (4.15) to (4.17) at the Long-Term Record Station 3012208

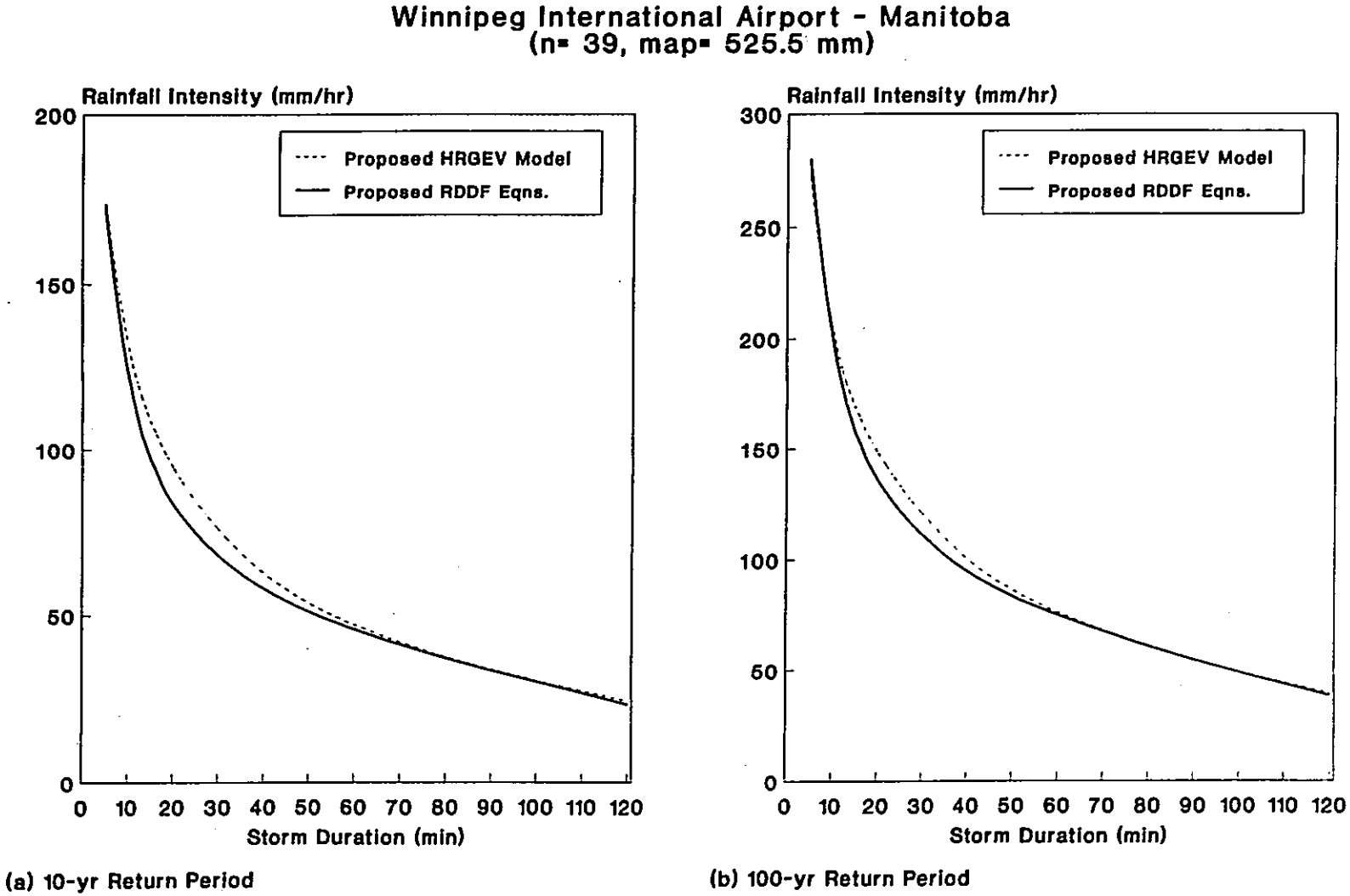

Figure 4.42: Verification of RDDF Equations (4.15) to (4.17) at the Long-Term Record Station 5023222

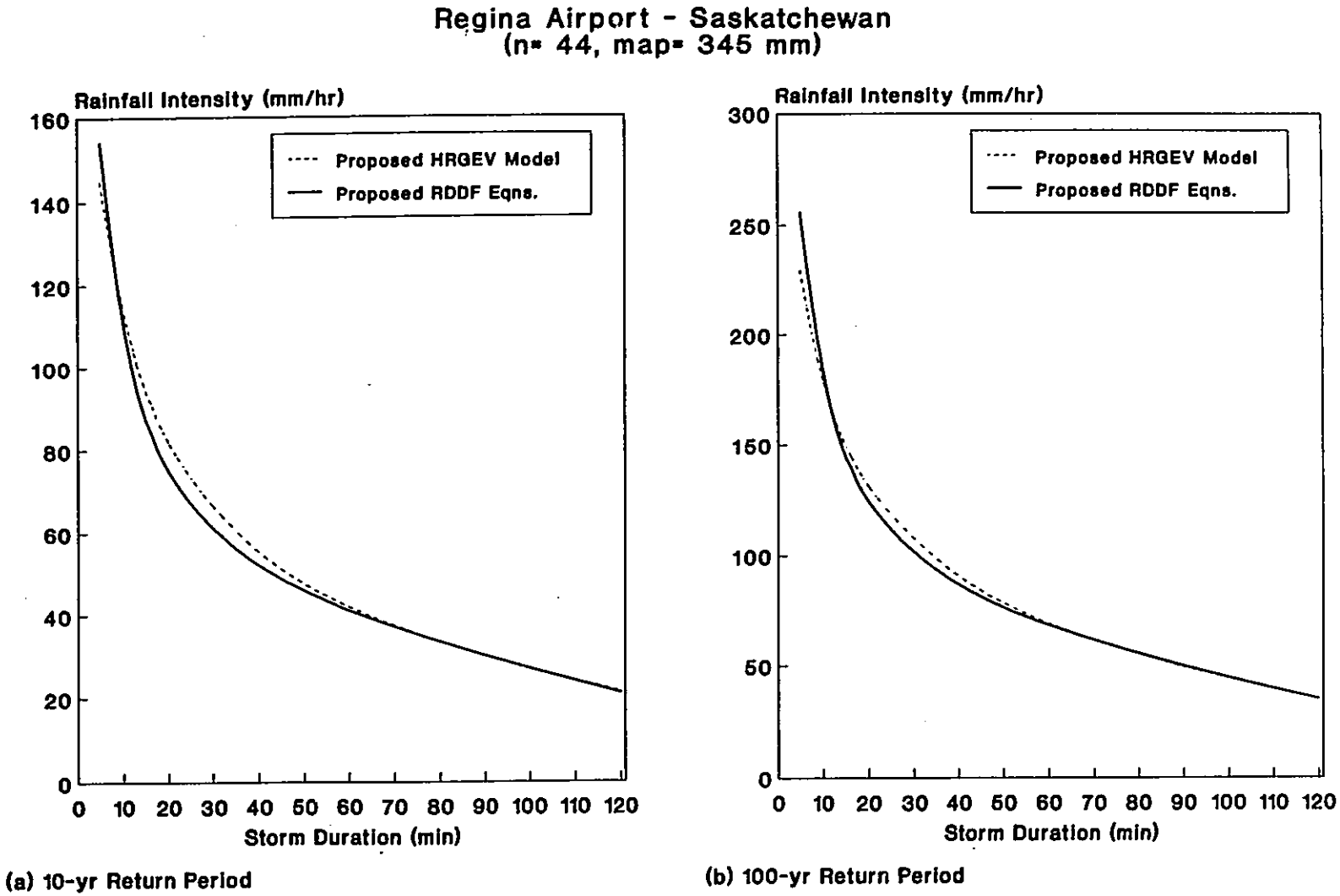

Figure 4.43: Verification of RDDF Equations (4.15) to (4.17) at the Long-Term Record Station 4016560

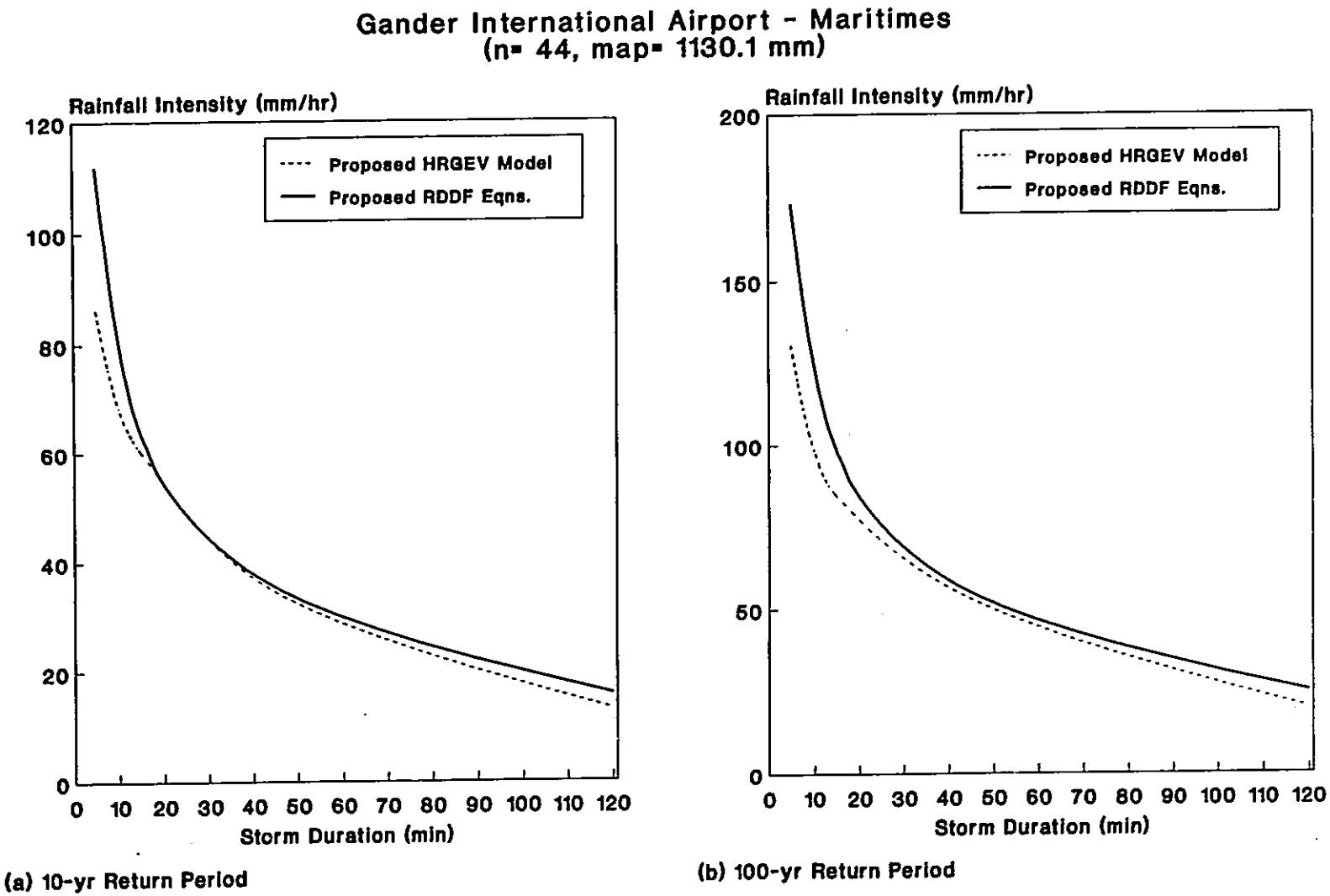

Figure 4.44: Verification of RDDF Equations (4.15) to (4.17) at the Long-Term Record Station 8401700

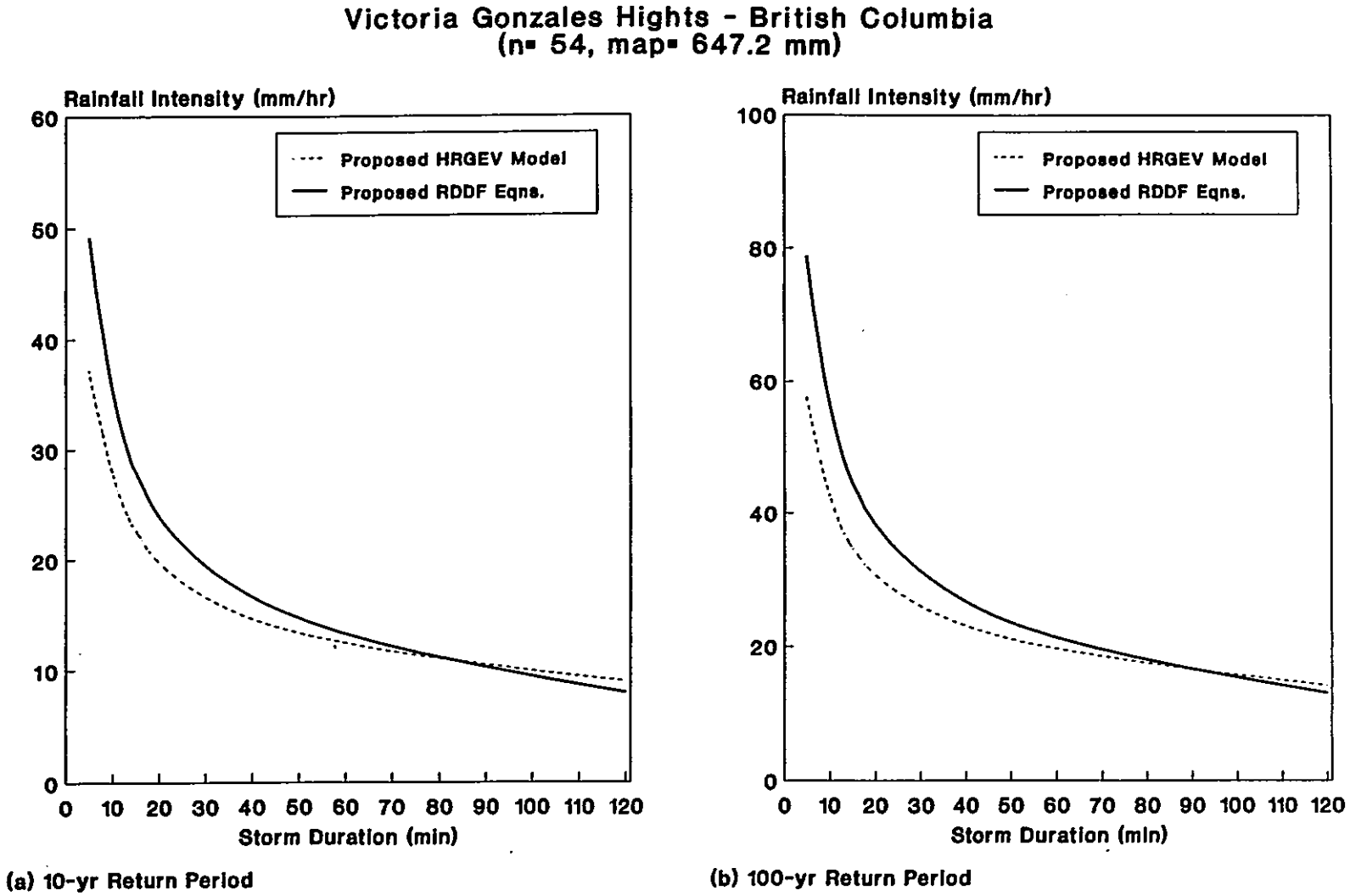

Figure 4.45: Verification of RDDF Equations (4.15) to (4.17) at the Long-Term Record Station 1018610

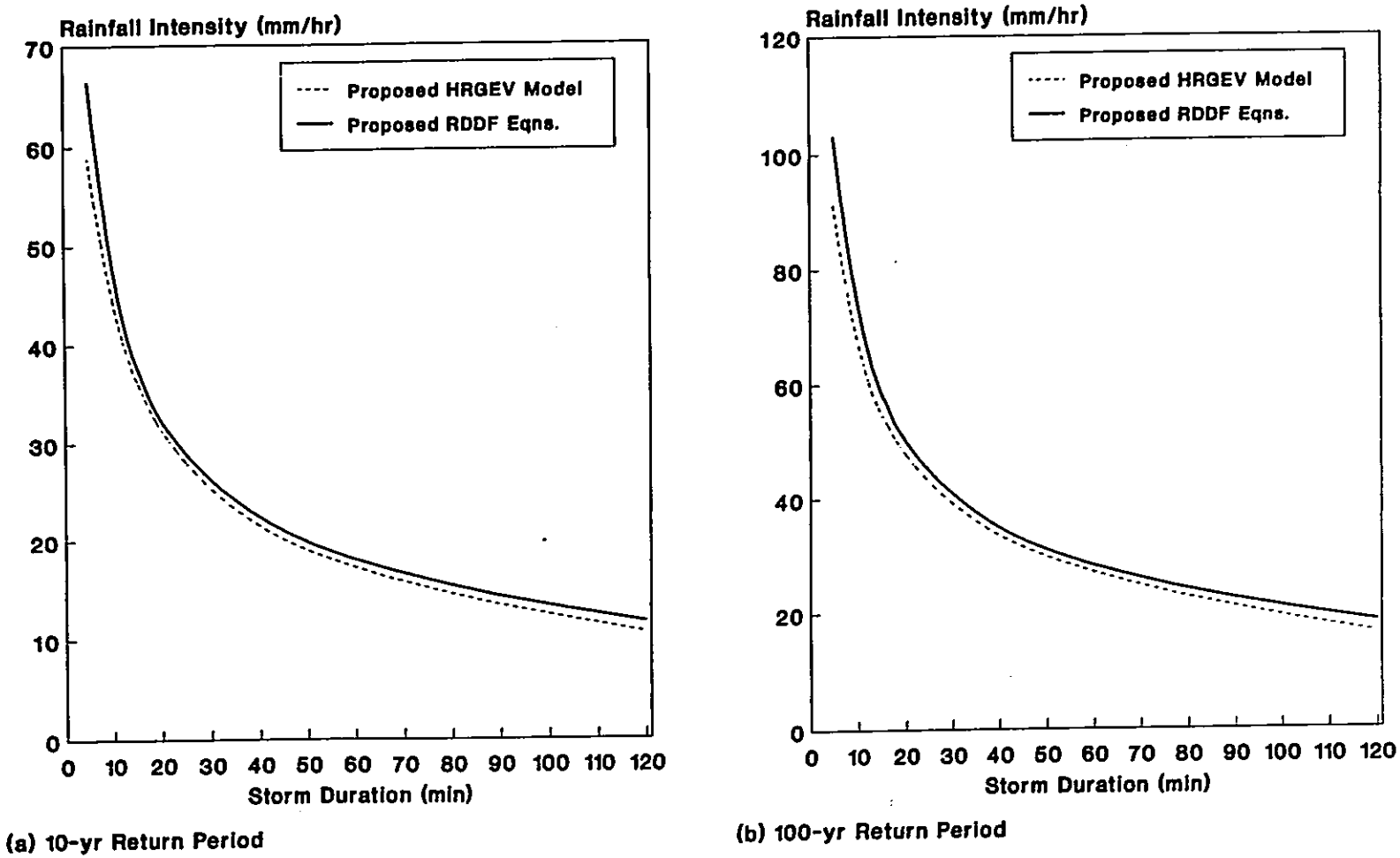

Figure 4.46: Verification of RDDF Equations (4.15) to (4.17) at the Long-Term Record Station 1108447

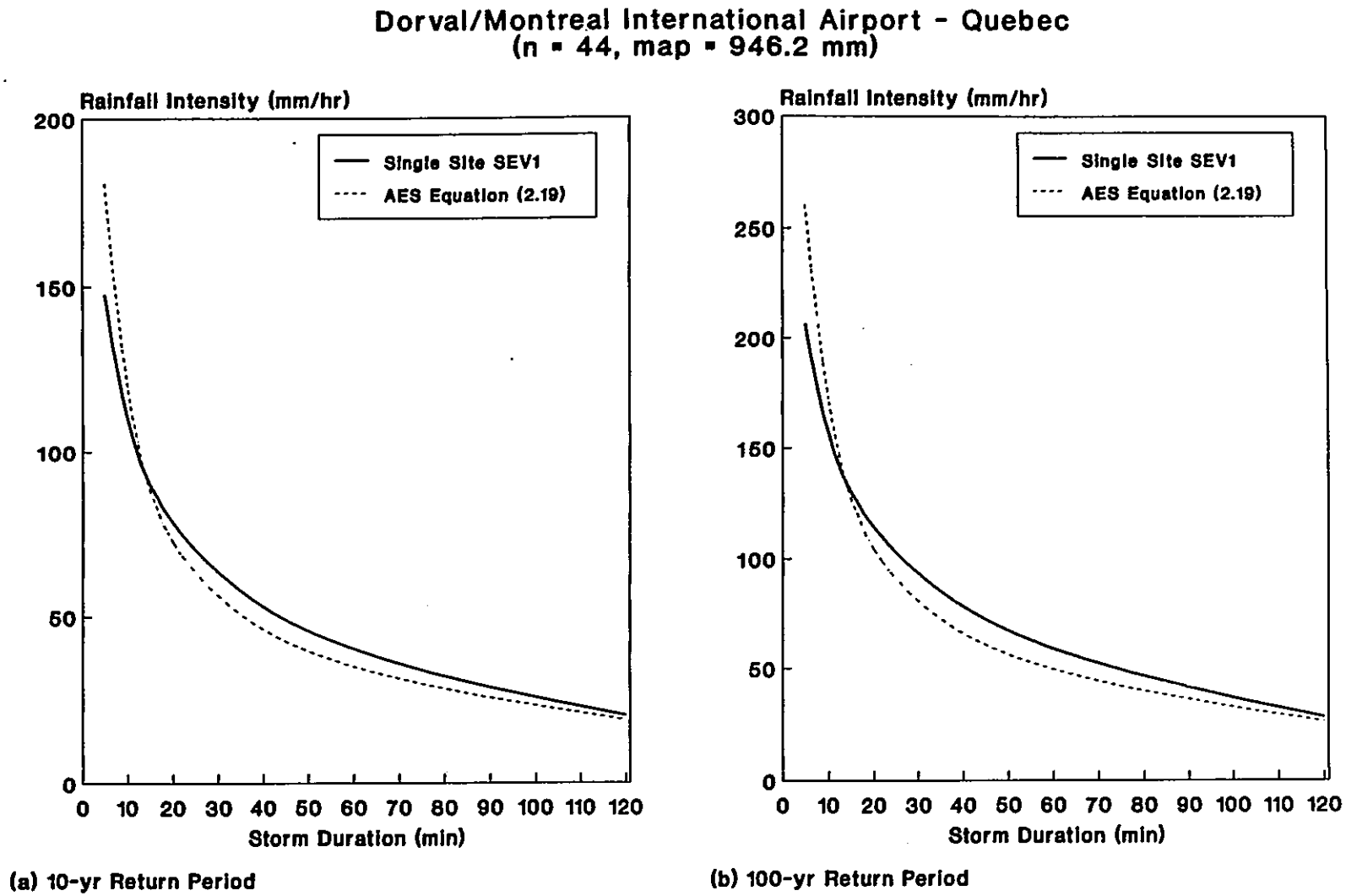

Figure 4.47: Comparison of AES Equation (2.19) and SEV1 Model at the Long-Term Record Station 7025250

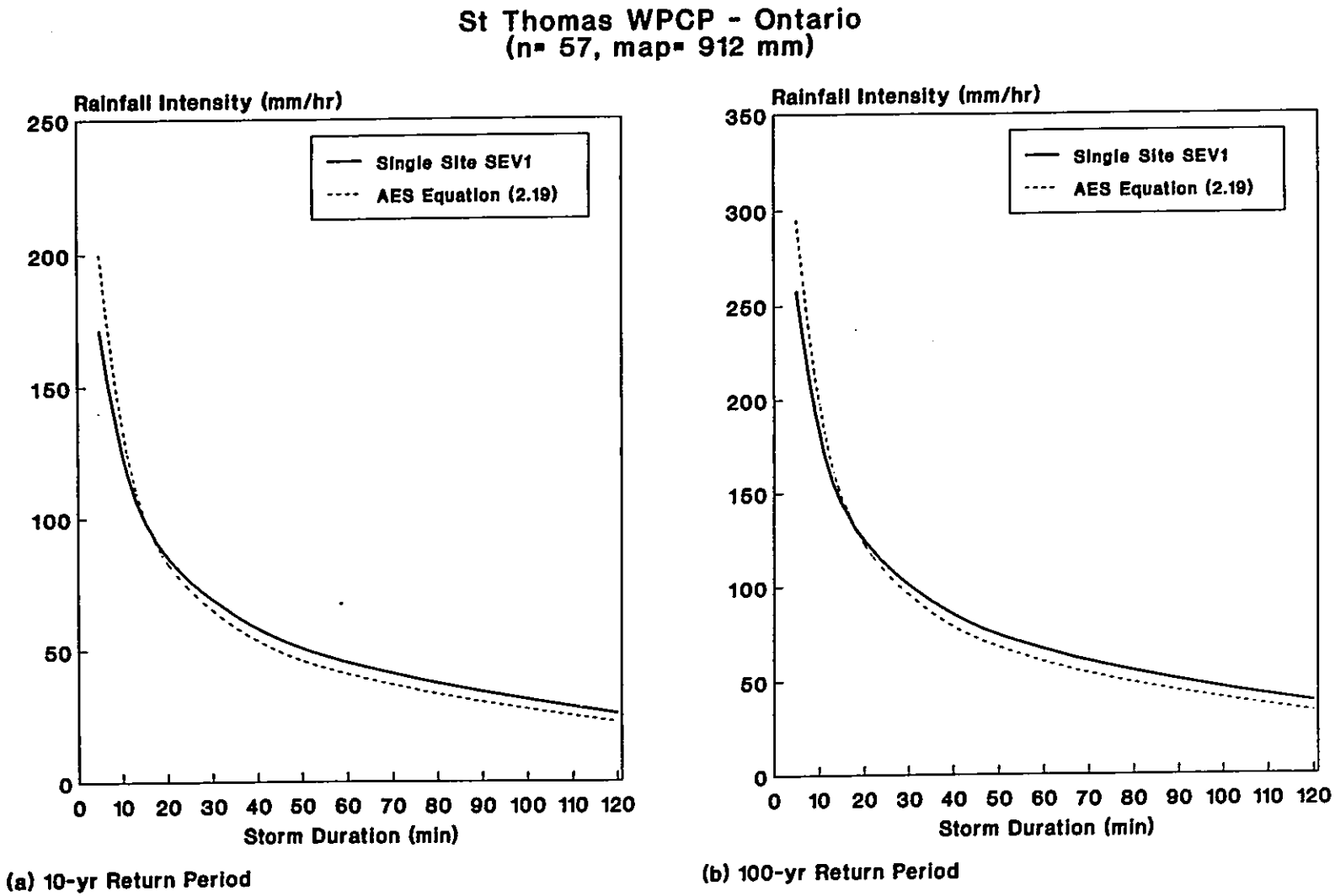

Figure 4.48: Comparison of AES Equation (2.19) and SEV1 Model at the Long-Term Record Station 6137362

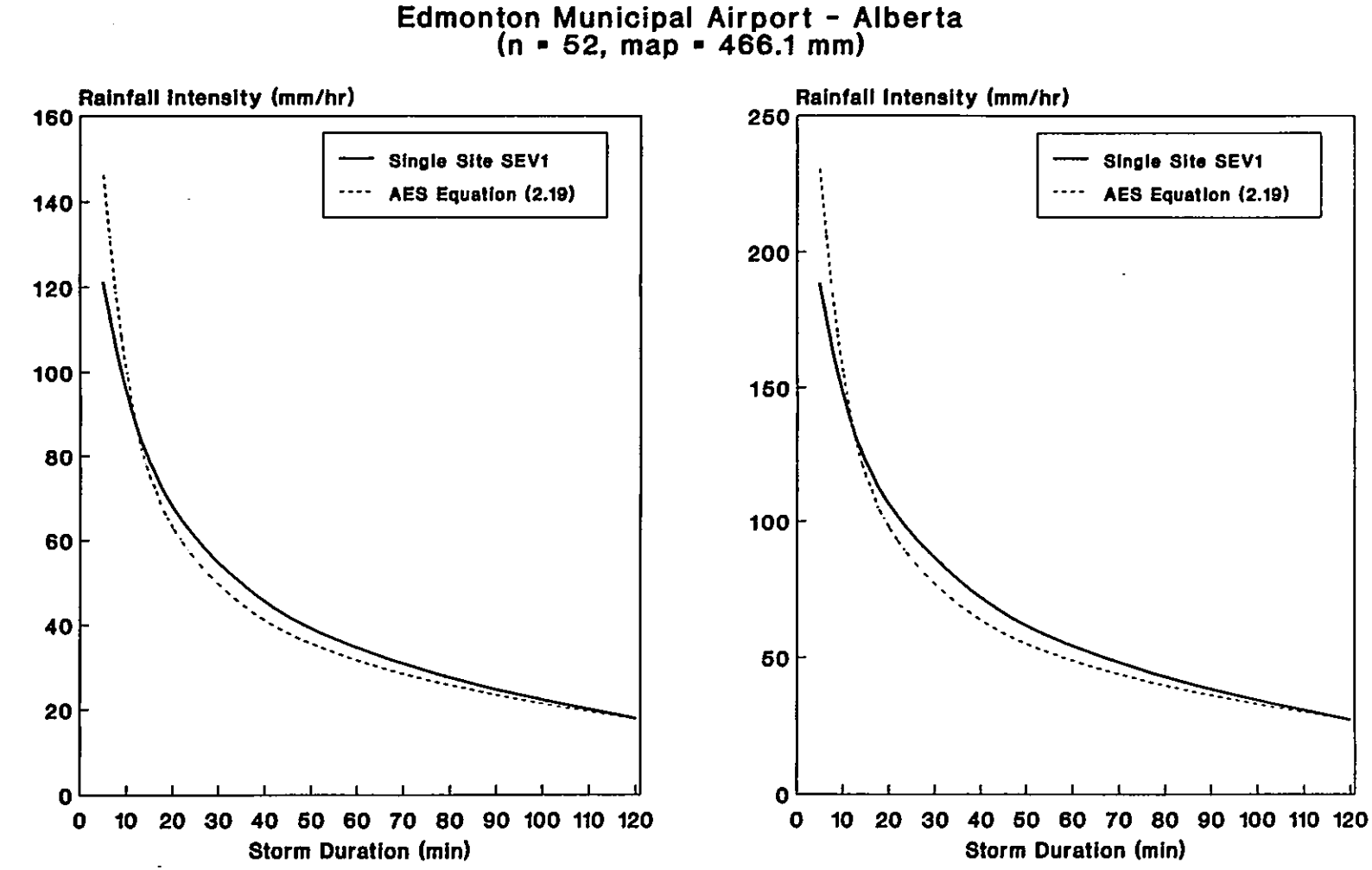

Figure 4.49: Comparison of AES Equation (2.19) and SEV1 Model at the Long-Term Record Station 3012208

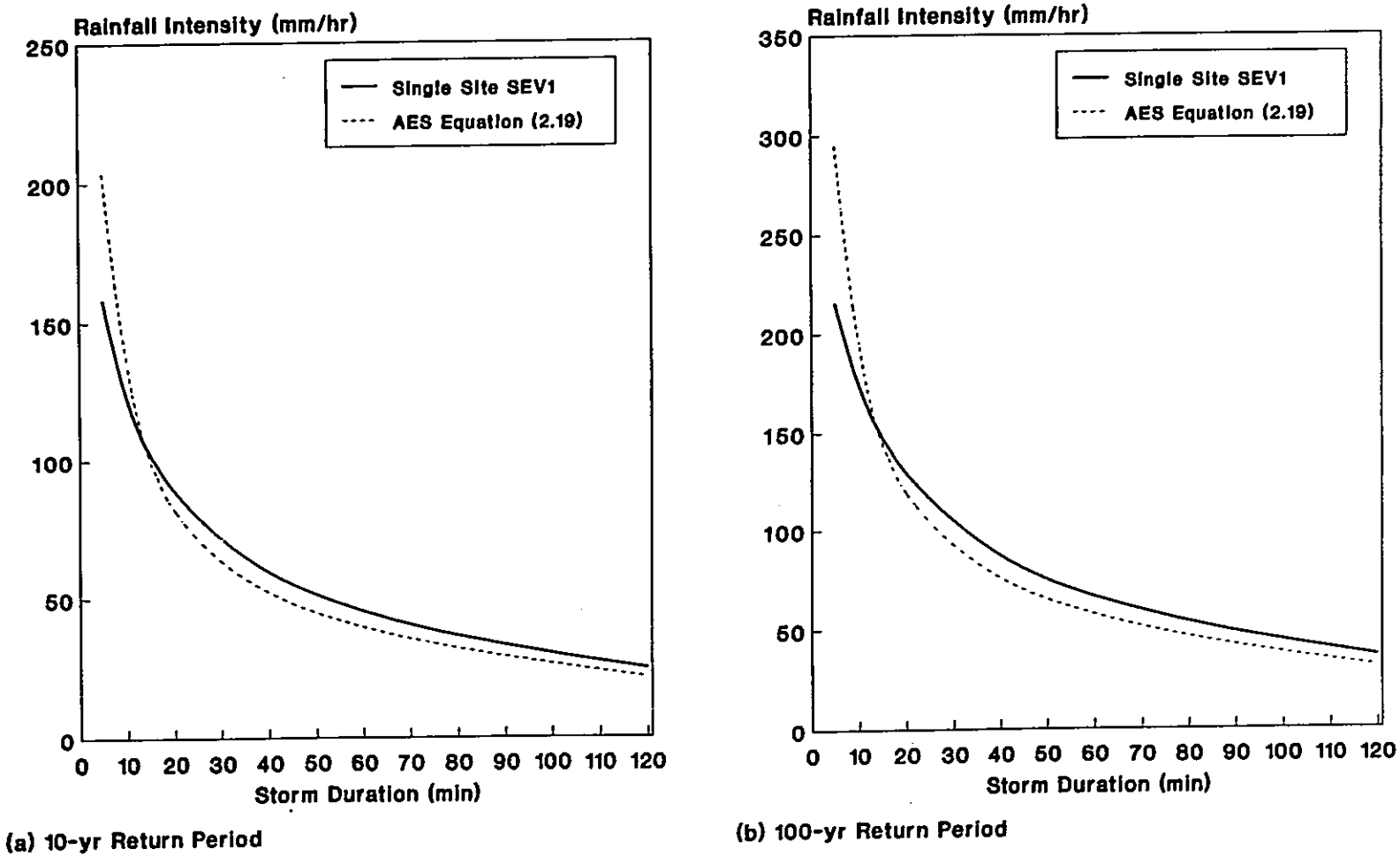

Figure 4.50: Comparison of AES Equation (2.19) and SEV1 Model at the Long-Term Record Station 5023222

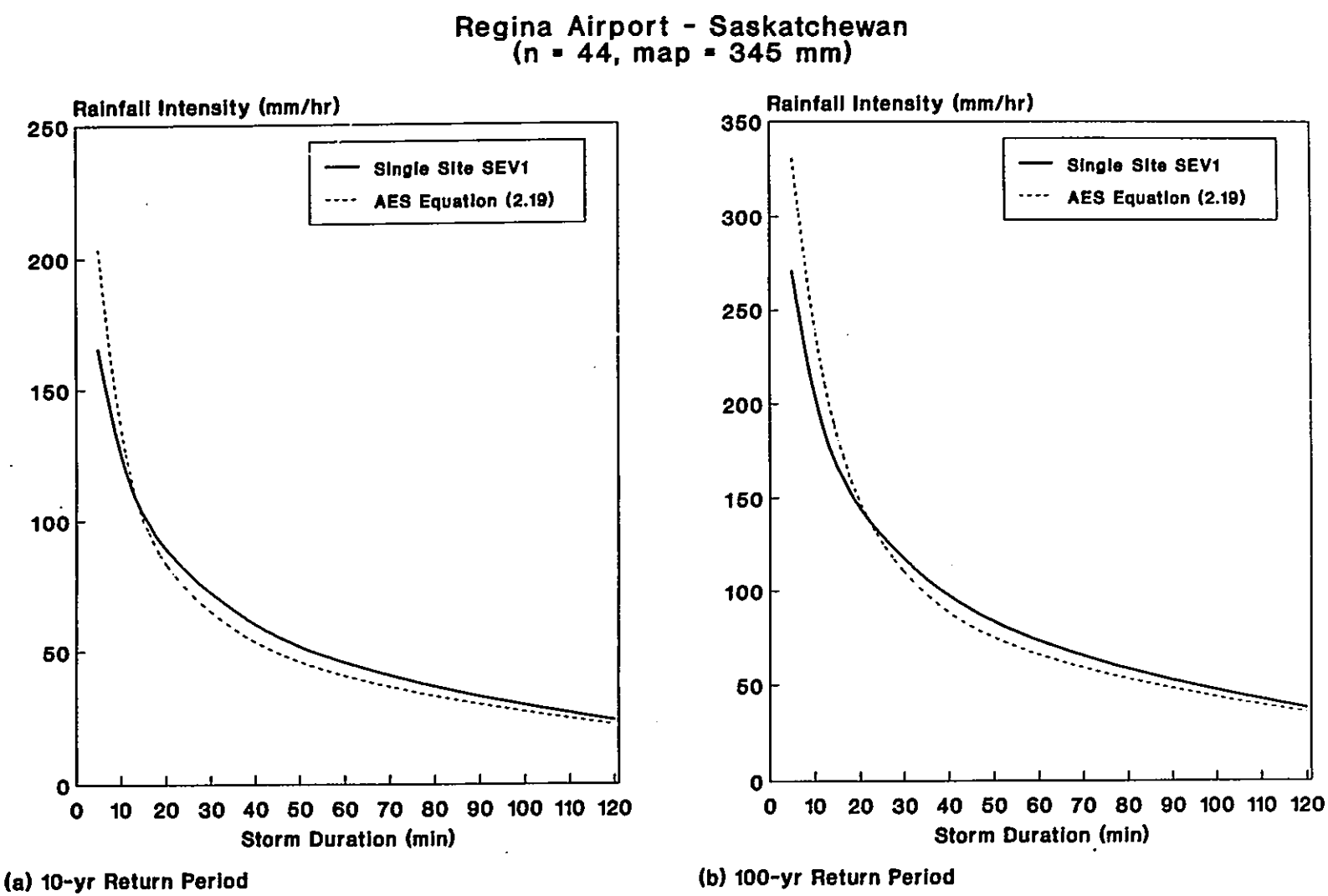

Figure 4.51: Comparison of AES Equation (2.19) and SEV1 Model at the Long-Term Record Station 4016560

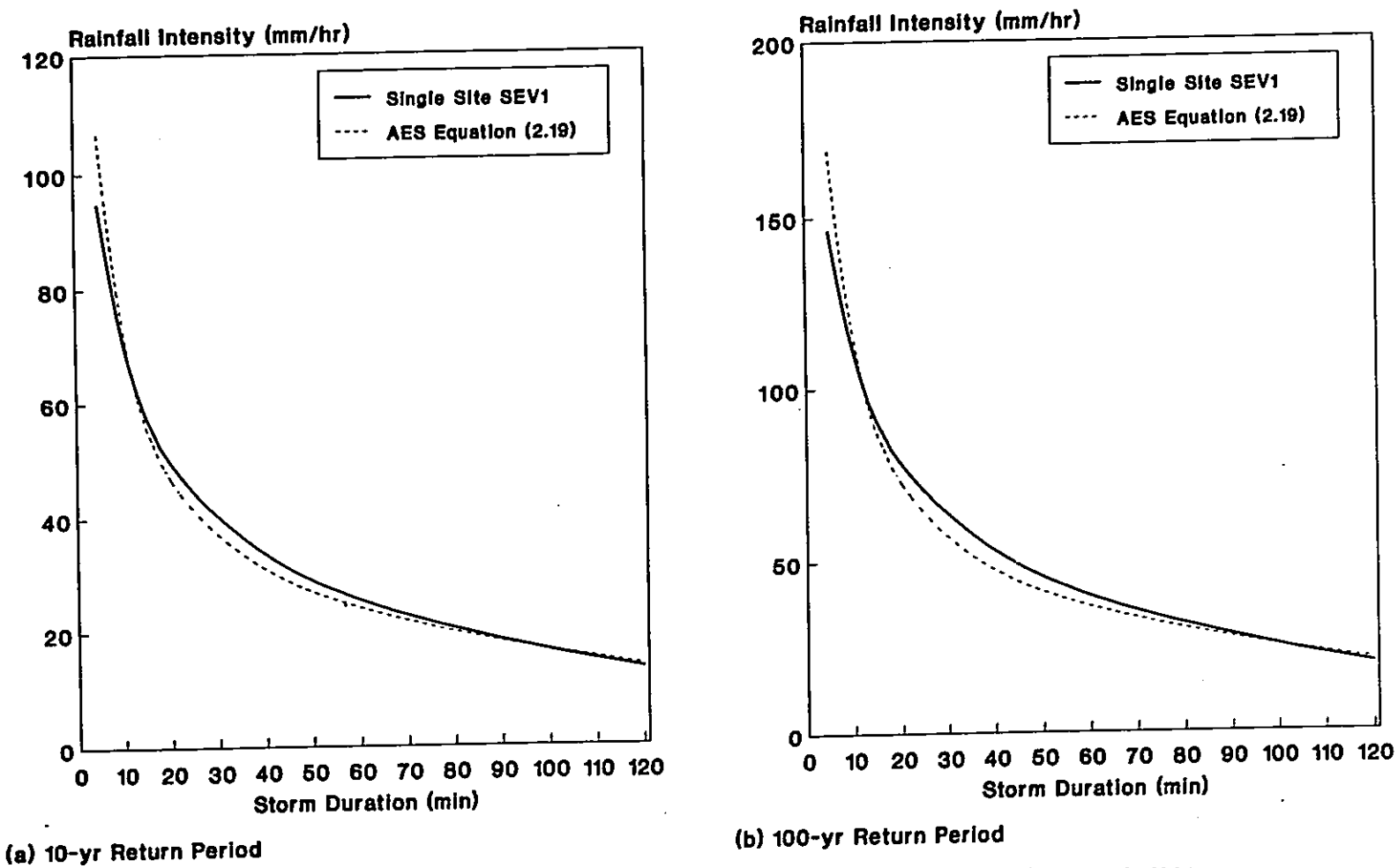

Figure 4.52: Comparison of AES Equation (2.19) and SEV1 Model at the Long-Term Record Station 8401700

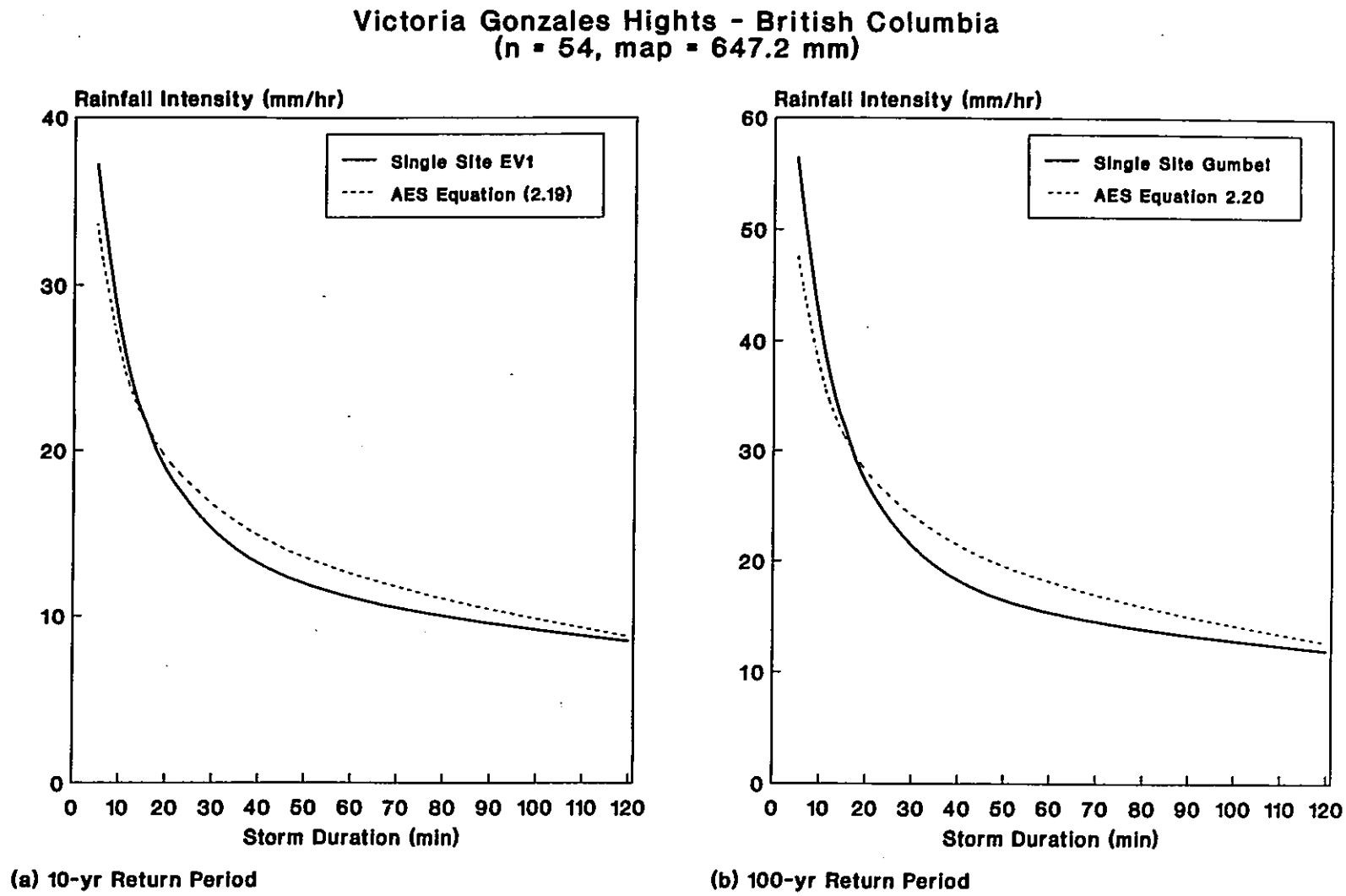

Figure 4.53: Comparison of AES Equation (2.19) and SEV1 Model at the Long-Term Record Station 1018610

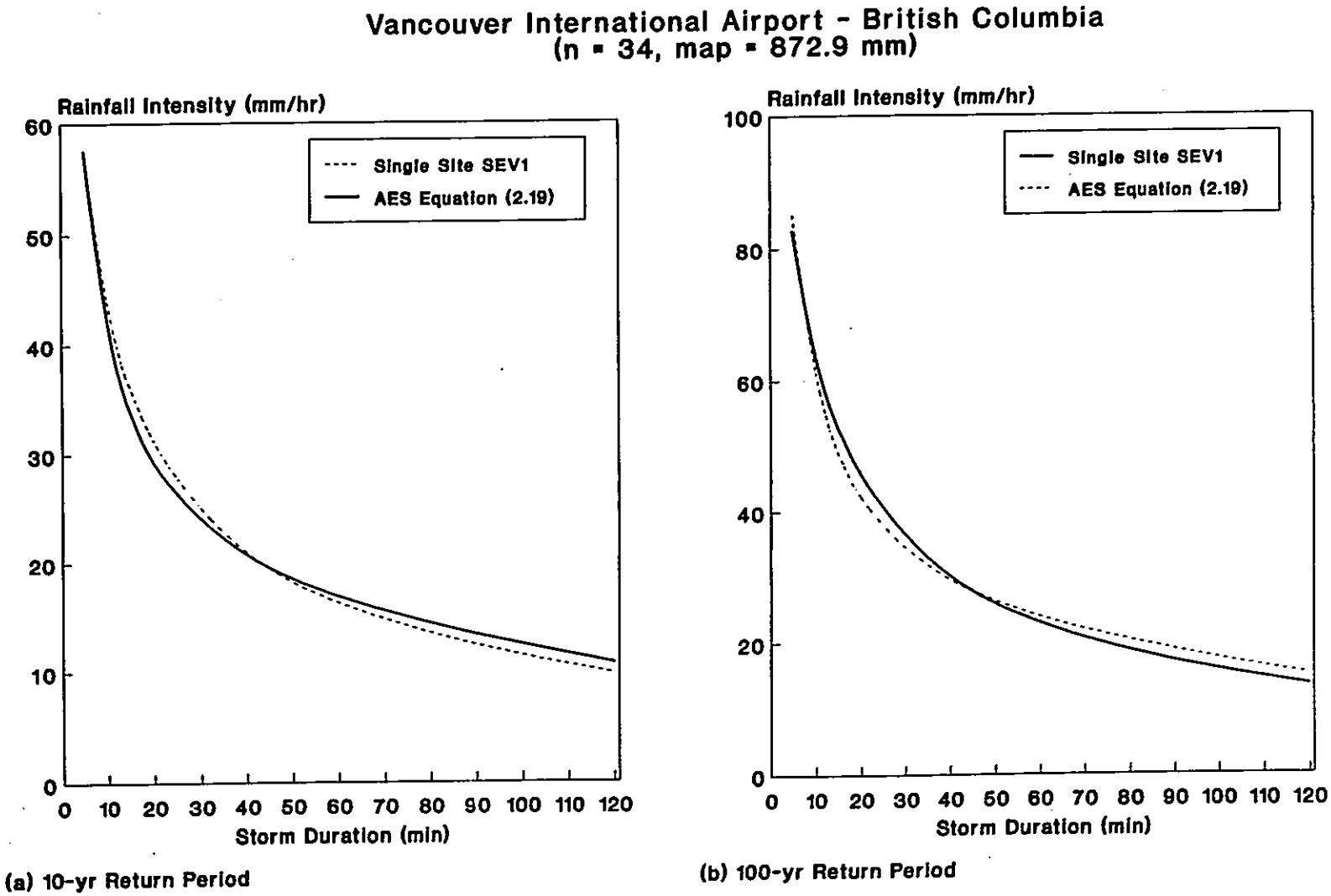

Figure 4.54: Comparison of AES Equation (2.19) and SEV1 Model at the Long-Term Record Station 1108447

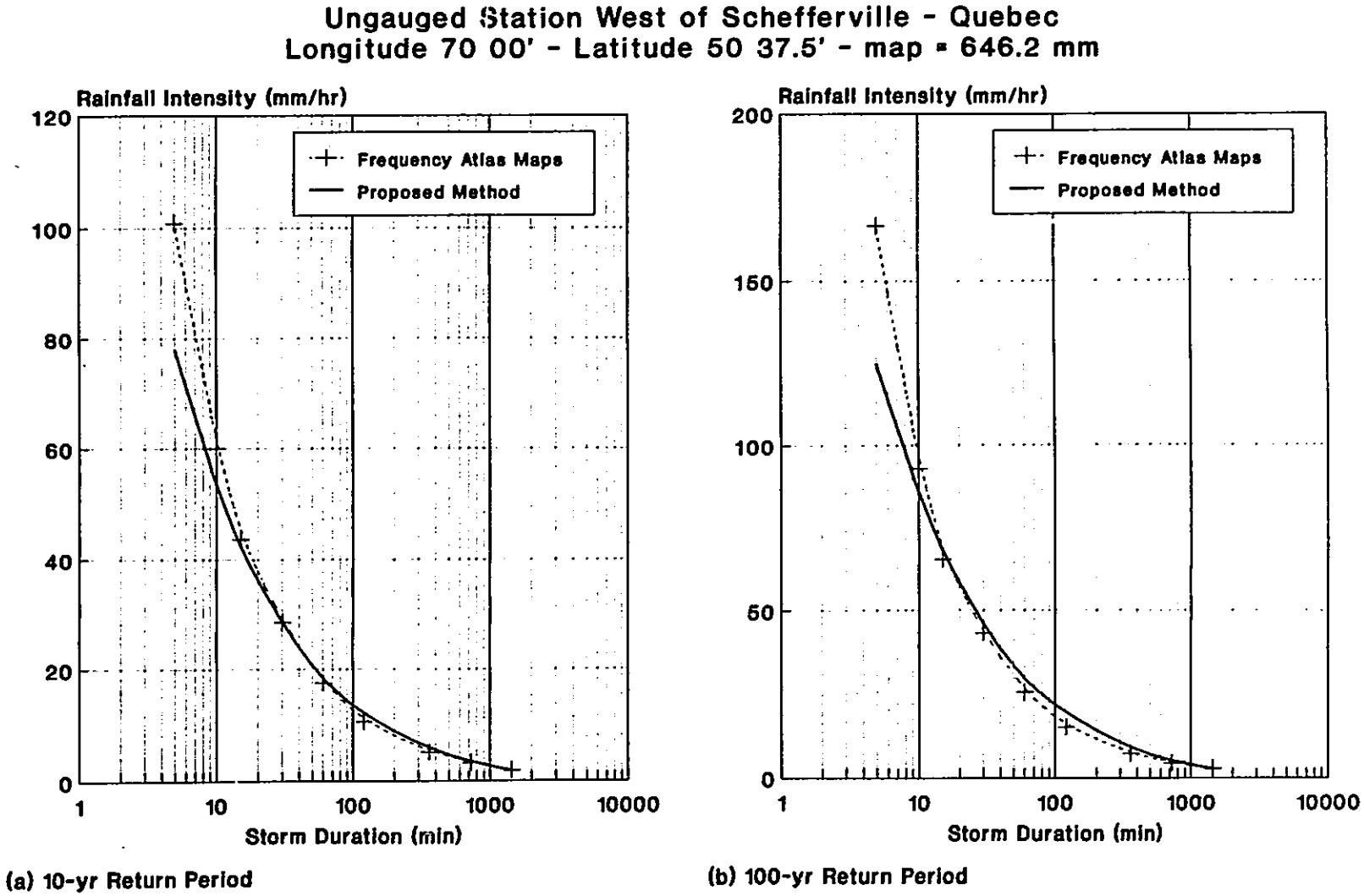

Figure 4.55: Comparison of IDF Curves Computed by Proposed Method of Section 4.8 and those Interpolated from Rainfall Frequency Atlas Maps

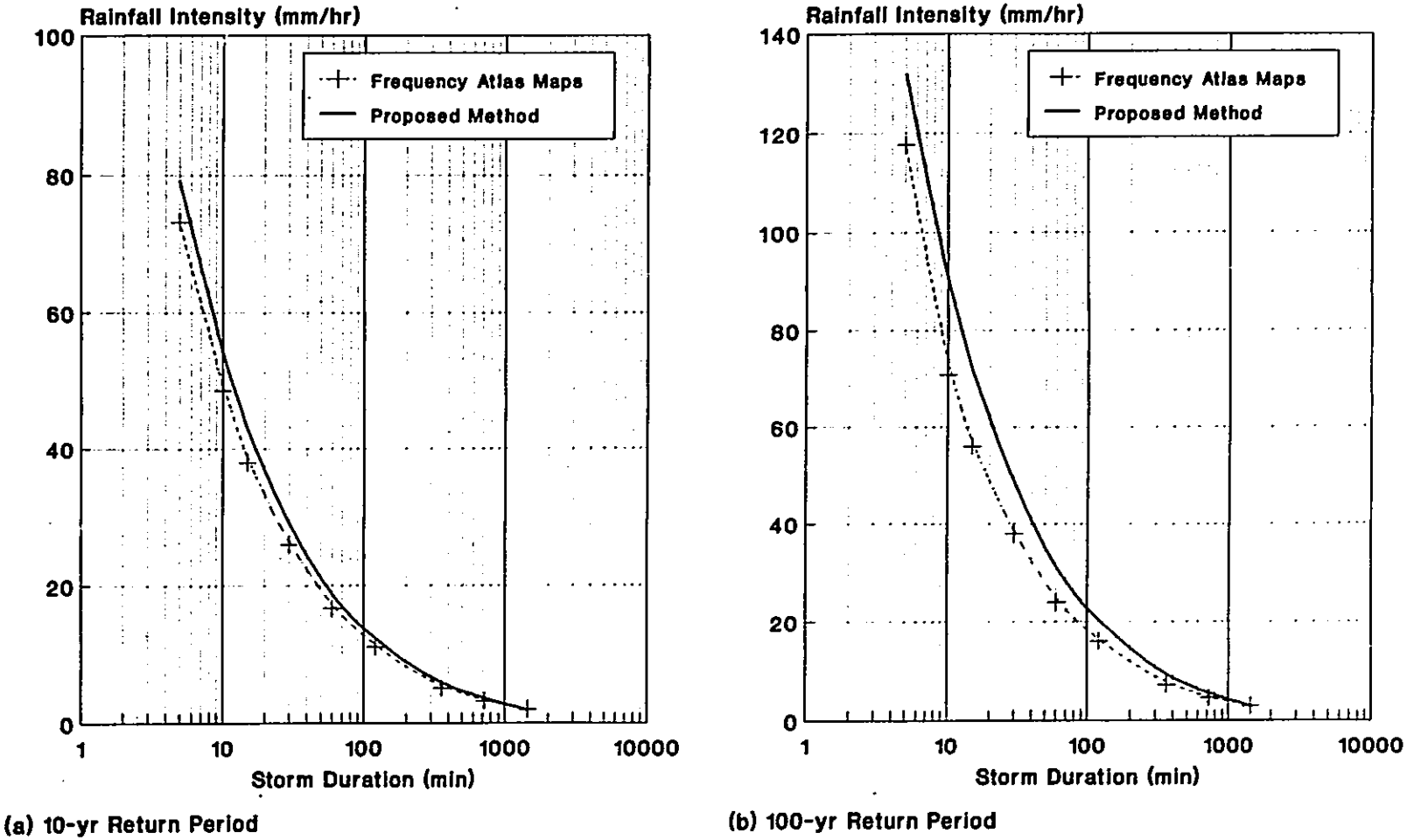

Figure 4.56: Comparison of IDF Curves Computed by Proposed Method of Section 4.8 and those Interpolated from Rainfall Frequency Atlas Maps

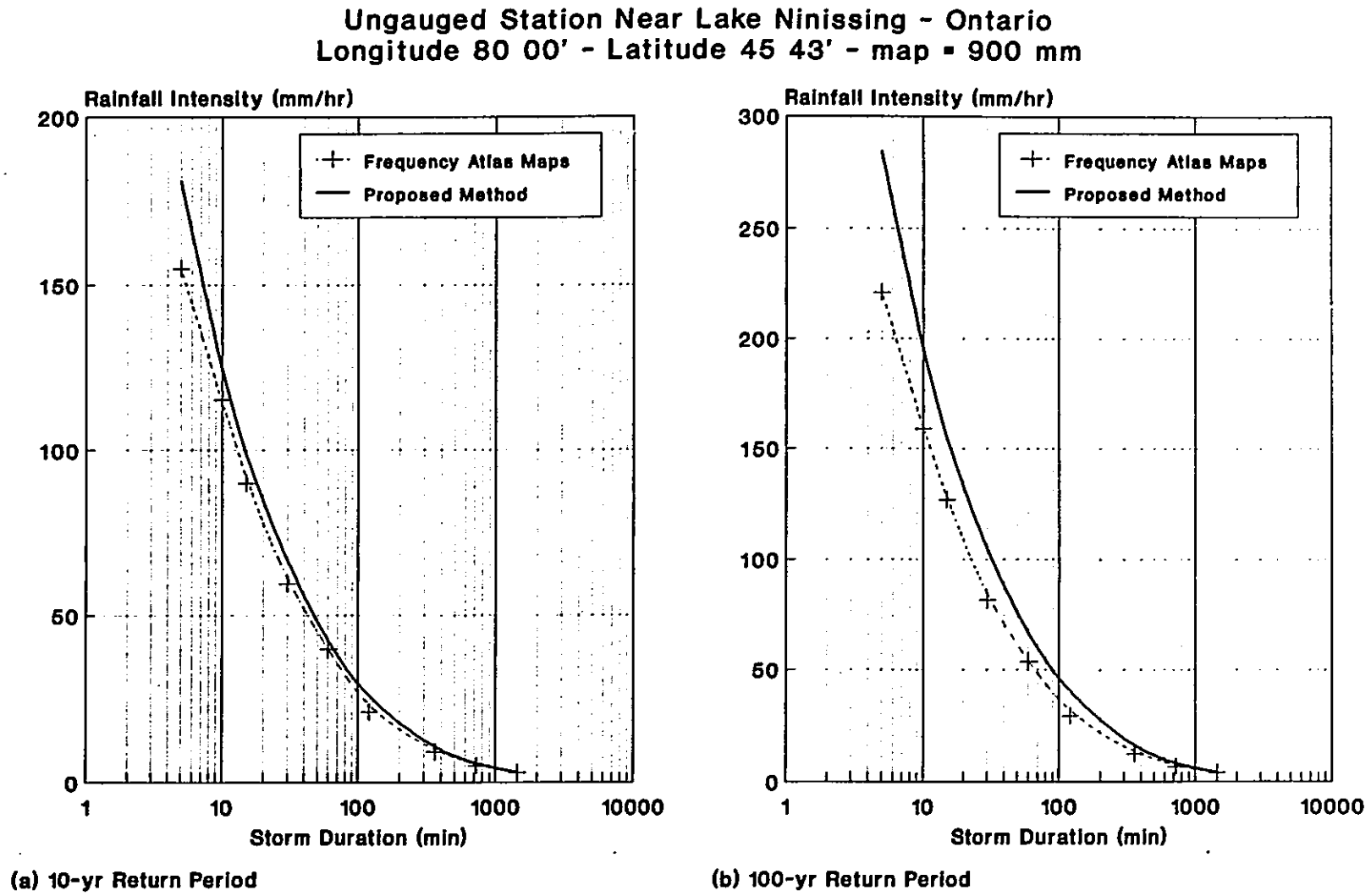

Figure 4.57: Comparison of IDF Curves Computed by Proposed Method of Section 4.8 and those Interpolated from Rainfall Frequency Atlas Maps

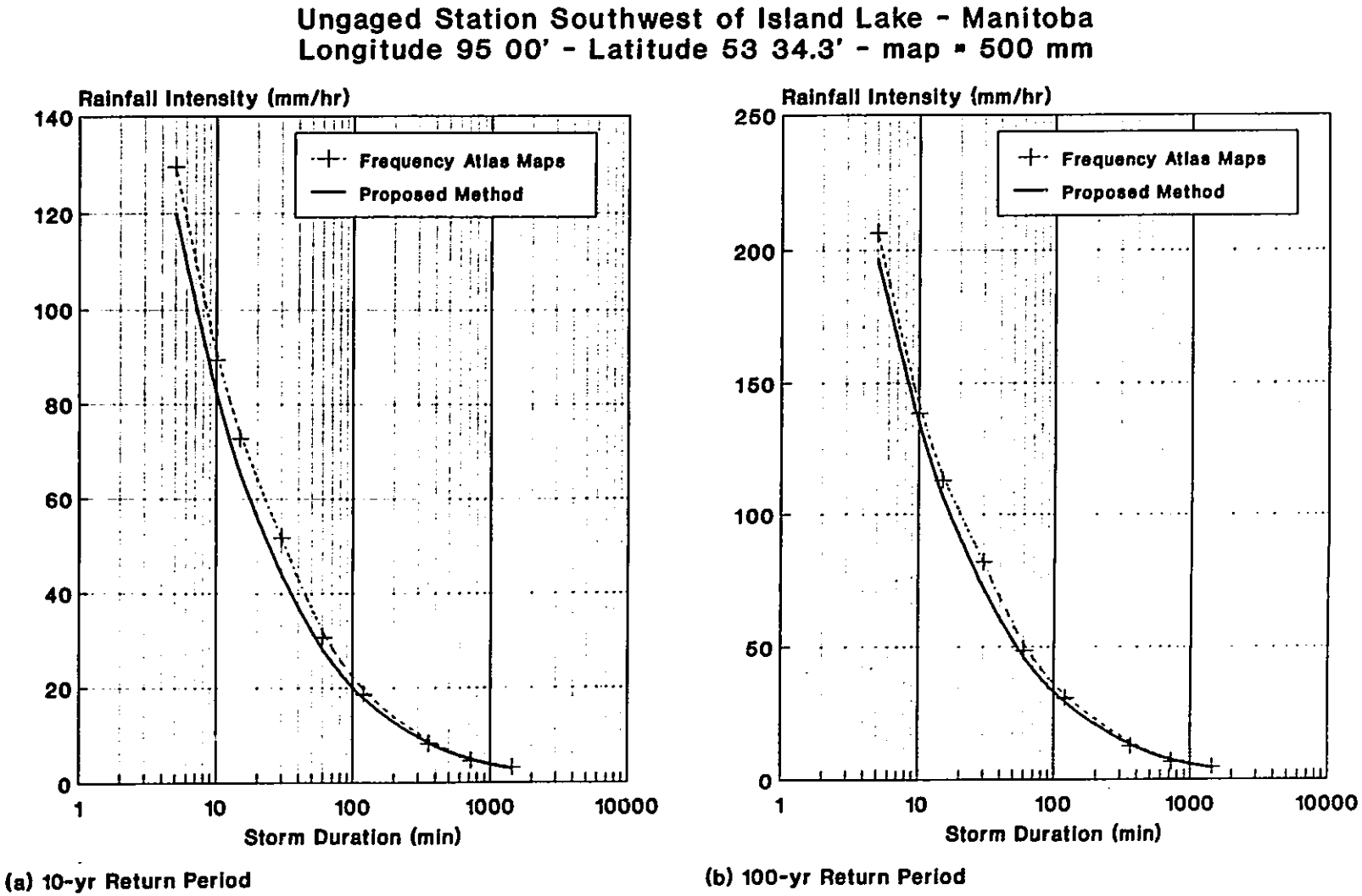

Figure 4.58: Comparison of IDF Curves Computed by Proposed Method of Section 4.8 and those Interpolated from Rainfall Frequency Atlas Maps

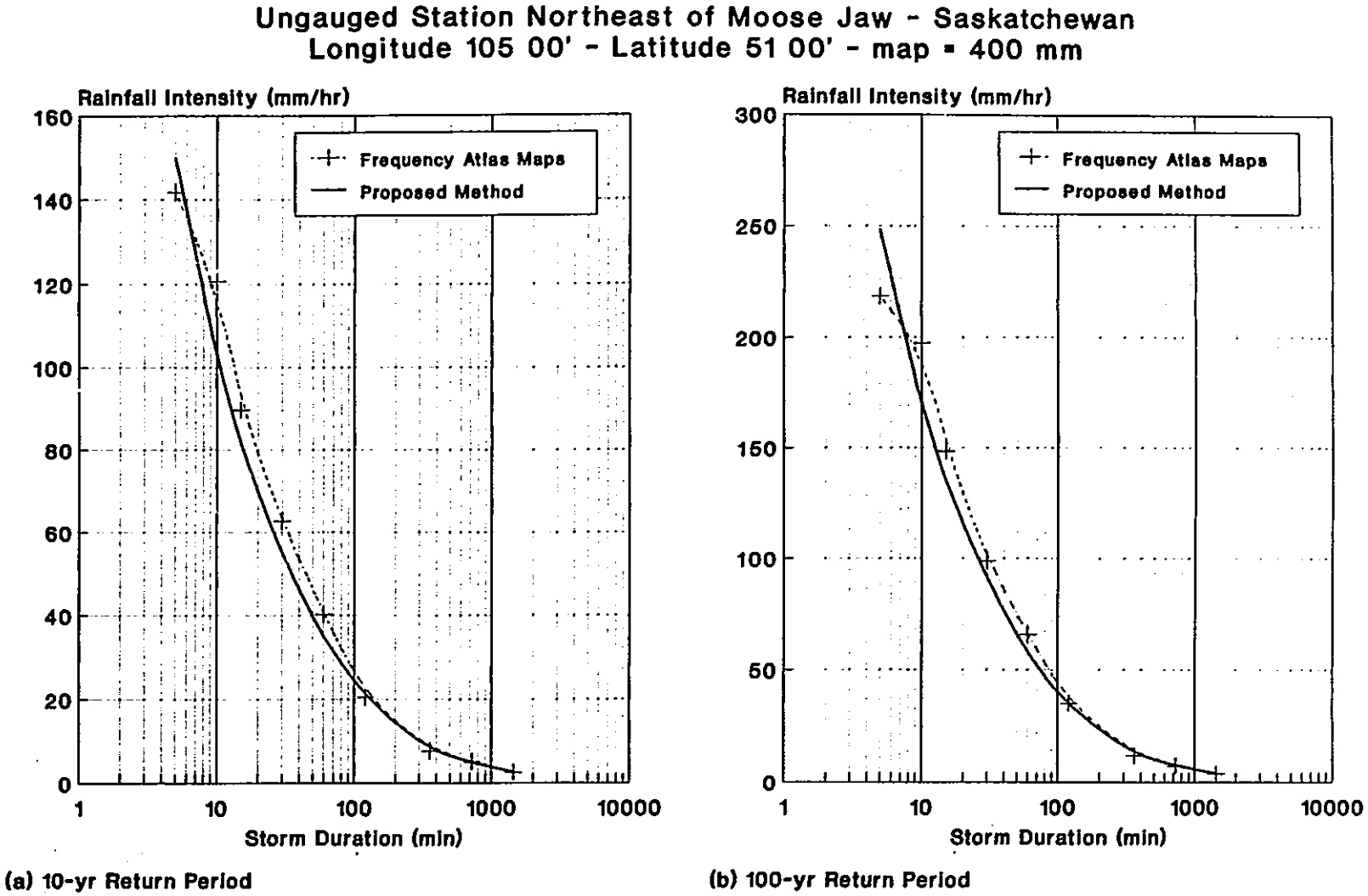

Figure 4.59: Comparison of IDF Curves Computed by Proposed Method of Section 4.8 and those Interpolated from Rainfall Frequency Atlas Maps

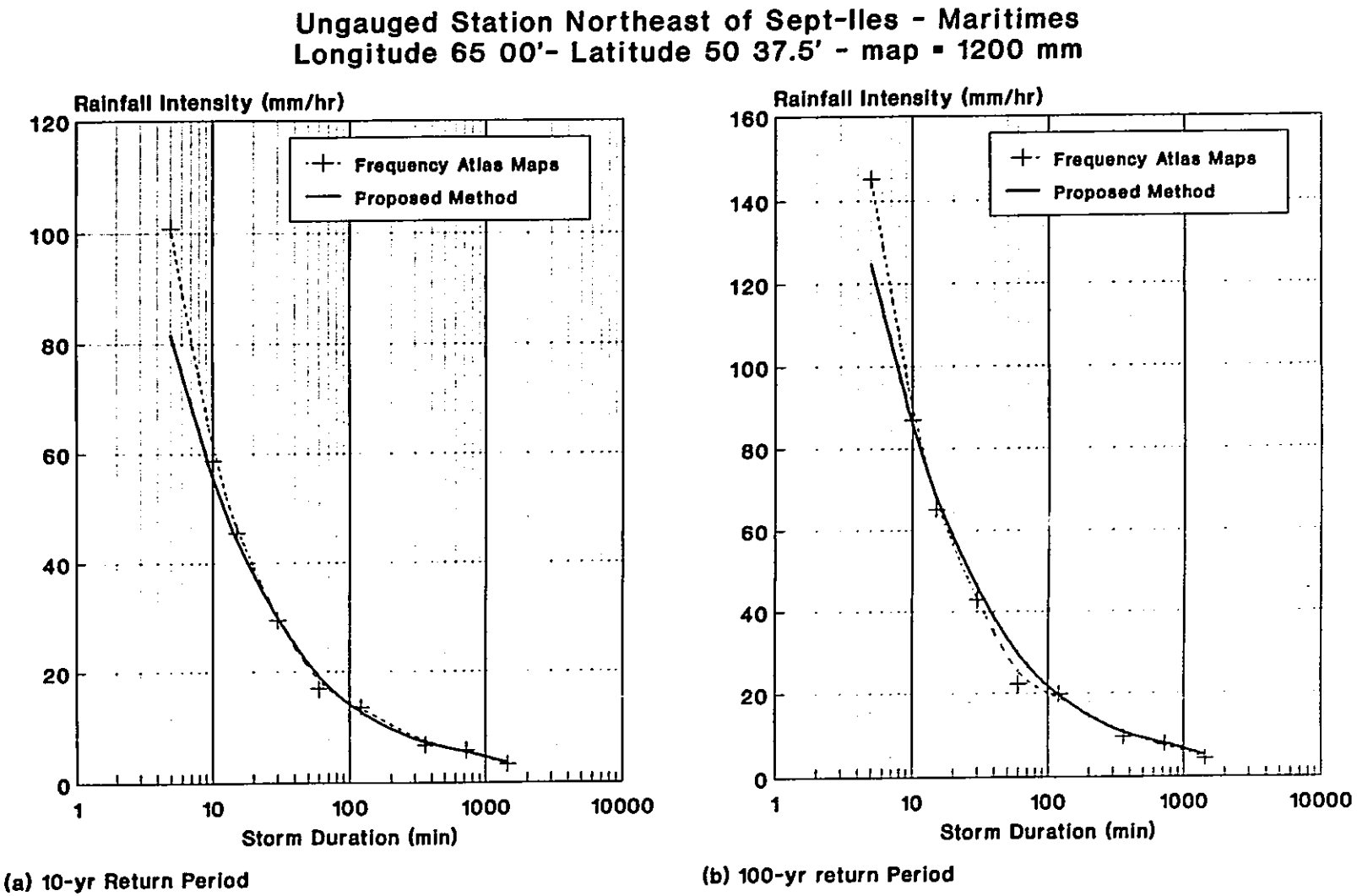

Figure 4.60: Comparison of IDF Curves Computed by Proposed Method of Section 4.8 and those Interpolated from Rainfall Frequency Atlas Maps

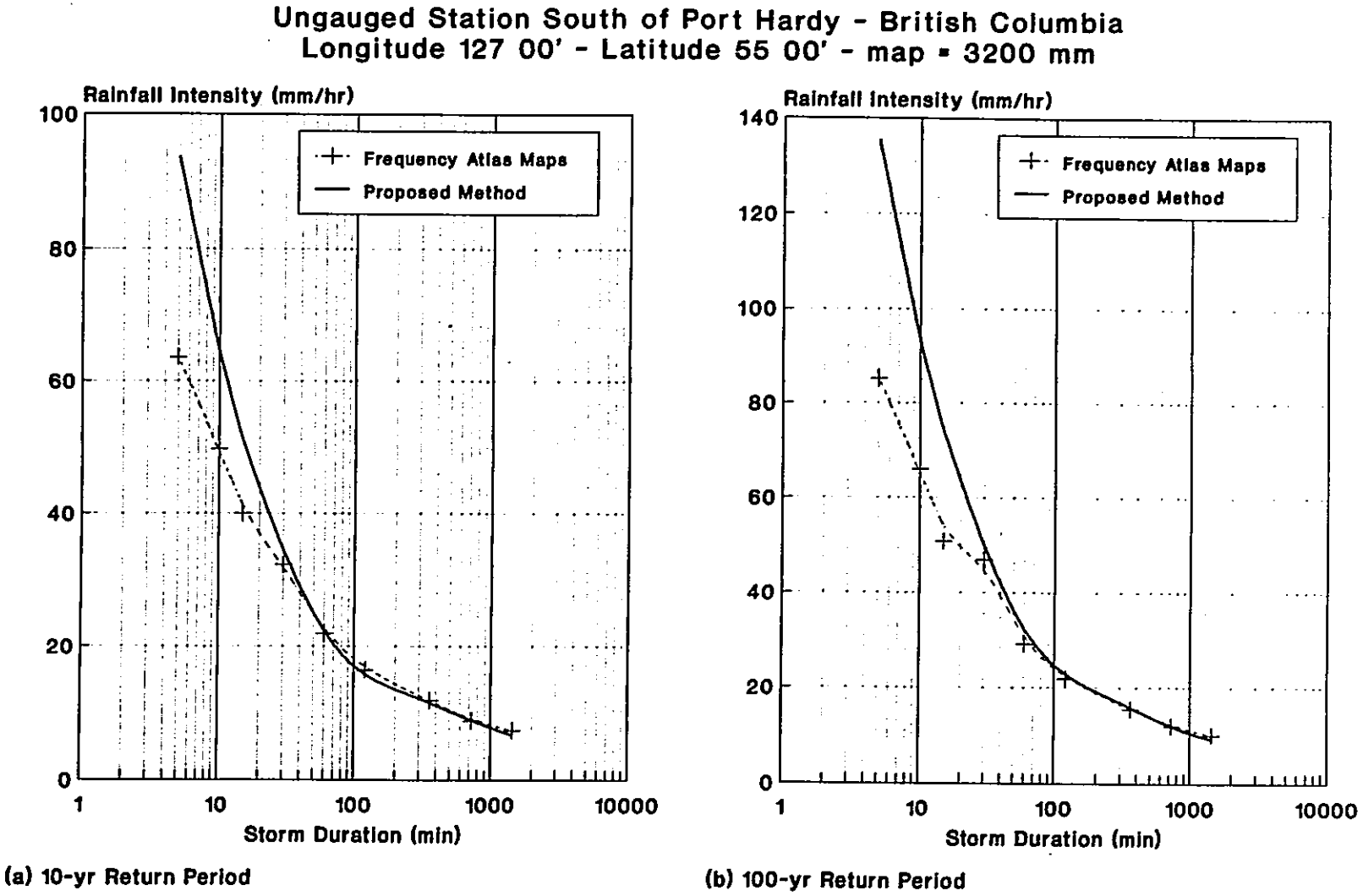

Figure 4.61: Comparison of IDF Curves Computed by Proposed Method of Section 4.8 and those Interpolated from Rainfall Frequency Atlas Maps

Appendix B

Tables

Table 4.1a: Rainfall Gauging Network Information for Study Area

Storm Duration	Minimum Record Length = 10 yr		Minimum Record Length = 15 yr		Minimum Record Length = 20 yr	
	Years of Record	Number of Sites	Years of Record	Number of Sites	Years of Records	Number of Sites
5 min	6207	318	5256	241	3375	130
10 min	6236	319	5297	243	3418	132
15 min	6251	320	5325	244	3483	135
30 min	6239	320	5327	246	3464	136
60 min	7151	375	5913	275	3767	148
2 hr	7136	374	5897	275	3787	149
6 hr	7154	375	5914	275	3787	149
12 hr	7119	374	5879	273	3789	149
24 hr	7157	375	5917	275	3790	149

Table 4.1b: Total Number of Gauged Stations and Average Record Length per Province

Povince	Storm Duration 5 min $\leq$ t $\leq$ 30 min		Storm Duration 1 hr $\leq$ t $\leq$ 24 hr	
	Number of Sites	Average Record Length	Number of Sites	Average Record Length
Alberta	24	22	24	22
British Columbia	60	18	99	17
Manitoba	22	20	22	21
Maritimes	40	20	40	20
Ontario	70	21	80	20
Quebec	74	18	80	18
Saskatchewan	30	21	30	22
Canada	320	19	375	19

Table 4.2: Results of H and S Statistical Tests of Homogeneity for Canadian Rainfall Data

Storm Duration	L-Coefficient of Variation		L-Skewness		L-Kurtosis	
	H	S (%)	H	S (%)	H	S (%)
5 min	6.5	48	1.8	-2	0.7	27
10 min	7.7	53	3.9	16	1.7	40
15 min	8.5	56	3.0	-3	1.2	30
30 min	7.6	52	0.9	-11	-0.1	15
60 min	7.7	53	0.8	-22	0.2	6
2 hr	6.7	47	-0.9	-42	-1.9	-9
6 hr	6.7	51	0.5	-11	-1.7	20
12 hr	6.3	45	0.3	-14	0.3	-14
24 hr	6.3	44	-0.2	-13	-1.2	17

Table 4.3: Sub-Regional L-Coefficient of Variation as a Function of *map*

Storm Duration	Regional Transfer Function	Coefficient of Determination	Standard Error of Estimate (%)
5 min	$t_2 = 0.469 - 0.037 \ln(map)$	0.73	9.6
10 min	$t_2 = 0.862\ (map)^{-0.208}$	0.85	7.8
15 min	$t_2 = 1.167\ (map)^{-0.253}$	0.91	7.0
30 min	$t_2 = 0.627 - 0.061 \ln(map)$	0.93	6.7
60 min	$t_2 = 0.606 - 0.059 \ln(map)$	0.94	6.4
2 hr	$t_2 = 0.592 - 0.059 \ln(map)$	0.91	9.2
6 hr	$t_2 = 1.301\ (map)^{-0.298}$	0.84	11.9
12 hr	$t_2 = 0.482 - 0.045 \ln(map)$	0.88	8.4
24 hr	$t_2 = 0.613\ (map)^{-0.182}$	0.85	7.2

Table 4.4: Weighted Average Third and Fourth L-Moment Ratios for Short Duration Rainfall Extremes in Canada

Storm Duration	Regional L-Skewness	Regional L-Kurtosis
5 min	0.195	0.163
10 min	0.184	0.158
15 min	0.191	0.156
30 min	0.204	0.154
60 min	0.221	0.168
2 hr	0.227	0.178
6 hr	0.212	0.171
12 hr	0.201	0.168
24 hr	0.193	0.156

Table 4.4a: Results of the Z Goodness-of-fit Test for Canadian Rainfall Data

	5 min	10 min	15 min	30 min	60 min	2 hr	6 hr	12 hr	24 hr
GLO	5.45	5.88	6.83	7.57	5.84	4.81	4.94	5.34	7.46
GEV	-1.06	-1.01	-0.09	1.13	-0.38	-1.36	1.48	-1.57	-0.09
GNO	-2.43	-2.15	-1.44	-0.45	-2.37	-3.52	-3.27	-3.15	-1.60
P3	-5.41	-4.87	-4.45	-3.70	-6.19	-7.60	-6.84	-6.48	-4.94
GPA	-15.82	-16.36	-15.69	-13.66	-15.05	-16.05	-16.39	-17.35	-17.15

Table 4.5: Bias (mm) of HRGEV and SGEV Rainfall Frequency Models Based on 10000 Synthetic Replications

	Sample Size n											
	10		20		30		50		75		100	
Return Period (yr)	SGEV	HRGEV	SGEV	HRGEV	SGEV	HRGEV	SGEV	HRGEV	SGEV	HRGEV	SGEV	HRGEV
2	0.1	0.0	0.1	0.0	0.1	0.0	0.0	0.0	0.0	0.0	0.0	0.0
5	-0.3	0.0	-0.1	0.0	-0.1	0.0	-0.1	0.0	0.0	0.0	0.0	0.0
10	-0.7	0.0	-0.3	0.0	-0.2	0.0	-0.1	0.0	-0.1	0.0	-0.1	0.0
20	-0.7	0.0	-0.3	0.0	-0.2	0.0	-0.1	0.0	-0.1	0.0	-0.1	0.0
50	-0.1	0.0	0.1	0.0	0.0	0.0	0.0	0.0	0.0	0.0	0.0	0.0
100	1.3	0.0	0.9	0.0	0.5	0.0	0.3	0.0	0.2	0.0	0.2	0.0
200	3.9	0.0	2.2	0.0	1.3	0.0	0.8	0.0	0.5	0.0	0.4	0.0
500	10.2	0.0	5.3	0.0	3.2	0.0	2.0	0.0	1.3	0.0	1.0	0.0

Table 4.6: RMSE (mm) of HRGEV and SGEV Rainfall Frequency Models Based on 10000 Synthetic Replications

	Sample Size n											
	10		20		30		50		75		100	
Return Period (yr)	SGEV	HRGEV	SGEV	HRGEV	SGEV	HRGEV	SGEV	HRGEV	SGEV	HRGEV	SGEV	HRGEV
2	2.7	2.7	1.9	1.9	1.5	1.6	1.2	1.2	1.0	1.0	0.8	0.8
5	4.2	3.6	3.0	2.6	2.4	2.1	1.8	1.6	1.5	1.3	1.3	1.1
10	5.9	4.3	4.2	3.1	3.5	2.5	2.7	1.9	2.2	1.6	1.9	1.4
20	8.7	5.0	6.4	3.6	5.2	2.9	4.0	2.2	3.3	2.2	2.8	1.6
50	14.8	6.0	10.7	4.3	8.7	3.5	6.7	2.7	5.5	2.5	4.7	1.9
100	22.2	6.8	15.7	4.8	12.6	3.9	9.7	3.0	7.9	2.8	6.7	2.1
200	33.0	7.6	22.9	5.4	17.9	4.4	13.6	3.4	11.1	3.2	9.3	2.4
500	55.9	8.8	36.7	6.3	27.7	5.1	20.6	3.9	16.6	3.5	13.8	2.8

Table 4.7: Long-Term Record Stations Used for Comparison Between SEV1 and HRGEV Models and for Verification of RDDF Equations by Split Sampling Experiment

Station Name	Stn Number	Location	Record Length	map (mm)
Montreal/Dorval	7025250	Quebec	44	946.2
St Thomas	6137362	Ontario	57	912.0
Edmonton	3012208	Alberta	52	466.1
Winnipeg	5023222	Manitoba	39	525.5
Regina	4016560	Saskatchewan	44	345.0
Gander	8401700	Mritimes	44	1130.1
Victoria	1018610	British Columbia	54	647.2
Vancouver*	1108447	British Columbia	34	872.9

* this station is only used in the split sampling experiment

Table 4.8: Rainfall statistics at the Long-Term Record Station 5023222-Winnipeg International Airport - Manitoba

Storm Duration	Mean (mm)	At-Site Standard Deviation	Sub-Regional L-Standard Deviation	Regional L-Skewness
5 min	9.2	3.1	2.18	0.195
10 min	13.4	4.7	3.14	0.184
15 min	16.9	6.1	4.03	0.191
30 min	22.2	8.4	5.42	0.204
60 min	26.2	9.9	6.18	0.221
2 hr	31.7	12.9	7.01	0.227
6 hr	40.5	14.6	8.13	0.212
12 hr	45.3	15.8	9	0.201
24 hr	51.6	16.9	10.1	0.193

Table 4.9: The 10-yr and 100-yr Design Storms Estimated by HRGEV and SEV1 Models at the Long-Term Record Station 5023222 - Winnipeg International Airport

Return Period	10-yr			100-yr		
Storm Duration	SEV1	HRGEV	Deviation (%)	SEV1	HRGEV	Deviation (%)
5 min	158.4	174	9	216	272	21
10 min	117.6	126	7	169.8	193.8	12
15 min	99.6	106.4	6	144.4	166	13
30 min	66.4	70.4	6	97.4	112.2	13
60 min	39.1	41.1	5	57.2	66.5	14
2 hr	24.3	24.3	0	36.1	39	7
6 hr	9.9	10	1	14.4	15.4	6
12 hr	5.5	5.6	2	7.9	8.4	6
24 hr	3.1	3.2	3	4.4	4.7	6

Table 4.10: Absolute Deviation in Percent Between Design Storms Estimated by HRGEV and SEV1 Models at Long-Term Record Stations

Station Name	Station Number	10-yr 5-min	10-yr 60-min	100-yr 5-min	100-yr 60-min
Montreal/Dorval	7025250	8	1	15	5
St Thomas	6137362	4	7	3	3
Edmonton	3012208	3	1	1	5
Winnipeg	5023222	9	5	21	14
Regina	4016560	14	8	18	4
Gander	8401700	10	17	12	18
Victoria	1018610	0	11	2	23
Average Deviation		7	7	10	10

Table 4.11: Short -Term Record Stations Used for Comparison Between HRGEV and SEV1 Models

Station Name	Station Number	Location	Record Length	map (mm)
St Modeste	7057504	Quebec	11	935.6
Slave Lake	3066001	Alberta	14	488.1
Point Pelee	613FN58	Ontario	12	846.2
The Pas River	5052880	Manitoba	16	453.7
Collins Bay	4061630	Saskatchewan	13	522.6
Beechwood	8100512	Mritimes	10	1056.8
Port Mellon	1046330	British Columbia	11	3322.0

Table 4.12: Absolute Deviation in Percent Between Design Storms Estimated by HRGEV and SEV1 Models at Short-Term Record Stations

Station Name	Station Number	10-yr 5-min	10-yr 60-min	100-yr 5-min	100-yr 60-min
St Modeste	7057574	15	12	27	25
Slave Lake	3066001	5	11	10	22
Point Pelee	613FN58	13	5	23	3
The Pas River	5052880	14	1	18	8
Collins Bay	4061630	0	7	1	16
Beechwood	8100512	5	7	5	18
Port Mellon	1046330	8	9	12	21
Average Deviation		9	7	14	16

Table 4.13a: Regression Results of the Linear Depth-Duration Relationship (Equation 4.3) for the 5-min Storm

Return Period (yr)	Slope	Intercept (mm)	Coefficient of Determination	Standard Error of Estimate (mm)
2	0.333	0.19	0.91	0.8
5	0.349	0.04	0.92	1.1
10	0.351	-0.03	0.92	1.3
20	0.352	-0.11	0.92	1.5
50	0.351	-0.15	0.92	1.7
100	0.347	-0.19	0.93	1.9
Average	0.347	-0.04	0.92	1.4

Table 4.13b: Regression Results of the Linear Depth-Duration Relationship (Equation 4.3) for the 10-min Storm

Return Period (yr)	Slope	Intercept (mm)	Coefficient of Determination	Standard Error of Estimate (mm)
2	0.492	0.19	0.93	1.1
5	0.505	0.01	0.93	1.4
10	0.506	-0.08	0.94	1.6
20	0.503	-0.17	0.94	1.8
50	0.496	-0.26	0.95	2.1
100	0.491	-0.32	0.95	2.3
Average	0.499	-0.11	0.94	1.7

Table 4.13c: Regression Results of the Linear Depth-Duration Relationship (Equation 4.3) for the 15-min Storm

Return Period (yr)	Slope	Intercept (mm)	Coefficient of Determination	Standard Error of Estimate (mm)
2	0.616	-0.09	0.94	1.1
5	0.631	-0.37	0.95	1.5
10	0.631	-0.55	0.95	1.7
20	0.629	-0.72	0.95	1.9
50	0.623	-0.94	0.96	2.2
100	0.617	-1.11	0.96	2.5
Average	0.625	-0.63	0.95	1.82

Table 4.13d: Regression Results of the Linear Depth-Duration Relationship (Equation 4.3) for the 30-min Storm

Return Period (yr)	Slope	Intercept (mm)	Coefficient of Determination	Standard Error of Estimate (mm)
2	0.833	-0.61	0.98	0.9
5	0.852	-1.08	0.98	1.3
10	0.856	-1.41	0.98	1.5
20	0.857	-1.74	0.98	1.7
50	0.856	-2.17	0.98	2.1
100	0.852	-2.51	0.98	2.2
Average	0.851	-1.59	0.98	1.62

Table 4.14a: Comparison Between Computed Depth-Duration Ratios for Canada and for other Places in the World*

Time (min)	USA	Australia	USSR	Sicily	Sardinia	Canada
5	0.292	0.3	0.315	0.387	0.425	0.347
10	0.45	0.46	0.44	0.615	0.544	0.5
15	0.569	0.58	0.55	0.637	0.633	0.625
30	0.79	0.77	0.79	0.77	0.794	0.851

* - Bell (1969), Cao et al. (1969), Ferreri and Ferro (1990), and Maksimov (1964)

Tabe 4.14b: Values of 's' Coefficient in the Depth-Duration Equation (4.6) for Different Geographical Regions

Region	's' Coefficient
Sicily*	0.386
Sardinia*	0.345
United States*	0.451
India*	0.29
Canada**	0.393

* Ferro (1993)

** Equation (4.6)

Table 4.15a: Regression Results of the Linear Depth-Duration Relationship (Equation 4.3) for the 120-min Storm Based on Subnetwork I*

Return Period (yr)	Slope	Intercept (mm)	Coefficient of Determination	Standard Error of Estimate (mm)
2	1.128	2	0.93	1.7
5	1.092	3.1	0.93	2.3
10	1.08	3.9	0.93	2.7
20	1.068	4.7	0.93	3.1
50	1.058	5.8	0.92	3.8
100	1.053	6.7	0.92	4.3
Average	1.08	4.37	0.93	3.0

* Sites with a mean annual precipitation value less than or equal to 1200 mm

Table 4.15b: Regression Results of the Linear Depth-Duration Relationship (equation 4.3) for the 120-min Storm Based on Subnetwork II**

Return Period (yr)	Slope	Intercept (mm)	Coefficient of Determination	Standard Error of Estimate (mm)
2	1.256	2.8	0.9	1.9
5	1.2	4.1	0.9	2.4
10	1.179	5	0.91	2.7
20	1.165	5.8	0.91	3
50	1.152	6.9	0.91	3.4
100	1.146	7.8	0.92	3.8
Average	1.18	5.40	0.91	2.9

** Sites with a mean annual precipitation value greater than 1200 mm

Table 4.16a: Regression Results of the Logarithmic Depth-Frequency Relationship (Equation 4.10) for the 5-min Storm.

Return Period (yr)	Slope	Intercept	Coefficient of Determination	Standard Error of Estimate
2	0.042	0.322	0.98	0.3
5	0.017	0.724	0.98	0.1
20	-0.017	1.127	0.98	0.3
50	-0.039	1.635	0.98	0.4
100	-0.057	1.917	0.98	0.5

Table 4.16b: Regression Results of the Logarithmic Depth-Frequency Relationship (Equation 4.10) for the 10-min Storm.

Return Period (yr)	Slope	Intercept	Coefficient of Determination	Standard Error of Estimate
2	0.053	0.257	0.99	0.07
5	0.021	0.700	0.99	0.04
20	-0.021	1.292	0.99	0.05
50	-0.048	1.676	0.99	0.08
100	-0.069	1.970	0.99	0.11

Table 4.16c: Regression Results of the Logarithmic Depth-Frequency Relationship (Equation 4.10) for the 15-min Storm.

Return Period (yr)	Slope	Intercept	Coefficient of Determination	Standard Error of Estimate
2	0.045	0.177	0.98	0.14
5	0.026	0.666	0.98	0.06
20	-0.026	1.328	0.98	0.06
50	-0.060	1.764	0.98	0.13
100	-0.087	2.100	0.98	0.18

Table 4.16d: Regression Results of the Logarithmic Depth-Frequency Relationship (Equation 4.10) for the 30-min Storm.

Return Period (yr)	Slope	Intercept	Coefficient of Determination	Standard Error of Estimate
2	0.073	0.119	0.99	0.26
5	0.030	0.639	0.99	0.11
20	-0.030	1.360	0.99	0.11
50	-0.070	1.847	0.99	0.26
100	-0.102	2.228	0.99	0.38

Table 4.16e: Regression Results of the Logarithmic Depth-Frequency Relationship (Equation 4.10) for the 60-min Storm.

Return Period (yr)	Slope	Intercept	Coefficient of Determination	Standard Error of Estimate
2	0.074	0.118	0.99	0.27
5	0.031	0.633	0.99	0.11
20	-0.031	1.373	0.99	0.11
50	-0.074	1.888	0.99	0.27
100	-0.109	2.298	0.99	0.41

Table 4.16f: Regression Results of the Logarithmic Depth-Frequency Relationship (Equation 4.10) for the 120-min Storm.

Return Period (yr)	Slope	Intercept	Coefficient of Determination	Standard Error of Estimate
2	0.076	0.118	0.98	0.11
5	0.032	0.631	0.98	0.61
20	-0.032	1.377	0.98	0.25
50	-0.078	1.901	0.98	0.61
100	-0.114	2.323	0.98	0.91

Table 4.17a: Comparison of the HRGEV Model and RDDF Equations at the Long-Term Record Station 6137362 , St. Thomas WPCP - Ontario (n=57)

Storm Duration (min)	Design Storm Estimated by HRGEV (mm/hr)		Design Storm Estimated by RDDF Equations (mm/hr)		Deviation* (%)	
	10-yr	100-yr	10-yr	100-yr	10-yr	100-yr
5	166.8	255.6	169.0	265.4	-1	-4
10	119.4	178.8	114.4	179.4	4	0
15	96.4	145.2	91.2	143.1	5	1
30	64.0	98.4	61.7	97.0	4	1
60	40.2	62.7	41.8	65.7	-4	-5
120	24.1	37.1	22.9	36.3	5	2
Absolute Average Deviation					4	2

* Deviation (%)=((Estimate by HRGEV - Estimate by RDDF)/Estimate by HRGEV)*100

Table 4.17b: Comparison of the SEV1 Model and AES Equation (2.19) at the Long-Term Record Station 6137362 , St. Thomas WPCP - Ontario (n=57)

Storm Duration (min)	Design Storm Estimated by SEV1 (mm/hr)		Design Storm Estimated by AES Equation (mm/hr)		Deviation** (%)	
	10-yr	100-yr	10-yr	100-yr	10-yr	100-yr
5	171.6	258.0	200.4	285.2	-17	-14
10	117.6	170.4	124.2	183.0	-6	-7
15	95.2	139.2	94.0	138.4	1	1
30	63.4	92.8	58.0	85.6	9	8
60	40.6	59.7	36.0	53.0	11	11
120	25.5	38.2	22.3	32.8	13	14
Absolute Average Deviation					9	9

** Deviation (%)=((Estimate by SEV1 - Estimate by AES Equation)/Estimate by SEV1)*100

Table 4.18a: Comparison of the HRGEV Model and RDDF Equations at the Long-Term Record Station 7025250, Dorval/Montreal Airport - Quebec (n=44)

Storm Duration (min)	Design Storm Estimated by HRGEV (mm/hr)		Design Storm Estimated by RDDF Equations (mm/hr)		Deviation* (%)	
	10-yr	100-yr	10-yr	100-yr	10-yr	100-yr
5	159.6	243.6	147.1	230.5	8	5
10	111.0	165.6	99.7	156.1	10	6
15	90.0	135.2	79.4	124.3	12	8
30	58.6	90.0	53.8	84.2	8	6
60	35.0	54.5	36.4	57.1	-4	-5
120	20.2	31.2	20.2	32.0	0	-3
Absolute Average Deviation					7	5

* Deviation (%)=((Estimate by HRGEV - Estimate by RDDF)/Estimate by HRGEV)x100

Table 4.18b: Comparison of the SEV1 Model and AES Equation (2.19) at the Long-Term Station 7025250, Dorval/Montreal Airport - Quebec (n=44)

Storm Duration (min)	Design Storm Estimated by SEV1 (mm/hr)		Design Storm Estimated by AES Equation (mm/hr)		Deviation** (%)	
	10-yr	100-yr	10-yr	100-yr	10-yr	100-yr
5	147.6	206.4	181.0	260.1	-23	-26
10	104.4	148.8	110.2	158.4	-6	-6
15	87.6	126.4	82.5	118.0	6	7
30	59.0	87.2	50.3	71.6	15	18
60	35.4	52.0	30.6	43.5	14	16
120	19.9	28.3	18.6	26.4	7	7
Absolute Average Deviation					11	13

** Deviation (%)=((Estimate by SEV1 - Estimate by AES Equation)/Estimate by SEV1)x100

Table 4.19a: Comparison of the HRGEV Model and RDDF Equations at the Long-Term Record Station 5023222, Winnipeg Int'l Airport - Manitoba (n=39)

Storm Duration (min)	Design Storm Estimated by HRGEV (mm/hr)		Design Storm Estimated by RDDF Equations (mm/hr)		Deviation* (%)	
	10-yr	100-yr	10-yr	100-yr	10-yr	100-yr
5	174.0	272.4	172.2	280.0	1	-3
10	126.0	193.8	116.6	189.7	7	2
15	106.4	166.0	92.9	151.0	13	9
30	70.4	112.2	62.9	102.3	11	9
60	41.1	66.5	42.6	69.3	-4	-4
120	24.3	39.0	23.3	38.1	4	2
Absolute Average Deviation					7	5

* Deviation (%)=((Estimate by HRGEV - Estimate by RDDF)/Estimate by HRGEV)x100

Table 4.19b: Comparison of the SEV1 Model and AES Equation (2.19) at the Long-Term Station 5023222, Winnipeg Int'l Airport - Manitoba (n=39)

Storm Duration (min)	Design Storm Estimated by SEV1 (mm/hr)		Design Storm Estimated by AES Equation (mm/hr)		Deviation** (%)	
	10-yr	100-yr	10-yr	100-yr	10-yr	100-yr
5	158.4	216.0	204.0	295.2	-29	-37
10	117.6	169.8	124.2	180.0	-6	-6
15	99.6	144.4	92.8	134.8	7	7
30	66.4	97.4	56.6	82.2	15	16
60	39.1	57.2	34.6	50.1	12	12
120	24.3	36.1	21.1	30.6	13	15
Absolute Average Deviation					13	15

** Deviation (%)=((Estimate by SEV1 - Estimate by AES Equation)/Estimate by SEV1)x100

Table 4.20a: Comparison of the HRGEV Model and RDDF Equations at the Long-Term Record Station 4016560, Regina Airport - Saskatchewan (n=44)

Storm Duration (min)	Design Storm Estimated by HRGEV (mm/hr)		Design Storm Estimated by RDDF Equations (mm/hr)		Deviation* (%)	
	10-yr	100-yr	10-yr	100-yr	10-yr	100-yr
5	145.2	229.2	154.3	255.9	-6	-12
10	110.4	173.4	104.5	173.3	5	0
15	91.2	145.2	83.3	138.0	9	5
30	62.0	101.0	56.4	93.5	9	7
60	36.9	61.2	38.2	63.3	-4	-3
120	21.4	35.2	21.1	35.1	1	0
Absolute Average Deviation					6	5

* Deviation (%)=((Estimate by HRGEV - Estimate by RDDF)/Estimate by HRGEV)x100

Table 4.20b: Comparison of the SEV1 Model and AES Equation (2.19) at the Long-Term Station 4016560, Regina Airport - Saskatchewan (n=44)

Storm Duration (min)	Design Storm Estimated by SEV1 (mm/hr)		Design Storm Estimated by AES Equation (mm/hr)		Deviation** (%)	
	10-yr	100-yr	10-yr	100-yr	10-yr	100-yr
5	165.2	271.2	204.0	331.2	-23	-22
10	120.6	194.4	125.4	229.8	-4	-18
15	99.2	160.4	94.4	170.0	5	-6
30	67.4	109.2	58.2	94.2	14	14
60	39.9	63.9	35.9	57.9	10	9
120	23.7	38.1	22.1	35.6	7	7
Absolute Average Deviation					10	13

** Deviation (%)=((Estimate by SEV1 - Estimate by AES Equation)/Estimate by SEV1)x100

Table 4.21a: Comparison of the HRGEV Model and RDDF Equations at the Long-Term Record Station 3012208, Edmonton Municipal Airport- Alberta (n=52)

Storm Duration (min)	Design Storm Estimated by HRGEV (mm/hr)		Design Storm Estimated by RDDF Equations (mm/hr)		Deviation* (%)	
	10-yr	100-yr	10-yr	100-yr	10-yr	100-yr
5	116.4	182.4	118.9	194.8	-2	-7
10	88.8	136.8	80.6	131.9	9	4
15	72.4	113.6	64.1	105.0	11	8
30	47.2	75.6	43.5	71.2	8	6
60	28.4	46.3	29.4	48.2	-4	-4
120	14.8	24.0	16.7	26.2	-13	-9
Absolute Average Deviation					8	6

* Deviation (%)=((Estimate by HRGEV - Estimate by RDDF)/Estimate by HRGEV)x100

Table 4.21b: Comparison of the SEV1 Model and AES Equation (2.19) at the Long-Term Station 3012208, Edmonton Municipal Airport - Alberta (n=52)

Storm Duration (min)	Design storm Estimated by SEV1 (mm/hr)		Design Storm Estimated by AES Equation (mm/hr)		Deviation** (%)	
	10-yr	100-yr	10-yr	100-yr	10-yr	100-yr
5	121.1	188.4	146.4	230.4	-22	-22
10	92.4	143.4	92.4	144.6	0	-1
15	75.6	118.0	70.8	110.0	6	7
30	50.6	80.6	44.6	69.2	12	14
60	30.3	47.6	28.1	43.5	7	9
120	17.9	27.3	17.7	27.3	1	0
Absolute Average Deviation					8	9

** Deviation (%)=((Estimate by SEV1 - Estimate by AES Equation)/Estimate by SEV1)x100

Table 4.22a: Comparison of the HRGEV Model and RDDF Equations at the Long-Term Record Station 1108447, Vancouver Airport- British Columbia (n=34)

Storm Duration (min)	Design Storm Estimated by HRGEV (mm/hr)		Design Storm Estimated by RDDF Equations (mm/hr)		Deviation* (%)	
	10-yr	100-yr	10-yr	100-yr	10-yr	100-yr
5	58.8	91.2	66.5	103.0	-13	-13
10	42.6	63.6	45.0	69.8	-6	-10
15	35.2	53.2	35.9	55.6	-2	-5
30	23.2	36.0	24.3	37.7	-5	-5
60	15.8	24.7	16.5	25.5	-4	-3
120	10.6	16.4	11.7	18.4	-10	-12
Absolute Average Deviation					7	8

* Deviation (%)=((Estimate by HRGEV - Estimate by RDDF)/Estimate by HRGEV)x100

Table 4.22b: Comparison of SEV1 Model and AES Equation (2.19) at Long-Term Station 1108447, Vancouver Airport - British Columbia (n=34)

Storm Duration (min)	Design Storm Estimated by SEV1 (mm/hr)		Design Storm Estimated by AES Equation (mm/hr)		Deviation** (%)	
	10-yr	100-yr	10-yr	100-yr	10-yr	100-yr
5	57.6	82.8	57.6	85.2	0	-3
10	42.0	61.2	40.2	58.2	4	5
15	35.2	51.6	32.4	46.8	8	9
30	23.0	33.4	22.4	31.8	3	5
60	14.4	19.7	15.5	21.8	-8	-11
120	9.8	13.3	10.8	14.9	-10	-12
Absolute Average Deviation					5	7

** Deviation (%)=((Estimate by SEV1 - Estimate by AES Equation)/Estimate by SEV1)x100

Table 4.23a: Comparison of the HRGEV Model and RDDF Equations at the Long-Term Record Station 1018610, Victoria/Gonzales - British Columbia (n=54)

Storm Duration (min)	Design Storm Estimated by HRGEV (mm/hr)		Design Storm Estimated by RDDF Equations (mm/hr)		Deviation* (%)	
	10-yr	100-yr	10-yr	100-yr	10-yr	100-yr
5	37.2	57.6	49.1	78.8	-32	-37
10	26.4	40.2	33.3	53.4	-26	-33
15	21.6	33.6	26.5	42.5	-23	-26
30	15.4	24.2	17.9	23.8	-16	-19
60	11.7	18.6	12.1	19.5	-3	-5
120	9.0	14.2	8.0	13.1	11	8
Absolute Average Deviation					19	21

* Deviation (%)=((Estimate by HRGEV - Estimate by RDDF)/Estimate by HRGEV)x100

Table 4.23b: Comparison of the SEV1 Model and AES Equation (2.19) at the Long-Term Station 1018610, Victoria/Gonzales - British Columbia (n=54)

Storm Duration (min)	Design Storm Estimated by SEV1 (mm/hr)		Design Storm Estimated by AES Equation (mm/hr)		Deviation** (%)	
	10-yr	100-yr	10-yr	100-yr	10-yr	100-yr
5	37.2	56.4	33.6	48.0	10	15
10	26.4	39.6	25.2	36.0	5	9
15	21.2	30.8	21.2	30.4	0	1
30	13.6	18.6	15.8	22.8	-13	-23
60	10.4	14.3	11.8	17.0	-13	-19
120	8.5	12.0	8.8	12.7	-4	-6
Absolute Average Deviation					7	12

** Deviation (%)=((Estimate by SEV1 - Estimate by AES Equation)/Estimate by SEV1)x100

Table 4.24a: Comparison of the HRGEV Model and RDDF Equations at the Long-Term Record Station 8401700, Gander Int'l Airport - Maritimes (n=44)

Storm Duration (min)	Design Storm Estimated by HRGEV (mm/hr)		Design Storm Estimated by RDDF Equations (mm/hr)		Deviation* (%)	
	10-yr	100-yr	10-yr	100-yr	10-yr	100-yr
5	86.4	130.8	111.9	173.4	-39	-33
10	64.4	91.2	75.8	117.4	-18	-29
15	61.8	85.0	60.4	93.5	2	-10
30	40.2	61.6	40.9	63.4	-2	-3
60	26.6	41.5	27.7	42.9	-4	-3
120	13.1	19.8	15.9	24.9	-21	-26
Absolute Average Deviation					14	17

* Deviation (%)=((Estimate by HRGEV - Estimate by RDDF)/Estimate by HRGEV)x100

Table 4.24b: Comparison of the SEV1 Model and AES Equation (2.19) at the Long-Term Station 8401700, Gander Int'l Airport - Maritimes (n=44)

Storm Duration (min)	Design Storm Estimated by SEV1 (mm/hr)		Design Storm Estimated by AES Equation (mm/hr)		Deviation** (%)	
	10-yr	100-yr	10-yr	100-yr	10-yr	100-yr
5	94.8	146.4	106.8	169.2	-13	-16
10	68.4	106.8	68.4	106.8	0	0
15	54.8	86.0	52.4	81.6	4	5
30	37.8	60.2	33.6	51.4	11	15
60	22.2	34.1	21.6	32.4	3	5
120	13.4	19.4	13.9	20.5	-4	-6
Absolute Average Deviation					6	8

** Deviation (%)=((Estimate by SEV1 - Estimate by AES Equation)/Estimate by SEV1)x100

Table 4.25: Ungauged Sites Used for Comparison of the Proposed Method of Section 4.8 and Interpolation Procedure from Rainfall Frequency Atlas Maps

Station Proximity	Longitude	Latitude	Location	map (mm)
West of Schefferville	70 00'	50 50.5'	Quebec	646.2
Southwest of Fitzgerald	115 00'	59 25'	Alberta	350.0
Near Lake Ninissing	80 00'	45 43'	Ontario	900.0
Southwest of Island Lake	95 00'	53 34.3 '	Manitoba	500.0
Northeast of Moose Jaw	105 00'	51 00'	Saskatchewan	400.0
Northeast of Sept-Iles	65 00'	50 37.5'	Maritimes	1200.0
South of Port Hardy	127 00'	55 00	British Columbia	3200.0

Table 4.26: Comparison of the Proposed Method and Interpolation from Rainfall Frequency Atlas Maps at the Ungauged Site West of Schefferville - Quebec (Longitude 70 00' and Latitude 50 37.5' - map= 646.2 mm)

Storm Duration	Design Storm by Proposed Method (mm/hr)		Design Storm by Interpolation from Frequency Atlas Maps (mm/hr)		Deviation* (%)	
	10-yr	100-yr	10-yr	100-yr	10-yr	100-yr
5 min	78.0	124.8	100.6	166.8	-29	-34
10 min	52.8	84.6	60.0	93.0	-14	-10
15 min	41.6	67.2	43.6	65.6	-5	2
30 min	28.2	45.2	28.6	43.2	-1	4
60 min	17.7	28.3	17.5	25.4	1	10
2 hr	11.8	19.0	10.6	15.0	10	21
6 hr	5.5	8.3	5.1	7.1	7	15
12 hr	3.2	4.8	3.1	4.3	3	10
24 hr	1.8	2.7	1.8	2.6	1	3
Absolute Average Deviation					8	12

* Deviation (%)=((Estimate by Proposed Method - Estimate by Interpolation)/Estimate by Proposed Method)*100

Table 4.27: Comparison of the Proposed Method and Interpolation from Rainfall Frequency Atlas Maps at the Ungauged Site Southwest of Fitzgerald - Alberta (Longitude 115 00' and Latitude 59 25' - map=350 mm)

Storm Duration	Design Storm by Proposed Method (mm/hr)		Design Storm by Interpolation from Frequency Atlas Maps (mm/hr)		Deviation* (%)	
	10-yr	100-yr	10-yr	100-yr	10-yr	100-yr
5 min	79.2	132.0	73.2	117.6	8	11
10 min	53.4	89.4	48.6	70.6	9	21
15 min	42.4	70.8	38.0	56.0	10	21
30 min	28.6	47.8	26.0	38.0	9	21
60 min	18.0	30.0	16.7	24.0	7	20
2 hr	11.9	19.8	11.0	16.0	8	19
6 hr	5.3	8.4	5.0	7.1	6	16
12 hr	3.4	5.2	3.1	4.4	8	15
24 hr	1.8	2.8	1.9	2.8	-4	-1
Absolute Average Deviation					8	16

* Deviation (%)=((Estimate by Proposed Method - Estimate by Interpolation)/Estimate by Proposed Method)*100

Table 4.28: Comparison of the Proposed Method and Interpolation from Rainfall Frequency Atlas Maps at the Ungauged Site Near Lake Ninissing - Ontario (Longitude 80 00' and Latitude 45 43' - map=900 mm)

Storm Duration	Design Storm by Proposed Method (mm/hr)		Design Storm by Interpolation from Frequency Atlas Maps (mm/hr)		Deviation* (%)	
	10-yr	100-yr	10-yr	100-yr	10-yr	100-yr
5 min	181.2	284.4	154.8	220.8	15	22
10 min	122.4	192.0	115.2	159.0	6	17
15 min	97.2	152.8	90.0	126.8	7	17
30 min	65.6	103.0	59.6	81.6	9	21
60 min	41.1	64.6	39.8	53.6	3	17
2 hr	24.4	38.5	20.8	29.1	14	24
6 hr	9.4	13.9	9.1	12.4	3	11
12 hr	5.0	7.4	4.9	6.7	3	9
24 hr	3.0	4.3	2.8	3.9	6	10
Absolute Average Deviation					7	16

* Deviation (%)=((Estimate by Proposed Method - Estimate by Interpolation)/Estimate by Proposed Method)*100

Table 4.29: Comparison of the Proposed Method and Interpolation from Rainfall Frequency Atlas Maps at the Ungauged Site Southwest of Island Lake - Manitoba (Longitude 95 00' and Latitude 53 34.3' map = 900 mm)

Storm Duration	Design Storm by Proposed Method (mm/hr)		Design Storm by Interpolation from Frequency Atlas Maps (mm/hr)		Deviation* (%)	
	10-yr	100-yr	10-yr	100-yr	10-yr	100-yr
5 min	120.0	196.8	129.6	206.4	-8	-5
10 min	81.0	132.6	89.4	138.4	-10	-4
15 min	64.4	105.2	72.8	113.2	-13	-8
30 min	43.6	71.0	51.8	82.6	-19	-16
60 min	27.3	44.5	30.7	48.5	-13	-9
2 hr	17.0	27.7	18.7	30.6	-10	-11
6 hr	7.6	11.7	8.1	12.4	-7	-6
12 hr	4.4	6.6	4.5	6.6	-3	1
24 hr	2.9	4.4	3.1	4.6	-6	-5
Absolute Average Deviation					10	7

* Deviation (%)=((Estimate by Proposed Method - Estimate by Interpolation)/Estimate by Proposed Method)*100

Table 4.30: Comparison of the Proposed Method and Interpolation from Rainfall Frequency Atlas Maps at the Ungauged Site Northeast of Moose Jaw - Saskatchewan (Longitude 105 00' and Latitude 51 00' map= 400 mm)

Storm Duration	Design Storm by Proposed Method (mm/hr)		Design Storm by Interpolation from Frequency Atlas Maps (mm/hr)		Deviation* (%)	
	10-yr	100-yr	10-yr	100-yr	10-yr	100-yr
5 min	150.0	248.4	141.6	218.4	6	12
10 min	101.4	167.4	120.6	197.4	-19	-18
15 min	80.4	132.8	89.6	148.4	-11	-12
30 min	54.2	89.8	62.6	98.8	-16	-10
60 min	34.0	56.2	40.3	65.9	-19	-17
2 hr	20.6	34.0	20.5	35.1	0	-3
6 hr	7.0	11.0	7.6	11.9	-9	-9
12 hr	5.0	7.7	5.1	7.4	-1	4
24 hr	2.6	3.9	2.5	3.8	3	3
Absolute Average Deviation					9	10

* Deviation (%)=((Estimate by Proposed Method - Estimate by Interpolation)/Estimate by Proposed Method)*100

Table 4.31: Comparison of the Proposed Method and Interpolation from Rainfall Frequency Atlas Maps at the Ungauged Site Northeast of Sept-Iles - Maritimes (Longitude 65 00' and Latitude 50 37.5' map= 1200 mm)

Storm Duration	Design Storm by Proposed Method (mm/hr)		Design Storm by Interpolation from Frequency Atlas Maps (mm/hr)		Deviation* (%)	
	10-yr	100-yr	10-yr	100-yr	10-yr	100-yr
5 min	81.6	124.8	100.8	145.2	-24	-16
10 min	54.6	84.6	58.8	87.0	-8	-3
15 min	43.6	67.2	45.6	65.24	-5	3
30 min	29.4	45.2	29.4	43.0	0	5
60 min	18.4	28.4	17.0	22.4	8	21
2 hr	12.2	19.0	13.5	19.8	-11	-5
6 hr	6.5	9.4	6.7	9.5	-4	-1
12 hr	5.8	8.3	5.7	7.8	2	7
24 hr	3.5	5.1	3.2	4.3	9	15
Absolute Average Deviation					8	8

* Deviation (%)=((Estimate by Proposed Method - Estimate by Interpolation)/Estimate by Proposed Method)*100

Table 4.32: Comparison of the Proposed Method and Interpolation from Rainfall Frequency Atlas Maps at the Ungauged Site South of Port Hardy - British Columbia (Longitude 127 00' and Latitude 55 00' map= 3200 mm)

Storm Duration	Design Storm by Proposed Method (mm/hr)		Design Storm by Interpolation from Frequency Atlas Maps (mm/hr)		Deviation* (%)	
	10-yr	100-yr	10-yr	100-yr	10-yr	100-yr
5 min	93.6	135.6	63.6	85.2	32	37
10 min	63.6	91.8	49.8	66.0	22	28
15 min	50.4	72.8	40.0	50.8	21	30
30 min	34.0	49.2	32.4	47.0	5	5
60 min	21.3	30.8	21.9	29.2	-3	5
2 hr	14.8	21.8	16.4	21.9	-11	-1
6 hr	11.8	16.0	11.8	15.4	0	4
12 hr	8.5	11.5	8.8	11.9	-3	-3
24 hr	6.7	9.3	7.3	10.0	-9	-8
Absolute Average Deviation					12	13

* Deviation (%)=((Estimate by Proposed Method - Estimate by Interpolation)/Estimate by Proposed Method)*100

Appendix C

Database

RAIN GAUGE DATA BASE USEDIN THE ANALYSIS
PROVINCE OF QUEBEC
(AES FORMAT)

FILE : INDEX DISK IDENT : A:IDF_QU.D1

7025745ORMSTOWN	QUE19631986	214507	7403	4521
7022720GEORGEVILLE	QUE19681986	194508	7214	26519
7027040STE CLOTHILDE CDA	QUE19691986	174510	7341	5417
7020840BROME	QUE19711986	154511	7234	20415
7027120STE EDWIDGE	QUE19681984	164512	7141	38016
7027372ST ISIDORE D'AUCKLAND	QUE19651981	164516	7131	39316
7021320CHARTIERVILLE	QUE19681986	194517	7112	51819
7024624MAPLE LEAF EAST	QUE19651980	164520	7124	44116
7024280LENNOXVILLE CDA	QUE19601986	264522	7150	15826
7027802SAWYERVILLE NORD	QUE19661986	204522	7132	34420
7023312ISLAND BROOK	QUE19661981	164523	7128	34416
7022800GRANBY	QUE19701986	174523	7242	16717
7028946WOBURN	QUE19731986	144523	7052	39614
7028906WEST DITTON	QUE19651986	214524	7118	50521
7028120SHERBROOKE	QUE19591971	134524	7154	17913
7026839STE ANNE DE BELLEVUE	QUE19631986	234526	7356	3923
7028124SHERBROOKE A	QUE19621986	244526	7141	23724
7025250MONTREAL/DORVAL INT'L A	QUE19431986	444528	7345	3044
7015730OKA	QUE19691985	174530	7404	9117
7025260MONTREAL JEAN BREBEUF	QUE19691985	174530	7337	13116
7025280MONTREAL MCGILL	QUE19061986	764530	7335	5428
7027320ST HUBERT A	QUE19651986	204531	7325	2720
7025267MONTREAL LAFONTAINE	QUE19731986	134531	7334	3913
7016906ST BENOIT	QUE19731986	134534	7403	5113
7023677LAC MEGANTIC 2	QUE19701986	174536	7053	46317
7038040SHAWVILLE	QUE19701986	174536	7630	16717
7024320LINGWICK	QUE19681986	184538	7122	26518
7027725ST SEBASTIEN	QUE19731986	144546	7057	44114
7037400ST JEROME	QUE19711986	144548	7403	16714
7014160L'ASSOMPTION CDA	QUE19631986	244549	7326	1824
7027302ST GUILLAUME	QUE19731986	144553	7246	4214
7022160DRUMMONDVILLE	QUE19671986	174553	7229	8216
7031375CHENEVILLE	QUE19721986	134554	7505	22213
7027750ST THEOPHILE	QUE19661986	194556	7029	50919
7013362JOLIETTE VILLE	QUE19671984	144600	7325	4514
7020305ARTHABASKA	QUE19631986	194601	7157	13419
7036762STE AGATHE DES MONTS	QUE19661986	214603	7417	39921
7027200ST EPHREM	QUE19661986	194604	7058	31019
7028441THETFORD MINES	QUE19671986	204606	7121	38020
7027785ST ZACHARIE	QUE19731986	144607	7023	47814

RAIN GAUGE DATA BASE USED IN THE ANALYSIS
PROVINCE OF QUEBEC (continued)
(AES FORMAT)

FILE : INDEX DISK IDENT : A:IDF_QU.D2

7027283ST GEORGES	QUE19661986	204609	7042	16720
7027656ST PIERRE DE BROUGHTON	QUE19721986	154615	7113	36515
7017100ST DONAT	QUE19701986	134619	7412	38713
7035520NOMININGUE	QUE19711986	154623	7503	30415
7034480MANIWAKI	QUE19651986	214623	7558	16721
7028676VALLEE JONCTION	QUE19661986	184623	7056	15218
701HE63TROIS RIVIERES AQUEDUC	QUE19771986	104623	7237	5410
7057287STE GERMAINE	QUE19661986	214625	7028	50921
7022494FORTIERVILLE	QUE19741986	134629	7203	5113
7057518ST MALACHIE	QUE19661986	214633	7049	21921
7018000SHAWINIGAN	QUE19681986	194634	7245	12119
7011982DESCHAMBAULT	QUE19731986	144640	7156	1514
7077570ST MICHEL DES SAINTS	QUE19701986	164641	7355	35016
7016800ST ALBAN	QUE19691986	174643	7205	7617
7030457BARRAGE MERCIER	QUE19671979	134643	7559	23413
7080468BARRAGE TEMISCAMINGUE	QUE19681986	194643	7906	17919
7016900ST AUGUSTIN	QUE19661986	214644	7130	5721
7017B65STE FOY MATAPEDIA	QUE19691984	134645	7117	4513
7017BFNSTE FOY (PIE XII)	QUE19721986	154646	7119	7915
7016280QUEBEC CITY	QUE19141943	304648	7113	8830
7016294QUEBEC A	QUE19611986	264648	7123	7026
7012232DUBERGER	QUE19721986	144649	7118	1514
7016932STE CATHERINE	QUE19681986	194651	7137	15219
7012240DUCHESNAY	QUE19711986	154652	7139	16415
7011309CHARLESBOURG PARC ORLEAN	QUE19721986	154652	7116	11215
701A9E0COURVILLE DE POISSY	QUE19711981	114653	7110	11211
7041177CAP TOURMENTE	QUE19731984	114704	7047	611
7042388FORET MONTMORENCY	QUE19671986	204719	7109	64020
7054095LA POCATIERE CDA	QUE19621986	254721	7002	3025
7056922ST BRUNO KAMOURASKA	QUE19691986	174727	6947	19817
7080452BARRAGE DES QUINZE	QUE19671986	204733	7914	26520
7042870GRAND FONDS	QUE19701985	144745	7007	36514
7056615RIVIERE DU LOUP	QUE19681980	114748	6933	14610
7057574ST MODESTE	QUE19741984	114751	6923	15211
7065100MONT APICA	QUE19701986	164758	7125	54816
7098600VAL D'OR A	QUE19611986	254804	7747	33525
7055705NOUVELLE	QUE19711986	154806	6618	1515
7053649LAC HUMQUI	QUE19731986	144817	6734	23414
7066080PORTAGE DES ROCHES	QUE19691984	164818	7113	16415
7056970ST CHARLES GARNIER	QUE19701986	154820	6803	32315

RAIN GAUGE DATA BASE USED IN THE ANALYSIS
PROVINCE OF ALBERTA
(AES FORMAT)

FILE : INDEX DISK IDENT : A:IDF_AL.D1

3044200MANYBERRIES CDA	ALTA19641986	17490711028	93216
3035202PINCHER CREEK AIRPORT	ALTA19651986	22493111400118822	
3033880LETHBRIDGE AIRPORT	ALTA19601986	27493811248	92627
3034480MEDICINE HAT AIRPORT	ALTA19711986	16500111043	71616
3036681VAUXHALL CDA	ALTA19561986	31500311208	77731
3030856BROOKS AHRC	ALTA19651986	20503311151	75520
3031093CALGARY INT'L AIRPORT	ALTA19471986	36510611401108236	
3025480RED DEER AIRPORT	ALTA19591986	23521111354	90223
3015522ROCKY MTN HOUSE AIRPORT	ALTA19641986	21522611455	98721
3023720LACOMBE CDA	ALTA19701986	17522811345	84717
3053520JASPER	ALTA19631986	23525311804106023	
3012205EDMONTON INTL AIRPORT	ALTA19611986	25531811335	71325
3012295ELLERSLIE	ALTA19651986	19532511333	69119
3016761VEGREVILLE CDA	ALTA19711986	13532911202	63313
3012208EDMONTON MUNICIPAL A	ALTA19141986	54533411331	67054
3062244EDSON AIRPORT	ALTA19701986	17533511628	92017
3012210EDMONTON NAMAO AIRPORT	ALTA19651986	22534011328	68522
3081680COLD LAKE AIRPORT	ALTA19661986	21542511017	53921
3072920GRANDE PRAIRIE AIRPORT	ALTA19681986	18551111853	66718
3070560BEAVERLODGE CDA	ALTA19611986	25551211924	74324
3066001SLAVE LAKE AIRPORT	ALTA19731986	14551811447	57914
3077246WATINO	ALTA19631986	15554311738	39615
3075040PEACE RIVER AIRPORT	ALTA19661986	21561411726	56921
3062693FORT MCMURRAY AIRPORT	ALTA19661986	21563911113	36821
3072658FORT CHIPEWYAN AIRPORT	ALTA19691986	18584611107	23118

RAIN GAUGE DATA BASE USED IN THE ANALYSIS
PROVINCE OF ONTARIO
(AES FORMAT)

FILE : INDEX DISK IDENT : A:IDF_ON.D1

613FN58POINT PELEE	ONT19751986	124157	8231	17612
6133360HARROW CDA	ONT19661986	194202	8254	18819
6139525WINDSOR AIRPORT	ONT19461986	404216	8258	18840
6139538WINDSOR UNIV	ONT19681979	124218	8304	17912
6131415CHATHAM WPCP	ONT19661986	214223	8212	17620
6137147RIDGETOWN	ONT19591985	274227	8153	20427
6134610LONG POINT	ONT19671985	184233	8003	17318
6137362ST THOMAS WPCP	ONT19261986	574246	8113	20757
6137730SIMCOE	ONT19621986	254251	8016	23725
6131982DELHI CDA	ONT19621986	244252	8033	23124
6136606PORT COLBORNE	ONT19641986	234253	7915	17323
6127514SARNIA AIRPORT	ONT19701986	174300	8218	17917
6144475LONDON AIRPORT	ONT19431986	394302	8109	27739
6140954BRANTFORD MOE	ONT19611986	254308	8014	19525
6149625WOODSTOCK	ONT19621971	104308	8046	28010
6135638NIAGARA FALLS	ONT19651986	224308	7905	18222
6153194HAMILTON AIRPORT	ONT19711986	164310	7956	23416
6139145VINELAND STATION	ONT19631986	194311	7924	7919
6137287ST CATHARINES AIRPORT	ONT19541986	244312	7910	9724
6146745PROSPECT HILL	ONT19561970	104313	8114	31010
6153300HAMILTON RBG	ONT19631986	234317	7953	10023
6151059BURLINGTON FIRE	ONT19701982	104321	7949	11210
6148105STRATFORD MOE	ONT19661986	204322	8100	35320
6146714PRESTON WPCP	ONT19711986	144323	8021	27114
6149387WATERLOO WELLINGTON A	ONT19711986	164327	8023	31316
6144241KITCHENER CITY ENG	ONT19551967	134328	8029	31613
615N745OAKVILLE SE OWRC	ONT19651976	124329	7938	8512
6143087GUELPH SMALLFIELD	ONT19541964	114332	8018	34411
6143069GUELPH ARBORETUM	ONT19541986	314333	8013	32631
6140818BLUE SPRINGS CRK	ONT19671977	114338	8007	37111
6158665TORONTO ISLAND AIRPORT	ONT19711986	164338	7924	7616
6158525TORONTO ETOBICOKE	ONT19641980	164338	7932	11816
6142285ELORA RESEARCH STN	ONT19701986	174339	8025	37417
6158764TORONTO OLD WESTON RD	ONT19661986	214339	7928	12121
6158406TORONTO BOOTH	ONT19661986	214339	7921	7621
6158733TORONTO PEARSON INTL A	ONT19501986	354340	7938	17035
6158575TORONTO GREENWOOD	ONT19661981	164340	7919	9716
6158350TORONTO	ONT19401986	434340	7924	10943
6142803GLEN ALLAN	ONT19601970	104341	8043	40210
6158732TORONTO LESLIE EGLINTON	ONT19731986	134343	7921	13112

RAIN GAUGE DATA BASE USED IN THE ANALYSIS
PROVINCE OF ONTARIO (continued)
(AES FORMAT)

FILE : INDEX DISK IDENT : A:IDF_ON.D2

6142400FERGUS SHAND DAM	ONT19621986	234344	8020	41723
615HHDFTORONTO YORK MILLS	ONT19731986	134345	7923	15213
6122849GODERICH AIRPORT	ONT19701980	114346	8142	21311
6158718TORONTO KEELE-FINCH	ONT19641986	204346	7929	19820
6158520TORONTO ELLESMERE	ONT19661986	204346	7916	16119
6158740TORONTO MET RES STN	ONT19661986	184348	7933	19218
6155878OSHAWA WPCP	ONT19701986	164352	7850	8216
6153020GREENWOOD MTRCA	ONT19601986	224354	7904	12822
6150830BOWMANVILLE MOSTERT	ONT19681986	184355	7840	9718
6154820MAIN DUCK ISLAND	ONT19661986	214356	7638	7621
6159510WILCOX LAKE	ONT19601970	104357	7926	28910
6158084STOUFFVILLE WPCP	ONT19611986	114358	7915	26511
6155722OAK RIDGES	ONT19271948	174358	7928	33817
6145503MOUNT FOREST	ONT19621986	254359	8045	41425
6156533PICTON	ONT19661986	214401	7708	7621
6151042BURKETON MCLAUGHLIN	ONT19691986	184402	7848	31018
6157831SMITHFIELD CDA	ONT19691986	144405	7740	12114
6158875TRENTON AIRPORT	ONT19651986	214407	7732	8521
6150689BELLEVILLE	ONT19601986	194409	7724	7619
6166418PETERBOROUGH AIRPORT	ONT19711986	164414	7821	18816
6104175KINGSTON PUMPING STATION	ONT19141986	434414	7629	7643
6166450PETERBOROUGH STP	ONT19651986	224417	7819	19222
6151137CAMPBELLFORD	ONT19731986	144418	7748	14614
6164432LINDSAY FILTRATION PLANT	ONT19651986	224421	7844	24922
6159010TWEED	ONT19571970	134430	7717	14313
6116132OWEN SOUND MOE	ONT19651986	214435	8056	17621
6100971BROCKVILLE PCC	ONT19671986	194436	7540	9119
6115820ORILLIA TS	ONT19651986	214437	7925	21921
6119500WIARTON AIRPORT	ONT19731986	144445	8106	21914
6107836SMITHS FALLS TS	ONT19641986	194453	7600	11219
6104025KEMPTVILLE	ONT19701986	174500	7538	9717
6116843RAGGED RAPIDS	ONT19521970	144501	7941	22814
6101901CORNWALL ONT HYDRO	ONT19571986	274502	7448	7627
6169453WEST GUILFORD	ONT19721986	154506	7841	32615
6119115UTTERSON ONT HYDRO	ONT19711983	114512	7921	29511
6112072DORSET MOE	ONT19621986	134513	7856	32313
6106000OTTAWA INTL AIRPORT	ONT19671986	204519	7540	11220
6121912COVE ISLAND	ONT19651985	194520	8144	17918
6101820COMBERMERE	ONT19541977	204522	7737	28620
6105976OTTAWA CDA	ONT19051986	344523	7543	7934

RAIN GAUGE DATA BASE USED IN THE ANALYSIS
PROVINCE OF MANITOBA
(AES FORMAT)

FILE : INDEX DISK IDENT : A:IDF_MN.D1

```
5022125PILOT MOUND (AUT)        MAN19651986 224912 9854 46922
5020720DEERWOOD                 MAN19641986 214924 9819 33821
5031320INDIAN BAY               MAN19611986 244937 9512 32624
5021054GLENLEA                  MAN19671986 204939 9707 23120
5010485BRANDON CDA              MAN19601985 254952 9959 36225
5023233WINNIPEG ST BONIFACE     MAN19611981 204953 9706 23120
5023222WINNIPEG INTL AIRPORT    MAN19441986 394954 9714 23739
5012320PORTAGE LA PRAIRIE A     MAN19641986 234954 9816 26823
5010480BRANDON AIRPORT          MAN19701986 174955 9957 40817
5023261WINNIPEG STP             MAN19611985 204957 9706 23119
5031038GIMLI                    MAN19641986 235037 9659 22223
5030282BISSETT                  MAN19691984 165102 9540 25616
5040680DAUPHIN AIRPORT          MAN19541986 33510610003 30133
5031111GRAND RAPIDS             MAN19661978 135309 9917 22213
5061376ISLAND LAKE AIRPORT      MAN19711986 165351 9439 23416
5052880THE PAS AIRPORT          MAN19711986 16535810106 26816
506B0M7NORWAY HOUSE FORESTRY    MAN19631986 185400 9748 21618
5050960FLIN FLON AIRPORT        MAN19701986 16544110141 30115
5062922THOMPSON AIRPORT         MAN19711986 165548 9752 21316
5061001GILLAM AIRPORT           MAN19721986 155621 9442 14315
5061646LYNN LAKE AIRPORT        MAN19691986 18565210104 35618
5060600CHURCHILL AIRPORT        MAN19631986 245845 9404  3324
```

RAIN GAUGE DATA BASE USED IN THE ANALYSIS
PROVINCE OF SASKATCHEWAN
(AES FORMAT)

FILE : INDEX DISK IDENT : A:IDF_SA.D1

```
4012400ESTEVAN AIRPORT          SASK19641986 23490410300 56923
4018760WEYBURN                  SASK19621986 24493910350 56624
4015680ORMISTON                 SASK19691986 16494310522 68516
4028060SWIFT CURRENT CDA        SASK19591986 28501610744 82228
4028040SWIFT CURRENT AIRPORT    SASK19701986 17501710741 81617
4015320MOOSE JAW AIRPORT        SASK19601986 27502010533 57627
4012164DAVIN 5                  SASK19521986 25502210410 65525
4010879BROADVIEW                SASK19651986 22502310241 59722
4016560REGINA AIRPORT           SASK19411986 44502610440 57644
4013490INDIAN HEAD PFRA         SASK19611986 26503010341 60325
4013480INDIAN HEAD CDA          SASK19621986 25503210340 58225
4019080YORKTON AIRPORT          SASK19701986 17511610228 49617
404037QBAD LAKE IHD 102         SASK19721986 15511910825 63715
4043900KINDERSLEY AIRPORT       SASK19661986 21513110910 69121
4055736OUTLOOK PFRA             SASK19631985 23512910703 53922
4019035WYNYARD                  SASK19651986 22514610412 56022
4057200SASKATOON U OF S.        SASK19261959 33520810638 51533
4057120SASKATOON AIRPORT        SASK19601986 26521010641 49926
4047240SCOTT CDA                SASK19611986 24522210850 65824
4045600NORTH BATTLEFORD AIRPORTSASK19751986 12524610815 54512
4055085MELFORT CDA              SASK19741986 13524910436 47813
4083321HUDSON BAY AIRPORT       SASK19661986 21524910219 35621
4056240PRINCE ALBERT AIRPORT    SASK19601986 24531310541 42624
4075518NIPAWIN AIRPORT          SASK19741986 13532010400 37113
4064150LA RONGE AIRPORT         SASK19661986 21550910515 37421
4063560ISLAND FALLS             SASK19661986 19553210221 29819
4060982BUFFALO NARROWS AIRPORT  SASK19681986 17555010826 43217
4061861CREE LAKE                SASK19701986 17572110708162717
4061630COLLINS BAY              SASK19731986 13581110342 48713
4068340URANIUM CITY AIRPORT     SASK19651985 20593410829 31620
```

RAIN GAUGE DATA BASE USED IN THE ANALYSIS
MARITIME REGION
(AES FORMAT)

FILE : INDEX DISK IDENT : A:IDF_MA.D1

8104800SAINT JOHN	N.B.	19241950	204517	6605	2720
8104900SAINT JOHN AIRPORT	N.B.	19581986	294519	6553	10629
8101600FREDERICTON CDA	N.B.	19591986	284555	6637	3928
8104480ROYAL ROAD	N.B.	19661986	204603	6643	11520
8104482ROYAL ROAD WEST	N.B.	19661978	124605	6644	15812
8103200MONCTON AIRPORT	N.B.	19461986	374607	6441	7037
8100512BEECHWOOD	N.B.	19591969	10	0	0	010
8101000CHATHAM AIRPORT	N.B.	19641986	234701	6527	3323
8105100SUMMIT DEPOT	N.B.	19551973	174747	6820	41117
8100514BELLEDUNE	N.B.	19711986	154754	6550	615
8100880CHARLO AIRPORT	N.B.	19591986	284759	6620	3628
8205126SHELBURNE	N.S.	19731986	144343	6515	2714
8206500YARMOUTH AIRPORT	N.S.	19711986	164350	6605	4216
8204700SABLE ISLAND	N.S.	19621986	254356	6001	325
8205090SHEARWATER AIRPORT	N.S.	19551986	314438	6330	4831
8202200HALIFAX	N.S.	19411973	234439	6334	3023
8202250HALIFAX INT'L AIRPORT	N.S.	19771986	104453	6331	14310
8202000GREENWOOD AIRPORT	N.S.	19641986	224459	6455	2722
8205085SHARPE BROOK	N.S.	19681977	104501	6438	13710
8202800KENTVILLE CDA	N.S.	19601986	254504	6429	4825
8205990TRURO	N.S.	19581985	264522	6316	3926
8201716EDDY POINT	N.S.	19721985	144531	6115	6413
8205700SYDNEY AIRPORT	N.S.	19611986	254610	6003	5425
8300400CHARLOTTETOWN CDA	PEI	19671986	204615	6308	2120
8300700SUMMERSIDE AIRPORT	PEI	19641986	234626	6350	2123
8403615ST LAWRENCE	NFLD	19691986	184655	5523	4518
8402975PORT AUX BASQUES	NFLD	19751986	124734	5910	3912
8400798BURGEO	NFLD	19671986	194737	5737	1219
8403506ST JOHN'S AIRPORT	NFLD	19491986	274737	5244	13127
8403290ST ALBANS	NFLD	19691983	144752	5551	1214
8403800STEPHENVILLE AIRPORT	NFLD	19671986	194832	5833	2419
8401700GANDER INT'L AIRPORT	NFLD	19391986	444857	5434	14944
8401501DEER LAKE AIRPORT	NFLD	19661986	214913	5724	2121
8401259COMFORT COVE	NFLD	19671986	194916	5453	9419
8401400DANIELS HARBOUR	NFLD	19691986	185014	5735	2418
8403401ST ANTHONY	NFLD	19711986	155122	5538	10315
8500398BATTLE HARBOUR LOR	NFLD	19721983	115215	5536	911
8504175WABUSH LAKE AIRPORT	NFLD	19741986	135256	6652	54813
8501900GOOSE AIRPORT	NFLD	19611986	245319	6025	4524
8501132CHURCHILL FALLS AIRPORT	NFLD	19691986	17	0	0	017

RAIN GAUGE DATA BASE USED IN THE ANALYSIS
PROVINCE OF BRITISH COLUMBIA
(AES FORMAT)

FILE : INDEX DISK IDENT : A:IDF_BC.D1

1018642VICTORIA MARINE	B.C.	19671986	20482212345 3020
1013755JORDAN RIVER GENERATING	B.C.	19731986	14482512403 314
1018610VICTORIA GONZALES HTS	B.C.	19251986	54482512319 6754
1018FF6VICTORIA U VIC	B.C.	19651985	20482812319 4520
1013754JORDAN RIVER DIVERSION	B.C.	19641986	20483012400 39320
1016941SAANICH CAMOSUM COLLEGE	B.C.	19641975	12483012325 3612
1016335PORT RENFREW BCFP	B.C.	19731982	10483512424 610
1018620VICTORIA INT'L AIRPORT	B.C.	19651986	22483912326 1822
1031413CARNATION CREEK CDF	B.C.	19751986	11485412500 6011
1108914WHITE ROCK STP	B.C.	19641986	23490112246 1523
1100030ABBOTSFORD AIRPORT	B.C.	19771986	10490212222 5710
1104555LANGLEY LOCHIEL	B.C.	19721986	15490312235 10015
1104473LADNER BCHPA	B.C.	19631978	13490512301 013
1038205TOFINO AIRPORT	B.C.	19701986	16490512546 1816
1107876SURREY MUNICIPAL HALL	B.C.	19631986	23490612250 7623
1101562CHILLIWACK MICROWAVE	B.C.	19641980	16490712154 22816
1105192MISSION WEST ABBEY	B.C.	19631986	24490912216 21924
1108447VANCOUVER INT'L AIRPORT	B.C.	19531986	34491112310 034
1148211TRAIL BIRCHBANK	B.C.	19651986	22491111744 59421
1125766OLIVER STP	B.C.	19731986	14491111933 29514
1103328HANEY MICROWAVE	B.C.	19641984	21491212231 32021
1107873SURREY KWANTLEN PARK	B.C.	19621986	25491212252 9125
110FAG9PITT MEADOWS STP	B.C.	19741986	12491312241 312
1025C70NANAIMO DEPARTURE BAY	B.C.	19711986	16491312357 616
1100120AGASSIZ CDA	B.C.	19551986	29491512146 1529
1108487VANCOUVER UBC	B.C.	19581986	29491512315 8529
1036206PORT ALBERNI AIRPORT	B.C.	19691986	18491512450 018
1103332HANEY UBC RF ADMIN	B.C.	19631986	24491612234 14324
1106256PORT COQUITLAM CITY YARD	B.C.	19711986	16491612247 616
1108453VANCOUVER KITSILANO	B.C.	19151944	30491612311 2130
1100360ALOUETTE LAKE	B.C.	19711982	12491712229 11512
110JA54BURNABY MTN BCHPA	B.C.	19741986	12491712255 46312
1106CL2PORT MOODY GULF OIL RFY	B.C.	19711986	16491712253 12816
1141455CASTLEGAR AIRPORT	B.C.	19731986	14491811738 49314
1108446VANCOUVER HARBOUR	B.C.	19701986	17491812307 017
1106180PITT POLDER	B.C.	19651986	22491812238 022
1141457CASTLEGAR BCHPA DAM	B.C.	19691984	16492111747 47516
1113540HOPE AIRPORT	B.C.	19641986	23492212129 3623
1101890COQUITLAM LAKE	B.C.	19711982	12492212248 15812
1105660N VANCOUVER LYNN CREEK	B.C.	19641983	19492212302 18819

RAIN GAUGE DATA BASE USED IN THE ANALYSIS
PROVINCE OF BRITISH COLUMBIA (continued)
(AES FORMAT)

FILE : INDEX DISK IDENT : A:IDF_BC.D2

1032730	ESTEVAN POINT	B.C.	19691978	10492312633 610
1101140	BUNTZEN LAKE	B.C.	19691983	15492312252 2115
1123970	KELOWNA AIRPORT	B.C.	19691986	18492811923 42618
1126150	PENTICTON AIRPORT	B.C.	19531986	30492811936 34130
1046330	PORT MELLON	B.C.	19641974	11493112329 611
1127800	SUMMERLAND CDA	B.C.	19551986	31493411939 45429
1152102	CRANBROOK AIRPORT	B.C.	19691986	18493611547 93818
1154203	KIMBERLEY PCC	B.C.	19761986	11493811559 88611
1021990	COURTENAY PUNTLEDGE BCHP	B.C.	19641986	23494112502 2423
1041710	CLOWHOM FALLS	B.C.	19691986	18494312332 2118
1021830	COMOX AIRPORT	B.C.	19631986	24494312454 2424
1123992	KELOWNA OK COLLEGE	B.C.	19691986	15495211929 34715
1142820	FAUQUIER	B.C.	19741986	12495211804 47212
1021261	CAMPBELL RIVER AIRPORT	B.C.	19701986	13495712516 10313
1042255	DAISY LAKE DAM	B.C.	19681983	15495912308 38015
1027775	STRATHCONA DAM	B.C.	19681982	14500012535 20114
1021265	CAMPBELL RIVER STP	B.C.	19731986	14500112514 314
1048898	WHISTLER	B.C.	19691986	16500812257 65816
1114741	LYTTON	B.C.	19701986	17501412135 25617
1142574	DUNCAN LAKE DAM	B.C.	19691986	17501411658 54817
1128551	VERNON	B.C.	19721986	15501411917 55415
1086083	PEMBERTON BCFS	B.C.	19691984	14501912249 21614
1114627	LILLOOET SETON BCHPA	B.C.	19731986	14504012155 19814
1166R45	SALMON ARM AIRPORT	B.C.	19641986	21504111914 52421
1026270	PORT HARDY AIRPORT	B.C.	19731986	13504112722 2113
1163780	KAMLOOPS AIRPORT	B.C.	19651986	22504212027 34422
1084490	LAJOIE DAM	B.C.	19701982	12505012252 68512
1176751	REVELSTOKE AIRPORT	B.C.	19701986	17505811811 44117
1173210	GOLDEN	B.C.	19731986	13511811659 78313
117R00	FYOHO NAT PARK BOULDER CR	B.C.	19741986	12512311632121912
1175122	MICA DAM	B.C.	19691982	10520311835 57910
1160899	BLUE RIVER AIRPORT	B.C.	19701986	17520811917 67617
1093599	HORSEFLY BCFS	B.C.	19701983	14522012125 78314
1060842	BELLA COOLA BC HYDRO	B.C.	19701985	16522212649 1216
1178CL9	VALEMOUNT NORTH	B.C.	19701986	15525111915 89015
1057050	SANDSPIT AIRPORT	B.C.	19721986	15531513149 315
1094955	MCBRIDE NORTH	B.C.	19731986	14532212015 77114
1096450	PRINCE GEORGE AIRPORT	B.C.	19601986	27535312241 67327
1064283	KITIMAT	B.C.	19661986	17540212842 917
1087600	SOUTHBANK	B.C.	19631975	12540212546 72812

RAIN GAUGE DATA BASE USED IN THE ANALYSIS
PROVINCE OF BRITISH COLUMBIA (continued)
(AES FORMAT)

FILE : INDEX DISK IDENT : A:IDF_BC.D3

1091169	BURNS LAKE	B.C.	19691986	17541412546 70417
1066481	PRINCE RUPERT AIRPORT	B.C.	19701986	17541813026 3317
1092970	FORT ST JAMES	B.C.	19761986	11542712415 68511
1068130	TERRACE AIRPORT	B.C.	19691986	18542812835 21618
1068131	TERRACE PCC	B.C.	19681986	18543012837 5718
1076638	QUICK	B.C.	19631986	21543712654 53319
1077500	SMITHERS AIRPORT	B.C.	19711986	16544912711 52116
1184790	MACKENZIE AIRPORT	B.C.	19711986	16551812308 69716
1181508	CHETWYND AIRPORT	B.C.	19701986	18554212138 60618
1182285	DAWSON CREEK AIRPORT	B.C.	19691986	15554412011 65214
1183090	GERMANSEN LANDING	B.C.	19641986	22554712442 74622
1183FLO	HUDSON HOPE BCHPA DAM	B.C.	19711986	15560112212 67614
1183000	FORT ST JOHN AIRPORT	B.C.	19731986	12561412044 69412
1188696	WARE	B.C.	19641981	13572612538 77713
1208202	TODAGIN RANCH	B.C.	19751986	12573613004 89911
1192340	DEASE LAKE	B.C.	19731986	14582513000 81314
1192940	FORT NELSON AIRPORT	B.C.	19661986	20585012235 38020
1200560	ATLIN	B.C.	19771986	10593413342 67310